# Gain and loss of information by decoherence

Quantum correlations and decoherent histories in diverse physical systems

**Michele Allegra**

PhD Thesis in Physics
Tesi di Dottorato in Fisica


Scuola di Dottorato in Scienza ed Alta Tecnologia
Indirizzo di Fisica e Astrofisica
XXVI ciclo
Università degli Studi di Torino

Academic Supervisor (Relatore Accademico) Prof. Lorenzo Magnea
External Supervisor (Relatore Esterno) Dr. Paolo Giorda

# Contents

# Introduction and synopsis

### Listening back to the whole piece

The experience of going through a PhD training is similar to listening for the first time to a long musical composition. Like the composition's movements, projects come in rapid succession and as you concentrate on single units you often miss to perceive the global coherence of the work. Writing up this thesis is the occasion for listening back to the whole piece, and appreciate its cohesion. This thesis shows both unity and variation. Unity has been provided by the firm guidance of my tutors, who have pushed me along a meaningful and clear research direction. Variation is due the freedom they have granted me to comply with the whims of interests, stimuli, and ideas.
By the nature of the work I have carried over, this cannot be a strictly monographic thesis – I haven't been working on a single research project from the beginning to the end. But it is certainly neither a mere collection of papers. If it were a music piece, it wouldn't have the monolithic character of Bach's *Goldberg variations*, with its obsessive exploration of a single aria, but it would't either resemble a collection of completely disparate and unrelated passages like Chopin's *Études*. It would probably sound like Schumann's *Carnaval*, a series of scenes with a *strong thematic unity* represented by a leitmotiv and the ubiquitous, recurring presence of four keys. The leitmotiv is *decoherence*, and the recurring keys are the concepts of *coherence*, *measurements*, *correlations*, *information*.

### Synopsis: decoherence and information

> "The inability to discard entails the impossibility to discern"
>
> Umberto Eco

When you measure a quantum system, you irremediably perturb it – so goes a common representation of Heisenberg's uncertainty principle. While this image is essentially faithful, it may fail to adequately depict the huge gap between classical and quantum physics. In fact, even by measuring a classical system you ought to perturb it. For instance, if you want to measure an electrostatic field you must use a test charge, whose presence will necessarily affect the field itself. However, there is a fundamental difference between this kind of disturbance and the kind of disturbance emerging from Heisenberg's uncertainty principle. The disturbance created by a classical measurement is not fundamental, and it can be made arbitrarily small, at least in principle. On

the contrary, the disturbance unleashed by a quantum measurement is lower-bounded by precise limits that depend on the measured observable, ant it cannot be reduced at will, not even in principle. This kind of disturbance is fundamental, and it stems from the fact that we are trying to *extract classical records from a quantum state*. When we measure a given observable, we obtain a classical record thereof. This comes at the price of losing all information about the quantum state's phases in the observable's eigenbasis.

The leitmotiv of this thesis is that *if we wish to obtain a classical record of a quantum property or process, we must usually discard some information*. The obstacle that impedes acquiring classical records of quantum phenomena is quantum *coherence*, in its multifarious manifestations. Correspondingly, the process of information loss that is needed to create classical records is *decoherence*.

Decoherence, as the product of physical processes affecting open quantum systems, has been studied since the 1980es. A major breakthrough in the understanding of quantum mechanics was the realization that decoherence can be the consequence of phase information dispersal among an ensemble of uncontrollable degrees of freedom external to the system, generally termed "environment". Decoherence, whether it is caused by a quantum measurement or not, effectively creates classical records of the system. It fragilizes quantum information, and stabilizes classical information.

While decoherence is now a well-known and well-studied phenomenon, its effects have not been explored in all possible directions yet. In particular, an interesting perspective on decoherence processes opens up by taking an informational approach. The immediate dividend of this choice is that one can use *information-theoretical quantifiers* to give a precise quantitative meaning to the ideas of information gain and information loss under the effect of decoherence. In several cases, the amount of information that is lost under decoherence is commensurate with the amount of coherence originally present in the system. Actually, it turns out that a good way to *define* and *assess* the degree of coherence, or quantumness of the system is exactly to consider the information lost under actual or potential decoherence processes. On the other side, the ability to quantify the classical information gained after the action of decoherence is a precious indication of how much an observer can learn about a quantum system through observation.

The thread binding together all studies presented in the forthcoming chapters is the *analysis of the effects of actual or potential decoherence processes on several physical systems, with the key aid of information-theoretical quantifiers.*

An important aspect of decoherence that has been properly highlighted only in recent years is its effect on the correlations between two subsystems. If a measurement-induced decoherence process locally affects a subsystem belonging to a correlated system, a part of the correlations can be irreversibly lost. Actually, unless correlations are in a specific, classical form, *any* local decoherence process entails a correlation loss. This was recognized by Ollivier and Zurek [26] as a blatantly nonclassical feature of correlations and they considered the minimal amount of correlations lost to define a genuine measure of *quantum correlations* called *quantum discord*. Complementarily, Henderson and Vedral [27] considered the maximum amount of correlations that can survive the effect of local decoherence to define a measure of classical correlations. Discord and classical correlations have been receiving growing attention in

recent years, as they are of relevance to the performance of several quantum information processing tasks. In the first part of this thesis I will present two research projects aimed at analyzing discord and classical correlations in physically important scenarios: a quantum many-body model (Chapter 2) and a quantum optical model (Chapter 3).
Another still poorly studied aspect of decoherence is its relation to *dynamical entropy*, that quantifies the amount of information generated by the time evolution of a system, i.e., that cannot be predicted on the basis of previous data on the system. This issue can be properly addressed within the general formalism of *decoherent histories*. Originally developed as an interpretational framework for quantum theory, decoherent histories provide a natural language to describe coherence in the evolution of quantum systems. Coherent effects reflect into the impossibility of assigning well-defined probabilities to different paths or "histories" of the system, and they are simply captured by the off-diagonal elements of a mathematical object called *decoherence matrix* (or *functional*). When the decoherence matrix is diagonal, a condition called *medium decoherence*, the evolution admits a perfectly classical description. Medium decoherence is usually obtained upon discarding information, a procedure caleed coarse-graining. The ignored information can be related either to an external environment, or to a part of the system itself. By framing the concept of dynamical entropy in the decoherent histories language, we will obtain a twofold yield. On one side, we will develop an information theoretical quantifier of coherence in the time-evolution of a system (the *relative entropy of decoherence*, Chapter 5), by comparing entropy production when coherent effects are neglected or taken into accout, respectively. This measure will be used to address a physically important problem, the emergence of pointer bases in Hilbert space after interaction with a noisy environment (chapter 7). Moreover, we will analyze the effects of decoherence and coarse-graining on entropy production by quantum systems, comparing chaotic and integrable dynamics, and establishing under which conditions both types of dyamics can lead to the effective production of classical information at a nonvanishing rate.
Quantum information theory has contributed to highlight the tight relation between physics and information theory. On one side, encoding, manipulating and extracting information are tasks that sensibly depend on the physical properties and behavior of information-bearing systems. On the other side, taking an informational perspective can shed light onto the physics of those systems, leading to significant advances in understanding.
Exploring the effects of decoherence from an informational perspective conforms to this general spirit. There are two main motivations for this exploration. From viewpoint of *applications*, understanding how decoherence, information extraction, and information loss affect quantum systems is essential to control them and put them to use for information processing tasks. From the point of view of *fundamental theory*, we can achieve a deeper comprehension of the difference between classical and quantum physics.

**Contents of the chapters**

- Chapter 1 contains an introductory review of quantum discord. I will highlight the derivation of discord from decoherence theory, explain its information-theoretic meaning and stress its potential for applications of quantum science and technology. The chapter should enable the reader to understand and contextualize the work in presented in Chapters 2 and 3.

- In Chapter 2, I investigate quantum discord and classical correlations in the extended Hubbard model, a reference model in the study of correlated electrons. This chapter significantly overlaps with an article that has been featured in Physical Review B [107], of which I am the first author. Since quantum information has highlighted strong ties between quantum entanglement and physical properties of many-body ground states, especially at quantum critical points, it is interesting to look for similar relations involving other types of quantum correlations like quantum discord. I will assess discord and classical correlations in all phases of the model, which has a complex phase diagram, and focus on the behavior of correlation measures in the proximity of quantum critical points. I will uncover a tie between long range correlations (off-diagonal long-range order) and quantum discord in parameter regions where entanglement is vanishing, pinpointing a possible general relation between discord and macroscopic quantum phenomena like superfluidity and superconductivity. Furthermore, the separation between discord and classical correlations at the critical points will prove essential to discriminate between phase transitions that are physically different depending on the appearance/disappearance of off-diagonal long-range order.

- In Chapter 3, I will address discord for Gaussian states of two bosonic modes. This chapter is essentially a reprint of a paper published in Physical Review A [64], of which I a contributing author. The computation of quantum discord is in general very difficult, since an optimization over all local measurements is required: One has to identify the optimal local measurement allowing for the maximal preservation of classical correlation between two correlated systems. The problem is interesting per se, besides the evaluation of discord, as it sheds light onto information extraction from the quantum system at hand. For Gaussian states, it has been shown that the maximization problem can be solved if one restricts the optimization to Gaussian measurements like homodyne detection, that maintain the Gaussian character of the state. This left open the question, whether non-Gaussian measurements may allow for a better optimization. I will focus on two large classes of Gaussian states, (squeezed thermal states and mixed thermal states) and evaluate discord comparing results obtained with Gaussian measurements, like homodyne detection, and non-Gaussian ones like photon counting. I will exhibit strong evidence that Gaussian measurements are optimal.

- Chapter 4 is a review of the decoherent histories formalism. The presentation is tailored to provide the reader with sufficient knowledge to understand the following chapters (5,6,7).

- In Chapter 5, I will introduce dynamical entropy and explain how this concept can be embedded in the decoherent histories formalism, by virtue of a general mapping between measurements and Hilbert space partitions. I will show that ALF-entropy, a quantum generalization of the classical Kolmogorov-Sinai entropy, is related to the von Neumann entropy of the decoherence matrix of a set of histories with fixed projections for all times. I will show that the decoherence matrix can be interpreted as the density matrix of a set of quantum registers that subsequently interact with the system, effectively performing the "measurements" that define the set of histories under attention. This picture allows to interpret ALF entropy as the rate of production of quantum information by the dynamics. Upon casting ALF entropy in the decoherent histories language, I will introduce a general measure of coherence for quantum histories, the relative entropy of decoherence. The latter is defined as the quantum relative entropy between the actual decoherence matrix and a decoherence matrix where off-diagonal entries are completely discarded.

- In Chapter 6, I will analyze dynamical entropy production by closed quantum systems in presence of two sources of randomness, (R1) randomness in the dynamics, i.e., in the choice of the evolution operator (R2) randomness in the choice of measurements. By using the decoherent histories formalism, I will be able to focus on the effects of decoherence and coarse-graining for dynamical entropy production. Both (R1) and (R2) lead to similar results: Upon sufficient coarse-graining, histories are decoherent and exhibit to a non-vanishing rate of entropy production. These results entail that both chaotic and integrable quantum systems can produce effectively classical information at a non-vanishing rate. This picture is obtained through a general, yet heuristic argument, and strengthened by a rigorous random matrix argument that proves results for the (R1) case. I will test theoretical results by numerically studying decoherent histories and dynamical entropy in the quantum standard map, a well-known model that has a chaotic/integrable transition. Results of this chapter are of interest for a general issue raised by Gell-Mann, that of fundamental sources of unpredictability in quantum mechanics.

- In Chapter 7, I will analyze the emergence of pointer bases (i.e., privileged bases in which the open system decoheres) in a two-level small system interacting with a non-Markovian environment. As previous literature has shown, pointer bases depend on the strength of the system-environment coupling. While weakly coupled systems decohere in their own energy eigenbasis, strongly coupled ones do so in a basis dictated by the interaction Hamiltonian. A recent paper has suggested that pointer bases exist also for intermediate values of the coupling, and they "interpolate" between the two extremes found at weak and strong coupling. By following previously developed methods, I will investigate pointer bases as a function of the system-environment coupling. In addition, I will study decoherent histories with fixed projections in different bases, focusing on the behavior of the relative entropy of decoherence introduced in Chapter 4. I will test the basic expectation that pointer bases should correspond to sets of mutually decoherent histories. At weak and strong coupling I will observe the appearance of clear

pointer bases, and correspondingly a small value of the relative entropy of decoherence. For intermediate values of the coupling, I will argue that no true pointer bases arise, showing that different initial states decohere in different bases. The behavior of the relative entropy of decoherence (that shows similar values for all bases) strengthens this conclusion.

**We, the authors of this thesis**

This is my thesis, but it also *our* thesis. No part of this manuscript arose from a solitary effort. In particular, I can claim no unshared credit for any of the scientific results presented in the following chapters. It is hard to delimit the contribution given by my supervisor at ISI, Paolo Giorda. Work presented in chapters 2 and 3 is the product of our direct collaboration, and his steady supervision. We were both involved in discussing ideas, making calculations, analyzing results, and writing. We also had the pleasure to collaborate with other people. Our project on discord in the extended Hubbard model (chapter 2) was done in collaboration with Arianna Montorsi, whose essential ideas and physical insights have determined the very shape of the work. For the work on non-Gaussian discord (chapter 3) we collaborated with Matteo Paris, who gave fundamental contributions in the framing, the analysis and the writing. All work related to decoherent histories (chapters 5,6,7) was done by me in collaboration with Seth Lloyd. Those projects were ignited by creative bursts of his, and he later carefully guided me along the most interesting research directions. Even if Paolo Giorda didn't directly collaborate on the projects described in chapter 5,6,7, his encouragement, as well as his comments and suggestions were invaluable in bringing those projects to an end. Although the review chapters on discord and decoherent histories were written solely by me, they reverberate many echoes of discussions we had together with Paolo and several other friends and colleagues.
I am sure that the merits, if any, of this thesis are largely a fruit of this range of collaborations, while I am the sole responsible for its possible flaws.

## My publications during this PhD

### Published papers included to this thesis

- M. Allegra, P. Giorda, A. Montorsi, *Quantum discord and classical correlations in the bond-charge Hubbard model: Quantum phase transitions, off-diagonal long-range order, and violation of the monogamy property for discord*, Phys. Rev. B **84** (24), 245133 (2011).
- P. Giorda, M. Allegra and M.G.A. Paris, *Quantum discord for Gaussian states with non-Gaussian measurements*, Phys. Rev. A **86**, 052328.

### Papers in progess from work included in this thesis

- M. Allegra and S. Lloyd, *Decoherent histories and entropy production by quantum systems*, in progress.
- M. Allegra and S. Lloyd, *Decoherent histories and pointer bases for a qubit subject to non-Markovian noise*, in progress.

### Papers not included in this thesis

- M. Allegra, M.G.A. Paris, and P. Giorda, *Robustness of Gaussian and non-Gaussian Entanglement in a Noisy Environment*, Int .J. Quant. Inf. **9** (1), 27 (2011).
- M. Allegra, M.G.A. Paris, and P. Giorda, *Allegra, Giorda, and Paris Reply*, Phys. Rev. Lett. **107**, 238902 (2011).
- M. Allegra and P. Giorda, *Topology and energy transport in networks of interacting photosynthetic complexes*, Phys. Rev. E **85**, 051917. (2012).

# Notations

We always consider units where $\hbar = 1$, unless otherwise specified. *Subscripts* on kets, density matrices ($\varrho$) and traces (Tr), and *superscripts* on measurement maps $\Pi$ and $\Phi$'s label subsystem label the subsystem(s) of reference. Primed quantities always indicate that they are evaluated after a measurement. Logarithms are taken in base 2, unless otherwise stated.

# List of symbols

| | |
|---|---|
| $a_X, a_X^\dagger$ | boson creator operators of mode $X$, *Chap. 3* |
| $\alpha$ | displacement parameter, *Chap. 3* |
| $\mathcal{A}_i$ | Kraus operators, *Chap. 1,4,5,7* |
| $\mathcal{A}_{j_\ell}^\ell$ | Kraus operator representing alternative $j_\ell$ at time $t_\ell$, *Chap. 4,5,7* |
| $A, B, C$ | subsystems, *Chap. 1,3* |
| $\|b_i\rangle$ | orthonormal basis, *Chap. 7* |
| $\beta$ | inter-basis angle, *Chap. 7* |
| $c_{i\sigma}, c_{i\sigma}^\dagger$ | fermion creation operator for site $i$ and spin $\sigma$, *Chap. 2* |
| $C_{\mathbf{j}}$ | history operator, *Chap. 4,5,6,7* |
| $\mathcal{C}_N$ | relative entropy of decoherence, *Chap. 5,6,7* |
| $d$ | space dimension, *all chapters* |
| $d_\pm$ | symplectic eigenvalues, *Chap. 3* |
| $D(\eta)$ | displacement operator, *Chap. 3* |
| $D(A\|B)$ | quantum discord with measurements on $B$, *Chap. 1,2,3* |
| $D(B\|A)$ | quantum discord with measurements on $A$, *Chap. 1,2,3* |
| $D_G(A\|B)$ | geometric discord, *Chap. 1,3* |
| $D^{\mathcal{G}}(A\|B)$ | Gaussian discord with measurements on mode $B$, *Chap. 3* |
| $D^{\mathcal{NG}}(A\|B)$ | non-Gaussian discord with measurements on mode $B$, *Chap. 3* |
| $D_G^{\mathcal{G}}(A\|B)$ | Gaussian geometric discord, *Chap. 3* |
| $D_G^{\mathcal{NG}}(A\|B)$ | non-Gaussian geometric discord, *Chap. 3* |
| $\mathcal{D}_{\mathbf{jk}}$ | decoherence matrix, *Chap. 4,5,6,7* |
| $\mathcal{D}^{(N,E)}$ | dec. matrix with $N$ measurements given by POVM $E$, *Chap. 4,5,6,7* |
| $\delta^2$ | coherence ratio between pair of histories, *Chap. 6* |
| $\delta_s$ | basis stability parameter, *Chap. 7* |
| $\Delta$ | coarse-graining dimension, *Chap. 5,6* |
| $\Delta t$ | time interval between projections in histories, *Chap. 4,5,6,7* |
| $\|e_i\rangle, \|f_i\rangle$ | orthonormal bases, *Chap. 1* |
| $\|e_i\rangle$ | Schmidt basis, *Chap. 7* |
| $\mathcal{E}$ | environment, *Chap. 1,4,7* |
| $\mathcal{E}$ | energy density, *Chap. 2* |
| $E_E(\varrho)$ | entanglement entropy of $\varrho$, *Chap. 1* |
| $E_F(\varrho)$ | entanglement of formation of $\varrho$, *Chap. 1,3* |
| $E_S(\varrho)$ | relative entropy of entanglement of $\varrho$, *Chap. 1* |
| $\eta$ | $\eta$-pair creation operator, *Chap. 2* |

| | |
|---|---|
| $f$ | fine-graining parameter ($f = d/\Delta$), *Chap. 5,6* |
| $\Phi$ | generalized measurement (POVM), *Chap. 1* |
| $\Phi^{\mathcal{G}}$ | Gaussian POVM, *Chap. 3* |
| $\gamma$ | dephasing constant, *Chap. 7* |
| $\Gamma$ | relaxation constant, *Chap. 7* |
| $h(p_A)$ | Shannon entropy of $p_A$, *Chap. 1* |
| $h_{ALF}$ | Alicki-Fannes entropy, *Chap. 5,6* |
| $h_{KS}$ | Kolmogorov-Sinai entropy, *Chap. 5* |
| $h_N(\Omega)$ | Shannon entropy of refined partition after $N$ iterations of $\mathcal{T}$, *Chap. 5* |
| $h_N(E)$ | von Neumann entropy $\mathcal{D}^{(N,E)}$, *Chap. 5,6,7* |
| $h_N^{(c)}(E)$ | Shannon entropy of diagonal elements of $\mathcal{D}^{(N,E)}$, *Chap. 5,6,7* |
| $\mathfrak{h}$ | history, *Chap. 4* |
| $\mathcal{H}$ | Hilbert space, *all chapters* |
| $H_X$ | Hamiltonian of system $X$, *all chapters* |
| $H_{int}$ | interaction Hamiltonian, *Chap. 6* |
| $H(p_A\|p_b)$ | (classical) conditional entropy of $p_A$ given $p_B$, *Chap. 1,5* |
| $I, II, III, IV$ | regions of Hubbard model, *Chap. 2* |
| $I_{1,2,3,4}$ | symplectic invariants, *Chap. 3* |
| $I(A:B)$ | classical mutual information, *Chap. 1* |
| $\mathcal{I}(A:B)$ | quantum mutual information, *Chap. 1,2,3* |
| $I_{acc}(A:B)$ | accessible information information, *Chap. 1* |
| $I(A\rangle B)$ | coherent information, *Chap. 1* |
| Im | imaginary part, *all chapters* |
| $\mathbf{j} \equiv i_1 \dots i_N$ | multi-index for quantum history, *Chap. 4,5,6,7* |
| $\bar{\mathbf{j}} \equiv \bar{j}_1 \dots \bar{j}_N$ | multi-index for coarse-grained history, *Chap. 4,5,6,7* |
| $\tilde{\mathbf{j}} \equiv \tilde{j}_1 \dots \tilde{j}_N$ | multi-index for fine-grained history, *Chap. 4* |
| $\mathbf{j} \vee \mathbf{k}$ | coarse-graining by logical sum of histories $\mathbf{i}$ and $\mathbf{j}$, *Chap. 4* |
| $\mathcal{J}(A:B)$ | classical correlations, *Chap. 1,2,3* |
| $\mathbf{k}, \bar{\mathbf{k}}, \tilde{\mathbf{k}}$ | same as $\mathbf{j}, \bar{\mathbf{j}}, \tilde{\mathbf{j}}$, *Chap. 4* |
| $K$ | concurrence, *Chap. 1,2* |
| $\mathcal{K}_{t\ t0} \quad (\tilde{\mathcal{K}}_{t\ t0})$ | propagator (reduced propagator) between time $t_0$ and time $t$, *Chap. 4,7* |
| $L$ | length of chain, *Chap. 2* |
| $\lambda$ | coupling constant, *Chap. 7* |
| $\lambda$ | two-mode squeezing parameter, *Chap. 3* |
| $\lambda_k$ | state eigenvalues, *Chap. 1,2* |
| $\Lambda$ | quantum operation (TPCP map), *Chap. 1* |
| $m_\ell, n_\ell$ | number of projectors at time $t_\ell$, *Chap. 4* |
| $\mathcal{M}(A:B)$ | entanglement monotone, *Chap. 1* |
| $\mu$ | chemical potential, *Chap. 2* |
| $n$ | average per site filling, *Chap. 2* |
| $n_d \quad (n_s)$ | density of doubly (singly) occupied sites, *Chap. 2* |
| $n_{i\sigma}$ | fermion number operator for site $i$ and spin $\sigma$, *Chap. 2* |
| $n_T$ | thermal number, *Chap. 7* |
| $N$ | number of projections in decoherent histories, *all chapters* |
| $N_d \quad (N_s)$ | number of doubly (singly) occupied sites, *Chap. 2* |

| | |
|---|---|
| $N_t$ | total number of particles, *Chap. 2* |
| $N_1, N_2$ | thermal numbers of modes $A$, $B$, *Chap. 3* |
| $\mathcal{N}(A:B)$ | negativity, *Chap. 1,2* |
| $\mathcal{N}_{\mathcal{P}}, \mathcal{N}'_{\mathcal{P}}$ | symmetry factors, *Chap. 6* |
| $\nu(N)$ | thermal state with thermal photon number $N$, *Chap. 3* |
| $O$ | generic operator, *Chap. 1,6* |
| $\Omega_j$ | phase-space partition elements, *Chap. 5* |
| $\Omega^{(N)}_{j_1 \ldots j_N}$ | elements of refined partition after $N$ iterations of $\mathcal{T}$, *Chap. 5* |
| $p$ | momentum coordinate of the kicked rotor, *Chap. 6,7* |
| $p_i$ | probability of $i$, *Chap. 1,2,3* |
| $p_{i\|j}$ | conditional probability of $i$ given $j$, *Chap. 1,2,3* |
| $p_{\mathbf{j}}$ | probability of history $\mathbf{j}$, *all chapters* |
| $p^{th}_s(N)$ | thermal distribution, *Chap. 3* |
| $P_i, Q_i$ | projectors, *all chapters* |
| $P^{\ell}_{j_\ell}$ | history proj. representing alternative $j_\ell$ time $t_\ell$ , *Chap. 4,5,6,7* |
| $\bar{P}^{\ell}_{\bar{j}_\ell}$ | history proj. representing coarse-grained alternative $\bar{j}_\ell$ time $t_\ell$, *Chap. 4* |
| $\tilde{P}^{\ell}_{\tilde{j}_\ell}$ | history proj. representing f-grained alternative $\tilde{j}_\ell$ time $t_\ell$, *Chap. 4* |
| $\Pi$ | projective measurement map, *Chap. 1,2,3* |
| $q$ | position coordinate of the kicked rotor, *Chap. 6,7* |
| $q(t), \quad (Q(t))$ | generalized coordinate (of neglected DOF), *Chap. 4* |
| $Q2, QS$ | two-point (multipartite) quantum correlations, *Chap. 2* |
| $\mathcal{Q}(A\|B)$ | measure of discord with measurements on $B$, *Chap. 1* |
| $r$ | single-mode squeezing parameter, *Chap. 3* |
| $R$ | register, *Chap. 5* |
| $R$ | quantum kicked rotor, *Chap. 6,7* |
| $R1$ | randomness in the dynamics, *Chap. 6* |
| $R2$ | randomness in the measurements, *Chap. 6* |
| Re | real part, *all chapters* |
| $R_M$ | monogamy ratio, *Chap. 2* |
| $\mathcal{R}$ | entanglement range, *Chap. 2* |
| $\varrho$ | density matrix, *all chapters* |
| $\varrho_0$ | initial state, *all chapters* |
| $\varrho^{(h)}$ | mixed state in Heisenberg notation, *Chap. 4,5* |
| $\varrho_{X\|j}$ | conditional density matrix of $X$, given outcome $j$, *Chap. 1,2,3* |
| $\bar{\varrho}_X$ | time-averaged density matrix of $X$, *Chap. 7* |
| $S$ | system label of $\varrho$, *all chapters* |
| $S(\varrho)$ | von Neumann entropy of $\varrho$, *all chapters* |
| $S(\varrho\|\|\sigma)$ | quantum relative entropy, *all chapters* |
| $S(A\|B)$ | quantum conditional entropy of $A$ given $B$, *Chap. 1* |
| $S(A\|\Pi^B)$ | quantum conditional entropy $A$ given a measurement $\Pi^B$ on $B$, *Chap. 1* |
| $S(A\|\Phi^B)$ | quantum conditional entropy $A$ given a POVM $\Phi^B$ on $B$, *Chap. 1* |
| $S(r)$ | squeezing operator, *Chap. 3* |
| $\Sigma$ | set of quantum histories, *all chapters* |
| $\mathcal{S}$ | action, *Chap. 4* |
| $\sigma_{x,y,z}$ | Pauli matrices, *all chapters* |

| | |
|---|---|
| $\sigma_X$ | covariance matrix of $X$, *Chap. 3* |
| $t$ | time, *all chapters* |
| $t_\ell$ | intermediate time in history, $1 \leq \ell \leq N$, *all chapters* |
| $T$ | temperature, *Chap. 1,2,3* |
| $T$ | kicked rotor period, *Chap. 6,7* |
| $\mathcal{T}$ | classical dynamical evolution, *Chap. 5* |
| Tr | trace, *all chapters* |
| $\theta$ | angle defining qubit basis in XY (or XZ) plane, *Chap. 7* |
| $\tau_D$ | decoherence time, *Chap. 4,7* |
| $\tau_\gamma$ | dephasing time, *Chap. 7* |
| $u$ | on-site repulsion, *Chap. 2* |
| $U, V, W$ | unitary operators, *all chapters* |
| $U(\phi)$ | two-mode mixing operator, *Chap. 3* |
| $\mathcal{U}(d)$ | unitary group, *all chapters* |
| $x(t)$ | (generalized) coordinate of system, *Chap. 4* |
| $X_i^{\alpha\beta}$ | Hubbard-like projection operator $\|\alpha\rangle_i\langle\beta\|_i$, *Chap. 2* |
| $\chi$ | characteristic function, *Chap. 3* |
| $\|\chi\rangle, \|\chi'\rangle$ | path-projected states, *Chap. 6* |
| $Wg(d, \sigma\tau^{-1})$ | Weingarten function, *Chap. 6* |
| $\uparrow, \downarrow$ | spin up/spin down, *Chap. 2* |
| $\|\psi_0\rangle$ | initial state, *all chapters* |
| $\|\psi^{(h)}\rangle$ | state in Heisenberg notation, *Chap. 4,5* |

# Chapter 1

# An introduction to quantum discord

## 1.1 Introduction

There are two points at which quantum mechanics radically departs from the classical picture of physics. The first, by far more popularized, is the impossibility to simultaneously assign values to all observables of a system ("Heisenberg's uncertainty principle"), which compels a probabilistic account of physics. The second are the collective properties of compound quantum systems. The most important example thereof are the symmetries obeyed by *identical particles*, which play a crucial role in the organization and behavior of matter. Another example, perhaps equally relevant, is the existence of several types of *quantum correlations* between different parts of a system. Although the study of quantum correlations has met changing fortunes in the course of time, the global trend has been one of growth in importance and attention.

The field originated in the 1930es and flourished in the 1950es, when it was still considered of merely foundational interest. Several physicists at that time believed that quantum mechanics should be ultimately reduced to classical mechanics, by virtue of a local hidden variable model that might explain quantum indeterminacy in terms of ignorance of some relevant variables. Much effort was payed to confirm or disprove this intuition. Quantum entanglement, a form of quantum correlation, was soon recognized as a key concept that might tip the scales againts a reduction of quantum to classical mechanics. Indeed, in the 1960es it was proved that entanglement is tied to the so-called nonlocality of quantum mechanics, as discussed in the seminal work by John Bell. The discovery of nonlocality severely diminished the appeal of local hidden variable models.

But not only could quantum correlations explain why quantum mechanics is not reducible to classical mechanics. In the 1980es, they were used as the picklock that opened the door to the quite opposite goal of reducing classical mechanics to quantum mechanics. The theory of *decoherence* showed that correlations between quantum systems and their environment are essential to explain the emergence of classical reality

from a quantum substrate.
In the early 1990es, the spring of quantum information theory projected quantum correlations out of the niche of foundational topics, for it was suddenly realized that quantum correlations are powerful in affecting the way information can be manipulated and transmitted by quantum systems. In fact, quantum correlations became the fundamental *resource* allowing for novel communicational and computational tasks at the quantum level: quantum computation, teleportation, dense coding. Finally, in the last decade quantum correlations have acquired a more central status in condensed matter theory, as a relevant concept to explain so-called new phases of matter.
Correlations reflect the fact that the information contained in the global state of a system is not equivalent to the information contained in the local states of its subsystems taken separately. The ability to perform global operations that jointly involve all subsystems or the availability of communication between subsystems allows for ways of encoding and decoding information beyond what can be achieved by means of separate local operations on each subsystem. What characterizes *quantum correlations*, as opposed to other (classical) types of correlations, is the quantum nature of the global operations and/or the type of communication involved.
Traditionally, quantum information theory has focused on entanglement, that distinguishes states that can be prepared by local quantum operations and classical communication (LOCC) from those whose preparation requires global quantum operations or, equivalently, peferct quantum communication. In the last years, a novel view of quantum correlations has emerged, based on the fundamental role bestowed on *measurements* rather than preparation. The essential idea that *correlations can be unstable under decoherence induced by local measurements* has led to the concept of *quantum discord*.
For pure states, entanglement and discord coincide, and they are simply related to the algebraic structure of the states. The complex, but interesting case is that of mixed states, where entanglement and discord differ in nontrivial ways. A better understanding of this difference is important to clarify the quantum aspect of correlations and delineate the boundary between classical and quantum physics. Moreover, discord has prompted an extended research effort aimed at elucidating the role of quantum correlations in mixed state quantum information processing. This chapter provides an introduction to quantum discord. I do not aim at a fully comprehensive review of the subject (which can be found elsewhere, e.g. in [25]), but only at a short (and highly personal) summary that may provide the reader with sufficient knowledge to understand later chapters. In § 1.2 I will introduce quantum discord by showing its genesis within the theory of decoherence. In § 1.3 I will present a more information-theoretical derivation of discord, which will allow to define classical correlations. Moreover, I will discuss properties of discord and classical correlations and their possible generalizations to the case of general measurements and multipartite systems. § 1.4 discusses the relevance of discord in quantum information processing. Throughout the chapter, I assume that the reader is familiar with the concepts of subsystems, Shannon and von Neumann entropy, mutual information, entanglement, LOCC, entanglement monotones. The reader who is not familiar with these concepts can read the background section § 1.5 where they are explained.

## 1.2 Einselection, local measurements and correlations

The fundamental idea by Zurek [26] was that entanglement is not the only possible form of quantum correlation. His pioneering work led to a novel view of quantum correlations, based on measurements rather than preparations. Although Zurek's idea was introduced in the context of measurement theory, it is of much wider applicability. In measurement theory, one focuses on correlations between a system $S$ under observation and an "apparatus" $A$. The process of measurement requires an interaction between the two, leading to a correlated state. Correlations can be regarded as a measurement of a fixed observable $F = \sum_j f_j |s_j\rangle\langle s_j|$ only if the states $|s_j\rangle$ of the system become univocally correlated with corresponding states $|a_j\rangle$ of the apparatus. Assuming that $S$ and $A$ interact unitarily, entanglement between the two is established. The $SA$ state can be written as:

$$|\psi\rangle_{SA} = \sum_i \alpha_i |s_i\rangle|a_i\rangle \tag{1.1}$$

where $|s_i\rangle$ and $|a_i\rangle$ are orthogonal bases of $S$ and $A$ respectively. Contrary to appearances, Eq. (1.1) cannot be seen as a measurement of $F$. Indeed, $|\psi_{SA}\rangle$ reflects the so-called *basis ambiguity* problem that we already noticed discussing the EPR paradox. Correlations between $S$ and $A$ can be expressed in several bases, not only in the *preferred basispreferred bases* corresponding to the eigenbasis of $F$. To see this, consider a change of basis in $S$ induced by a unitary rotation $U$, $|s_i\rangle = \sum_j U_{ij}|\tilde{s}_j\rangle$. The $SA$ state can be rewritten as

$$|\psi\rangle_{SA} = \sum_{ij} \alpha_i U_{ij} |\tilde{s}_j\rangle|a_i\rangle = \sum_j \beta_j |\tilde{s}_j\rangle|\tilde{a}_j\rangle \tag{1.2}$$

where $\beta_j|\tilde{a}_j\rangle = \sum_i \alpha_i U_{ij}$ and the $\beta_j$ are fixed by the requirement that the $|a_i\rangle$ be normalized. Then $|a_i\rangle$ is a new (not necessarily orthogonal) basis of $A$. If the $|\tilde{a}_j\rangle$ are sufficiently distinguishable, meaning that $\langle a_i|a_j\rangle \ll 1, \forall i \neq j$, then correlations can be expressed in the $|\tilde{s}_j\rangle, |\tilde{a}_j\rangle$ bases, and the interaction can be fairly seen as a measurement of a different observable with eigenbasis given by $|\tilde{s}_j\rangle$, viz., $G = \sum_j g_j |\tilde{s}_j\rangle\langle\tilde{s}_j|$. In the extreme case where the state is maximally entangled ($\alpha_i = 1/d, \forall i$), then for any $U$ the new basis $|\tilde{a}_j\rangle$ is orthogonal, hence $SA$ are correlated in any possible basis and their interaction can be seen as a measurement of an arbitrary (rather than a specified) observable. What leads to the overcoming of the basis ambiguity issue is *decoherence*. The (unavoidable) interaction with external degrees of freedom, usually collectively denoted as called "environment", has the effect of stabilizing the correlation in a given *preferred* basis. The effect of interaction with the environment $\mathcal{E}$ is that different states of $SA$ become correlated with (quasi) orthogonal states of $\mathcal{E}$. As a result, the reduced $SA$ state evolves into an incoherent mixture,

$$\varrho_{SA} = \sum_{ij} \alpha_i \alpha_j |s_i\rangle|\alpha_i\rangle\langle s_j|\langle\alpha_j| \rightarrow \varrho'_{SA} = \sum_i |\alpha_i|^2 |s_i\rangle\langle s_i| \otimes |\alpha_i\rangle\langle\alpha_i| \tag{1.3}$$

Now correlations cannot be expressed in a different basis: they are unambiguously fixed in the $|s_i\rangle, |a_i\rangle$ basis. This process through which the environment selects a preferred basis is called environment-induced superselection or *einselection*. Once einselection has happened, the state of the apparatus can be consulted in the preferred basis

leaving it unperturbed: if we perform an orthogonal measurement of $A$ in the $|a_i\rangle$ basis, $P_i^A = |a_i\rangle\langle a_i|$, then we have $\Pi_{P^A}(\varrho'_{SA}) = \varrho'_{SA}$ where $\Pi^A$ is the quantum operation corresponding to the orthogonal measurement, $\Pi^A(\varrho) \equiv \sum_i P_i^A \varrho P_i^A$. Moreover, $\varrho'_{SA}$ is also stable under further interaction with $\mathcal{E}$, whose net effect on $SA$ is the same as that of an orthogonal measurement $P$ (the environment can be thought of as effectively acting as a measuring device). Thus we are left with correlations that are stable under environmental perturbation and repeated measurement.
Einselection decreases correlations between $S$ and $A$, as measured by the quantum mutual information $\mathcal{I}(S:A)$ (Eq. 1.91). Indeed, we have

$$\mathcal{I}(S:A) = 2\sum_i |\alpha_i|^2 \log|\alpha_i|^2, \qquad \mathcal{I}'(S:A) = \sum_i |\alpha_i|^2 \log|\alpha_i|^2 \tag{1.4}$$

Hence, $\mathcal{I}(S:A) > \mathcal{I}'(S:A)$. However, the additional correlations present in $\varrho_{SA}$ have the drawback of being unstable under measurement and/or environmental perturbation. This feature is recognized as a quantum effect. Classically, when locally probing a subsystem we do not alter its correlations with the rest of the system. The instability of correlations under local measurement is a purely quantum phenomenon. The excess correlations that are disrupted by any local measurement define a peculiar kind of quantum correlation, that has been called *quantum discord*.
To introduce its formal definition, let us now leave aside the system-apparatus setting and just consider a generic system living in Hilbert space $\mathcal{H}_A \otimes \mathcal{H}_B$. Assume first that its state be in the form

$$\varrho^c_{AB} = \sum_{ij} p_{ij} |e_i\rangle_A\langle e_i| \otimes |f_j\rangle_B\langle f_j| \tag{1.5}$$

i.e. diagonal in a product eigenbasis $|e_i\rangle_A \otimes |f_j\rangle_B$. A state in this form is called *classically correlated state* or simply *classical-classical ($CC$) state*. I warn the reader that the terminology "classical state" used in the quantum discord literature may be slightly misleading. The classical aspect of these states resides the structure of correlations. From other standpoints, these states are not classical. In particular, they do not correspond to an embedding of a classical probability distribution in a quantum setting, unless one restricts to an observable algebra of local operations commuting with the state's eigenbasis. Much less can CC states be considered as a semiclassical approximation, i.e., do not correspond to a suitable quantum approximation of a phase space distribution (like, for instance, coherent states that are often termed "classical states" in the quantum optics literature).
For any $CC$ state, there exist (at least) one pair of local measurements $P^A$ on $A$ and $Q^B$ on $B$ that leave the total state – and correlations – unchanged. Indeed it is immediately seen that correlations are stable under local measurements in the $|e_i\rangle_A\langle e_i|$ or $|f_j\rangle_B\langle f_j|$ basis: upon performing the projective measurements $P_i^A = |e_i\rangle_A\langle e_i|$ and $Q_j^B = |f_j\rangle_B\langle f_j|$ then we obtain

$$\Pi^A(\varrho_{AB}) = \varrho^c_{AB}, \qquad \Pi^B(\varrho^c_{AB}) = \varrho^c_{AB} \tag{1.6}$$

where again $\Pi^A(\varrho) \equiv \sum_i P_i^A \varrho P_i^A$ and analogously $\Pi^B(\varrho) \equiv \sum_j Q_j^B \varrho Q_j^B$. As a consequence $\mathcal{I}(A:B) = \mathcal{I}(\Pi^A(\varrho_{AB})) = \mathcal{I}(\Pi^B(\varrho_{AB}))$. If a state is not classical,

then there is no pair of local measurements leaving the state unchanged. Here we can distinguish two cases. The first case is that of states that are "classical" in one of the two parties. States in the form

$$\varrho^{cq}_{AB} = \sum_i |e_i\rangle_A\langle e_i| \otimes \varrho_{B|i} \qquad \text{or} \qquad \varrho^{qc}_{AB} = \sum_j \varrho_{A|j} \otimes |f_j\rangle_B\langle f_j| \tag{1.7}$$

are called *classical-quantum* ($CQ$) or *quantum-classical* ($QC$) respectively. Such states are "classical" in one of the parties ($B$ or $A$ respectively), meaning that there exist a local measurement on that party leaving the states and correlations invariant. It is sufficient to consider $P$ and $Q$ defined above and get

$$\Pi^A(\varrho^{cq}_{AB}) = \varrho^{cq}_{AB} \qquad , \qquad \Pi^B(\varrho^{qc}_{AB}) = \varrho^{cq}_{AB} \tag{1.8}$$

The second case us that of states that are neither $CQ$ nor $QC$ (nor, *a fortiori*, $CC$) and hence are disturbed by any possible local measurement both on $A$ and on $B$. Such a disturbance always leads to a decrease in total correlations, as measured by the mutual information. Consider a general $\varrho_{AB}$ and a (projective) measurement on party $A$, $P^A_i = |e_i\rangle_A\langle e_i|$. We get

$$\varrho'_{AB} = \Pi^A(\varrho_{AB}) = \sum_i |e_i\rangle_A\langle e_i| \otimes \langle e_i|\varrho_{AB}|e_i\rangle \tag{1.9}$$

Let $\mathcal{I}(A:B)$ be the mutual information before the measurement, and $I'(A:B)_{\Pi^A}$ the mutual information after the measurement. We always have

$$\mathcal{I}'(A:B)_{\Pi^A} \leq \mathcal{I}(A:B) \tag{1.10}$$

with equality if and only if $\varrho^{AB}$ is $CQ$:

$$\mathcal{I}'(A:B)_{\Pi^A} = \mathcal{I}(A:B) \;\Leftrightarrow\; \varrho_{AB} = \Pi^A(\varrho_{AB}) \;\Leftrightarrow\; \varrho_{AB} = \sum_i |e_i\rangle_A\langle e_i| \otimes \varrho_{B|i} \tag{1.11}$$

The proof is postponed to the end of this section. The same results obviously hold true if a measurement ($\Pi^B$) is performed on party $B$.

## 1.3 Introducing quantum discord

### 1.3.1 The definition of quantum discord

**Excess correlations**

The minimal amount of excess correlations that are unavoidably lost in the process of local measurement defines the *quantum discord*. If the measured subsystem is $A$, the quantum discord $D(B|A)$ is defined as

$$D(B|A) \equiv \min_{\Pi^A}(\mathcal{I}(A:B) - \mathcal{I}'(A:B)_{\Pi^A}) = \mathcal{I}(\varrho) - \max_{\Pi^A}\mathcal{I}'(A:B)_{\Pi^A} \tag{1.12}$$

If the measured subsystem is $B$, the quantum discord $D(A|B)$ is defined as

$$D(A|B) \equiv \min_{\Pi^B}(\mathcal{I}(\varrho) - \mathcal{I}'(A:B)_{\Pi^B} = \mathcal{I}(\varrho) - \max_{\Pi^B}\mathcal{I}'(A:B)_{Q^B} \tag{1.13}$$

States that are not CC have a non-vanishing value of either $D(B|A)$ or $D(A|B)$ and they are termed *discordant* with respect to measurements on $A$ or $B$ respectively. It has been proven [35] that discordant states are dense in the set of all mixed states, which *a fortiori* implies that almost all states are discordant Notice that "almost all" refers to a mathematical framework where all states are granted equal *a priori* probability, in the same sense that almost all pure states are entangled. In reality, decoherence is ubiquitous and hence it is nontrivial to create states with a high amount of discord (or entanglement) in the lab (i.e., in the lab probabilities are biased in favor of classical states).
It is in general very hard to explicitly perform the maximization required by the above definition. So far, analytic solutions have been obtained only for finite-dimensional $2 \otimes 2$ [52, 53, 54, 55] and $2 \otimes d$ [56, 57, 58] systems, as well as two Gaussian modes in the continuous variable setting [59, 60].

**Quantum generalizations of the mutual information**

We have just introduced discord as the difference in the total correlations before and after a local measurement. The name *discord*, though, stems from a different interpretation of the same quantity which was also originally given by Zurek: the difference, or failure to agree, of two quantum generalizations of the mutual information. Let $p_{AB}$ be the joint probability distribution of random variables $A$ and $B$, and $p_A, p_B$ the marginal distributions of $A$ and $B$. Classically, the conditional entropy as of $A$ given $B$ is defined as

$$h(p_A|p_B) \equiv h(p_{AB}) - h(p_B) \tag{1.14}$$

where $h$ is the Shannon entropy (Eq. 1.88). The conditional entropy measures the residual uncertainty on variable $A$ once $B$ is known. The classical mutual information $I(A:B) = h(p_A) + h(p_B) - h(p_{AB})$ can thus be rewritten as

$$I(A:B) = h(p_A) - h(p_A|p_B) \tag{1.15}$$

Zurek noticed that we obtain two different quantities when we try to define a quantum mutual information by generalizing Eqs. (1.87) or (1.15). Starting from (1.87) and following the conventional prescription of replacing probability distributions with density matrices and Shannon entropies with von Neumann entropies, we just obtain the standard definition of quantum mutual information, $\mathcal{I}(\varrho_{AB}) = S(\varrho_A) + S(\varrho_A) - S(\varrho_{AB})$. It is less straightforward to "quantize" Eq. (1.15). Indeed, if we start from Eq. (1.14) and try to define a quantum conditional entropy as

$$S(A|B) \equiv S(\varrho_{AB}) - S(\varrho_B)$$

we obtain a quantity that is unsuitable as a quantum generalization of the conditional entropy. In particular, $S(\varrho_{AB}) - S(\varrho_B)$ can be negative. In fact, its opposite

$$I(A\rangle B) \equiv S(\varrho_B) - S(\varrho_{AB}) \tag{1.16}$$

is a well-known quantity in quantum information theory, called *coherent information*. When $A$ is a purification of $B$ and $B$ is sent across a noisy channel, $I(A\rangle B)$ measures the amount of quantum information that can be reliably transmitted across the channel [116, 117]. Unless $S(A|B) < 0$, no information can be transmitted. More recently, another informational meaning of $S(A|B)$ has been found. It measures the amount of shared entanglement needed to accomplish a protocol of state merging [119] (more in § 1.3.5). When $S(A|B) < 0$, the protocol can be carried over with no entanglement cost and additional gain of $I(A\rangle B)$ units of shared entanglement. Also an interesting thermodynamical meaning of $S(A|B)$ has been found in [131]) as the amount of work needed by an observer $B$ to erase $A$. When $(S(A|B) < 0$, erasure can be effected with a net work gain.
To sum up, $S(A|B)$ is a important and meaningful quantity, that, however, cannot be interpreted as a conditional entropy. Conceptually, conditional entropy should assess the uncertainty about system $A$ once we have information about system $B$. A satisfactory quantum definition can be obtained by adopting an operational approach and recognizing that information about $B$ must be acquired through a physical process, a local measurement process on $B$. Then we consider a measurement $\Pi^B$ on $B$. When outcome $i$ is obtained, the state of $A$ is projected onto

$$\varrho_{A|i} = \frac{1}{p_i}\mathrm{Tr}_B[Q_i^B \varrho_{AB} Q_i^B] \tag{1.17}$$

with probability $p_i = \mathrm{Tr}_{AB}[Q_i^B \varrho_{AB} Q_i^B]$. Therefore, the average uncertainty about $A$, one we have measured $B$, is given by

$$S(A|\Pi^B) = \sum_i p_i S(\varrho_{A|i}) \tag{1.18}$$

that we may consider as a measurement-dependent conditional entropy. We always have $S(A|\Pi^B) \geq 0$. To remove the dependence on the measurement, one can consider the optimal local measurement on $B$ allowing for the maximal reduction of uncertainty on the state of $A$. We thus define $S(A|B) = \min_{\Pi^B} S(A|\Pi^B)$. Now, a quantum generalization of Eq. (1.15) is achieved as

$$\mathcal{J}(A|B) \equiv S(\varrho_A) - \min_{\Pi^B} S(A|\Pi^B) \tag{1.19}$$

$\mathcal{J}(A|B)$ measures the amount of correlations that can be extracted by a local measurement, i.e., the amount of information about $A$ that we can extract via a measurement on $B$. The optimal measurement is the measurement that allows for optimal extraction of information. In general, $\mathcal{I}$ and $\mathcal{J}$ have different magnitudes. In particular, $\mathcal{J}(A|B) \leq \mathcal{I}(A:B)$. In fact, one can easily prove (the proof is postponed to the end of this section) that

$$\mathcal{J}(A|B) = \max_{\Pi^B} \mathcal{I}'(A:B)_{\Pi^B} \tag{1.20}$$

i.e., $\mathcal{J}$ corresponds to the (maximum) mutual information after the local measurement on $B$. Therefore the quantum discord $D(A|B)$ can be alternatively defined as the difference between $\mathcal{I}$ and $\mathcal{J}$,

$$D(A|B) \equiv \mathcal{I}(A:B) - \mathcal{J}(A|B) = S(\varrho_B) - S(\varrho_{AB}) + \min_{\Pi^B} S(A|\Pi^B) \tag{1.21}$$

Analogously, the quantum discord $D(B|A)$ can be defined by just swapping the roles of the two subsystems, hence by considering a measurement $P^A$ on system $A$:

$$D(B|A) \equiv \mathcal{I}(A:B) - \mathcal{J}(B|A) = S(\varrho_A) - S(\varrho_{AB}) + \min_{\Pi^A} S(B|\Pi^A) \tag{1.22}$$

**The pure state case**

A very simple case is that of pure states. In the Schmidt form (see § 1.5.3) we have $|\psi_{AB}\rangle = \sum_i \lambda_i |e_i\rangle_A |f_i\rangle_B$. Upon locally measuring $A$ in the Schmidt basis $P_i^A = |e_i\rangle\langle e_i|$ or $B$ in the Schmidt basis $Q_j^B = |f_j\rangle\langle f_j|$), we get

$$S(B|\Pi^A) = 0, \qquad S(A|\Pi^B) = 0 \tag{1.23}$$

Thus we simply obtain

$$\mathcal{J}(B|A) = S(\varrho_A) = S(\varrho_B), \qquad \mathcal{J}(A|B) = S(\varrho_A) = S(\varrho_B) \tag{1.24}$$

The discord is simply evaluated as

$$D(A|B) = D(B|A) = S(\varrho_A) = S(\varrho_B) \tag{1.25}$$

Then for pure states the discord is symmetric and it coincides with the entanglement entropy.

**Asymmetry of discord**

In general, the discord is non-symmetric under the exchange of the measured parties, i.e. $D(A|B) \neq D(B|A)$. Since $\mathcal{I}(A:B) = S(\varrho_{AB}||\varrho_A \otimes \varrho_B)$, we can write

$$D(B|A) = \min_{\Pi^A} \Big( S\big(\varrho_{AB}||\varrho_A \otimes \varrho_B\big) - S\big(\Pi^A(\varrho_{AB})||\Pi^A(\varrho_A) \otimes \varrho_B\big) \Big)$$
$$D(A|B) = \min_{\Pi^B} \Big( S\big(\varrho_{AB}||\varrho_A \otimes \varrho_B\big) - S\big(\Pi^B(\varrho_{AB})||\varrho_A \otimes \Pi^B(\varrho_B)\big) \Big)$$

In the special case in which the parties are symmetric, $\varrho_A = \varrho_B$, the discord and the classical correlations are symmetric too and we can write

$$D(A:B) \equiv D(A|B) = D(B|A), \qquad \mathcal{J}(A:B) \equiv \mathcal{J}(A|B) = \mathcal{J}(B|A) \tag{1.26}$$

In the general case, a symmetric version of discord can be defined by taking measurements on both sides $A$ and $B$ and looking at the mutual information before and after the paired measurements:

$$D(A:B) = \min_{\Pi^A,\Pi^B} \big(\mathcal{I}(A:B) - \mathcal{I}'(A:B)_{\Pi^A,\Pi^B}\big) = \tag{1.27}$$
$$\min_{\Pi^A,\Pi^B} \Big( S\big(\varrho_{AB}||\varrho_A \otimes \varrho_B\big) - S\big(\Pi^A \otimes \Pi^B(\varrho_{AB})||\Pi^A(\varrho_A) \otimes \Pi^B(\varrho_B)\big) \Big)$$

This equation can be also rearranged as

$$D(\varrho_{AB}) = \min_{\Pi^A,\Pi^B} \Big( S\big(\varrho_{AB}||\Pi_{\Pi^A \otimes \Pi^B}(\varrho_{AB})\big) \tag{1.28}$$
$$- S(\varrho_A||\Pi^A(\varrho_A)) - S\big(\varrho_B||\Pi^B(\varrho_B)\big) \Big)$$

### Proofs

Upon introducing a third party $C$ [47], originally in the state $|0\rangle$, the projective measurement on $A$ can be realized as a joint $AC$ unitary rotation $U|e_i\rangle_A|0\rangle_C = |e_i\rangle_A|g_i\rangle_C$ such that

$$\varrho'_{ABC} = \sum_{jk} |e_j\rangle_A\langle e_k| \otimes \langle e_j|\varrho_{AB}|e_k\rangle \otimes |g_j\rangle_C\langle g_k| \tag{1.29}$$

and we can obtain $\varrho'_{AB}$ as a partial trace over $C$, $\varrho'_{AB} = \mathrm{Tr}_C[\varrho'_{ABC}]$. Upon taking the partial trace of $\varrho'_{ABC}$ over $B$ we get:

$$\varrho'_{AC} = \sum_{jk} \langle e_j|\varrho_A|e_k\rangle \; |e_j\rangle_A\langle e_k| \otimes |g_j\rangle_C\langle g_k| \tag{1.30}$$

We have the following relations:

$$S(\varrho'_{ABC}) = S(\varrho_{AB}) \tag{1.31}$$
$$S(\varrho'_{AC}) = S(\varrho_A) \tag{1.32}$$
$$S(\varrho'_B) = S(\varrho_B) \tag{1.33}$$

To prove (1.31), expand $\varrho_{AB}$ in its eigenbasis $\varrho_{AB} = \sum_m \lambda_m |v_m\rangle_{AB}\langle v_m|$. Then

$$\begin{aligned}\varrho'_{ABC} &= \sum_{jkm} \lambda_m |e_j\rangle_A\langle e_k| \otimes \langle e_j|v_m\rangle\langle v_m|e_j\rangle \otimes |g_j\rangle_C\langle g_k| \\ &= \sum_m \lambda_m |u_m\rangle_{ABC}\langle u_m|,\end{aligned}$$

where we defined the orthogonal vectors $|u_m\rangle_{ABC} = \sum_j |e_j\rangle_A \otimes \langle e_j|v_m\rangle_B \otimes |g_j\rangle_C$. To prove (1.32), expand $\varrho_A$ in its eigenbasis $\varrho_A = \sum_n \mu_n |w_n\rangle_A\langle w_n|$. Then

$$\begin{aligned}\varrho'_{AC} &= \sum_{jkn} \mu_n \langle e_j|w_n\rangle\langle w_n|e_k\rangle \; |e_j\rangle_A\langle e_k| \otimes |g_j\rangle_C\langle g_k| \\ &= \sum_n \lambda_n |z_n\rangle_{AC}\langle z_n|,\end{aligned}$$

where we defined the orthogonal vectors $|z_n\rangle_{AC} = \sum_j \langle e_j|w_n\rangle \; |e_j\rangle_A \otimes |g_j\rangle_C$. To prove (1.33), just notice that $\varrho'_B = \varrho_B$ (a local measurement on $A$ cannot alter the reduced state on $B$). Finally, recall that the strong subadditivity of entropy [120] implies

$$S(\varrho'_{ABC}) + S(\varrho'_A) \leq S(\varrho'_{AC}) + S(\varrho'_{AB}) \tag{1.34}$$

Hence, by using all above relations we conclude that $\mathcal{I}(\varrho_{AB}) \leq \mathcal{I}(\varrho'_{AB})$.

$$\begin{aligned}&\mathcal{I}(\varrho_{AB}) \equiv S(\varrho'_B) + S(\varrho'_A) - S(\varrho'_{AB}) = \\ &S(\varrho_B) + S(\varrho'_A) - S(\varrho'_{AB}) \leq S(\varrho_B) + S(\varrho'_A C) - S(\varrho'_{ABC}) = \\ &S(\varrho_B) + S(\varrho_A) - S(\varrho_{AB}) \equiv \mathcal{I}(\varrho'_{AB})\end{aligned}$$

In the second line we have used (1.33) and (1.34), in the third line we have used (1.32) and (1.31).
Let us now inquire when the above inequality is saturated, i.e., when $\mathcal{I}(\varrho_{AB}) = \mathcal{I}(\varrho'_{AB})$ holds. Clearly, the inequality is saturated only if the state $\varrho'_{ABC}$ introduced above saturates the strong

subadditivity inequality. Now, it is known from Refs. [121] that a necessary and sufficient condition for saturation is that there exist a decomposition of $\mathcal{H}_A$ as

$$\mathcal{H}_A = \bigoplus_\alpha \mathcal{H}_{\alpha L} \otimes \mathcal{H}_{\alpha R}$$

such that $\varrho'_{ABC}$ is in the form

$$\varrho'_{ABC} = \sum_\alpha \lambda_\alpha \varrho_{\alpha LB} \otimes \varrho_{\alpha RC} \tag{1.35}$$

where $\lambda_\alpha$ is a probability distribution . Since $\varrho'_{ABC}$ is invariant under exchange of $A$ and $C$, we must also have a decomposition $\mathcal{H}_C = \bigoplus_\alpha \mathcal{H}_{\alpha L} \otimes \mathcal{H}_{\alpha R}$ such that

$$\varrho'_{ABC} = \sum_\alpha \mu_\alpha \varrho_{B\alpha L} \otimes \varrho_{A\alpha R} \tag{1.36}$$

where $\mu_\alpha$ is a probability distribution. If both (1.35) and (1.36) hold, we must have:

$$\varrho'_{ABC} = \sum_\alpha \lambda_\alpha \varrho_{B|\alpha} \otimes \varrho_{AC|\alpha} \tag{1.37}$$

i.e. the state is separable between $AC$ and $B$. Moreover, because of the orthogonality of the blocks $\alpha$ we must have $\varrho_{AC|\alpha} = \Pi_\alpha \varrho_{AC|\alpha} \Pi_\alpha$ where

$$\Pi_\alpha = \sum_l |e_{\alpha l}\rangle_A\langle e_{\alpha l}| \otimes |g_{\alpha l}\rangle_C\langle g_{\alpha l}|, \tag{1.38}$$

and $\sum_{\alpha l} |e_{\alpha l}\rangle\langle e_{\alpha l}| = \mathbb{I}_A$ (we have relabeled the $|e_j\rangle$ as $|e_{\alpha l}\rangle$ to explicitly distinguish those belonging to different blocks $\alpha$). Therefore,

$$\varrho'_{ABC} = \sum_{\alpha\ lm} \lambda_\alpha \varrho^{lm}_{A|\alpha} |e_{\alpha l}\rangle_A\langle e_{\alpha m}| \otimes \varrho_{B|\alpha} \otimes |g_{\alpha l}\rangle_C\langle g_{\alpha m}| \tag{1.39}$$

Upon tracing out $C$ we obtain

$$\varrho'_{AB} = \sum_{\alpha\ l} \lambda_\alpha \varrho^{ll}_{A|\alpha} |e_{\alpha l}\rangle_A\langle e_{\alpha l}| \otimes \varrho_{B|\alpha} \tag{1.40}$$

Upon undoing the measurement, we get,

$$\begin{aligned} \varrho_{ABC} &= \sum_{\alpha\ lm} \lambda_\alpha \varrho^{lm}_{A|\alpha} |e_{\alpha l}\rangle_A\langle e_{\alpha m}| \otimes \varrho_{B|\alpha} \otimes |0\rangle_C\langle 0| = \\ &= \sum_\alpha \lambda_\alpha \varrho_{A|\alpha} \otimes \varrho_{B|\alpha} \otimes |0\rangle_C\langle 0| \end{aligned} \tag{1.41}$$

hence, by tracing out $C$, we obtain

$$\varrho_{AB} = \sum_\alpha \lambda_\alpha \varrho_{A|\alpha} \otimes \varrho_{B|\alpha} \tag{1.42}$$

We can diagonalize $\varrho_{B|\alpha}$ as

$$\varrho_{A|\alpha} = \sum_l \nu_{\alpha l} |u_{\alpha l}\rangle_A\langle u_{\alpha l}| \tag{1.43}$$

where for any fixed $\alpha$ the $|u_{\alpha l}\rangle_A$ are linear combinations of the $|e_{\alpha l}\rangle_A$, and get

$$\varrho_{AB} = \sum_{\alpha\, l} \lambda_\alpha \nu_{\alpha l} |u_{\alpha l}\rangle_A \langle u_{\alpha l}| \otimes \varrho_{B|\alpha} \tag{1.44}$$

By just relabeling, we finally get:

$$\varrho_{AB} = \sum_j p_j |u_j\rangle_A \langle u_j| \otimes \varrho_{B|j} \tag{1.45}$$

Thus $\varrho_{AB}$ is a $QC$ state. The $\varrho_{B|j}$ are equal for all $j$ corresponding to the same block $\alpha$. If some block $\alpha$ is more than one-dimensional, then any measurement in the subspace identified by $\alpha$ attains zero discord. More in general, any measurement $\Pi = \{P_j\}$ whose projectors commute with the block structure, $[P_j, \Pi_\alpha], \forall j, \alpha$ attains zero discord.

### 1.3.2 Classical correlations

The quantum discord $D(A|B)$ ($D(B|A)$) has been defined as the amount of excess correlations in $\mathcal{I}(A:B)$ that are unavoidably lost if a local measurement is performed on $B$ ($A$). The correlations that are stable under repeated measurements are given by $\mathcal{J}(A|B)$ ($\mathcal{J}(B|A)$) and they are called *classical correlations*. Such a denomination is justified by several considerations. First, Henderson and Vedral [27] derived formula (1.19) while trying isolate the "classical part" of total correlations in $\mathcal{I}$. In particular, they required that a good measure of classical correlations $\mathcal{J}(A|B)$ satisfy the following properties:

1. $\mathcal{J}(A|B) \geq 0$ and $\mathcal{J}(A|B) = 0$ for product states
2. $\mathcal{J}(A|B)$ is invariant under local unitaries $U_A \otimes U_B$
3. $\mathcal{J}(A|B)$ is non-increasing under local operations
4. $\mathcal{J}(A|B) = E_E(\varrho)$ for pure states

that coincide with those of an entanglement measure (see § 1.5.5), except for point 3. Point 1. is obvious. Point 2. is required because a local change of basis should not affect correlations. Point 3. is natural because classical correlations should not increase under local operations, but may be legitimately increased by classical communication, contrary to an entanglement measure. Point 4. is justified by the observation that total correlations for pure states are given by $I(A:B) = 2E_E(\varrho)$, while the quantum part of correlations should correspond to the entanglement $E_E(\varrho)$: thus classical correlations should amount to the difference.
The classical correlations $\mathcal{J}(A|B)$ represent the maximum amount of correlations that can be distributed among many parties by classical means (LOCC). Assume $\varrho_{AB}$ is a correlated state, and we have $n$ other systems $C_1, \ldots, C_n$, initially uncorrelated with $AB$. If we can use only LOCC among $B, C_1, \ldots, C_n$, then the maximum amount of correlations between $A$ and each of the $B, C_1, \ldots, C_n$ is given by $\mathcal{J}(A|B)$, as proven by Zurek [44]. In the limit $n \to \infty$, even allowing quantum communication among the $B, C_1, \ldots, C_n$ does not change the picture. As a consequence, only if $\varrho_{AB}$ is $QC$ (classical in $B$) can we distribute the entirety of correlations with $A$, measured

by $\mathcal{I}(A:B)$ to additional parties $C_1,\ldots,C_n$. The classical correlations represent the amount of correlations that can be shared among arbitrarily many parties. This result, which pinpoints a limitation on the sharability of correlations, is in agreement with other results. For instance, the no-local-broadcasting theorem [43] states that only $CC$ states can be locally "duplicated" (formally: given a state $\varrho_{AB}$ , there exists a state $\sigma_{AA'BB'}$ with $\mathcal{I}(\sigma_{AB}) = \mathcal{I}(\sigma_{A'B'}) = \mathcal{I}(\varrho_{AB})$, that can be obtained from $\varrho_{AB}$ by means of local operations, if and only if $\varrho_{AB}$ is $CC$).

### 1.3.3 Discord for general POVMs

So far, we have defined quantum discord and classical correlations by only considering projective (von Neumann) measurements. More in general, one can allow for generalized local measurements (POVMs), which is equivalent to allowing the use of local ancillas. POVMs $\Phi$ are described by a set of positive operators $\{E_i\}$ with $\sum_i E_i = \mathbb{I}$. To any POVM we can associate a quantum operation (see § 1.5.4) by choosing Kraus operators $\{\mathcal{A}_i\}$ such that $E_i = \mathcal{A}_i^\dagger \mathcal{A}_i$. Given a density matrix $\varrho$, the probability of measuring result $i$ is $p_i = \mathrm{Tr}[\varrho E_i]$ and the post-measurement state is $\varrho_i = \sum_i \mathcal{A}_i \varrho \mathcal{A}_i^\dagger$. The definition of classical correlations and quantum discord are simply replaced by

$$\mathcal{J}(A|B) = S(\varrho_A) - \min_{\Phi^B} S(A|\Phi^B), \quad D(A|B) = S(\varrho_B) - S(\varrho_{AB}) + \min_{\Phi^B} S(A|\Phi^B)$$

where $\Phi^B = \{E_j^B\}$ is a local POVM on $B$, and analogously for $\mathcal{J}(B|A)$ and $D(B|A)$. Actually, the minimization can be restricted without loss of generality to rank-one POVMs, i.e., POVMs such that all $E_j$ are one-dimensional projectors [65]. Indeed assume that $E_j^B$ can be refined, $E_j = \sum_k E_{jk}^B$. The refined post-measurement reduced states on $A$ are $\varrho_{A|jk} = \frac{1}{p_{jk}} \mathrm{Tr}_B[\varrho_{AB} E_{jk}]$ with $p_{jk} = \mathrm{Tr}[\varrho_{AB} E_{jk}]$. We have

$$\varrho_{A|j} = \frac{1}{p_j} \mathrm{Tr}_B[\varrho_{AB} E_j] = \sum_k \frac{p_{jk}}{p_j} \mathrm{Tr}_B[\varrho_{AB} E_{jk}]/p_{jk} = \sum_k \frac{p_{jk}}{p_j} \varrho^{A|jk} = \sum_k p_{k|j} \varrho_{A|jk}$$

where $p_{k|j} = \frac{p_{jk}}{p_j}$. Then we obtain

$$S(A|\Phi^B) = \sum_j p_j S(\varrho_j^A) = \sum_j p_j S(\sum_k p_{k|j} \varrho_{A|jk})$$

By the concavity of von Neumann entropy, we get

$$S(A|\Phi^B) \geq \sum_{jk} p_j p_{k|j} S(\varrho_{A|jk}) = \sum_{jk} p_{jk} S(\varrho_{A|jk})$$

Thus the refined POVM can only decrease the value of conditional entropy. Since any POVM can be written in terms of its eigendecomposition, the minimum conditional entropy is attained on a rank-1 POVM. Furthermore, $S(A|\Phi^B)$ is concave on the set of POVMs. If $E_j^B = \lambda E_{\alpha,j}^B + (1-\lambda) E_{\beta,j}^B$, we have

$$p_j \varrho_{B|j} = \lambda p_{\alpha,j} \varrho_{B|\alpha,j} + (1-\lambda) p_{\beta,j} \varrho_{B|\beta,j}, \qquad p_j = p_{\alpha,j} + p_{\beta,j}$$

Then by using again the concavity of von Neumann entropy we get

$$S(A|\Phi^B) \geq S(A|\Phi^{B,\alpha}) + S(A|\Phi^{B,\beta})$$

As a consequence, the minimum is attained on extremal points of the convex set of POVMs. In the case of rank-1 POVMs, a necessary and sufficient condition for extremality is that the set of $E_j$ be linearly independent [126].
One may ask whether the minimization over all POVMs leads to a significantly lower value of the conditional entropy. In Ref. [61], it was shown that the difference between the minimum over projective measurements and the minimum over all POVMs is very small (or the order $10^{-3}$), at least for two-qubit states.

### 1.3.4 Measures of discord

Entanglement is regarded as a property of all entangled states, regardless of the specific measure (entanglement monotone) used to quantify it. In full analogy, all discordant states are characterized by a property – having excess quantum correlations that are lost under local measurements, independent of how they are measured. Unfortunately, in the literature this property is simply referred to as *discord*, with a patent abuse of terminology because *discord* also designates a specific measure of nonclassical correlations). Henceforth, we will follow the literature use the word *discord* also. With this proviso, we may say that all discordant states have some discord, that may be assessed via *measures of discord*. Paralleling the definition of entanglement monotones (see § 1.5.5), we may require measures of discord $\mathcal{Q}(A|B)$ to satisfy a minimal set of properties. If only one party ($B$) is measured, a convenient list of properties is given by

1. $\mathcal{Q}(A|B) \geq 0$ and $\mathcal{Q}(A|B) = 0$ for all $CQ$ states
2. $\mathcal{Q}(A|B)$ is invariant under local unitaries $U_A \otimes U_B$
3. $\mathcal{Q}(A|B)$ is non-increasing under local operations on $A$
4. $\mathcal{Q}(A|B) = E_E(\varrho)$ for pure states

If both parties are measured, we ought to replace 1. with $1^{(b)}$: $\mathcal{Q} = 0$ for $CC$ states and 3. with $3^{(b)}$: $\mathcal{Q}$ is non-increasing under local operations.
Among the proposed measures of discord, we have the *relative entropy of discord* [29]

$$D_S(A|B) \equiv \inf_{\varrho_{qc} \in QC} S(\varrho_{AB}||\varrho_{qc}) \tag{1.46}$$

defined as the minimum statistical distance between a state $\varrho$ and a classical state $\varrho_{qc}$. Upon considering the geometric distance induced by the trace norm (instead of an entropic distance) one obtains a widely used measure of discord called *geometric discord* [29]

$$D_G(A|B) \equiv \inf_{\varrho_{qc} \in QC} ||\varrho_{AB} - \varrho_{qc}||_2^2 \tag{1.47}$$

Surprisingly, it was proven in [30] that the same measure of geometric discord can be obtained upon minimization with respect to local (orthogonal) measurements

$$D_G(A|B) = \inf_{\Pi^A} ||\varrho_{AB} - \Pi^A(\varrho_{AB})||_2^2$$

However, the geometric discord does not satisfy 3), as proved in [31], and, hence, is considered by many Authors as a bad measure of quantum correlations.
Another measure of discord is based on the fact, first highlighted in [40], that discordant states are such that any local measurement probing the system necessarily creates entanglement between the system and the external apparatus that realizes the measurement. Thus generic quantum correlations can be *activated* into entanglement [41]. The entanglement created in the local measurement can be measured by the negativity. Upon minimizing the system-apparatus negativity over all possible local measurements one obtains a measure of quantum correlations called *negativity of quantumness* [41, 42].
Before closing this paragraph, let us comment on 3. If the measured party is $B$, often a local operation on $B$ can create discord [46]: for example consider a $2 \otimes 2$ system and an operation $\Lambda^B$ acting as

$$\Lambda^B|0\rangle_B\langle 0| = |0\rangle_B\langle 0|, \qquad \lambda|1\rangle_B\langle 1| = |+\rangle_B\langle +|$$

(as usual, $|+\rangle_B = \frac{1}{\sqrt{2}}(|0\rangle_B + |1\rangle_B)$). This map can be realized by a introducing an ancilla $B_1$ in the state $|0\rangle_{B_1}$, performing a unitary $U_\Lambda$ on $BB_1$ such that

$$U_\Lambda|0\rangle_B|0\rangle_{B_1} = |0\rangle_B|0\rangle_{B_1}, \qquad U_\Lambda|1\rangle_B|0\rangle_{B_1} = |+\rangle_B|1\rangle_{B_1}$$

and finally tracing out the $B_1$. Under $\Lambda$ the $CC$ state

$$\frac{1}{2}(|0\rangle_A\langle 0| \otimes |0\rangle_B\langle 0| + |1\rangle_A\langle 1| \otimes |1\rangle_B\langle 1|) \tag{1.48}$$

is mapped into the state

$$\frac{1}{2}(|0\rangle_A\langle 0| \otimes |0\rangle_B\langle 0| + |1\rangle_A\langle 1| \otimes |+\rangle_B\langle +|) \tag{1.49}$$

that has non-vanishing discord $D(A|B)$ (while $D(B|A) = 0$). It should perhaps not come as a surprise that quantum correlations are created after a (quantum) operation is performed on the system whose classicality is tested. Of course, local operations do not increase the total amount of correlations (in this case, there is a loss of correlations as measured by the quantum mutual information). By correlating $B$ with a local ancilla that is later discarded, some of the $AB$ correlations become inaccessible to local measurements on $B$, so that not all correlations are classical any more. The creation of quantum correlations occurs at the price of a loss of classical correlations (this phenomenon is at the root of quantum data locking [124, 72]). Nevertheless, several Authors consider the increase under local operations as a sign that discord cannot be considered as a true measure of correlations, but only as a measure of the quantumness of the state. Recently, Gessner *et al.* [45] have proposed a different way to define quantum correlations, based on looking at the operator Schmidt rank of the state. Given local bases $\{A_i\}$ and $\{B_j\}$ of Hermitian operators, any state can be written as

$$\varrho_{AB} = \sum_{ij} M_{ij} A_i \otimes B_j \tag{1.50}$$

Via the same reasoning used for the Schmidt decomposition of pure states, we can find rotated bases $\{E_i\}$ and $\{F_j\}$ such that

$$\varrho_{AB} = \sum_{i=1}^{n_s} \lambda_i E_i \otimes F_j \tag{1.51}$$

where $n_s$ is called opersator Schmidt rank. $CC$ states are such that $n_s < \min(d_A, d_B)$. It can be proved that discordant states that can be locally created from $CC$ states also respect $n_s < \min(d_A, d_B)$ and are zero-measure in the set of all dicordant states. A measure of quantum correlations that does not increase under local operations can be obtained by a suitable function of $n_s$.

### 1.3.5 Monogamy of discord and Koashi-Winter relation

It is well known that entanglement cannot be shared among many parties: if two systems are maximally entangled, they cannot be entangled with a third system. This property is called *monogamy* and it is expressed by general inequalities of the type

$$\mathcal{M}(A:B) + \mathcal{M}(A:C) \leq \mathcal{M}(A:BC) \tag{1.52}$$

where $\mathcal{M}$ is an entanglement measure (see § 1.5.5). In general, contrary to entanglement, discord is non-monogamous. This was revealed by a few studies [33, 32, 107], including my work with Paolo Giorda and Arianna Montorsi [107], to be presented in later chapters. By means of a general argument, Streltsov *et al.* [34] later proved that monogamy is a property of strictly entangled correlations. Consider a generic measure of discord $\mathcal{Q}(A|B)$ satisfying properties 1., 2. above and

5. $\mathcal{Q}(A|B)$ is invariant under addition of a local ancilla in a pure state on both sides

which all meaningful measures of discord satisfy. Assume further that $\mathcal{Q}$ is monogamous,

$$\mathcal{Q}(A|B) + \mathcal{Q}(A|C) \leq \mathcal{Q}(A|BC) \tag{1.53}$$

We can prove that $\mathcal{Q}$ must vanish on separable states, and hence, can be seen as a measure of entanglement. Let $\varrho_{AC} = \sum_i p_i |\psi_i\rangle_A\langle\psi_i| \otimes |\phi_i\rangle_C\langle\phi_i|$ be a general separable state. We can extend $\varrho_{AC}$ as

$$\varrho_{ABC} = \sum_i p_i |\psi_i\rangle_A\langle\psi_i| \otimes |i\rangle_B\langle i| \otimes |\phi_i\rangle_C\langle\phi_i|$$

The quantity $\mathcal{Q}(A|BC)$ is equal for $\varrho_{ABC}$ and $\varrho'_{ABC} = \sum_i p_i |\psi_i\rangle_A\langle\psi_i| \otimes |i\rangle_B\langle i| \otimes |0\rangle_C\langle 0|$ because $\varrho_{ABC}$ and $\varrho'_{ABC}$ are related by a local (on $AC$) unitary and we assume 2). Moreover, since by 5. adding ancilla $C$ does not alter $\mathcal{Q}$, we must have $\mathcal{Q}'(A|BC) = \mathcal{Q}'(A|B)$. Hence because of the monogamy relation (1.53) we must have

$$\mathcal{Q}'(A|B) \geq \mathcal{Q}(A|B) + \mathcal{Q}(A|C)$$

But $\mathcal{Q}'(A|B) = \mathcal{Q}(A|B)$, whence we infer $\mathcal{Q}(A|C) = 0$. Since $\varrho_{AC}$ is a general separable state, $\mathcal{Q}$ must vanish on separable states. Even if we discard assumption 5., we can show that $\mathcal{Q}$ must vanish for separable states by making a much weaker assumption:

6. $\mathcal{Q}(A|B)$ remains finite for a fixed subsystem dimension, $\mathcal{Q}(A|B) < f(d_A) < \infty$ ($d_A$ is the subsystem dimension and $f$ a generic function).

Let $\varrho_{AB}$ be a general separable state. It admits a symmetric extension $\varrho_{AB_1\dots B_n}$ such that $\varrho_{AB_i} = \varrho_{AB}, \forall i \in \{1\dots n\}$. Because of 6., $\mathcal{Q}(A|B_1\dots B_n)$ must remain finite for all $n$, including the limit $n \to \infty$. Assuming that $\mathcal{Q}$ is monogamous, the relation

$$\mathcal{Q}(A|B_1\dots B_n) \geq n\mathcal{Q}(A|B),\ \forall n$$

must hold. Thus we must have $D(A|B) = 0$, lest the last inequality be violated for sufficiently large $n$.

Although monogamy, Eq. (1.53) does not generally hold for measures of quantum discord, it is possible to find "hybrid" monogamy relations involving a measure of discord and other information-theoretical measures. The most well-known is the Koashi-Winter relation [39] that involves the quantum discord and the entanglement of formation for different partial traces of a tripartite state $\varrho_{ABC}$. The relation can be expressed as

$$E_F(\varrho_{AB}) \leq D(A|C) + S(A|C) \tag{1.54}$$

where $D(A|C)$ is evaluated with respect to all POVM measurements on $C$. Since

$$D(A|C) + S(A|C) = \mathcal{I}(A:C) - \mathcal{J}(A|C) + S(\varrho_{AC}) - S(\varrho_C) = S(\varrho_A) - \mathcal{J}(A|C)$$

Eq. (1.54) can be seen as a monogamy relation involving $E_F(\varrho_{AB})$ and the classical correlations $\mathcal{J}(A|C)$,

$$E_F(\varrho_{AB}) + \mathcal{J}(A|C) \leq S(\varrho_A) \tag{1.55}$$

If the $ABC$ state is a pure tripartite state $|\psi\rangle_{ABC}$, the above relations hold with equality,

$$E_F(\varrho_{AB}) = D(A|C) + S(A|C), \qquad E_F(\varrho_{AB}) + \mathcal{J}(A|C) = S(\varrho_A) \tag{1.56}$$

Let us prove (1.56). By using $\mathcal{J}(A|C) = S(\varrho_A) - \min_{\Phi^C} S(A|C)_{\Phi^C}$, we have to prove

$$E_F(\varrho_{AB}) = \min_{\Phi^C} S(A|\Phi^C) \tag{1.57}$$

Let us consider an ensemble $p_i, |\phi_i\rangle_{AB}$ for $\varrho_{AB}$ (i.e., $\varrho_{AB} = \sum_i p_i |\phi_i\rangle_{AB}\langle\phi_i|$) achieving the minimum of the entanglement of formation,

$$E_F(\varrho_{AB}) = \sum_i p_i S\big(\mathrm{Tr}_B[|\phi_i\rangle_{AB}\langle\phi_i|]\big)$$

There must exist a POVM $\Psi^C = \{E_i^C\}$ on $C$ such that

$$\mathrm{Tr}_C[E_i^C|\psi_{ABC}\rangle\langle\psi_{ABC}|] = p_i|\phi_i\rangle_{AB}\langle\phi_i|$$

(consider e.g. $E_i = |\psi_i\rangle_C\langle\psi_i|$ where $\sqrt{p_i}|\psi_i\rangle_C = {}_{AB}\langle\phi_i|\psi\rangle_{ABC}$). If we neglect system $B$ and apply $\Psi^C$ on $\varrho_{AC}$ we get outcome $i$ with probability $p_i$, leaving $A$ in the conditional state $\varrho_{A|i} = Tr_B[|\phi_i\rangle_{AB}\langle\phi_i|]$. We have

$$E_F(\varrho_{AC}) = \sum_i p_i S(Tr_B[|\phi_i\rangle_{AB}\langle\phi_i|]) = S(A|\Psi^C) \leq \min_{\Phi^C} S(A|\Phi^C) \tag{1.58}$$

Conversely, consider a POVM $\Psi^C = \{E_i^C\}$ achieving the minimum of $S(A|\Phi^C)$. From the above discussion, we can take $\Psi^C$ to be a rank-one POVM. Let us apply $\Psi^C$ to $|\psi_{ABC}\rangle\langle\psi_{ABC}|$. Since $\Psi^C$ is rank-one, we obtain $Tr_C[E_i^C|\psi_{ABC}\rangle\langle\psi_{ABC}|] = p_i|\phi_i\rangle_{AB}\langle\phi_i|$. Hence we obtain an ensemble $\{p_i, |\phi_i\rangle_{AC}\}$ for $\varrho_{AB}$. We must have

$$S(A|\Psi^C) = \sum_i p_i S(Tr_B[|\phi_i\rangle_{AB}\langle\phi_i|]) \leq \min_{\mathcal{E}} \sum_i p_i E_E(|\psi_i\rangle_{AB}) = E_F(\varrho_{AB}) \tag{1.59}$$

From (1.58) and (1.59) we get the desired result, (1.57). If $\varrho_{ABC}$ is not pure, we can always purify it with $\varrho_{ABC} = \mathrm{Tr}_D[|\psi_{ABCD}\rangle\langle\psi_{ABCD}|]$. Upon regarding systems $C$ and $D$ as a single system $C'$, we get

$$E_F(\varrho_{AB}) = \min_{\Phi^{C'}} S(A|\Phi^{C'})$$

Since $\min_{\Phi^{C'}} S(A|\Phi^{C'}) \leq \min_{\Phi^C} S(A|\Phi^C)$, we get

$$E_F(\varrho_{AB}) \leq \min_{\Phi^C} S(A|\Phi^C)$$

hence retrieving (1.55).

Eq. (1.56) can be also used to obtain an operational interpretation of discord as the total entanglement cost in the quantum state merging protocol [48]. The latter is a scheme where two parties $A$ and $B$ are required to swap correlations with a third system $C$ via LOCC. More in detail, starting from a pure state $|\psi_{ABC}\rangle$, the goal is to create a state $|\psi_{B'BC}\rangle$, where $B'$ is a local ancilla on $B$'s side. In general, LOCC on $A$ and $B$ are insufficient to perform the task, and some prior shared entanglement entanglement (in terms of the asymptotic number of singlets) is given by $S(A|B)$. If $S(A|B) \leq 0$, not only does no shared entanglement have to be spent, but the protocol can be carried over obtaining in return an additional amount $-S(A|B)$ of shared entanglement. At the end of the protocol, the initial entanglement between $A$ and $B$ present in $|\psi_{ABC}\rangle$ is completely lost. If we measure such entanglement with the entanglement of formation $E_F(A:B)$, then the total loss of $AB$ entanglement in the state merging protocol is

$$E_F(A:B) - I(A\rangle B) = D(A|C) \tag{1.60}$$

where equality comes from Eq. (1.56). Thus the discord $D(A|C)$ of a state $\varrho_{AC}$ acquires an operational interpretation as the total entanglement cost of performing state merging between $A$ and a third party $B$ holding the remainder of a purification $|\psi_{ABC}\rangle$ of $\varrho_{AC}$.

We mention for completeness that a different interpretation of discord within a noisy version of the state merging protocol has been given in [50]. We consider state merging between $A$ and $B$ where $A$ is subject to a generic decoherence process, modeled as a quantum operation $\Phi^A$ acting on $A$. $\Phi^A$ can be effectively realized by coupling $A$ to an external ancilla $C$ in some pure state $|0\rangle$ through some unitary $V$ and then tracing out $C$. After action of $\Phi^C$, it can be readily computed that

$$S'(A|B) \equiv S(\varrho'_{AB}) - S(\varrho'_B) = S(B|\Phi^A)$$

hence the additional entanglement cost due to decoherence on $A$ is given by

$$S'(A|B) - S(A|B) = S(\varrho_A) - S(\varrho_{AB}) + S(B|\Phi^A) \tag{1.61}$$

The minimum additional cost over all possible decoherence processes is just the discord $S(\varrho_A) - S(\varrho_{AB} + \min_{\Phi^A} S(B|\Phi^A) \equiv D(B|A)$. Since several quantum communication protocols (including teleportation and dense coding) can be derived from the state merging protocol, discord also measures the additional entanglement cost to perform such protocols in the presence of noise [82].

### 1.3.6 Multipartite setting

To conclude this section, we analyze how the previous definitions can be extended to a multipartite setting. A state of an $r$-partite system can be said to be classical in $s \leq r$ parties identified by $\mathcal{C} \subseteq \{1, \ldots, r\}$ if it has the form

$$\varrho_{1\ldots r} = \sum_{j_1 \ldots j_s \in \mathcal{C}} \sum_{j_{s+1} \ldots j_r \in \bar{\mathcal{C}}} p_{j_1 \ldots j_r} |e_{j_1}\rangle_1\langle e_{j_1}| \otimes \cdots \otimes |e_{j_s}\rangle_r\langle e_{j_s}| \otimes \varrho_{j_{s+1}} \otimes \cdots \otimes \varrho_{j_r} \tag{1.62}$$

In this case, there is an $s$-tuple of local measurements on subsystems $\mathcal{C}$ leaving the state (and correlations) unchanged. Such local measurements can be specified $P^\ell_{j_\ell} = |e_{j_\ell}\rangle_\ell\langle e_{j_\ell}|$ with $\ell = 1, \ldots, s$. A state is classical in all parties if it is in the form

$$\varrho_{1\ldots r} = \sum_{j_1 \ldots j_r} p_{j_1 \ldots j_r} |e_{j_1}\rangle_1\langle e_{j_1}| \otimes \cdots \otimes |e_{j_r}\rangle_r\langle e_{j_r}| \tag{1.63}$$

i.e., diagonal in a product eigenbasis $\{|e_{j_\ell}\rangle_\ell\}$ with $\ell = 1, \ldots, r$.
A multipartite version of discord can thus be obtained upon considering the $r$-party state $\varrho_{1\ldots r}$) and the multipartite extension of the mutual information,

$$\mathcal{I}(1 : \cdots : r) = S(\varrho_{1\ldots r} || \varrho_1 \otimes \cdots \otimes \varrho_r) \tag{1.64}$$

which in classical information theory is called "total information" and can be expressed as $I(1 : \cdots : r) = H(1) + \cdots + H(r) - H(1 \ldots r)$. Upon extending equation (1.28) to $r$ parties undergoing local measurements $\Pi^1 \ldots \Pi^r$, Rulli and Sarandy [36] define a symmetrized multipartite discord as

$$\begin{aligned} D(1 : \cdots : r) = \min_{\Pi^1 \ldots \Pi^r} \Big( & S\big(\varrho_{1\ldots r} || \Pi^1 \otimes \cdots \otimes \Pi^r(\varrho_{1\ldots r})\big) \\ & - S\big(\varrho_1 || \Pi^1(\varrho_1)\big) - \cdots - S\big(\varrho_r || \Pi^r(\varrho_r)\big) \Big) \end{aligned} \tag{1.65}$$

A different route to define the multipartite discord was taken in [37]. Classically, the total information (like in the $r = 2$ case of the bipartite mutual information) can be re-expressed by using conditional probabilities, $p_{12\ldots r} = p_{1|2\ldots r} p_{2|3\ldots r} \ldots p_r$ and introducing conditional entropies. In the $r = 3$ instance we have

$$I(A : B : C) = H(B) - H(B|A) + H(C) - H(C|AB)$$

This formula can be "quantized" by introducing local measurements $\Pi^A = \{P_i^A\}$ on $A$ and $\Pi^B = \{Q_j^B\}$ on $B$, with post-measurement reduced density matrices $\varrho_{C|ij} = \frac{1}{p_{ij}}\mathrm{Tr}_{AB}[P_i^A Q_j^B \varrho_{ABC} P_i^A Q_j^B]$, $\varrho_{B|i} = \frac{1}{p_i}\mathrm{Tr}_{AC}[P_i^A \varrho_{ABC} P_i^A]$. We can then define and defining a tripartite version of the classical correlations $\mathcal{J}$ as

$$\mathcal{J}(C|A:B) = \max_{\Pi^A,\Pi^B}[S(\varrho_B) - S(B|\Pi^A) + S(\varrho_C) - S(C|\Pi^A,\Pi^B)] \tag{1.66}$$

where $S(B|\Pi^A) = \sum_i p_i S(\varrho_{B|i})$, $S(C|\Pi^A,\Pi^B) = \sum_i p_{ij} S(\varrho_{C|ij})$. The tripartite discord can then be defined as

$$D(C|A:B) = \mathcal{I}(A:B:C) - \mathcal{J}(C|A:B) \tag{1.67}$$

By following the same procedure, one can define classical correlations and discord for $r > 3$.

## 1.4 Discord in quantum information processing

Discord received little attention until it was suggested that it might be regarded as a *resource* for quantum information processing, not unlike entanglement. In particular, interest in discord boomed when some evidence was given [66] that discord, rather then entanglement, might be the essential type of quantum correlation enabling quantum speedup in a relevant protocol of mixed-state quantum computation, the so-called *power of one qubit* model [141]. On one hand, the question whether some kind of quantum correlation (and which then) can be considered the source of the quantum advantage in the power of one qubit model (and by extension in the complexity class DQC1 where it belongs) has not been fully settled yet. On the other hand, the significant research effort dedicated thenceforth to discord has allowed to highlight a precise role of discord in several quantum information processing tasks that are unrelated to computation. In particular, discord can be quantitatively related to the performance of a variety of protocols that effectively exploit the fact that a part of correlations are hidden to local measurements. These protocols make use of discordant states, where global measurements display advantage in performance over local measurements and classical communication. In what follows we shall briefly discuss the potential role of discord in mixed-state quantum computations, reviewing the power of one qubit model, and then succinctly list a few information processing tasks where discord leads to a performance enhancement.

### 1.4.1 Discord and mixed-state quantum computing

Quantum computation consists in encoding information in a quantum state and subsequently applying some logical operations (for instance, gates in the circuit model, measurements in the measurement-based model). If there is an efficient classical description of both the states and the operations applied, the quantum process can be efficiently simulated by a classical computer. The classical description is efficient if it scales at most polynomially with the amount of qubits, and the classical simulation is

efficient if it has at most polynomial overhead with respect to the quantum computation. In a seminal paper [138], Jozsa proved that a quantum computation can be efficiently simulated if there is a fixed $p$, independent of the total number of qubits $m$, such that the states at all steps in the computation are $p$-*blocked*, meaning that the qubits can be partitioned into $K$ blocks such that

$$\varrho = \varrho_1 \otimes \varrho_2 \otimes \cdots \otimes \varrho_K \tag{1.68}$$

and each block contains at most $p$ qubits. In the case of pure states, $p$-blocking is violated only if $n$-partite entanglement is created during the computation, where $n$ grows without bounds with the input size. Thus, exponential speedup requires the generation of entanglement. This is intuitively appealing, as there is no efficient classical description of entangled quantum states - the information required to specify the state scales exponentially with the amount of qubits. In a following study, Vidal showed that exponential speedup demands that the maximum Schmidt rank among all bipartitions scales exponentially. Otherwise, one has an efficient representation of the state as a matrix product state [16] which allows to efficiently simulate the quantum computation on a classical computer.
In the case of mixed states, the violation of $p$-blocking does not imply entanglement: even fully separable states need not be $p$-blocked. As a consequence, entanglement is not a necessary condition for exponential speedup in mixed-state quantum computation. In fact, a mixed separable state has in general the same capacity for coding information as a general mixed state (note that mixed separable states have a finite volume in the space of density matrices) and correspondingly it may not have an efficient classical description. Accordingly, Jozsa [138] deemed it plausible that separable mixed states may have the same computational power as general mixed states. With the same reasoning used in the pure-state case, Vidal showed that exponential speedup in the mixed-state case requires that the maximum *operator Schmidt rank* over all bipartitions scales exponentially. Otherwise there is an efficient representation of a state in terms of a tree-tensor network, implying that an efficient classical simulation is possible. An exponential scaling of the operator Schmidt rank does not imply entanglement, though, but only the presence of (possibly unentangled or even classical) correlations.
A prominent example of mixed-state quantum computing protocol is the power-of-one-qubit model. Even if it is not computationally universal, it can evaluate the trace of a unitary matrices with an exponential speedup over the best-known classical algorithm (it is thus believed, yet not proven, that it affords an exponential advantage over classical algorithms). This property can be put to use in various problems, including estimating the density of states to the decay of fidelity in chaotic systems. We have a set of $n+1$ qubits, the first (control qubit $C$) initialized in the pseudo-pure state

$$(1-\alpha)\mathbb{I}_C + \alpha|0\rangle_C\langle 0| \tag{1.69}$$

and the remaining ones (target qubits $T$) initialized in the fully mixed state $\mathbb{I}$. Conditioning on the state of $C$, a unitary $U \in SU(2^n)$ is applied to $T$, i.e., the system undergoes a unitary evolution represented by $|0\rangle_C\langle 0| \otimes \mathbb{I}_T + |1\rangle_C\langle 1| \otimes U$. The initial

$CT$ state evolves into

$$\varrho_{CT} = \frac{1}{2^{n+1}}\mathbb{I}_C \otimes \mathbb{I}_T + \frac{\alpha}{2^{n+1}}[|0\rangle_C\langle 0| \otimes U^\dagger + |1\rangle_C\langle 1| \otimes U] = \tag{1.70}$$
$$= \frac{1}{2^{n+1}}(|0\rangle_C\langle 0| \otimes (\mathbb{I}_T + \alpha U^\dagger) + |1\rangle_C\langle 1| \otimes (\mathbb{I}_T + \alpha U)]$$

The final reduced state of $C$ is

$$\varrho_C = \frac{1}{2}\begin{pmatrix} 1 & \frac{\alpha}{2^n}\mathrm{Tr}[U] \\ \frac{\alpha}{2^n}\mathrm{Tr}[U^\dagger] & 1 \end{pmatrix} = \frac{1}{2}\begin{pmatrix} 1 & \alpha\tau \\ \alpha\tau^* & 1 \end{pmatrix} \tag{1.71}$$

where $\tau = \tau_R + i\tau_I \equiv \frac{1}{2^n}\mathrm{Tr}[U]$. This allows to evaluate the trace of $U$ by measuring $\sigma_x$ and $\sigma_y$ on $C$, as

$$\mathrm{Tr}[\sigma_x\varrho_C] = \frac{\alpha}{2}\tau_R, \quad \mathrm{Tr}[\sigma_y\varrho_C] = \frac{\alpha}{2}\tau_I$$

The estimation error depends only on the purity of the control qubit $\alpha$ and the number of trials, but is independent of the size of the problem $n$. It is conjectured that there is no classical algorithm that can efficiently solve this problem. Datta and Vidal [144] showed that the maximum operator Schmidt rank in the model scales exponentially, strengthening this hypothesis. This implies the presence of correlations, but not necessarily entanglement. It is immediate that the control qubit $C$ is always separable from the target qubits $T$. Therefore there can be entanglement only among the $T$ qubits. The negativity $\mathcal{N}$ was used to measure entanglement across any bipartite splitting including $C$. For $\alpha < \frac{1}{2^n}$, $\mathcal{N}$ is bounded by a constant independent of $n$, and hence vanishes for $n \to \infty$. For $\alpha < \frac{1}{2^n}$, $\mathcal{N} = 0$. In summary, only multipartite entanglement between the $T$ qubits is present. The seemingly marginal role of entanglement in the model has led to propose that the speedup may be due to nonzero quantum discord in the model. For a typical unitary $U$, chosen according to the Haar measure, we can evaluate the discord between $T$ and $C$ ($C$ is measured) in the final state [66, 69]:

$$D(T|C) = S(\varrho_C) - S(\varrho_{CT}) + \min_{\Pi^C} S(T|\Pi^C) \tag{1.72}$$

Here I sketch the case $\alpha = 1$. Consider the measurement $P_\phi = \frac{1\pm\sigma_\phi}{2}$ with $\sigma_\phi = \cos\phi\sigma_x + \sin\phi\sigma_y$. The reduced conditional density matrices of $T$ after the measurement are

$$\mathrm{Tr}_C[P_\phi\varrho_{CT}P_\phi] = \frac{1}{p_\pm}\left(\frac{\mathbb{I}_T}{2^n} \pm \frac{e^{i\phi}Re(U) + e^{-i\phi}Im(U)}{2^{n+1}}\right) \tag{1.73}$$

with $p_\pm = 1/2[1 \pm (\cos\phi\tau_R + \sin\phi\tau_I)]$. Their eigenvalues are

$$\lambda_k^\pm = \frac{1}{2^n}\frac{1 \pm \cos(\theta_k - \phi)}{1 \pm (\cos\phi\tau_R + \sin\phi\tau_I)}$$

where we have used the eigendecomposition of $U$, $U = \sum_j e^{i\theta_j}|\theta_j\rangle\langle\theta_j|$. For a typical $U$ and large $n$, the $\theta_j$ are uniformly distributed in $[0, 2\pi]$ and we get $\tau_R, \tau_I \ll 1$, hence

$p_\pm \simeq 1/2,\ \lambda_k^\pm = \frac{1}{2^n}(1 \pm \cos(\theta_k - \phi))$. The results are approximately independent of $\phi$ and we can choose $\phi = 0$. The conditional entropy of $T$ given $C$ is computed as

$$S(T|\Pi_x^C) \simeq -\frac{1}{2^{n+1}} \sum_k (1+c_k)\log((1+c_k)/2^n) + (1-c_k)\log((1-c_k)/2^n)$$

Since $S(\varrho_{CT}) = n$, $S(\varrho_C) = H_2(\frac{1-|\tau|}{2}) \sim 1$ we finally find $D(T|C) \simeq 2 - \log e$. For general $\alpha$, one finds

$$D(T|C) \simeq 2 - H_2(\frac{1-\alpha}{2}) - \log(1+\sqrt{1-\alpha^2}) - (1-\sqrt{1-\alpha^2})\log e \quad (1.74)$$

Thus, for a *typical* unitary $U$ there is non-vanishing discord between $C$ and $T$ for all values of $\alpha$. This supports the hypothesis that quantum discord is involved in the quantum speedup offered by the model. A contrary position was held by Dakić *et al.*, o proved [49] that for unitaries such that $U = e^{i\gamma}U^\dagger$ the quantum discord $D(T|C)$ exactly vanishes. However, Datta and Shaji [47] later noticed that discord among the parties can be created during the computational process when $U$ has to be realized by subsequently applying a series of (one and two-qubit) gates, $U = W_1 \ldots W_n$, suggesting that for all unitaries discord is created during the computational process. The idea that quantum discord must be created if the computation is to offer an exponential speedup is further supported by a completely general argument by Eastin [68]. He devised a general procedure and showed that computations with classical states (states with vanishing discord among all qubits) can be efficiently simulated by a classical computer. Such a result, though strong, only concerns exactly classical state. Therefore it does not suffice to qualify discord as a resource for quantum computation, because it remains to be shown that a minimum amount of discord (actually, minimum scaling) is necessary to achieve exponential speedup.

At the time of this writing, the role of discord in quantum computation is still controversial. Following a penetrating discussion by Jozsa [138], many lean to the opinion that it is meaningless to look for a single "source" of the exponential speedup in quantum computation. In particular, there is no need to associate the speedup to a measure of correlations (entanglement or discord). In principle there are several different ways to classically describe a quantum computational process, depending on how states and operations are represented. For instance, one can represent states as amplitudes (in a given basis) and reproduce classically the quantum evolution with respect to this description. Unless the states are sufficiently entangled, this yields an efficient classical description of the quantum computation, and no exponential speedup is possible. An alternative formalism is the stabilizer formalism [140], where one considers the Pauli group on $n$ qubits and classifies states according to the subgroup elements that leave them invariant. In the stabilizer formalism, one can identify a class $\mathcal{X}$ of states that have a polynomial-sized stabilizer description. In this formalism, computations admit an efficient classical description whenever computations remain in $\mathcal{X}$, regardless of the amount of quantum correlations among qubits. Thus, if $p(\mathcal{X})$ stands for the property of a state that does not have a polynomially sized stabilizer description, then one can say that $p(\mathcal{X})$ is responsible for quantum-computational power.

### 1.4.2 Discord-assisted information processing tasks

Quantum discord has been found to be qualitatively, and in some cases quantitatively related to "quantum enhancements" in several quantum information processing tasks (by "quantitatively" I mean that discord proves a valid figure of merit to measure the quantum advantage of these protocols).
Discord (as a property) is arguably a resource for protocols of remote state preparation [70], whose efficiency can be quantified, at least in some cases, by geometric discord. Discord (as a property) is needed to perform quantum state discrimination of nonorthogonal states [76]. Discord (as a measure) is quantitatively related to the quantum enhancement of different tasks involving the discrimination of local channels: the performance gain of quantum illumination [128, 74], the sensitivity enhancement of quantum metrology schemes [127, 75], and the advantage of global over local measurements in a scheme involving local encoding of information [71]. Discord (as a measure) quantifies the amount of correlations that can be "unlocked" in the phenomenon of locking of classical correlations [72]. Discord (as a property)is necessary to perform quantum key distribution, since $CC$ correlations between the communicating parties can be locally duplicated by an eavesdropper without disturbing the system. Furthermore, discord (as a measure) is an upper bound to security rates in noise-assisted key distribution protocols [73]. Finally, discord (as a property) has a deep thermodynamic meaning [78, 77, 79]. The presence of discord implies that global strategies involving joint coherent operations allow for the extraction of more work then purely local strategies in different settings.
Intuitively, what groups all such cases together is a nonclassical effect where global measurements are insufficient for a better extraction of information than local measurement assisted by classical communication. Discussing each of these cases is outside the scope of this chapter, and I shall just describe a simple example, an instance of a quantum protocol which I consider the most convincing example of a discord-assisted process: quantum locking of classical information.

As we explained above in detail, some correlations are not accessible to local POVMs, as if they were "locked" in the global state. The accessible correlations are measured by the *accessible information*, defined as

$$I_{acc}(A:B) = \max_{\Pi^A,\Pi^B} I'(A:B) \tag{1.75}$$

where $\varrho'_{AB} = \Pi^A \otimes \Pi^B(\varrho_{AB})$. For a $CQ$ state, the accessible information just coincided with the classical correlations $I_{acc}(A:B) = \mathcal{J}(A|B)$. The amount of locked correlations is given by $\mathcal{I}(A:B) - I_{acc}(A:B)$, that coincides with $D(A|B)$ for a $CQ$ state. DiVincenzo *et al.* [124] discovered that the locked correlations can be "unlocked" by allowing a small amount of classical communication between the parties. If sending $n$ bits of classical communication, the parties can increase $\mathcal{I}$ by at most $n$ bits, but they can increase $I_{acc}$ by $n' > n$ bits, unlocking $\Delta = n' - n$ bits of information. This is a purely quantum phenomenon that has no classical analogue. If $A$ and $B$ originally share a $CQ$ state, we have $\Delta = D(A|B)$ as proved by Boixo *et al.* [72]. Let us illustrate this with a simple example.

Party $A$ aims to sent a classical message of length $m$ (a bit string of length $m$ to a receiving party $B$. The message can be encoded in a string of $m$ qubits

$$|a\rangle_A = s_{1A_1} \dots s_{1A_m} \tag{1.76}$$

where $A_1 \dots A_m$ are $A$'s qubits and $s_k = 0, 1$. $A$ can copy the string and send it to $B$ via a quantum channel $\Phi$. If all strings are produced with equal probability, the $AB$ state is

$$\varrho_{AB}^{(0)} = \frac{1}{2^m} \sum_a |a\rangle_A\langle a| \otimes \sigma_a \tag{1.77}$$

where $\sigma_a = \Phi(|a\rangle_B\langle a|)$. The maximal information that $B$ can gain about $A$'s message by making a POVM on his qubits is given by $I_{acc}^{(0)}(A:B) = \mathcal{J}^{(0)}(A|B) \leq m$. Let us consider an ideal channel for which we have $\sigma_a = |a\rangle_B\langle a|$ and hence $I_{acc}^{(0)}(A:B) = \mathcal{J}^{(0)}(A|B) = \mathcal{I}^{(0)}(A:B) = m$, i.e., the message can be perfectly decoded. In order to improve the communication security, $A$ can encrypt the message with a classical key $K$. Before sending $|a\rangle$ to $B$, she applies a unitary $U_k$ on $|a\rangle$ depending on the key. She can choose $U_k$ to be such that $U_k|a\rangle$ are mutually unbiased bases for all $k$. If the key is just one bit, the $AB$ state is

$$\varrho_{AB}^{(1)} = \frac{1}{2^{m+1}} \sum_a \sum_{k=0,1} |a,k\rangle_A\langle a,k| \otimes U_k|a\rangle_B\langle a|U_k^\dagger \tag{1.78}$$

where $U_0 = \mathbb{I}$ and $U_1$ is such that $U_1|a\rangle$ is maximally unbiased with respect to $|a\rangle$. After the encryption, we now have $\mathcal{I}^{(1)}(A:B) = m$, $I_{acc}^{(1)}(A:b) = \mathcal{J}^{(1)}(A|B) = m/2$. Therefore, $m/2$ bits of information are now locked. They can be unlocked by sending only one bit of information. Indeed, if $A$ copies and sends $K$ to $B$, their state becomes

$$\varrho_{AB}^{(2)} = \frac{1}{2^{m+1}} \sum_a \sum_k |a,k\rangle_A\langle a,k| \otimes U_k|a\rangle_B\langle a|U_k^\dagger\, |k\rangle_B\langle k| \tag{1.79}$$

Now $B$ can perfectly decode the message since $\mathcal{I}^{(2)}(A:B) = I_{acc}^{(2)}(A:B) = \mathcal{J}^{(2)}(A|B) = m+1$. Thus by sending only $n = 1$ bits of information, $A$ can effectively increases the accessible correlations of $n' = m/2 + 1$ bits, unlocking $\Delta = m/2$ bits of information. The amount of unlocked correlations is equivalent to the discord of the encrypted state, $D^{(1)}(A|B)$.

## 1.5 Background on quantum correlations

### 1.5.1 Definition of subsystems

The statement that a physical body is moving is incomplete, unless we specify which reference frame we are considering. Analogously, the statement that a quantum state is correlated (e.g., entangled) must be complemented with further information. In order to define and assess correlations a prior definition of how the total system is divided

into two or more subsystems is necessary. This division sets up a "reference frame" for correlations, called *tensor product structure*. Indeed for a quantum system, a division into subsystems is expressed by a tensor factorization of the Hilbert space $\mathcal{H}$ into $r \geq 2$ factors:

$$\mathcal{H} = \mathcal{H}_1 \otimes \mathcal{H}_2 \otimes \cdots \otimes \mathcal{H}_r \tag{1.80}$$

to which a tensor factorization of the observable algebra corresponds,

$$End\Big(\bigotimes_{i=1}^{r} \mathcal{H}_i\Big) \cong \bigotimes_{i=1}^{r} End(\mathcal{H}_i) \tag{1.81}$$

In general a large variety of tensor factorizations are possible for any system [4]. First, one has to specify the dimensions of the subsystems. Assume the Hilbert space has dimension $d$. Then the possible choices of the subsystem dimensions are in one-to-one mapping with the possible ways to factorize $d$,

$$\mathcal{F}_d \equiv \{F \subset \mathbb{N} \,/\, \prod_{m \in F} m = d\} \tag{1.82}$$

Any factorization $F = \{m_1 \leq m_2 \leq \ldots \leq m_{|F|}\} \in \mathcal{F}_d$ of $d$ provides a possible choice of the subsystem dimensions.
Second, given $F$, one has to specify which are the product vectors in $\mathcal{H}$. Choose any orthonormal set of vectors $\{|i\rangle\}, i = 1, \ldots, d$. By using $|F|$ indices $i_j \in \{1, \ldots, m_j\}$ we can relabel vectors as

$$|i\rangle \equiv |i_1 i_2 \ldots i_r\rangle, \tag{1.83}$$

and identify the set $\{|i_1 i_2 \ldots i_r\rangle\}$ as an (orthonormal) set of product vectors:

$$|i_1 i_2 \ldots i_r\rangle \equiv |i_1\rangle \otimes |i_2\rangle \otimes \cdots \otimes |i_r\rangle \tag{1.84}$$

Upon rotating the given set by $U \in \mathcal{U}(d)$, we generally obtain a different set of vectors. However, that are two kinds of unitary operators that leave the set of product states invariant: i) factorized unitaries in the form $U = \bigotimes_{j=1}^{r} U_j$ where each $U_j$ acts only on $\mathcal{H}_j = span\big(\{|i_j\rangle\}\big)$ ii) "exchange" unitaries that permute the tensor factors $\mathcal{H}_1, \ldots, \mathcal{H}_{|F|}$. Thus possible choices of product vectors are parametrized by $U(d)/(U(m_1) \times \cdots \times U(m_r) \times \mathfrak{P})$ where $\mathfrak{P}$ is a discrete permutation group. A choice of $F$, together with a choice of the product vectors, identifies a *tensor product structure* (TPS) on $\mathcal{H}$.
What the meaningful TPS are depends on the context. In many cases, a TPS may naturally reflect the fact that the degrees of freedom (DOF) of the system are naturally split among different physical entities. For instance, if we have two spins (e.g. two atoms, neglecting the orbital DOF), then the four DOF of the joint system can be naturally divided into two pairs, each pertaining to one spin. Correspondingly, we identify a natural TPS in the total Hilbert space $\mathcal{H} \cong \mathbb{C}^4 \cong \mathbb{C}^2 \otimes \mathbb{C}^2$, that also induces a tensor factorization $End(\mathbb{C}^4) \cong End(\mathbb{C}^2) \otimes End(\mathbb{C}^2)$ of the observable algebra. More in general, a partition of the DOF into separated sets may depend on our ability to measure and manipulate the system [5]. If the DOF can be split into $r$ sets that can be

separately, but not jointly addressed, then the actions that we can perform on the system have a factorized form $A_1 \otimes \cdots \otimes A_r$, and correspondingly the Hilbert space has a meaningful tensor factorization as $\mathcal{H}_1 \otimes \cdots \otimes \mathcal{H}_r$ .

### 1.5.2 Correlations and mutual information

Upon fixing a tensor factorization, and hence a definition of subsystems, we are able to define correlations. If $\mathcal{H} = \mathcal{H}_1 \otimes \cdots \otimes \mathcal{H}_r$, a state represented by the density matrix $\varrho$ is uncorrelated whenever it is in the product form:

$$\varrho = \varrho_1 \otimes \cdots \otimes \varrho_r \tag{1.85}$$

else it is *correlated*. For a pure state represented by vector, the above definition reduces to

$$|\psi\rangle = |\psi\rangle_1 \otimes \cdots \otimes |\psi\rangle_r \tag{1.86}$$

Correlation implies that the subsystems are not statistically independent. In classical information theory, a general measure of statistical dependence is the *mutual information*. Let $p_{AB}$ be the joint probability distribution of random variables $A$ and $B$, and $p_A, p_B$ the marginal distributions of $A$ and $B$. The classical mutual information is defined as

$$I(A:B) \equiv h(p_A) + h(p_B) - h(p_{AB}) \tag{1.87}$$

where $h(p)$ is the Shannon entropy

$$h(p) = \sum_i p_i \log p_i \tag{1.88}$$

$I(A:B)$ vanishes only if $A$ and $B$ are independent, $p_{AB} = p_A p_B$. The quantum analogue of this function can be obtained by replacing probability distributions $p$ with density matrices $\varrho$ and Shannon entropies $h(p)$ with von Neumann entropies $S(\varrho)$, where

$$S(\varrho) \equiv -\mathrm{Tr}[\varrho \log \varrho] \tag{1.89}$$

Marginal probability distributions are to be replaced with *reduced states*

$$\varrho_A \equiv \mathrm{Tr}_B[\varrho_{AB}], \qquad \varrho_B \equiv \mathrm{Tr}_B[\varrho_{AB}] \tag{1.90}$$

This prescription has its origin in a classical study by Schumacher [115], where he proved the quantum noiseless coding theorem: just as $H(p)$ represents the number of bits (asymptotically) required to encode a signal represented by $p$, the von Neumann entropy $S(\varrho)$ represents the number of qubits necessary to represent a quantum signal represented by $\varrho$. Starting from (1.87) and applying this prescription, we obtain the *quantum mutual information* [118]:

$$\mathcal{I}(\varrho_{AB}) \equiv S(\varrho_A) + S(\varrho_A) - S(\varrho_{AB}) \tag{1.91}$$

This quantity vanishes if and only if the state is uncorrelated, $\varrho_{AB} = \varrho_A \otimes \varrho_B$. Indeed Eq. (1.91) can be rewritten as

$$\begin{aligned}\mathcal{I}(\varrho_{AB}) &= -\mathrm{Tr}_A[\varrho_A \log \varrho_A] - \mathrm{Tr}_B[\varrho_B \log \varrho_B] + \mathrm{Tr}_{AB}[\varrho_{AB} \log \varrho_{AB}] = \\ &= -\mathrm{Tr}_{AB}[\varrho_{AB} \log \varrho_A] - \mathrm{Tr}_{AB}[\varrho_{AB} \log \varrho_B] + \mathrm{Tr}[\varrho_{AB} \log \varrho_{AB}] = \\ &= \mathrm{Tr}_{AB}[\varrho_{AB} \log \varrho_{AB} - \varrho_{AB} \log(\varrho_A \otimes \varrho_B)] = S(\varrho_{AB}||\varrho_A \otimes \varrho_B)\end{aligned}$$

where $S(\varrho||\sigma) = \mathrm{Tr}[\varrho \log \varrho - \varrho \log \sigma]$ is the quantum relative entropy that measures the "statistical distance" between states $\varrho$ and $\sigma$ (with $S(\varrho||\sigma) = 0$ if and only if $\varrho = \sigma$). Thus $\mathcal{I}$ represents a "statistical distance" between $\varrho_{AB}$ and the fully uncorrelated state $\varrho_A \otimes \varrho_B$. $\mathcal{I}$ can be regarded as a measure of total correlations, since it is equivalent to the amount of local randomness necessary in order t bring the state to an uncorrelated form [28] (this is the most important operational interpretation, but other exist, for instance as the maximal amount of classical information that can be securely exchanged in a one-time pad cryptographic protocol between two parties sharing a state $\varrho_{AB}$ [133]). The fundamental idea behind all notions of *quantum* correlations is some of the correlations accounted for by $\mathcal{I}$ can neither be created nor extracted by local operations on the subsystem – joint quantum operations and/or quantum communication between subsystems is required. The notion of entanglement focuses on the preparation of states, while that of discord focuses on information retrieval by measurements.

### 1.5.3 Entanglement for pure states

Given an arbitrary tensor factorization $\mathcal{H} = \mathcal{H}_1 \otimes \cdots \otimes \mathcal{H}_r$ of the Hilbert space, the general notion of entanglement for pure states is formulated as a straightforward algebraic condition. By definition, a pure state is *separable* if and only if it can be written as a product vector:

$$|\psi\rangle = |\psi_1\rangle_1 \otimes \cdots \otimes |\psi_r\rangle_r \tag{1.92}$$

else it is *entangled*. Thus any correlated pure state is entangled. Entanglement always implies that contrary to the global system, each subsystem cannot be ascribed a state vector but only a density matrix. It has recently been proved in full generality [8] that all entangled pure states are "nonlocal" in that they violate a Bell's inequality, a result referred to as "Gisin's theorem" since Gisen was the first to prove it, albeit for the restricted case of bipartite states of two qubits [7]. If $r = 2$ (bipartition), it is easy to characterize entangled states and even assess the amount of their entanglement. Let us start from an arbitrary bipartite state $|\psi\rangle = \sum_{ij} M_{ij}|i\rangle_A \otimes |j\rangle_B$. The matrix $M$ admits a singular value decomposition $M = U\Lambda V^\dagger$ where $U, V$ are unitaries and $\Lambda = \mathrm{diag}(\lambda_i)$. Upon defining new local orthonormal bases $|e_k\rangle_A = U_{ik}|i\rangle_A$, $|f_k\rangle_B = V_{jk}|j\rangle_B$, we can bring $|\psi\rangle$ in a standard form called *Schmidt form*,

$$|\psi\rangle = \sum_k \lambda_k |e_k\rangle_A \otimes |f_k\rangle_B \tag{1.93}$$

The number $n_s$ of nonzero singular values of $M$ is called *Schmidt rank*. Whenever $n_s > 1$, the state is entangled. The reduced states of the subsystems are $\varrho_A =$

$\sum_k \lambda_k |e_k\rangle_A\langle e_k|$ and $\varrho_B = \sum_k \lambda_k |f_k\rangle_B\langle f_k|$ and whenever $n_s > 1$ they are mixed. The extent to which the reduced states are mixed can be seen as a measure of the degree of entanglement present in the global state $|\psi\rangle$. It can be assessed by the von Neumann entropy of the reduced states, called *entanglement entropy* ($E_E$):

$$E_E(|\psi\rangle) \equiv S(\varrho_A) = S(\varrho_B) = -\sum_{k=1}^{n_s} \lambda_k \log \lambda_k \tag{1.94}$$

The entanglement entropy holds as a universal quantifier of entanglement for pure bipartite states. When $n_s = n = \min(\dim \mathcal{H}_A, \dim \mathcal{H}_B)$ and $\lambda_i = \frac{1}{\sqrt{n}}$ the entanglement entropy reaches its maximum values $S(\varrho_A) = S(\varrho_B) = \log n$ and the states are called *maximally entangled* . For a generic bipartition, almost all states with respect to the uniform measure on the complex $n$-sphere are entangled (i.e., separable states are a set of null measure). For large Hilbert space dimension, almost all pure states are even close to being maximally entangled [9].

### 1.5.4 LOCC and entanglement for mixed states

The definition of entanglement for mixed states cannot be achieved by simply identifying the set of entangled states with the set of correlated states, as in the pure state case, lest entanglement lose its characteristic traits. A defining trait of pure entangled states is that they cannot be prepared by means of a product of local operators $\mathcal{E}^1 \otimes \cdots \otimes \mathcal{E}^r$, but only through a global, non-factorized operator acting on all subsystems jointly (for instance, a unitary operator that couples all subsystems). Consider now a correlated state that is simply a mixture of separable (product) pure states $|\phi_i\rangle$:

$$\varrho = \sum_i p_i |\phi_i\rangle\langle\phi_i|, \qquad |\phi_i\rangle = |\varphi_1\rangle_1 \otimes \cdots \otimes |\varphi_r\rangle_r \tag{1.95}$$

Such a state can be prepared from an uncorrelated state by applying for each $i$ a different set of local operators $\mathcal{E}_i^1 \otimes \cdots \otimes \mathcal{E}_i^r$ with probability $p_i$ – a procedure involving only local operations and classical communication (LOCC, to be precisely described later). In fact, Werner proved [10] that states in the form (1.95) are "local" in the sense that they cannot violate any Bell inequality (and hence admit a local hidden variable model description). For this reason, Werner defined the set of separable states as those states that can be written as mixtures of product states (which also matches the intuitive expectation that a statistical mixture of separable states should be itself separable). Conversely, if a state cannot be written as a mixture of product states it is entangled. This definition of separable and entangled states obviously reduces to the previous one in the pure state case.

This definition of entanglement is fully grounded within the operational framework of local operations and classical communication (LOCC). The LOCC paradigm is meaningful in the "distant lab" scenario [10, 11], where the subsystems are at different locations (widely) separated in space, so that experimenters ad different locations cannot perform joint operations, but only local operations, possibly assisted

by classical communication among them. LOCC are defined as follows (we describe the bipartite case, but the following discussion trivially generalizes to more than two parties). A general *quantum operation* is defined by a trace-preserving, completely positive (TPCP) map $\Lambda$. For any such $\Lambda$, there exists a set of Kraus operators $\{\mathcal{A}_i\}$ such that $\sum_i \mathcal{A}_i^\dagger \mathcal{A}_i = \mathbb{I}$ and $\Lambda(\varrho) = \sum_i \mathcal{A}_i \varrho \mathcal{A}_i^\dagger$. Any operation can be seen as a measurement, followed by a unitary "feedback" [129]. Indeed, by virtue of the polar decomposition we have $\mathcal{A}_i = \mathcal{U}_i \mathcal{P}_i$ where $\mathcal{P}_i$ is positive and $\mathcal{U}_i$ is unitary. We thus obtain $\Lambda(\varrho) = \sum_i U_i \mathcal{P}_i \varrho \mathcal{P}_i U_i^\dagger$. This can be seen as a measurement whereby outcome $i$ is obtained with probability $p_i = \mathrm{Tr}[\mathcal{P}_i \varrho \mathcal{P}_i]$, projecting the state to $\varrho_i = \frac{1}{p_i}\mathcal{P}_i \varrho \mathcal{P}_i$. Depending on the outcome $i$, the state is rotated by $U_i$: $\Lambda(\varrho) = \sum_i p_i U_i \varrho_i U_i^\dagger$. Given a bipartition $\mathcal{H} = \mathcal{H}_A \otimes \mathcal{H}_B$, *separable operations* are such that $\mathcal{A}_i = \mathcal{A}_i^A \otimes \mathcal{A}_i^B$. LOCC form a subset of separable operations in which the Kraus operators $\mathcal{A}_i \otimes \mathcal{B}_i$ are restricted by the requirement that they be generated according to the following procedure. $A$ performs an operation $\Lambda^{(1)}$ with Kraus operators $\{\mathcal{A}_i^{(1)}\}$ and transmits the measurement outcome $i$ to $B$ via a classical communication channel. On the basis of $i$, $B$ chooses and performs operation $\Lambda^{(2,i)}$ with Kraus operators $\mathcal{B}_j^{(2,i)}$, and transmits the outcome $j$ back to $A$. $A$'s next operation can depend on $i$ and $j$, and so forth. The final result of this procedure is a separable operation, but it is very difficult to describe in precise mathematical terms what distinguishes LOCC from more general separable operations [13, 14].

Entanglement of a state is equivalent to the impossibility of preparing it with the sole aid of LOCC starting from an uncorrelated state. States that can be prepared by LOCC, and hence are separable have the general form of a convex combination of product states:

$$\varrho \neq \sum_{i=1}^{r} p_i \varrho_1^i \otimes \cdots \otimes \varrho_r^i \tag{1.96}$$

(with no loss of generality, the $\varrho_i$ can be chosen to be pure). The set of separable states is by definition convex, and hence compact. Therefore, in the space of density matrices there is a clear boundary between separable and entangled states. In general, it is very hard to decide whether a given state is separable or entangled, i.e., whether a state admits a decomposition of the type (1.96). This is the so-called *separability problem*. In fact, it has been proven that for states that are close to the boundary of the separable set (i.e, states that are slightly entangled) the separability problem becomes NP-hard [15].

### 1.5.5 Entanglement monotones and monogamy

Another closely related, and hence difficult task is to assess the *amount of entanglement* present in a state. For general bipartite states, there is a class of entanglement measures called *entanglement monotones* [16]. Any such measure $\mathcal{M}(A:B)$ is required to have the following properties:

1. $\mathcal{M}(A:B) \geq 0$ and $\mathcal{M}(A:B) = 0$ for all separable states
2. $\mathcal{M}(A:B)$ is invariant under local unitaries $U_A \otimes U_B$

3. $\mathcal{M}(A:B)$ is non-increasing under LOCC

4. $\mathcal{M}(A:B) = E_E(\varrho_{AB})$ for pure states

In addition, one may demand that the entanglement monotone be *faithful*, modifying 1) in 1'): $\mathcal{M}(A:B) \geq 0$ and $\mathcal{M}(A:B) = 0$ if and only if the state is separable. In general, entanglement monotones are very hard to compute because some optimization procedure is involved in their definition. An example of faithful entanglement monotone is the *relative entropy of entanglement* [18]

$$E_S(\varrho_{AB}) \equiv \inf_{\sigma \in SEP} S(\varrho_{AB}||\sigma) \tag{1.97}$$

defined as the minimum statistical distance between a state $\varrho_{AB}$ and a separable state $\sigma$. Another faithful monotone is the *entanglement of formation* [17]

$$E_F(\varrho_{AB}) \equiv \min_{\mathcal{E}} \sum_i p_i E_E(|\psi_i\rangle) \tag{1.98}$$

where $\sum_i p_i |\psi_i\rangle\langle\psi_i|$ is a given ensemble realization of $\varrho_{AB}$. The entanglement of formation corresponds to the minimum number of maximally entangled qubits (singlets or ebits) needed to synthesize $\varrho_{AB}$ by LOCC. A third faithful entanglement monotone is the *squashed entanglement* [21, 122] , defined as

$$E_{CMI}(\varrho_{AB}) \equiv \frac{1}{2} \min_{\varrho_{ABC}} \mathcal{I}(AB|C), \tag{1.99}$$

where $\varrho_{ABC}$ is an extension of $\varrho_{AB}$ (a state such that $\mathrm{Tr}_C[\varrho_{ABC}] = \varrho_{AB}$) and $\mathcal{I}(AB|C)$ is the conditional mutual information (CMI) $\mathcal{I}(AB|C) = S(\varrho_{AC}) + S(\varrho_{BC}) - S(\varrho_C) - S(\varrho_{ABC})$. A widely used, though non-faithful monotone is the *negativity* [19]

$$\mathcal{N}(\varrho_{AB}) \equiv \frac{||\varrho^{\Gamma_A}||_1 - 1}{2} \tag{1.100}$$

where $\varrho^{\Gamma_A}$ is the partial transpose of $\varrho$ with respect to subsystem $A$. The negativity is based on the fact that $\Gamma^A$ is a positive map when acting on separable states, but it can be negative on entangled states. Therefore $\varrho^{\Gamma_A}$ has in general negative eigenvalues. Since $\Gamma^A$ is trace-preserving, $\mathrm{Tr}[\varrho^{\Gamma_A}] = 1$ and hence $|\varrho^{\Gamma_A}||_1 \geq 1$.
For two qubits, there exists a faithful entanglement monotone that can be expressed in a simple analytical form for all states. The *concurrence* [20] is defined as

$$K(\rho_{AB}) \equiv \max(0, \lambda_1 - \lambda_2 - \lambda_3 - \lambda_4) \tag{1.101}$$

where $\lambda_1, \ldots, \lambda_4$ are the eigenvalues, in decreasing order, of the Hermitian matrix $R = \sqrt{\sqrt{\varrho_{AB}}\tilde{\varrho}_{AB}\sqrt{\varrho_{AB}}}$ with $\tilde{\varrho}_{AB} = (\sigma_y \otimes \sigma_y)\varrho^*_{AB}(\sigma_y \otimes \sigma_y)$ the spin-flipped state of $\varrho_{AB}$, $\sigma_y$ a Pauli spin matrix, and the eigenvalues listed in decreasing order (alternatively, the $\lambda_i$'s represent the square roots of the eigenvalues of the non-Hermitian matrix $\varrho_{AB}\tilde{\varrho}_{AB}$). From the concurrence, the entanglement of formation can be calculated as

$$E_F(\varrho_{AB}) = h\left(\frac{1 + \sqrt{1 - K(\varrho_{AB})^2}}{2}\right) \tag{1.102}$$

where $h(x) \equiv -x \log x - (1-x)\log(1-x)$.

An important property of entanglement is that two maximally correlated systems cannot be entangled with a third system: if a tripartite state $\varrho_{ABC}$ is such that $\varrho_{AB} = \mathrm{Tr}_C[\varrho_{ABC}] = |\phi_m\rangle\langle\phi_m|$ where $|\phi_m\rangle$ is a maximally entangled state, then we must have $\varrho_{ABC} = |\phi_m\rangle\langle\phi_m| \otimes \varrho_C$. Such a property is called *monogamy of entanglement* . More in general, two strongly entangled systems cannot share but a limited amount of entanglement with other systems. This limitation can captured by *monogamy relations*, i.e., inequalities involving entanglement monotones in the form:

$$\mathcal{M}(A:BC) \geq \mathcal{M}(A:B) + \mathcal{M}(A:C) \tag{1.103}$$

where $\mathcal{M}(X,Y)$ represents the monotone $\mathcal{M}$ calculated across the bipartition $X,Y$. This inequality may be extended for an arbitrary number of parties as

$$\mathcal{M}(A:B_1 \ldots B_k) \geq \mathcal{M}(A:B_1) + \cdots + \mathcal{M}(A:B_k) \tag{1.104}$$

Eq. (1.103) was proved to hold for the squared concurrence $K^2$ in Ref. [22], and the proof was later extended to a multiqubit system proving Eq. (1.104) [23]. In Ref. [122], it was proved that squashed entanglement is monogamous in all dimensions. Not all entanglement measures satisfy monogamy inequalities. For instance, Eq. (1.103) is not satisfied for the entanglement of formation nor for the relative entropy of entanglement.

# Chapter 2

# Quantum discord in the extended Hubbard model

## 2.1 Introduction

A very fertile interplay between the theories of quantum-information and condensed matter has developed during the last decade. On one side, condensed-matter theory has suggested a wide range of possibilities for the implementation of quantum communicational [137] and computational [142] tasks. On the other side, quantum information theory has yielded novel insights into the physics of condensed-matter systems.
One of the main intersection points between the two fields is the study of the ground state structure of many-body systems. As several models show – e.g., the Laughlin theory of quantum Hall systems and the BCS theory of superconduction – ground states can be dominated by quantum correlations, which frustrates attempts to describe them by means of simple and classical-like ansätze. Quantum information theory provides a conceptual toolkit that facilitates addressing the role of correlations in many-body states within a general perspective. In particular, quantum information theoretical notions have become relevant in characterizing quantum critical phenomena [84]. Quantum phase transitions (QPT) occur in quantum systems at zero temperature. For critical values of some parameters (quantum critical points), the structure of the ground states changes abruptly. QPTs are usually associated with a singular behavior of correlation functions and the correlation length. These indicators of correlations should not be independent from the behavior of *quantum correlations* in the sense outlined in the previous chapter, e.g., entanglement and discord. Thus one expects to find a critical behavior of quantum correlations measures, too. The critical behavior of quantum correlations has been extensively studied, mainly in one-dimensional integrable spin models that offer the advantage of analytical tractability. Two pioneering works [85, 86] addressed entanglement (as measured by single-site entropy and two-site concurrence) in simple spin chain models. These works showed that entanglement has a non-analytic behavior at the transition points, where it generally has a peak. More importantly, it exhibits universal behavior, e.g., in the finite-size scaling. A stronger sign of universality came

from analyzing the entanglement entropy between a block of $L$ sites and the rest of the chain (block entropy) [87]. In the noncritical regime, the entropy saturates as $L \to \infty$, while in the critical regime $L$ has a logarithmic divergence. The coefficient of the logarithmic divergence is manifestly universal, and it is related to the central charge of the associated $1 + 1$ conformal field theory. Thus the entanglement entropy of critical spin chains behaves like the entanglement entropy of the vacuum in conformal field theories [88]. As was later shown in [89], the non-analytic behavior of quantum correlation measures at quantum critical points is a general feature, which implies a capability of entanglement to mark quantum phase transitions (QPT). Moreover, the logarithmic divergence in the critical regime suggests that entanglement spreads over all scales, a hypothesis that was given support in [90]: At the quantum-critical point, a deep minimum in the pairwise-to-global entanglement ratio shows that multipartite entanglement between the spins is strongly enhanced.

In all these studies, quantum correlations and entanglement have been usually identified as one and the same concept. However, as we have discussed at length in the former chapter, the notion of entanglement is unfit to wholly capture the quantum character of correlations present in a system. The theory of quantum discord has shown that a part of the total correlations present in quantum states are unstable under (and inaccessible) under local measurements – a highly nonclassical feature which qualifies these correlations as quantum. Quantum discord has proved effective in better explaining the nonclassicality of several phenomena, including the quantum advantage of many quantum information processing tasks. Therefore, it is natural to inquire whether quantum discord can be also useful in characterizing quantum features of many-body systems, in particular critical ones . Unsurprisingly then, the behavior of discord has been analyzed in several one-dimensional many-body systems, especially in relation to QPTs and thermal effects [100, 101, 102, 103, 104, 106, 105]. The main results of these analyses show that two-point discord and classical correlations between near as well as distant sites show clear signatures of QPTs (discontinuities or divergences), which can be understood within a general framework [100] and agree with finite-size scaling theory in the case of finite chains. Research has mostly concentrated on spin-$1/2$ models [100, 101, 102, 103, 104, 105] (except for the Lipkin-Meshkov-Glick model [101] and the Castelnovo-Chamon model [106], where a topological QPT occurs). Therefore, a thorough analysis of discord and classical correlations in correlated electron systems was still lacking. The latter, at variance with the simplest spin systems, requires the evaluation of the discord for pairs of q-dits and hence presents more difficulties. A first step in filling this gap was taken in our paper [107], upon which the present chapter is based.

The subject of this chapter is the behavior of discord and classical correlations for the ground states of the one-dimensional bond-charge extended Hubbard model [162, 160], which is a reference model in correlated-electron theory. The model has an integrable point, and its entanglement properties have been the subject of recent studies [95, 97, 98, 99, 161] where use of two-point and multipartite entanglement measures led to a classification of QPTs into multipartite or two-point driven. These studies left open the problem of addressing the general role of bipartite correlations for all two-points driven QPTs, as well as their relation with the presence of off diagonal long range order (ODLRO) which characterizes some ordered phases of the model. The in-

troduction of discord and classical correlations allows to solve this problem in a proper framework. We will systematically consider the quantum discord and the classical correlations, in direct space between two-sites and in momentum space between two couples of modes, and we will study their interplay and their ability to properly describe the rich zero temperature phase diagram and the various phase transitions exhibited by the extended Hubbard model under consideration. We will show how that discord and classical correlations can highlight the presence of a so-called entanglement transition, where a different role of quantum and classical correlation at a transition is revealed by the different behavior of discord and classical correlations, both in their maxima and in the divergence of their derivatives (subsection 2.3.1). The study of the derivatives of discord and classical correlations close to the critical lines allows to confirm the two-point/multipartite nature of the various transitions and to distinguish transitions that are physically different based on a different role of long range quantum correlations(ODLRO) (subsection 2.3.3). I will demonstrate that these long-range correlations correlations, which are at the basis of superconductivity, are related to two-point discord rather than two-point entanglement: indeed a direct relation between ODLRO and discord can be found (subsection 2.3.2). This relation is true both in the direct and in the reciprocal lattice picture, since a functional relation between the two-site discord and the two mode discord can be established (subsection 2.3.4). As an example of how condensed matter systems constitute a natural playground to test quantum information concepts, the ground state properties also shed light onto an aspect of the quantum correlations that is very relevant in the general context of quantum information theory: the monogamy property (I will address this issue in detail in the self-contained subsection 2.3.5). Upon considering ground states of the model also at finite system size, I will extend previous analyses of the monogamy relation to an $n$-partite setting with $n \geq 3$. In a phase of the model the ground states coincide with a class of permutation-invariant states, for which I will show that the monogamy relation is always violated, both in presence and in absence of entanglement. In the TDL the entanglement vanishes and the violation of the monogamy property for discord becomes maximal: due to the presence of ODLRO, a single qubit can exhibit finite amount of discord with an infinite number of other qubits. The monogamy relation can be violated also in absence of ODLRO, but in this case the violation is not maximal.

This chapter is organized as follows. § 2.2 is a brief review of the main features of the extended Hubbard model: Hamiltonian, phase diagram., etc. § 2.3 is the core of the chapter, where the behavior of discord and classical correlations in the whole phase diagram of the model is analyzed, with a special focus on quantum critical points/lines. In § 2.4 I will highlight and summarize the main conclusions. This chapter essentially reproduces an article of ours already published in Physical Review B [107].

## 2.2 The bond-charge extended Hubbard model

### 2.2.1 Basics of the model

The bond-charge extended Hubbard model was derived as an effective one-band Hamiltonian for the description of cuprate superconductors [162]. The model is described by

the following Hamiltonian:

$$H_{BC} = - \sum_{<i,j>\sigma} [1 - x(n_{i\bar{\sigma}} + n_{j\bar{\sigma}})] c^{\dagger}_{i\sigma} c_{j\sigma} - \mu \sum_{i\sigma} n_{i\sigma} + u \sum_{i} \left( n_{i\uparrow} - \frac{1}{2} \right) \left( n_{i\downarrow} - \frac{1}{2} \right) \quad (2.1)$$

where $c^{\dagger}_{i\sigma}$ and $c_{i\sigma}$ are fermionic creation and annihilation operators on a one-dimensional chain of length $L$; $\sigma = \uparrow, \downarrow$ is the spin label, $\bar{\sigma}$ denotes its opposite, $n_{j\sigma} = c^{\dagger}_{j\sigma} c_{j\sigma}$ is the spin-$\sigma$ electron charge, and $\langle i, j \rangle$ stands for neighboring sites on the chain; $u$ and $x$ ($0 \leq x \leq 1$) are the (dimensionless) on-site Coulomb repulsion and bond-charge interaction parameters; $\mu$ is the chemical potential, and the corresponding term allows for arbitrary filling.

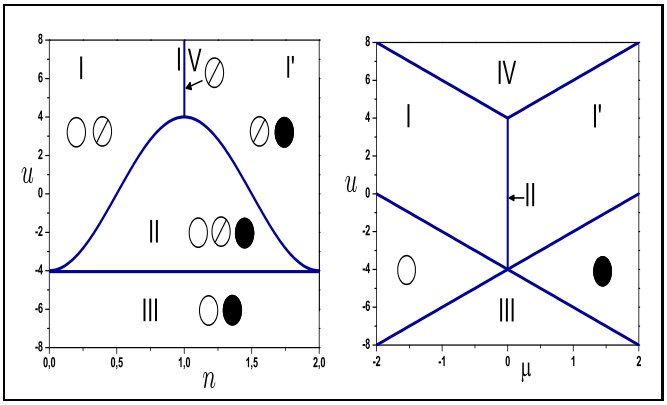


Figure 2.1: Ground-state phase diagram of $H$. LEFT: $n$-$u$ plane; empty circles stand for empty sites, slashed and full circles stand for singly and doubly occupied sites, respectively. RIGHT: $\mu$-$u$ plane.

The model is considered here at $x = 1$, in which case the system becomes integrable. This happens for two reasons. First, the $1 - x(n_{i\bar{\sigma}} + n_{j\bar{\sigma}})$ term suppresses several hopping possibilities. As a result, we can separate the four possible states at site $i$ into two groups, namely $A = \{|\uparrow\rangle, |\downarrow\rangle\}$ and $B = \{|0\rangle, |\uparrow\downarrow\rangle\}$: hopping permutes states of group $A$ with states of group $B$, but not states of the same group. The role of spin orientation becomes dynamically irrelevant, and the system behaves as if at each site the local space had dimension 3: $|\uparrow\rangle$ and $|\downarrow\rangle$ can be considered as the same state. Second, the hopping term commutes with the terms in $u, \mu$ and the number of doubly occupied sites becomes therefore a conserved quantity.
The physics of the system described by $H$ is basically that of $N_s$ spinless fermions – singly occupied sites– which move in a background of $L - N_s$ bosons, of which $N_d$ are doubly occupied sitesand the remaining are empty sites . Both $N_s$ and $N_d$ are conserved quantities, and determine the total number of electrons $N_t = N_s + 2N_d$.
The situation may be understood in the formalism developed by Sutherland in Ref.

[158]. We can say that, apart from constant terms, $H$ acts as a permutator of just two *Sutherland species* (SSs), the $N_s$ fermions, and the $L - N_s$ bosons. In practice, empty and doubly occupied sites —though different as physical species— belong to the same SS, since the off-diagonal part of the Hamiltonian (i.e., the hopping term) cannot distinguish between them. It is only the constant term counting doubly occupied sites which depends on the actual value of $N_d$.
It is convenient to rewrite both the Hamiltonian and the local vector space in terms of the Hubbard-like projection operators $X_i^{\alpha\beta} \doteq |\alpha\rangle_i\langle\beta|_i$, with local algebra $X_i^{\alpha\beta}X_i^{\gamma\delta} = \delta_{\beta\gamma}X^{\alpha\delta}$ and nonlocal (anti-)commutation relations given by

$$X_i^{\alpha\beta}X_j^{\gamma\delta} = (-)^{(\alpha+\beta)(\gamma+\delta)}X_j^{\gamma\delta}X_i^{\alpha\beta}\ ,\ i \neq j\,; \tag{2.2}$$

here $\alpha = 0, 1, 2$, $|0\rangle_i \equiv |\text{vac}\rangle_i$ is the local vacuum, $|1\rangle_i \doteq X_i^{10}|0\rangle_i$ is the singly occupied state (with odd parity), and $|2\rangle_i \doteq X_i^{20}|0\rangle_i$ is the doubly occupied state. More precisely, as far as the ground state is concerned, the model Hamiltonian in the one-dimensional case can be fruitfully written as

$$\begin{aligned} H = \ & - \sum_i \left(X_i^{10}X_{i+1}^{01} - X_i^{21}X_{i+1}^{12} + \text{H.c.}\right) + u\sum_i X_i^{22} \\ & - \left(\mu + \frac{u}{2}\right)\sum_i \left(X_i^{11} + 2X_i^{22}\right)\ . \end{aligned} \tag{2.3}$$

The eigenstates are easily worked out [160, 95], and read

$$|\psi(N_s, N_d)\rangle = \mathfrak{N}(\eta^\dagger)^{N_d}\tilde{X}_{k_1}^{10}\cdots\tilde{X}_{k_{N_s}}^{10}|\text{vac}\rangle\,; \tag{2.4}$$

Here $\mathfrak{N} = [(L - N_s - N_d)!/(L - N_s)!N_d!]^{1/2}$ is a normalization factor; $\tilde{X}_k^{10}$ is the Fourier transform of the Hubbard projection operator $X_j^{10}$, i.e.,

$$\tilde{X}_k^{10} = \sum_j \frac{1}{\sqrt{L}}\exp(i\frac{\pi}{L}jk)X_j^{10}$$

Moreover, $\eta^\dagger = \sum_{i=1}^{L} X_i^{20}$ is also known as the eta operator, commuting with $H$; $(\eta^\dagger)^{N_d}$ creates $N_d$ pairs which are fully spread over the chain. These are the $\eta$ pairs first introduced by Yang [159]. This structure corresponds to a very simple physical picture: eigenstates contain $N_s$ spinless fermions in momentum eigenstates $\{\frac{2\pi k_1}{L}, \ldots, \frac{2\pi k_{N_s}}{L}\}$ and $N_d$ spinless bosons ($\eta$ pairs).
The energy eigenvalues are given by

$$E(\{n_k\}, N_d) = -2\sum_{k=1}^{L}\cos(\frac{2\pi k}{L})n_k - 2\mu N_d - (\mu + \frac{u}{2})N_s \tag{2.5}$$

where $n_k = 0, 1$ is the number of fermions with momentum $\frac{2\pi k}{L}$. For any given $N_s = \sum_k n_k$ and $N_d$ the minimum is achieved by occupying with $N_s$ fermionic particles the momentum modes $\{\pi(N_s - 1)/L, \ldots, \pi(N_s - 1)/L\}$, the corresponding eigenvalue being

$$E(N_s, N_d) = -2\sin\left(\pi\frac{N_s}{L}\right)/\sin\left(\frac{\pi}{L}\right) - 2\mu N_d - \left(\mu + \frac{u}{2}\right)N_s$$

whence we obtain the ground state energy density in the TDL

$$\mathcal{E}(n_s, n_d) = -\frac{2}{\pi}\sin(\pi n_s) - 2\mu n_d - \left(\mu + \frac{u}{2}\right) n_s \tag{2.6}$$

with $\mathcal{E} = E/L, n_s = N_s/L, n_d = N_d/L$.
The actual ground state is found by requiring that $n_s$ and $n_d$ minimize (2.6).
For $\mu < 0$ we have $n_d = 0$, hence upon minimizing we get $n_s = \frac{1}{\pi}\arccos\left(-\frac{\mu}{2} - \frac{u}{4}\right)$.
For $-4 - 2\mu \leq u \leq 4 - 2\mu$ we have empty and singly occupied sites (phase I), for $u > 4 - 2\mu$ we have only singly occupied sites (phase IV) and for $u < -4 - 2\mu$ we have only empty sites.
For $\mu > 0$ we have $n_d = (1 - n_s)$, hence upon minimizing we get $n_s = \frac{1}{\pi}\arccos\left(\frac{\mu}{2} - \frac{u}{4}\right)$.
For $-4 + 2\mu \leq u \leq 4 + 2\mu$ we have doubly and singly occupied sites (phase I'), for $u > 4 - 2\mu$ we have only singly occupied sites (phase IV) and for $u < -4 - 2\mu$ we have only doubly occupied sites.
For $\mu = 0$ we get $n_s = \frac{1}{\pi}\arccos\left(-\frac{u}{4}\right)$. For $-4 \leq u \leq 4$ we have empty, doubly and singly occupied sites (phase II), while for $u > 4 - 2\mu$ we have only singly occupied sites (phase IV) and for $u < -4 - 2\mu$ we have empty and doubly occupied sites (phase III).
Hence we get in the $\mu$-$u$ plane the phase diagram depicted in Fig. 2.1, right. In the left part, the same ground-state phase diagram is drawn in the $n$-$u$ plane (with $n = N_t/L$ average per-site filling). The phase diagram presents various QPTs driven by parameters $u$ and $\mu$ (or $n$). Each transition is characterized by a change in the number of on-site levels involved in the state. Phase IV has just one level per site since each site is singly occupied. Phases I and I' (which is the particle-hole counterpart of phase I) have two on-site levels: singly occupied sites and empty or doubly occupied sites respectively. This holds for phase III as well, where only empty and doubly occupied sites appear. Phase II is the only phase in which all three on-site levels are involved. Phases II and III are characterized by the occurrence of off-diagonal long-range order (ODLRO)and superconducting correlations, evaluated as:

$$\lim_{r\to\infty} \langle X_i^{20} X_{i+r}^{02} \rangle = n_d(1 - n_d - n_s)\,. \tag{2.7}$$

Note that ODLRO —though not allowing real superconducting order at $x = 1$ due to spin degeneracy, which implies the vanishing of spin gap, is at the very root of superconducting order, which occurs at $x \neq 1$. [96]
Before discussing the various transitions in terms of the discord behavior, let us recall some feature of each of them in terms of standard theory. First of all, since $N_d$ and $N_s$ are both conserved quantities, the transitions should be originated from level crossing. Indeed, they also occur at finite $L$. Nevertheless, none of them is of first order, since it can be easily checked that the first derivative of $E_{GS}$ is always smooth. In fact, the transitions I (I') $\rightarrow$ IV and II $\rightarrow$ IV and II $\rightarrow$ III are second-order QPTs, while the transition II $\rightarrow$ I (I') is an infinite-order QPT.

### 2.2.2 Reduced density matrices

The present work focuses on two-point correlations. To evaluate them, knowledge of the ground-state reduced density matrices is necessary, and we shall report their ex-

pression for completeness (for a full derivation, the reader may refer to Refs. [97, 99]). Correlations can be analyzed within two different and complementary pictures. Obviously, one can examine correlations between sites of the lattice (direct lattice picture). In addition, the structure of eigenstates in the model suggests yet another approach, namely to consider the reciprocal lattice, whose elementary nodes are momentum modes $k_j = \frac{2\pi}{L} j$, $j = 0, \ldots, L-1$. In some respects, the reciprocal lattice picture affords a simpler description of the system [95, 98].

Let us start by giving reduced density matrices the direct lattice picture. The one-site reduced density matrix $\rho_i$ when expressed in terms of the basis $\{|0\rangle, |1\rangle, |2\rangle\}_i$ is diagonal in all the regions of the phase diagram:

$$\rho_i = \text{diag}\left\{1 - n_s - n_d, n_s, n_d\right\} \quad , \tag{2.8}$$

the two-site reduced density matrix $\rho_{ij}$ in the basis $\{|00\rangle, |01\rangle, |02\rangle, |10\rangle, |11\rangle, |12\rangle, |20\rangle, |21\rangle, |22\rangle\}_{ij}$ reads [97]:

$$\rho_{ij} = \begin{pmatrix} D_1 & 0 & 0 & 0 & 0 & 0 & 0 & 0 & 0 \\ 0 & O_1 & 0 & O_2 & 0 & 0 & 0 & 0 & 0 \\ 0 & 0 & Q & 0 & 0 & 0 & Q & 0 & 0 \\ 0 & O_2^* & 0 & O_1 & 0 & 0 & 0 & 0 & 0 \\ 0 & 0 & 0 & 0 & D_2 & 0 & 0 & 0 & 0 \\ 0 & 0 & 0 & 0 & 0 & P_1 & 0 & P_2 & 0 \\ 0 & 0 & Q & 0 & 0 & 0 & Q & 0 & 0 \\ 0 & 0 & 0 & 0 & 0 & P_2^* & 0 & P_1 & 0 \\ 0 & 0 & 0 & 0 & 0 & 0 & 0 & 0 & D_3 \end{pmatrix} . \tag{2.9}$$

Here

$$\begin{array}{lcllcl} D_1 &=& P_{ij}(1-c)^2\,, & O_2 &=& \Gamma_{ij}(1-c)\,, \\ D_2 &=& n_s^2 - |\Gamma_{ij}|^2\,, & P_1 &=& c\left(1 - n_s - P_{ij}\right)\,, \\ D_3 &=& c^2 P_{ij}\,, & P_2 &=& c\Gamma_{ij}\,, \\ O_1 &=& \left(1 - n_s - P_{ij}\right)(1-c)\,, & Q &=& c(1-c)P_{ij}\,, \end{array}$$

with $c = n_d/(1-n_s)$, $P_{ij} = (1-n_s)^2 - |\Gamma_{ij}|^2$, and $\Gamma_{ij} = \frac{\sin(n_s \pi |i-j|)}{\pi |i-j|}$.

Let us now turn to the reciprocal lattice picture. To each momentum mode $k_j$ corresponds a 4-dimensional Hilbert space, spanned by the basis

$$\mathcal{B}_{k_j} = |0\rangle_{k_j}\,,\ |\uparrow\rangle_{k_j}\,,\ |\downarrow\rangle_{k_j}\,,\ |\uparrow\downarrow\rangle_{k_j}\,, \tag{2.10}$$

The reduced density matrix for any such mode reads, in the TDL, and in the basis (2.10),

$$\rho_{k_j} = \text{diag}(a^2, ab, ab, b^2) \tag{2.11}$$

where $a = \frac{1-n_s-n_d}{1-n_s}$ and $b = \frac{n_d}{1-n_s}$.

The two-mode ($16 \times 16$) reduced density matrix for modes $k_i$ and $k_j$, $k_i \neq k_j$, is diagonal with respect to the local basis $\mathcal{B}_{k_i} \otimes \mathcal{B}_{k_j}$. In the TDL, the eigenvalues are $a^\alpha b^{4-\alpha}$ with multiplicity $m_\alpha = \binom{4}{\alpha}$.

The case $k_i = -k_j$ has to be treated separately. The two-mode ($16 \times 16$) reduced

density matrix for modes $k_j$ and $-k_j$ has support on a $4 \times 4$ subblock. Indeed the sole states that can be built by the action of the $\eta^\dagger_{k_j}$ operators belong to the subspace spanned by:

$$\mathcal{B}_{k_j,-k_j} = \{|0,0\rangle_j,\ |\uparrow,\downarrow\rangle_j,\ |\downarrow,\uparrow\rangle_j,\ |\uparrow\downarrow,\uparrow\downarrow\rangle_j\} \tag{2.12}$$

where $|\alpha\ \beta\rangle_j \equiv |\alpha\rangle_{k_j} \otimes |\beta\rangle_{-k_j}$.
In the TDL, and in this basis, the non-vanishing subblock of the matrix reads:

$$\rho|_{\mathcal{B}_{k_j,-k_j}} = \begin{pmatrix} a^2 & 0 & 0 & 0 \\ 0 & ab & ab & 0 \\ 0 & ab & ab & 0 \\ 0 & 0 & 0 & b^2 \end{pmatrix}. \tag{2.13}$$

### 2.2.3 Behavior of entanglement at QPTs

Two-point entanglement at the QPTs of the model was thoroughly analyzed in Refs. [95, 97, 98, 99], upon consideration of different correlation measures: the two-point concurrence $K(\varrho_{ij})$ (1.101) or the two-point negativity $\mathcal{N}(\varrho_{ij})$ (1.100) as measures of entanglement (notice that definition of concurrence is available for two-qutrit systems), the mutual information $\mathcal{I}(i:j)$ ( 1.87) as a measure of total two-point correlations, and the single site entropy $S(\varrho_i)$ as a measure of multipartite entanglement between one site and the rest of the chain. The behavior of all correlation measures was studied as a function of $x$ ($x = \mu$ or $x = u$) in the vicinity of the quantum critical points. Results are briefly summarized in the table below.

| transition | x | $\frac{dS(\varrho_i)}{dx}$ | $\frac{d\mathcal{I}(i:j)}{dx}$ | $\frac{dK(\varrho_{ij})}{dx}$ | $\frac{d\mathcal{N}(\varrho_{ij})}{dx}$ | ent |
|---|---|---|---|---|---|---|
| I $\to$ IV | $\mu$ | $\propto \frac{1}{\sqrt{\mu-\mu_c}}$ | $\propto \frac{1}{\sqrt{\mu-\mu_c}}$ | $\propto \frac{1}{\sqrt{\mu_c-\mu}}$ | | Q2 |
| II $\to$ I | u | $\propto \log(u_c - u)$ | finite | | finite | QS |
| II $\to$ III | u | $\propto \frac{1}{\sqrt{u-u_c}}$ | $\propto \frac{1}{\sqrt{u-u_c}}$ | | finite | Q2 |
| II $\to$ IV | u | $\propto \frac{1}{\sqrt{u_c-u}}$ | $\propto \frac{1}{\sqrt{u_c-u}}$ | | finite | Q2 |

The analysis of divergences allows to classify the different transitions into those driven by two-point correlations (Q2: II $\to$ III, II $\to$ IV, I $\to$ II), where some two-point correlation measure ($K(\varrho_{ij})$, $\mathcal{N}(\varrho_{ij})$ or $\mathcal{I}(i:j)$) diverges, and those driven by multipartite correlations (QS: II $\to$ I) where only $S_i$ diverges. However, the two-point character of the transitions II $\to$ III, II $\to$ IV is only detected by $\mathcal{I}(i:j)$ (a measure of total correlations), while $\mathcal{N}(\varrho_{ij})$ (the measure of quantum correlations used) is unfit to discriminate between those transitions and the multipartite-driven one (II $\to$ I).

## 2.3 Behavior of discord and classical correlations

In the following, we will evaluate two-site correlations (discord and classical correlations) in all phases of the model. The two-site density matrix is symmetric in the exchange of parties, $\varrho_i = \varrho_j$. Therefore, both discord and classical correlations are symmetric, too, and we can use the notation $D(i:j)$, $\mathcal{J}(i:j)$ introduced in Eq.(1.26).

The difficult step in evaluating the discord is the minimization of the conditional entropy $S(\rho_{ij}|\Pi^j)$ with respect all local measurements $\Pi^j$ (with no loss of generality, we assume that the measurement is performed on $j$ but the same results would be obtained for measurements $\Pi^i$ on $i$). As we discussed in §1.3.3, allowing for general POVMs instead of just von Neumann measurements may allow for a better minimization, but the results are not significantly different from the numerical standpoint. Therefore, in the following we will restrict to von Neumann measurements.
The minimization can be done analytically for some simple cases of two-qubits, namely for the class of X states which have non-zero entries only on the diagonal and antidiagonal and include states with maximally mixed marginals (see Refs. [52, 53] and [54, 55] for recent developments). On the contrary, the two-qutrit case must be handled numerically.

### 2.3.1 Region I (I')

We start our analysis by evaluating two-site correlations (discord and classical correlations) in phase I. Results for phase I' are omitted, since they are exactly equal (by virtue of the particle-hole symmetry one just has to replace empty with doubly occupied sites).
Phase I (I') is characterized by the absence of doubly occupied (empty) sites, so that the effective number of on-site levels reduces to 2. Consequently, the 2-site reduced $9 \times 9$ density matrix $\rho_{ij}$ has nonzero entries only in the $4 \times 4$ subblock spanned by $\{|00\rangle, |01\rangle, |10\rangle, |11\rangle\}_{ij}$ . $D$ and $\mathcal{J}$ can be evaluated analytically through the methods developed in Refs [52, 53, 54, 55].

Since in phases I and III the density matrix $\rho_{ij}$ corresponds to an X-state for which $\min_{\Pi^j} S(\rho_{ij}|\Pi^j)$ can be easily evaluated with a fully analytical way by resorting to the method developed in [53], which we briefly review.
An arbitrary (single-qubit) von Neumann measurement is defined by a couple of orthogonal projectors $P_0$ and $P_1$, which can be obtained from $|0\rangle\langle 0|$ and $|1\rangle\langle 1|$ by an arbitrary $SU(2)$ rotation $V$:

$$P_0 = V|0\rangle\langle 0|V^\dagger \qquad P_1 = V|1\rangle\langle 1|V^\dagger \tag{2.14}$$

Since $V = tI + i\vec{y}\cdot\vec{\sigma}$ with $t^2 + y_1^2 + y_2^2 + y_3^2 = 1$, von Neumann measurements are parametrized by three independent numbers.
The key result of [53] is that the minimum of $S(\rho_{ij}|\Pi^j)$ is always attained for some special values of the parameters $m = (ty_1 + y_2y_3)^2$, $n = (ty_2 - y_1y_3)(ty_1 - y_2y_3)$,$k = t^2 + y_3^2$, namely

$$\begin{aligned} &\{k = 0, m = 0, n = 0\}\text{and} \\ &\{k = 1/2, m = 0, 1/4, n = 0, \pm 1/8\} \end{aligned} \tag{2.15}$$

Therefore the minimization procedure reduces to comparing the expressions $S(\rho_{ij}|\Pi^j)$ obtained in correspondence of these two sets of values. Furthermore, when the two-site reduced density matrix element $(\rho_{ij})_{1,4} = 0$, which is our case, $m$ and $n$ become irrelevant and $S(\rho_{ij}|\Pi^j)$ depends only on $k$. Therefore, we only have to compare

$S(\rho_{ij}|\Pi^j)$ for $k = 1/2$ and $k = 0$.
By the formulas in Ref. [53], for $k = 1/2$ we have

$$S(\rho_{ij}|\Pi^j) \equiv S_1(\rho_{ij}) = \\ -\frac{1-\theta_1}{2}\log_2\frac{1-\theta_1}{2} - \frac{1+\theta_1}{2}\log_2\frac{1+\theta_1}{2} \tag{2.16}$$

where

$$\theta_1 = \sqrt{[(\rho_{ij})_{11} - (\rho_{ij})_{33} + (\rho_{ij})_{22} - (\rho_{ij})_{44}]^2 + 4|(\rho_{ij})_{23}|^2} \tag{2.17}$$

while for $k = 0$ we have

$$S(\rho_{ij}|\Pi^j) \equiv S_2(\rho_{ij}) = \\ -(1-p_0)\frac{1-\theta_2}{2}\log_2\frac{1-\theta_2}{2} - (1-p_0)\frac{1+\theta_2}{2}\log_2\frac{1+\theta_2}{2} \\ -p_0\frac{1-\theta_3}{2}\log_2\frac{1-\theta_3}{2} - p_0\frac{1+\theta_3}{2}\log_2\frac{1+\theta_3}{2} \tag{2.18}$$

where $p_0 = (\rho_{ij})_{11} + (\rho_{ij})_{33}$ and

$$\theta_2 = \frac{|(\rho_{ij})_{22} - (\rho_{ij})_{44}|}{|(\rho_{ij})_{22} + (\rho_{ij})_{44}|},\ \theta_3 = \frac{|(\rho_{ij})_{11} - (\rho_{ij})_{33}|}{|(\rho_{ij})_{11} + (\rho_{ij})_{33}|} \tag{2.19}$$

All we must do is take the minimum between (2.16) and (2.18):

$$\min_{\Pi^j} S(\rho_{ij}|\Pi^j) = \min\{S_1, S_2\} \tag{2.20}$$

Evaluating the mimimum of the reduced conditional entropy reduces, Eq. (2.20), to taking the minimum among two functions, i.e., $\min_{\Pi^j} S(\rho_{ij}|\Pi^j) = \min\{S_1, S_2\}$, where $S_1, S_2$ depend on $\theta_1 = \sqrt{(1+4n^2-4n)+4|\Gamma_{ij}|^2}$ , $\theta_2 = \frac{|n-2n^2+2|\Gamma_{ij}|^2|}{n}$ , $\theta_3 = \frac{|1+2n^2-3n-2|\Gamma_{ij}|^2|}{1-n}$ (2.16-2.19).
We verify that for all values of $|i-j|$ we always have $S_1 \leq S_2$ and therefore two-point classical correlation $\mathcal{J}(i:j)$ and quantum discord $D(i:j)$ can be written in terms of $S_1$.
In order to compare quantum discord and entanglement, we also evaluate two-point concurrence [97]

$$K(\varrho_{ij}) = \min\left\{0, \left|\Gamma_{ij} - \sqrt{((1-n)^2 - |\Gamma_{ij}|^2)(n^2 - |\Gamma_{ij}|^2)}\right|\right\}. \tag{2.21}$$

In the following, letters $D(i:j), \mathcal{J}(i:j), \mathcal{I}(i:j), K(\varrho_{ij})$ always denote quantum discord, classical correlations, mutual information and concurrence respectively. The values of $\mathcal{I}(i:j)$, $\mathcal{J}(i:j)$, $D(i:j)$ and $K(\varrho_{ij})$ for region I and different values of $|i-j|$ are plotted in Fig. 2.2.

We first see that the $D(i:j)$ and $\mathcal{J}(i:j)$ have the typical oscillating behavior already shown by the mutual information [97]. At variance with the previous analysis, where the quantum correlations measured by the concurrence were different from zero only in

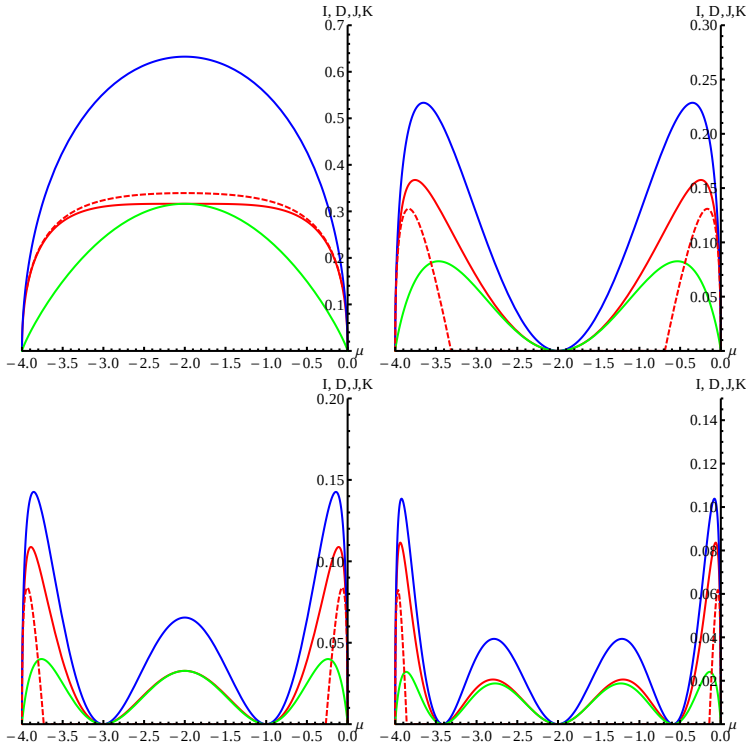


Figure 2.2: quantum mutual information $\mathcal{I}(i:j)$ (blue, solid), quantum discord $D(i:j)$ (red, solid), classical correlation $\mathcal{J}(i:j)$ (green, solid), concurrence $K(\varrho_{ij})$ (red, dashed) as a function of $\mu$ in region I ($u=4$), for $|i-j|=1$ (top, left), $|i-j|=2$ (top, right), $|i-j|=3$ (bottom, left), $|i-j|=4$ (bottom, right).

proximity of the borders of the regions i.e., for $\mu \to -4, 0$, here we see that the system exhibits non zero discord within the whole region I except at some nodal points defined by the equation $\Gamma_{ij} = \langle c_i^\dagger c_j \rangle = \frac{\sin(n_s\pi|i-j|)}{\pi|i-j|} = 0$ where all correlation measures vanish, $\mathcal{I}(i:j) = \mathcal{J}(i:j) = D(i:j) = 0$. Classical correlations show a similar behavior. Therefore, in the central region of phase I, where $K(\varrho_{ij})$ vanishes $\forall |i-j| > 1$, two-point discord and classical correlations are still present. Correlations are modulated by the sinusoidal behavior induced by $\Gamma_{ij}$ and *at fixed* $\mu$ they all decay algebraically with the distance: $\mathcal{I}(i:j), D(i:j), \mathcal{J}(i:j) \simeq |i-j|^{-2}$, see Fig.2.3.

In proximity of the transition I $\to$ IV it was shown in [97] that the system exhibits an *entanglement transition*[91]: the entanglement range $\mathcal{R}_K$, i.e., the maximal distance $|i-j|$ for which $K(\varrho_{ij}) \neq 0$, goes to infinity when approaching the transition. In particular, $K(\varrho_{ij})$ have a maximum value for $n_s \to 1$ as $|i-j| \to \infty$. This behavior is reflected in that of $\mathcal{I}(i:j), D(i:j), \mathcal{J}(i:j)$, which also exhibit a global maximum at a value $n_s^{(i,j)} \approx 1 - 1/(2|i-j|)$ which approaches $n_s = 1$ for $|i-j| \to \infty$. Hence,

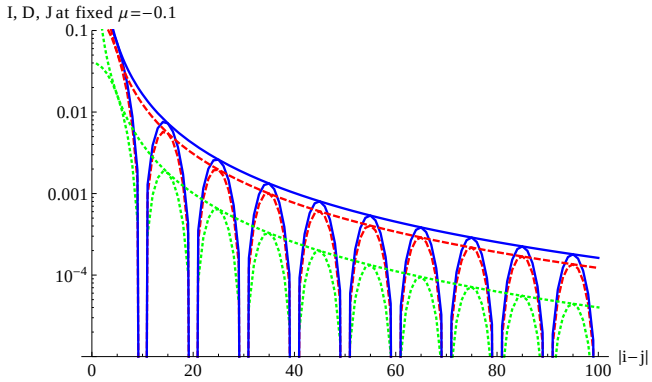


Figure 2.3: quantum mutual information $\mathcal{I}(i:j)$ (blue, solid), quantum discord $D(i:j)$ (red, solid), classical correlation $\mathcal{J}(i:j)$ (green, solid) as a function of $|i-j|$ in region I for $\mu = -0.1, u = 4$. Upper dashed lines represent the envelope of the respective maxima which exhibits a power law decay ($\sim |i-j|^{-2}$)

the behavior of discord mirrors that of the entanglement. This behavior is depicted in Fig.2.4. In fact, also the mutual information and the classical correlations exhibit the same kind of behavior. However the values of the maxima for the various measures $\mathcal{I}(i:j), D(i:j), \mathcal{J}(i:j)$ scale in a different way with the distance:

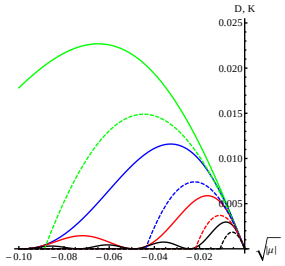


Figure 2.4: maxima of quantum discord $D(i:j)$ (solid lines) and concurrence $K(\varrho_{ij})$ (dashed lines) for $|i-j| = 16$ (blue), $|i-j| = 32$ (red), $|i-j| = 64$ (green), $|i-j| = 128$ (black) as a function of $\sqrt{|\mu|}$ in region I ($u = 4$)

$$\mathcal{I}(n_s^{(i,j)}, |i-j|) \simeq \frac{1}{|i-j|} \tag{2.22}$$

$$D(n_s^{(i,j)}, |i-j|) \simeq \frac{1}{|i-j|} \tag{2.23}$$

$$\mathcal{J}(n_s^{(i,j)}, |i-j|) \simeq \frac{\log(|i-j|)}{|i-j|^2} \tag{2.24}$$

$$\tag{2.25}$$

Therefore, when approaching the metal insulator transition I→IV the maxima of correlation measures ($\mathcal{I}(i:j), D(i:j), \mathcal{J}(i:j)$) decay in algebraic way along the chain. Quantum discord dominates for high distances, since the spreading of the classical correlation is suppressed by a factor $\log(|i-j|)/|i-j|$. This difference in the behavior of discord and classical correlations defines the different role that they have at the transition and can be further appreciated by studying the derivatives of the different correlation measures with respect to $\mu$. In the critical limit $\mu \to 0, -4$ we have

$$\partial_\mu D(i:j) \simeq -\frac{1}{\pi\sqrt{|\mu-\mu_c|}} \tag{2.26}$$

while

$$\partial_\mu \mathcal{J}(i:j) \simeq \frac{1}{\pi^2}\log|\mu-\mu_c| \tag{2.27}$$

Therefore, while the $\partial_\mu D(i:j)$ correctly agrees with the scaling behavior of $\partial_\mu \mathcal{I}(i:j)$ and $\partial_\mu K(\varrho_{ij})$ evaluated in [97], $\partial_\mu \mathcal{J}(i:j)$ though being singular has a lower degree of divergence, so that classical correlations are subleading in the vicinity of the critical point.

We therefore see that the introduction of the new measures of correlations $D(i:j)$ and $\mathcal{J}(i:j)$ and the study of their derivatives allows on one hand to properly identify the metal-insulator transition and to properly classify it as a two-point QPT [97], and on the other hand allows for a refinement in description of the QPT. The importance of this feature will be more evident in the following paragraphs where we will describe the other two-point QPTs i.e., II → IV and II→ II. We close this subsection by discussing the role of the divergences of the different correlation measures and their relation with the divergences of the energy density of the system. In [89], the authors found a direct relationship between the singularities (discontinuities and divergences) in the derivatives of the energy density of the system $\mathcal{E} = E/L$ with respect to the parameter $\lambda$ that drives the QPTs, and the singularities in the elements of the two-point reduced density matrix $\rho_{ij}$ or their derivatives with respect to $\lambda$. In our case the, the divergences in $\partial_\lambda \mathcal{I}(i:j)$ and $\partial_\lambda D(i:j)$ inherit the non-analyticities of the derivatives of the elements of $\rho_{ij}$ at the critical point. In particular the elements:

$$\partial_\lambda D_2, \partial_\lambda O_1, \partial_\lambda O_2 \to \frac{1}{\sqrt{|\lambda-\lambda_c|}} \tag{2.28}$$

show the same divergences exhibited by the second derivative of the energy density (2.6) with respect to $\lambda = \mu$ (I→IV), i.e., $\partial_\mu^2 \mathcal{E} \sim 1/\sqrt{|\mu-\mu_c|}$. However, as we have

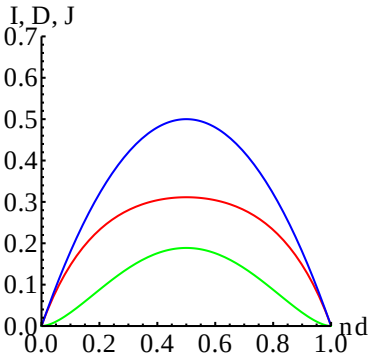


Figure 2.5: quantum mutual information $\mathcal{I}$ (blue), quantum discord $D$ (red), classical correlation $\mathcal{J}$ (green) as a function of $n_d$ in region III

seen above, classical correlations, though diverging, show a logarithmic divergence instead of an algebraic one, and accordingly one might believe that this is an accidental fact due to the definition of the correlation measure (i.e., that classical correlations always display a lower degree of divergence). However, as we will see in the next sections, the classical correlations $\mathcal{J}(i:j)$ behave like $D(i:j)$ and $\mathcal{I}(i:j)$, in terms of their derivatives with respect to $\lambda = u$, at the transition II$\rightarrow$III, and therefore they coherently behave as the energy density at that transition i.e., $\partial_u^2 \mathcal{E} \sim 1/\sqrt{|u-u_c|}$. In summary, while the derivatives of different elements of $\rho_{ij}$ and of some of the correlations measures defined on the $\rho_{ij}$ show the same divergent behavior at the various transitions, which agrees with that of the energy density $\partial_\lambda^2 \mathcal{E}$, the classical correlations may show different kind of divergences and are thus able to discriminate between quantum phase transitions that are physically different.

### 2.3.2 Region III: discord and ODLRO

Phase III is characterized by the absence of singly occupied sites, so that the number of on-site levels effectively reduces to 2, and the quantum discord can be evaluated analytically in the same way as above. Moreover in this case the number of Sutherland species reduces to 1. The quantum discord may be evaluated in the same way as above. We have $\min_{\Pi^j} S(\rho_{ij}|\Pi^j) = \min\{S_1, S_2\}$, where $S_1, S_2$ depend on $\theta_1 = (1-n_d)^2 + n_d^2$ and $S2$ on $\theta_2 = 1-2n_d, \theta_3 = 1-2n_d$ (2.16-2.19). Since two-site density matrices $\rho_{ij}$ are equal for all $i, j$, the values of two-site correlations are equal for each pair of sites, $\mathcal{I}(i:j) = \mathcal{I}$,$\mathcal{J}(i:j) = \mathcal{J}$,$D(i:j) = D$. We have $S_1 \leq S_2$ and therefore the classical correlations and the discord can be written in terms of $S_1$.
The values of $\mathcal{I}$, $\mathcal{J}$ and $D$ for region III are plotted in Fig. 2.5.
The first result of our analysis is that while in the TDL the concurrence $K(\varrho_{ij}) = \min\{0, -2n_d^2(1-n_d)^2\} = 0$ vanishes everywhere in region III, the discord is always different from zero in the region; we thus have that the $\eta$-pair states display two-point quantum correlations, though not in the form of entangled correlations but rather in the form of discord. Moreover, we notice that discord, as well as classical correlations,

between any two sites has the same value, irrespective of their distance: this reflects the way in which the $\eta$-paring mechanism spreads the correlations equally along the whole chain. The $\eta$-pairing is also the ground for the appearance of ODLRO, which follow directly from (2.7). It is intuitive to suppose that these superconducting correlations might be related to some kind of two-point quantum correlations, and indeed many authors have tried to find such a relation, see for example [92, 93]. While a relation with the entanglement properties in $k$ space was found in [99] in the case of for $\eta$-pairs and BCS states, in direct space this relation could not be established in terms of the concurrence since the latter vanishes in the TDL [97].

While ODLRO in $\eta$-pair states cannot be related to two-point entanglement, our analysis allows instead to connect the ODLRO to the two-point quantum discord. Indeed we find that in the TDL $D(i:j) = D_2^{TDL}, \forall i,j$ and we have

$$D_2^{TDL} = f(x) = \tfrac{1}{\log 4}[4x \text{ arctanh}(1-2x) + x\log 16 + \sqrt{1-4x}\log(-1 - \tfrac{2}{-1+\sqrt{1-4x}}) + \log(\tfrac{1}{(x-1)^2}) + \log x] \tag{2.29}$$

where $f(x)$ a monotonically increasing function of $x = n_d(1-n_d)$, i.e., of the ODLRO. The above analysis allows to establish a *direct relation between a fundamental quantum property such as ODLRO and the presence of two-point (two-qubit) discord*. It therefore seems that the important two-point quantum correlations necessary in direct space for the appearance of the ODLRO are represented by the discord and not by the entanglement.
We finally note that the presence of the ODLRO in $\eta$-paris states is reflected also by the behavior of classical correlations, which also are a monotonically increasing function of $n_d(1-n_d)$. The relation between classical correlations and ODLRO will be important in the discussion of the transitions described in the next section.

### 2.3.3 Region II

Region II contains empty as well as singly and doubly occupied sites, so that there are 3 on-site levels. This means that the evaluation of discord and classical correlations is more difficult than in the previous cases. In order to evaluate $D(i:j)$ and $\mathcal{J}(i:j)$ we used two numerical recipes. As for the two-qutrit case, we have that the possible von Neumann measurements correspond to unitary rotations,

$$P_0 = V|0\rangle\langle 0|V^\dagger\,, P_1 = V|1\rangle\langle 1|V^\dagger\,, P_2 = V|2\rangle\langle 2|V^\dagger \tag{2.30}$$

where now $V \in SU(3)$.
Unfortunately, to proceed forward in the computation of the discord, one cannot simply mimic the procedure described for qubits. The main difficulty is that no easy, explicit parametrization of $V \in SU(3)$ by 8 real parameters (the group dimension) can be found. [222]. We therefore must compute the discord *numerically*. Our strategy is to minimize $S(\rho_{ij}|\Pi^j)$ over a (large) set of randomly-generated unitary matrices [224]. More precisely, we generate a large ensemble of unitary matrices taken from the uniform distribution over the $SU(3)$ group manifold, evaluating $S(\rho_{ij}|\Pi^j)$ for each matrix. We then keep the minimum as our esteem of $\inf_{\{B_k\}} S(\rho_{ij}|\Pi^j)$. To be rigorous,

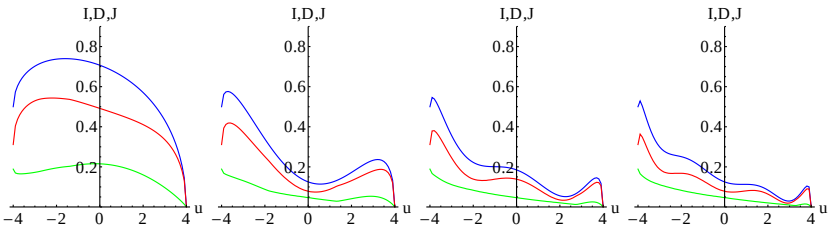


Figure 2.6: quantum mutual information $\mathcal{I}(i:j)$ (blue), quantum discord $D(i:j)$ (red), classical correlation $\mathcal{J}(i:j)$ (green) as a function of $u$ in region II for $n=1$, $|i-j|=1$ (top, left), $|i-j|=2$ (top, right), $|i-j|=3$ (bottom, left), $|i-j|=4$ (bottom, right)

this esteem is to be regarded as an upper bound: however, since we are generating a rather large set of random matrices we are confident that the bound is very stringent.
Alternatively, we can use the $SU(3)$ parametrization given in Ref. [223]. This allows to parametrize $SU(3)$ in terms of trigonometric functions of $8$ independent parameters, $3$ angles $\eta_1, \eta_2, \eta_3$ and $5$ phases $\alpha, \beta, \gamma, \rho, \sigma$. This parametrization makes it apparent that the phases $\rho$ and $\sigma$ are completely irrelevant for the computation of the discord, since orthonormal projectors (von Neumann measurements) are independent of the choice of such phases. This method has the advantage that it is based on a more transparent parametrization of von Neumann measurements. Again, we generate a large ensemble of unitary matrices find the minimum of $S(\rho_{ij}|\Pi^j)$
In all cases under study, the two methods applied led to the same results, which provides us with full confidence on their reliability. In particular, the two methods show perfect agreement in the value of the discord throughout the whole region, and this is a first indication of their reliability. A further element of confidence in the methods used is the fact that $D(i:j)$ and $\mathcal{J}(i:j)$ must be continuous in the transitions II $\rightarrow$ I , III (since all matrix elements of $\rho_{ij}$ are): when we approach the phase boundaries, the numerical limits of $D(i:j)$ and $\mathcal{J}(i:j)$ in region II coincide with the analytical values determined in region I and III.

In Fig. 2.6 and Fig. 2.7 we plot $\mathcal{I}(i:j)$, $\mathcal{J}(i:j)$, $D(i:j)$ in region II as a function of $u$ for $|i-j|=1,2,3,4$, and for $n=1$ and $n=0.5$ respectively. In the Table below, we summarize the critical behavior of the derivatives of quantum discord $D(i:j)$ and classical correlations $\mathcal{J}(i:j)$ for the transitions II $\rightarrow$ I, II $\rightarrow$ III, IV. These values are obtained as follows. We find numerically (with either of the procedures sketched above) the optimal measurement which minimizes the reduced conditional entropy. Contrary to what happens in region I, the orthogonal measurement minimizing the conditional entropy varies throughout region II, i.e., the parameters of the unitary rotation $V$ are not constant throughout the whole region. However, in the neighborhood of the critical lines ($u \rightarrow -4$ and $u \rightarrow -4\cos\pi n$) they are found to remain constant at any fixed $n$. We therefore use these constant values in the expressions for the reduced conditional entropy and obtain analytical formulas for $D(i:j)$ and $\mathcal{J}(i:j)$ as a function of $u$. We then extrapolate the critical behavior by studying these functions in the

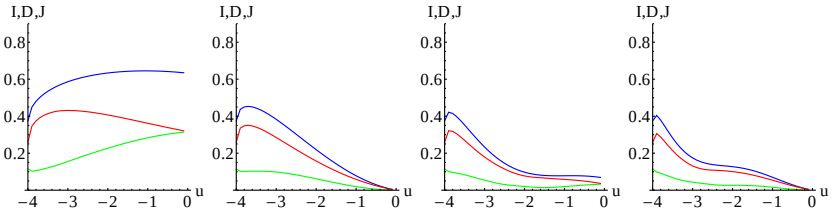


Figure 2.7: quantum mutual information $\mathcal{I}(i:j)$ (blue), quantum discord $D(i:j)$ (red), classical correlation $\mathcal{J}(i:j)$ (green) as a function of $u$ in region II for $n=1$, $|i-j|=0.5$ (top, left), $|i-j|=2$ (top, right), $|i-j|=3$ (bottom, left), $|i-j|=4$ (bottom, right). We note that at the multipartite transition II→I ($u=0$) all the two-point correlation measures behave in a smooth way

critical limit.

| transition | n | u | $\frac{d\mathcal{I}}{du}$ | $\frac{dD}{du}$ | $\frac{d\mathcal{J}}{du}$ |
|---|---|---|---|---|---|
| II $\to$ I | $1/2$ | $\to 0$ | finite | finite | finite |
| II $\to$ III | $1/2$ | $\to -4$ | $\propto \frac{1}{\sqrt{u-u_c}}$ | $\propto \frac{1}{\sqrt{u-u_c}}$ | $\propto \frac{1}{\sqrt{u_c-u}}$ |
| II $\to$ IV | $1$ | $\to 4$ | $\propto \frac{1}{\sqrt{u_c-u}}$ | $\propto \frac{1}{\sqrt{u_c-u}}$ | $\propto \log(u_c-u)$ |
| II $\to$ III | $1$ | $\to -4$ | $\propto \frac{1}{\sqrt{u-u_c}}$ | $\propto \frac{1}{\sqrt{u-u_c}}$ | $\propto \frac{1}{\sqrt{u_c-u}}$ |

The results can be summarized as follows. In the transition II $\to$ I o (or I') two-point $D(i:j)$, $\mathcal{I}(i:j)$, $\mathcal{J}(i:j)$ are regular, thus confirming that this transition has a multipartite nature.

As for the transitions II→IV and II→III, previous analyses [97] have shown that both transitions have a two-point character. As a first result, we see that at both transitions quantum discord is able to correctly detect the divergence expected, whereas negativity fails for this aspect[95] (see Sec. 2.2.3). The two transitions are however physically inequivalent, since they lead to two completely different phases: transition II→IV is characterized by the disappearance of ODLRO, whereas at transition II→III ODLRO is present. We now show how this difference can be properly described by the study of the two-point classical correlations.

In the transition II $\to$ III, while $\partial_u \mathcal{I}(i:j), \partial_u D(i:j) > 0$ and $\partial_u \mathcal{J}(i:j) < 0$ all the derivatives display the same kind of algebraic singularity. On the other hand, in the transition II $\to$ IV, we have that $\partial_u \mathcal{I}(i:j), \partial_u D(i:j), \partial_u \mathcal{J}(i:j) < 0$, they all diverge, but $\mathcal{J}(i:j)$ has a lower degree of divergence i.e., it is logarithmic; this property allows to correctly describe the transition as a two-point one and furthermore to assimilate it to the metal-insulator transition I→IV, where the classical correlations show the same kind of divergence.

The result can be further deepened by considering the following argument. All two-point correlations in region II can always be split into a finite and an infinite range contributions: $A^{II}_{i,j} = \tilde{A}_{i,j} + A^{II}_{\infty}$, where $A = I, \mathcal{J}, D$ and $A^{II}_{\infty} = \lim_{|i-j|} A^{II}_{i,j}$.

The infinite range contributions can be analytically evaluated and they all explicitly

depend on the value of the ODLRO in this phase, $n_d(1-n_s-n_d)$. Therefore, their derivatives with respect to $u$ have all the same behavior: they display the same type of algebraic singularity in case of transition II→III (ODLRO), while they do not display any singularity in case of transition II→IV (disappearance of ODLRO).
On the other hand, as for the finite range contributions we find that $\partial_u \tilde{\mathcal{J}}_{i,j}$ diverges at both transitions but with a logarithmic behavior that is dominant only in the transition II→IV (where $\partial_u \tilde{\mathcal{J}}_{\infty}$ is regular) while its quantum counterpart $\partial_u \tilde{D}_{i,j}$ diverges algebraically. The above results show that the introduction of the discord and classical correlations allows to discriminate between two apparently similar but inequivalent two-point QPTs, and to root their difference in the persistence (disappearance) of ODLRO at the transitions.

### 2.3.4 Reciprocal Lattice

We now consider quantum discord between two momentum modes in the reciprocal lattice; the analysis is significant in region II and III, where $\eta$-pairs are present, and for values of $k_j > k_s$ where $k_s = \frac{2\pi N_s}{L}$ is the maximum single-fermion momentum, since the portion of k-space pertaining to single fermions is factorized. Let us fist consider two modes $k_j \neq k_j$. From the results derived in [98] we have that the measures of correlations all depend on a single parameter $a$ linked to the average occupation number of a generic mode $k_j$, $a = \langle n_{k_j}\rangle/2 = n_d/(1-n_s), \ \ \forall k_j$. In particular, the only pairs of modes $(k_i, k_j)$ which are correlated are the ones for which $k_i = -k_j$, while if $k_i \neq -k_j$ the relative momentum modes are completely uncorrelated i.e., $\mathcal{I}(k_i : k_j) = 0$ and therefore $D(k_i : k_j) = 0$. When $k_i = -k_j$ the single-mode von Neumann entropy reads $S(\rho_{k_j}) = -2(a\log a + (1-a)\log(1-a))$, the two-mode von Neumann entropy is $S(\rho_{k_i,k_j}) = S(\rho_{k_j}) + 2a(1-a)$ and hence the mutual information is $\mathcal{I}(k_i : k_j) = -2(a\log a + b\log b - ab)$.
In order to evaluate the quantum discord, we should now consider the reduced conditional entropy after a generic measurement is performed on mode $k_j$, and minimize with respect to all measurements. It turns out that, a von-Neumann measurement $B = \{\Pi_0, \Pi_\uparrow, \Pi_\downarrow, \Pi_{\uparrow\downarrow}\}$ onto the trivial basis $\mathcal{B}_{-k_j}$ yields

$$\begin{aligned}
\rho_0 &= \frac{1}{p_0}\mathrm{Tr}_{-k_j}\Pi_0\rho_{k_j,-k_j}\Pi_0 = a^2|0\rangle\langle 0| \\
\rho_\uparrow &= \frac{1}{p_\uparrow}\mathrm{Tr}_{-k_j}\Pi_\uparrow\rho_{k_j,-k_j}\Pi_\uparrow = ab|\uparrow\rangle\langle\uparrow| \\
\rho_\downarrow &= \frac{1}{p_\downarrow}\mathrm{Tr}_{-k_j}\Pi_\downarrow\rho_{k_j,-k_j}\Pi_\downarrow = ab|\downarrow\rangle\langle\downarrow| \\
\rho_{\uparrow\downarrow} &= \frac{1}{p_{\uparrow\downarrow}}\mathrm{Tr}_{-k_j}\Pi_{\uparrow\downarrow}\rho_{k_j,-k_j}\Pi_{\uparrow\downarrow} = b^2|\uparrow\downarrow\rangle\langle\uparrow\downarrow|
\end{aligned} \tag{2.31}$$

so that $\sum_\alpha p_\alpha S(\rho_\alpha) = 0$ and the minimum is immediately attained. Consequently we have that the quantum discord has a simple expression

$$D(k_j : -k_j) = \mathcal{I}(k_j : -k_j) - S(\rho_{k_j}) = 2a(1-a) \propto \mathcal{N}(\varrho_{k_j,-k_j}) \tag{2.32}$$

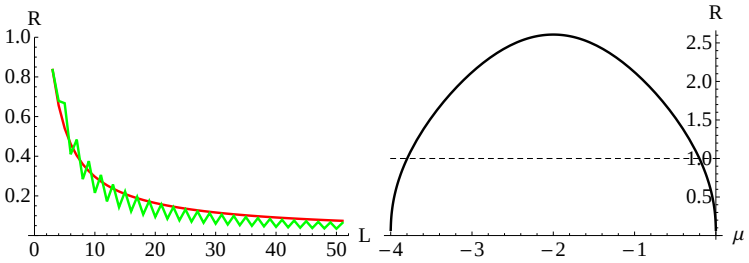


Figure 2.8: Left: monogamy ratio $R_M$ in phase III for chains of varying length $L$, with $N_d = 1/L$ (red), $N_d = \lfloor L/2 \rfloor / L$ (green). Right: monogamy ratio $R_M$ in phase I in the TDL.

and it is simply proportional to the negativity $\mathcal{N}(\varrho_{k_j,-k_j})$[99]. . This result allows us to derive some important conclusions. On one hand, the relationship found in [99] between ODLRO and negativity in region II can be rewritten in terms of the discord $D(k_j : -k_j)$ showing once again the quantum roots of the ODLRO:

$$\lim_{|i-j|\to\infty} \langle X_i^{20} X_j^{02} \rangle = (1-n_s)^2 a(1-a) = (1-n_s)^2 D(k_j : -k_j)/2. \qquad (2.33)$$

This result, together with Eq. 2.29, allows to establish a functional relation between the two-site discord $D(i : j)$ and the two mode discord $D(k_i : -k_i)$.

On the other hand, the line $n = 1$ is an *iso-correlation* line [98]: since $a = 1/2 = const$, and therefore the momentum particle density $\langle n_{k_j} \rangle$, and all the correlations between subsystem in the momentum picture are maximal and constant in the whole phase II. In particular, they are constant at the transition II→III, therefore this transition cannot be identified by studying the derivatives of the correlation measures in $k$ space. On the other hand, at the transition II→IV there is a sudden change in all correlations that discontinuously drop to zero in correspondence of the insulating phase that is characterized by a ground state which is factorized also in the momentum space i.e., $|\psi\rangle = \otimes_{k_j} |\sigma\rangle_{k_j}$, with $\sigma = \uparrow, \downarrow$. We therefore see that the two-point transitions II→III and II→IV can be distinguished even in momentum space, and this reinforces the result obtained in the previous section in the direct lattice picture, where the difference between the two transitions is highlighted by the behavior of $\mathcal{J}(i : j)$.

### 2.3.5 Monogamy of quantum discord

The study of the ground state properties of the extended Hubbard model can be fruitfully extended in order to assess a relevant quantum information problem: the relations between entanglement and discord. In this framework an interesting question to address is whether the discord may satisfy a *monogamy* relation like (1.104). As we know from §1.3.5, this relation cannot be satisfied for all states (otherwise the quantum discord would vanish for all separable states). Nevertheless, it is still possible that the relation holds for a given class of states. In fact, the satisfaction/violation of a monogamy inequality highlights the structure of multipartite correlations in the state,

as we will now show by focusing on the ground states in region III and I.
In Region III, the $\eta$-pairs states coincide with class of two-qubits permutation-invariant states that can be written as

$$|\psi(N_d, L)\rangle = \left( \begin{array}{c} L \\ N_d \end{array} \right)^{-1} \sum_P P|N_d, L - N_d\rangle \tag{2.34}$$

where $\left( \begin{array}{c} L \\ N_d \end{array} \right)$ is the binomial coefficient, $|N_d, L - N_d\rangle$ is a fixed state with a given sequence of $N_d$ ones (pairs) and $L - N_d$ zeros (empty sites), and the sum is taken over all possible permutations $P$s (the 3-partite $W$ state belongs to this class of states). For states of these form, at fixed $N_d < L$ the single and two site reduced density matrices can be easily evaluated from (2.8) and (2.9) and they are equal for all sites, i.e., $\rho_i = \rho_1$ and $\rho_{ij} = \rho_2$ and the discord can be evaluated as described in the previous sections. Since $|\psi(N_d, L)\rangle$ is a pure state the discord between one site and the rest of the chain is equal for all sites $D(1|2, \cdots, L)) = D_1$ and it simply coincides with the entanglement between the site and the rest of the chain, $D_1 = S(\rho_1)$. Thus $D_1$ is a function of $n_d$ only and and it is bounded by 1. Both for finite $N_d, L$ and in the TDL the two point discord $D(1 : j) = D_2(n_d, L)$ does not depend on $j$ and therefore $\sum_j D_2(n_d, L) = (L - 1)D_2(n_d, L)$. As already mentioned, similar arguments can be applied to the concurrence $K$: with $n_s = 0$ the dependence on $|i-j|$ disappears and, in particular for large $L$ one has $K(\varrho_{1,j}) \approx 1/L$; for finite $N_d, L$ the concurrence is small but different from zero, and the monogamy property is always satisfied by the squared concurrence. On the other hand, a direct evaluation of the above quantities shows that $\forall N_d$ and $L \geq 3$ one has

$$R_M \equiv D_1/[(L - 1)D_2(n_d, L)] < 1 \tag{2.35}$$

In Fig. 2.8 (left panel) we show the *monogamy ratio* $R_M$ for $N_d = 1/L, \lfloor L/2 \rfloor / L$ and different values of $L$. While a general analytical demonstration of this result is not straightforward, one can note that in the case of permutation-invariant states, for any fixed value of $n_d$ it is always possible to find an infinite number of states $|\psi(N_d, L)\rangle$ with $L = N_d/n_d$ and such that $D_1 \leq (L - 1)D_2(n_d, L)$, i.e., the monogamy relation is violated. Indeed, while $D_1$ just depends on $n_d$, $D_2(N_d, L)$ is a decreasing function of $L$ which is lower bounded by its TDL expression (2.29). Therefore all the states for which $L = N_d/n_d$ satisfies the relation $D_1 \leq (L - 1)D_2^{TDL}$ will violate the monogamy relation.
As for the TDL, while $K_{1,j} \to 0$, $D_s$ is constant at fixed $n_d$ and $D_2 = D_2^{TDL}$ as in (2.29) and therefore $R_M \to 0$.
Since the above arguments apply to a whole class of permutation invariant $n$-partite two-qubit states (2.34), we can state in full generality a property of two-qubit discord: *for $n$-partite states ($n \geq 3$) discord can be polygamous both in presence (for finite $N_d, L$) and in absence (TDL) of two point entanglement.*

While it is tempting to relate the violation of a monogamy relation by the discord to the presence of those correlations that are typical of $\eta$-pairs states, and that give rise in the TDL to ODLRO, our model shows that there are other classes of states in which

such violation can occur. Indeed, in Fig. 2.8 (right panel) we report the ratio $R_M$ for the ground state of region I, which reads:

$$|\psi(N_s, L)\rangle = |k_1, \ldots, k_{N_s}\rangle = \tilde{X}^{10}_{k_1} \cdots \tilde{X}^{10}_{k_{N_s}} |\text{vac}\rangle \tag{2.36}$$

i.e., contains $N_s$ fermions in momentum eigenmodes $(k_1, \ldots, k_{N_s})$, created by action of the Fourier transform of the Hubbard projection operator $\tilde{X}^{10}_k$ onto the vacuum. The results refer to the TDL case and they show that for such states, although $D(i : j)$ does depend on the distance $|i - j|$, the monogamy property is violated by the two point discord in proximity of the QPT I $\rightarrow$ IV. This feature reflects the fact discussed in Section 2.3.1 that when $\mu \rightarrow 0$, there is a spreading of the quantum correlations over the whole chain. Indeed, the violation of the monogamy condition starts in correspondence of $\mu \approx -0.2$, where the entanglement has already started to spread along the chain and has a finite range ($\mathcal{R}_N$ diverges only at the transition).
This result has two interesting consequences. On one hand the ground states in region I show that, depending on the parameters that define them ($n_s$ in this case) for the same class of states the discord may or may not violate a monogamy relation [32]. On the other hand the behavior of the discord allows to refine the description about region I carried out in [97]. There, by means of the entanglement and correlation ratio it was pointed out that the ground states in region I have a truly multipartite character in the center of the region, while when approaching the transition the weight of the two-point correlations starts to increase; and this agrees with the two-point character of this transition. Here this picture is revealed by the violation of the monogamy property displayed by the discord: In order to prepare the two-point transition at $\mu = 0$, the system reorganizes its correlations in such a way that their two point character starts to prevail; one can therefore identify the point in which this process starts with the value of the parameters i.e., $\mu \approx -0.2$ at which the monogamy property is violated by the discord.

We finally compare the two above cases in terms of the violation of the monogamy property. Here the key observation is the different kind of violation exhibited by the discord. In region I the discord can be polygamous but the amount of quantum correlations shared by a single site with the other sites of the chain is finite i.e., $0 < R_M < 1$ for $\mu \neq 0$ and it vanishes at the transition $\mu = 0$ because $D_1 \rightarrow 0$, while $\sum_j D(i : j)$ tends to a finite value. On the contrary, for $\eta$-pair states the violation has a completely different nature: Each site can be equally correlated with all the other sites of the chain: $R_M \equiv 0 \,\forall\, n_d$. This difference is indeed rooted in the presence of ODLRO in the TDL and in the previously found relation between discord and ODLRO. This kind of violation is associated by the disappearance of the two-sites entanglement, while for the state in region I, the violation occurs in presence of bipartite entanglement.
The above results allows to give a general statement about quantum discord for multipartite pure states: It can be non-monogamous both in presence and in absence of bipartite entanglement. However the violation of the monogamy property can be maximal when ODRLO is established in the TDL and no bipartite entanglement is present in the state.

## 2.4 Conclusions

In this chapter we have addressed several important questions related to the ground state correlation properties of a reference fermionic model, the bond-charge Hubbard model. We have applied quantum discord and classical correlations to study how these relate to quantum phase transitions displayed by the model. By means of analytical and numerical analysis we have derived and analyzed the expressions of discord and classical correlations for two-qubits and two-qutrits systems both in the direct lattice and in momentum space. Our results allow to describe the different quantum phase transitions in terms of the divergences of the various correlation measures. As shown in [95, 97, 98] the transitions can be classified on the basis of the relevance of the two-point and multipartite correlations involved. At variance with other entanglement measures [95], such as negativity, discord (and classical correlations) exhibits the expected non analyticities that define the two-point transitions. Moreover, the comparison of their behavior allows to discriminate between two apparently similar kind of two-point transitions. In particular, a careful study of the contributions in which classical correlations can be decomposed gives the possibility to detect the presence (disappearance) of the off diagonal long range order (ODLRO) and to identify its consequences at the various transitions.
Furthermore, the study of the discord between two generic sites $i, j$ and two momenta modes $k_i, -k_i$ allows to establish a direct relation between ODLRO and the two-site/momenta modes discord, which turns out to be a monotonic function of ODLRO. This result is remarkable, since in the TDL no two-site entanglement is present in this states. By means of the same analysis it is possible to establish a functional relation between the two-sites discord in direct space $D(i : j)$ and two-modes discord in momentum space $D(k_i : -k_i)$.

The study of $D(i : j)$ for $\eta$-pairs states is also important for describing the behavior of the discord with respect to the *monogamy* property. [22, 23]. Indeed, the $\eta$-pairs states are isomorphic to a relevant class of permutational invariant multipartite qubit states. While in the finite size case, all the states in the class display non-zero two-qubit entanglement, in the TDL the latter vanishes. However, in both cases we have shown that two-qubit discord is in general different from zero and furthermore it violates a monogamy relation. Finally, we have shown for another class of states, the non-interacting fermionic ground states in region I, the discord can be polygamous depending on the values of the parameters. The main difference between the two class of states analyzed resides in the kind of violation of the monogamy property: only for the $\eta$-pair states the single qubit can be arbitrarily correlated with all the other infinite sites, thus leading to a maximal violation of the monogamy property. This fact is rooted in the presence of ODLRO in these states and in the direct relation between ODLRO and discord.

Our results confirm that the application of quantum information concepts to condensed matter systems can fruitfully lead to a precise description of the role of correlations in quantum phase transitions and at the same time to the development of useful relations that shed new light on the nature of quantum correlations as measured by discord.

# Chapter 3

# Non-Gaussian quantum discord for Gaussian states

## 3.1 introduction

In the realm of continuous variable (CV) systems, initial research efforts on quantum discord have focused on Gaussian measurements. The Gaussian quantum discord, proposed in [59, 60], is defined by restricting the minimization involved in the definition of discord to the set of Gaussian POVMs [125] and it can be analytically computed for Gaussian states. Its behavior in noisy channels has been studied in Ref. [109, 110] – where it was shown that it is more robust than entanglement to the decorrelating effect of independent baths and more likely to yield non-zero asymptotic values in the case of a common bath – while its relation to the synchronization properties of detuned, correlated oscillators has been analyzed in Ref. [80].

It is natural to investigate CV quantum discord beyond Gaussian measurements: non-Gaussian ones may indeed allow for a stronger minimization of discord, and in this case the Gaussian discord would be an overestimation of the true discord. Here we focus on Gaussian states and ask whether Gaussian measurements are optimal in this case, i.e., *whether the Gaussian discord is the true discord for Gaussian states*. This question is relevant for two main reasons: On one hand, if discord is a truly useful resource for quantum information protocols [71, 82], then it is crucial to have a reliable estimate of its actual value. On the other hand, from a fundamental point of view it is important to establish how different kinds of measurements can affect correlations in quantum states. A further motivation comes from the fact that indeed for some non-Gaussian states e.g., CV Werner states, non-Gaussian measurements such as photon counting have been proven to lead to a better minimization [62].

The optimality of Gaussian measurements has already been proven analytically for two-mode Gaussian states having one vacuum normal mode [60], by use of the Koashi-Winter relation (1.56), but no analytic argument is available in the general case. We address the question numerically, for the case of two-modes, upon considering two large classes of Gaussian states, the squeezed thermal states (STS) and the mixed thermal

states (MTS), and allowing for a range of experimentally feasible non-Gaussian measurements based on orthogonal bases: the number basis, the squeezed number basis, the displaced number basis. As a result, we provide evidence that Gaussian quantum discord is indeed optimal for the states under study. In addition, we also investigate the CV geometric discord [63], comparing the case of Gaussian and non-Gaussian measurements.

This work is structured as follows. In § 3.2 we review Gaussian quantum discord; in § 3.3 we thoroughly describe the basic question we want to address in this work and introduce non-Gaussian measurements and non-Gaussian discord; in § 3.4, 3.5, 3.6, we present our key results concerning non-Gaussian discord upon measurements in the number basis, squeezed number basis and displaced number basis; in § 3.7 we discuss the behavior of non-Gaussian geometric discord; finally, § 3.8 closes the paper discussing our main conclusions.
This chapter essentially reproduces our paper [64], previously published in Physical Review A.

## 3.2 Gaussian discord

In the realm of continuous-variable systems, the *Gaussian discord* [59, 60] is defined by restricting the set of possible measurements in Eq. (1.21) to the set of Gaussian POVMs [125], and minimizing only over this set. The Gaussian discord can be analytically evaluated for two-mode Gaussian states, where one mode is probed through (single-mode) Gaussian POVMs. The latter can be written in general as

$$\Phi_B^{\mathcal{G}}(\eta) = \pi^{-1} D_B(\eta) \varrho_M D_B^\dagger(\eta)$$

where $D_B(\eta) = \exp(\eta b^\dagger - \eta^* b)$ is the displacement operator, and $\varrho_M$ is a single-mode Gaussian state with zero mean and covariance matrix $\sigma_M = \begin{pmatrix} \alpha & \gamma \\ \gamma & \beta \end{pmatrix}$. Two-mode Gaussian states can be characterized by their covariance matrix $\sigma_{AB} = \begin{pmatrix} A & C \\ C^T & B \end{pmatrix}$. By means of local unitaries that preserve the Gaussian character of the state, i.e. local symplectic operations, $\sigma_{AB}$ may be brought to the so-called standard form, i.e. $A = \mathrm{diag}(a, a)$, $B = \mathrm{diag}(b, b)$, $C = \mathrm{diag}(c_1, c_2)$. The quantities $I_1 = \det A$, $I_2 = \det B$, $I_3 = \det C$, $I_4 = \det \sigma_{AB}$ are left unchanged by the transformations, and are thus referred to as symplectic invariants. The local invariance of the discord has therefore two main consequences. On the one hand, correlation measures may be written in terms of symplectic invariants only. On the other hand, we can restrict to states with $\sigma$ already in the standard form. Before the measurement we have

$$S(\varrho_{AB}) = f(d_+) + f(d_-), \tag{3.1}$$

$$S(\varrho_A) = f(\sqrt{I_1}),\ S(\varrho_B) = f(\sqrt{I_2}) \tag{3.2}$$

where $f[x] = (x+1/2)\log(x+1/2) - (x-1/2)\log(x-1/2)$ and $d_\pm$ are the symplectic eigenvalues of $\varrho_{AB}$ expressed by $d_\pm^2 = 1/2[\Delta \pm \sqrt{\Delta^2 - 4I_4}$, $\Delta = I_1 + I_2 + 2I_3$. After the measurement, the (conditional) post-measurement state of mode $A$ is a Gaussian

state with covariance matrix $\sigma_P$ that is independent of the measurement outcome and is given by the Schur complement $\sigma_P = A - C(B+\sigma_M)^{-1}C^T$. The Gaussian discord is therefore expressed by

$$D^{\mathcal{G}}(A|B) = f(\sqrt{I_2}) - f(d_-) - f(d_+) + \min_{\sigma_M} f(\det\sqrt{\sigma_P}) \tag{3.3}$$

where we use two key properties: i) the entropy of a Gaussian state depends only on the covariance matrix, and ii) the covariance matrix $\sigma_P$ of the conditional state does not depend on the outcome of the measurement. The minimization over $\sigma_M$ can be done analytically. For the relevant case of states with $C = \text{diag}(c, \pm c)$, including STS and MTS (see below), the minimum is obtained for $\alpha = \beta = 1/2, \gamma = 0$ i.e. when the covariance matrix of the measurement is the identity. This corresponds to the coherent state POVM, i.e. to the joint measurement of canonical operators, say position and momentum, which may be realized on the radiation field by means of heterodyne detection. For *separable* states the Gaussian discord grows with the total energy of the state and it is bounded, $D^{\mathcal{G}} \leq 1$; furthermore, we have $D^{\mathcal{G}} = 0$ iff the Gaussian state is in product form $\varrho_{AB} = \varrho_A \otimes \varrho_B$.

## 3.3 Non-Gaussian discord

In this work we consider Gaussian states, and ask whether non-Gaussian measurements can allow for a better extraction of information than Gaussian ones, hence leading to lower values of discord.

The optimality of Gaussian measurements has been already proven for a special case [60]: that of two-mode Gaussian states having one vacuum normal mode. Indeed any bipartite state $\varrho_{AB}$ can be purified, $\varrho_{AB} \Longrightarrow |\psi\rangle_{ABC}$; then, the Koashi-Winter relation (1.56),

$$D(A|B) = E_F(A:C) + S(\varrho_B) - S(\varrho_{AB}) \tag{3.4}$$

relates the quantum discord $D$ and the entanglement of formation $E_F$ of reduced states $\varrho_{AB}$ and $\varrho_{AC}$ respectively. Given a (mixed) two-mode Gaussian state $\varrho_{AB}$, there exists a Gaussian purification $|\psi\rangle_{ABC}$. In general, the purification of $\varrho_{AB}$ requires two additional modes, so that $\varrho_{AC}$ is a three-mode Gaussian state. In the special case when one normal mode is the vacuum, the purification requires one mode only. In this case, $\varrho_{AC}$ represents a two-mode Gaussian state and $E_F(A:C)$ can be evaluated [24]. From $E_F(A:C)$, by means of Eq. ([39]), one can obtain $D(A|B)$ (the exact discord) and a comparison with $D^{\mathcal{G}}(A|B)$ proves that $D(A|B) = D^{\mathcal{G}}(A|B)$.

In the general case, there is no straightforward analytical way to prove that Gaussian discord is optimal. Therefore, we perform a numerical study. Since taking into account the most general set of non-Gaussian measurements is an extremely challenging task, one can rather focus on a restricted subset. We choose to focus on a class of measurements that are realizable with current or foreseeable quantum optical technology. These are the the projective POVMs, $\Pi = \{P_n\}$, represented by the following orthogonal measurement bases:

$$P_n = D(\alpha)S(r)|n\rangle\langle n|S(r)^\dagger D(\alpha)^\dagger, \quad n = 0, \cdots, \infty \tag{3.5}$$

where $S(r) = \exp\left(-r^* \frac{a^2}{2} - r\frac{(a^\dagger)^2}{2}\right)$ and $D(\alpha) = \exp(\alpha a^\dagger - \alpha^* a)$ are respectively the single-mode squeezing and displacement operators [150]. The set of projectors in (3.5) is a POVM for any fixed value of $\alpha$ and $r$. If $\alpha = r = 0$ we have the spectral measure of the number operator, describing ideal photon counting $P_n = |n\rangle\langle n|$. If $\alpha > 0, r = 0$ we are projecting onto displaced number states [151], if $\alpha = 0, r > 0$ onto squeezed number states [153, 154, 155]. While more general non Gaussian measurements are in principle possible, the class (3.5) encompasses most of the measurements that can be realistically accessed.

In the following, we will evaluate the non-Gaussian quantum discord defined by

$$D^{\mathcal{NG}}(A|\Pi^B) = f(\sqrt{I_2}) - f(d_-) - f(d_+) + S^{\mathcal{NG}}(A|\Pi^B) \tag{3.6}$$

where the non-Gaussian measurements are given by Eq. (3.5) above. For the non-Gaussian conditional entropy we have

$$\begin{aligned} S^{\mathcal{NG}}(A|\Pi^B) &= \sum_n p_n S(\varrho_{A|n})\,, \\ \varrho_{A|n} &= \frac{1}{p_n}\mathrm{Tr}_B[P_n \varrho_{AB} P_n]\,, \\ p_n &= \mathrm{Tr}_{AB}[P_n \varrho_{AB} P_n] \end{aligned} \tag{3.7}$$

In the following we consider two classes of Gaussian states in order to assess the performances of the above measurements. These are the two-mode squeezed thermal states (STS) [146, 147, 148]:

$$\varrho = S(\lambda)\nu_A(N_1) \otimes \nu_B(N_2) S(\lambda)^\dagger \tag{3.8}$$

and the two-mode mixed thermal states (MTS) [149]

$$\rho = U(\phi)\nu_A(N_1) \otimes \nu_B(N_2) U(\phi)^\dagger \tag{3.9}$$

where $\nu_X(N_i)$ are 1-mode thermal states ($X = A, B$) with thermal photon number $N_i$ ($i = 1, 2$); $S(\lambda) = \exp\{\lambda(a_A^\dagger a_B^\dagger - a_A a_B)\}$ is the two-mode squeezing operator (usually realized on optical modes through parametric down-conversion in a nonlinear crystal); and $U(\phi) = \exp\{\phi(a_A^\dagger a_B - a_A a_B^\dagger)\}$ is the two-mode mixing operator (usually realized on optical modes through a beam splitter).

In particular, in the following we will focus on the simplest case of symmetric STS with $N_1 = N_2 \in [10^{-5}, 1]$ $\lambda \in [0, 0.5]$. As for MTS, we cannot consider the symmetric case (since if $N_1 = N_2$ then the mutual information vanishes and there are no correlations in the system), therefore we consider the unbalanced case and focus on $\phi \in [0, \pi/2]$ and $N_1, N_2 \in [10^{-5}, 1]$.

## 3.4 Number basis

Let $P_n = |n\rangle\langle n|$. In this case, the post-measurement state is

$$\varrho_{A|n} = \otimes|n\rangle\langle n| = \left(\sum_{h,k} \varrho_{(h,k),(n,n)}|h\rangle\langle k|\right) \otimes |n\rangle\langle n| \tag{3.10}$$

and we have the following expression for the density matrix elements

$$\varrho_{(h,k),(n,n)} = \sum_{s,t} p_s^{th}(N_1) p_t^{th}(N_2) O_{hn}(st) O_{kn}^*(st) \tag{3.11}$$

where $p_s^{th}(N) = N^s\ (1+N)^{-(s+1)}$ and $O_{hn}(st) = \langle hn|O|st\rangle$ with $O = S(\lambda), U(\phi)$ for STS and MTS respectively. The post-measurement state

$$\varrho_{A|n} = \mathrm{Tr}_B[\mathbb{I}\otimes|n\rangle\langle n|\ \varrho\ \mathbb{I}\otimes|n\rangle\langle n|]/p_n \tag{3.12}$$

(here, $p_n = \mathrm{Tr}[\varrho\mathbb{I}\otimes|n\rangle\langle n|]$) of STS and MTS after local measurement in the number basis is diagonal,

$$\langle h|\varrho_{A|n}|k\rangle = \delta_{hk}\ \varrho_{(h,h),(n,n)} \tag{3.13}$$

**Proof.** We have indeed:

$$\varrho = \sum_{s,t} p_s^{th}(N_1) p_t^{th}(N_2) O|st\rangle\langle st|O^\dagger =$$

$$= \sum_{(h,n),(k,m)} |hn\rangle\langle km| \left( \sum_{s,t} p_s^{th} p_t^{th} O_{hn}(st) O_{km}^*(st) \right) \tag{3.14}$$

where $p_s^{th}(N) = N^s\ (1+N)^{-(s+1)}$ where $O_{hn}(st) = \langle hn|O|st\rangle$ and $O_{km}^*(st) = \langle st|O^\dagger|km\rangle = \langle km|O|st\rangle^*$, where $O = S(\lambda)$, $O = U(\phi)$ for STS and MTS respectively. The post measurement states can be written as:

$$\varrho_{A|n}\otimes|n\rangle\langle n| = \left( \sum_{h,k} \varrho_{(h,k),(n,n)}|h\rangle\langle k| \right) \otimes |n\rangle\langle n| \tag{3.15}$$

and therefore we need to evaluate the matrix elements

$$\varrho_{(h,k),(n,n)} = \sum_{s,t} p_s^{th} p_t^{th} O_{hn}(st) O_{kn}^*(st) \tag{3.16}$$

The elements of the two-mode squeezing operator are given in [155] (Eq. 22):

$$\langle hn|S(\lambda)|st\rangle = \delta_{t+h,s+n} f^\lambda(h,n,s,t) = \delta_{t+h,s+n} \times$$
$$\sum_{a=0}^{min(s,t)} \sum_{b=0}^{min(h,n)} (-1)^{a+b} (sech\lambda)^{t+h-a-b-1} \mu^{a-b+h-s} \times$$
$$\frac{(t+h-a-b)![s!t!h!n!]^{1/2}}{a!(t-a)!(s-a)!b!(n-b)!(h-b)!} \tag{3.17}$$

where $\mu = e^{\lambda}$, while the elements of the two-mode mixing operator

$$\langle hn|U(\phi)|st\rangle = \delta_{h+n,s+t} \sum_{a=\max\{0,h-t\}}^{\min\{h,s\}} A_{a\ h-a}^{s\ t}$$

$$= \delta_{h+n,s+t} \sum_{a=\max\{0,h-t\}}^{\min\{h,s\}} \sqrt{\frac{h!(s+t-h)!}{s!t!}}(-1)^{h-a} \times$$

$$\binom{s}{a}\binom{t}{h-a} \sin\phi^{s+h-2a} \cos\phi^{t+2a-h} \tag{3.18}$$

In order to evaluate (3.16), we need $O_{hn}(st)O_{kn}^{*}(st)$. Due to the $\delta$'s appearing in both (3.17) and (3.18), the following relations must be satisfied:

$$\begin{aligned} t-s &= n-h \\ t-s &= n-k. \end{aligned}$$

and this implies $h = k$; therefore the post-measurement state is diagonal in the number basis:

$$(\varrho_{A|n})_{h,k} = \delta_{h,k} \sum_{s,t} p_s^{th}(N_1) p_t^{th}(N_2) |O_{hk}(st)|^2 \tag{3.19}$$

*QED.*

As a consequence, the entropy of the post-measurement state can be expressed as: $S(\varrho_n^A) = H(\{\varrho_{(h,h),(n,n)}\}) = H(\vec{p}(A|B=n))$ where $H$ is the Shannon entropy of the conditional probability $\vec{p}(A|B=n) = (p(0,n), p(1,n), \cdots)/p_n$, and therefore the overall conditional entropy can be simply expressed in terms of the photon number statistics:

$$\begin{aligned} S(A|\{P_n\}) &= \sum_n p_n h(\vec{p}(A|B=n)) = \\ &= h(\vec{p}(A,B)) - h(\vec{p}(B)) \end{aligned} \tag{3.20}$$

with $\vec{p}(A,B) = \{p(A=n, B=m)\}$ and $\vec{p}(B) = \{p(B=n)\}$. In view of this relation, the only elements of the number basis representation of the density matrix $\varrho$ that are needed are the diagonal ones, i.e. one has to determine the photon number statistics for the two-mode STS or MTS state. The required matrix elements can be obtained in terms of the elements of the two-mode squeezing and mixing operators (see Eqs. (3.17) and (3.18) above). One has of course to define a cutoff on the dimension of the density matrix. This can be done upon requiring that the error on the trace of each state considered be sufficiently small: $\epsilon_{err} = 1 - \mathrm{Tr}\varrho \leq 10^{-3}$.

We have compared Gaussian and non-Gaussian quantum discord (with the non-Gaussian measurements corresponding to photon number measurements) for STS and MTS states with a wide range of squeezing, mixing and thermal parameters. In Fig. 3.1 we show results for STS with varying $\lambda$ and $N_1 = N_2 = 10^{-2}$, $N_1 = N_2 = 1$. The

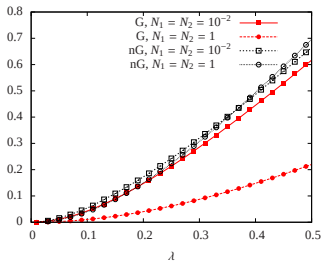


Figure 3.1: Gaussian and non-Gaussian quantum discord for STS as a function of $\lambda$, for different values of $N_1 = N_2$

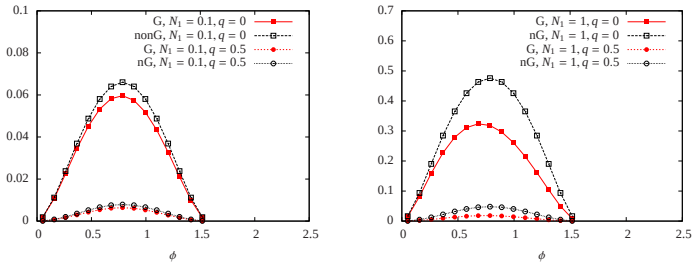


Figure 3.2: Gaussian and non-Gaussian quantum discord for MTS states as a function of $\phi$ for different values of $N_1$ and $q = N_2/N_1$

key result is that the non-Gaussian quantum discord is always greater than its Gaussian counterpart for all values of $N_1$ and $\lambda$. The gap grows with increasing $N_1$ and $\lambda$. In Fig. 3.2 we show results for MTS $N_1 = \{0.1, 1\}$ and $q = N_2/N_1 = \{0, 0.1, 0.4, 0.5\}$. Also in this case, the non-Gaussian discord is always higher than the Gaussian one. Both results indicate that the Gaussian (heterodyne) measurement is optimal for STS and MTS states, at least compared to photon counting, in the sense that it allows for a better extraction of information on mode $A$ by a measurement on mode $B$.

## 3.5 Squeezed Number basis

We now analyze the case of non-Gaussian measurements represented by the squeezed number basis $|n_r\rangle\langle n_r| = S(r)|n\rangle\langle n|S(r)^\dagger$, where $S(r) = \exp\left(-r^* \frac{a^2}{2} - r\frac{(a^\dagger)^2}{2}\right)$ is the single mode squeezing operator. A local measurement in the squeezed number basis is equivalent to a measurement in the number basis, performed on a locally squeezed state. In formulas, the probability of measuring $n_r$ on one subsystem when the state is the $\varrho$ is

$$\begin{aligned} p_\varrho(n_r) &= \mathrm{Tr}(\mathbb{I}\otimes|n_r\rangle\langle n_r|\varrho) = \mathrm{Tr}(\mathbb{I}\otimes|n\rangle\langle n|S^\dagger(r)\varrho S(r)) = \\ &= \mathrm{Tr}(\mathbb{I}\otimes|n\rangle\langle n|\varrho^r) = p_{\varrho^r}(n) \end{aligned} \tag{3.21}$$

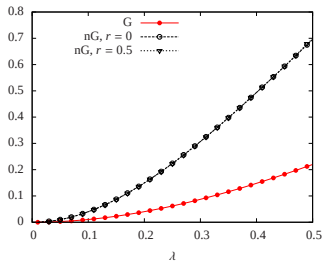


Figure 3.3: Gaussian and non-Gaussian quantum discord for STS with $N_1 = 1$ as a function of $\lambda$ and for different values of local squeezing $r$

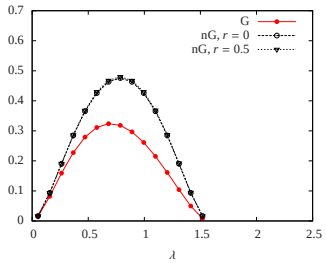


Figure 3.4: Gaussian and non-Gaussian quantum discord for MTS states for $N_1 = 1$, $N_2 = 0$ as a function of $\phi$ and for different values of local squeezing $r$

i.e., is equal to the probability of measuring $n$ on the locally squeezed state $\varrho^r = S(r)\varrho S(r)^\dagger$, and the relative post-measurement state is

$$\begin{aligned} \varrho_{A|n_r} &= \mathrm{Tr}_B[\mathbb{I}\otimes|n_r\rangle\langle n_r|\varrho\mathbb{I}\otimes|n_r\rangle\langle n_r|]/p_\varrho(n_r) = \\ &= \mathrm{Tr}_B[\mathbb{I}\otimes|n\rangle\langle n|\varrho^r\mathbb{I}\otimes|n\rangle\langle n|]/p^r_\varrho(n) = \varrho^r_{A|n} \end{aligned} \tag{3.22}$$

The general idea is that measurements on a state $\varrho$ in a basis that is obtained by performing a unitary (Gaussian) operation $V$ on the number basis $|n\rangle\langle n|$ can be represented as measurements on the number basis of a modified state $\varrho_V = V\varrho V^\dagger$ on which the local unitary operation acts.
In the case of the squeezed number basis, the post-measurement state is not diagonal, therefore the reasoning leading to Eq. (3.20) does not hold. The post-measurement state matrix elements $(\varrho^r_{A|n})_{h,k} = \varrho_{(h,k),(n,n)}$ can be obtained directly by evaluating the expression (3.11) where now the expression $O_{hk}(st) = \langle hk|O|st\rangle$ (where $O = S(\lambda), U(\phi)$) must be replaced with

$$O'_{hk}(st) = \langle hk|S(r)O|st\rangle = \sum_q \langle k|S(r)|q\rangle\langle hq|O|st\rangle$$

and the elements of the single mode squeezing operator are given in [156] (Eq. 20) or in [153] (Eq. 5.1).

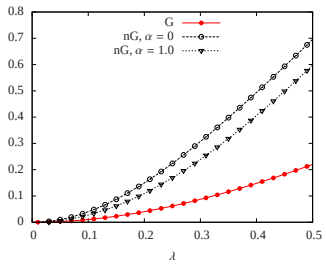


Figure 3.5: Gaussian and non-Gaussian quantum discord for STS with $N_1 = 1$ as a function of $\lambda$ and for different values of local displacement $\alpha$

We have evaluated the Gaussian and non-Gaussian quantum discord for STS and MTS states with a wide range of two-mode squeezing and thermal parameters. Non-Gaussian measurements are done in the squeezed photon number basis, $P_n = S(r)|n\rangle\langle n|S(r)^\dagger$ with variable $r \in [0, 0.5]$. The effect of local squeezing on non-Gaussian quantum discord is negligible in the whole parameter range under consideration: we compare the non-Gaussian discord for different values of $r$ and find that all curves collapse. This can be seen in Fig. 3.3 and Fig. 3.4 where plot the behavior for $N_1 = N_2 = 0.01$ (STS) and $N_1 = 1, N_2 = 0$ (MTS). The same behavior is observed in the whole parameter range under investigation. We have verified numerically that the post-measurement states of mode $A$ $\varrho^r_{A|n}$ are not equal as $r$ varies (i.e., the post-measurement states corresponding to measurement result $n_r$ change with $r$), yet the sum $\sum_n p_n S(\varrho^r_{A|n})$ is equal for all values of $r$ under investigation. Therefore, the squeezing in the measurement basis has no effect on the discord, at least for the values of squeezing considered: in particular, it cannot afford a deeper minimization than that obtained without local squeezing. This indicates that the heterodyne measurement remains optimal also with respect to measurement in the squeezed number basis.

## 3.6 Displaced Number basis

We finally analyze the case of non-Gaussian measurements represented by the displaced number basis $|n_\alpha\rangle\langle n_\alpha| = D(\alpha)|n\rangle\langle n|D(\alpha)^\dagger$, where $D(\alpha) = \exp(\alpha a^\dagger - \alpha^* a)$ is the single mode displacement operator. According to the general considerations above, a local measurement in the displaced number basis is equivalent to a measurement in the number basis, performed on a locally displaced state $\varrho^\alpha$. As in the case of the squeezed number basis, the post-measurement state is not diagonal and we need all matrix elements $(\varrho^\alpha_{A|n})_{h,k} = \varrho_{(h,k),(n,n)}$. They can be obtained directly by evaluating the expression (3.11) where the expression $O_{hk}(st) = \langle hk|S(\lambda)|st\rangle$ (where $O = S(\lambda), U(\phi)$) must be substituted with $O'_{hk}(st) = \langle hk|D(\alpha)O|st\rangle = \sum_q \langle k|D(\alpha)|q\rangle\langle hq|O|st\rangle$, and the elements of the single mode displacement operator are given in [145] (Eq. 1.46).

The evaluation of the non-Gaussian quantum discord can be simplified by first noticing that one can consider real values of $\alpha$ only. Indeed, we can prove that the

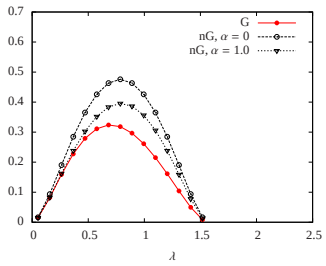


Figure 3.6: Gaussian and non-Gaussian quantum discord for MTS states for $N_1 = 1$, $N_2 = 0$ as a function of $\phi$ and for different values of local displacement $\alpha$

quantum discord only depends on the modulus $|\alpha|$. Before proceeding to the detailed proof (that requires the characteristic function formalism), let us just sketch the argument. Consider $\varrho^{\alpha}_{A|n}$, the post-measurement state of mode $A$ after measurement result $n_\alpha$ is obtained on $B$. If we change the phase of $\alpha$, $\alpha \to \alpha' \equiv e^{i\theta}\alpha$ we find that

$$\varrho^{\alpha'}_{A|n} = U \varrho^{\alpha}_{A|n} U^{\dagger} \tag{3.23}$$

where $U$ is a unitary operation corresponding to a simple quadrature rotation

$$a_A \to a_A e^{i\theta} \quad a_A^{\dagger} \to a_A^{\dagger} e^{-i\theta} \tag{3.24}$$

Therefore, we have $\varrho^{\alpha'}_{A|n} \neq \varrho^{\alpha}_{A|n}$, but $\varrho^{\alpha}_{A|n}$ and $\varrho^{\alpha'}_{A|n}$ have the same spectrum, since they are related by a unitary. Therefore, the entropy of the reduced post-measurement state $\varrho^{\alpha}_{A|n}$ does not depend on the phase of $\alpha$ but just on $|\alpha|$. If follows that the non-Gaussian quantum discord of $\varrho^{\alpha}$ does not depend on the phase of $\alpha$.

**Proof.** We show that the (non-Gaussian) discord in the displaced number basis does not depend on the phase of displacement for STS and MTS. The arguments is best given in the characteristic function representation of the states [145]. The STS and MTS states have a Gaussian characteristic function $\chi[\varrho](\mathbf{\Lambda}) = \exp(-\frac{1}{2}\mathbf{\Lambda}^T \sigma \mathbf{\Lambda})$ where $\mathbf{\Lambda} = \frac{1}{\sqrt{2}}(\mathrm{Re}\lambda_A, \mathrm{Im}\lambda_A, \mathrm{Re}\lambda_B, \mathrm{Im}\lambda_B)$ and the covariance matrix is given by

$$\sigma = \begin{pmatrix} A & C \\ C^T & B \end{pmatrix} = \begin{pmatrix} a & 0 & c & 0 \\ 0 & a & 0 & \pm c \\ c & 0 & b & 0 \\ 0 & \pm c & 0 & b \end{pmatrix} \tag{3.25}$$

where $\pm c$ is $-c$ in the case of STS and $+c$ in the case of MTS. For STS we have

$$\chi[\varrho](\lambda_A, \lambda_B) = \exp(-a|\lambda_A|^2 - b|\lambda_B|^2 + 2c\mathrm{Re}[\lambda_A \lambda_B]) \tag{3.26}$$

while for MTS the same expression holds upon changing $2c\mathrm{Re}[\lambda_A\lambda_B] \to 2c\mathrm{Re}[\lambda_A^* \lambda_B]$. In the following, we shall carry on the argument for STS, but the MTS case is fully equivalent. If we perform a displacement on one mode, $\varrho \to D(\alpha)\varrho D^{\dagger}(\alpha) \equiv \varrho^{\alpha}$, the

effect on the characteristic function is easy to evaluate. Using the relation $D(\alpha)D(\lambda)D^\dagger(\alpha) = D(\lambda)\exp(-2i\text{Im}[\lambda\alpha^*])$ [145] we obtain

$$\chi[\varrho^\alpha](\lambda_A,\lambda_B) = \chi[\varrho](\lambda_A,\lambda_B)\exp(-2i\text{Im}[\lambda_B\alpha^*]) \tag{3.27}$$

Suppose we perform a measurement on mode $B$ in the number basis $\{P_n = |n\rangle\langle n|\}$. The post-measurement state of mode $A$ is $\varrho^\alpha_{A|n} = \frac{1}{p_n}\text{Tr}_B[\varrho^\alpha\Pi_n]$ where $p_n = \text{Tr}[\varrho^\alpha\Pi_n]$. By use of the trace formula [145]

$$\text{Tr}[O_1O_2] = \frac{1}{\pi}\int_{\mathbb{C}^m} d^{2m}\lambda\ \chi[O_1](\lambda)\chi[O_2](-\lambda)$$

we obtain the characteristic function

$$\chi[\varrho^\alpha_{A|n}](\lambda_A) = \frac{1}{\pi p_n}\int_{\mathbb{C}} d^2\lambda_B\ \chi[\Pi_n](\lambda_B)\ \chi[\varrho^\alpha](\lambda_A,-\lambda_B) \tag{3.28}$$

Since $\chi[\Pi_n](\lambda_B) = e^{-\frac{1}{2}|\lambda_B|^2}L_n(|\lambda_B|^2)$, where $L_n$ is the Laguerre polynomial $L_n(|\lambda_B|^2) = \sum_{i=0}^n \binom{n}{n-i}\frac{|\lambda_B|^{2i}}{i!}$, we have explicitly

$$\begin{aligned}\chi[\varrho^\alpha_{A|n}](\lambda_A) = \frac{1}{\pi p_n}\int_{\mathbb{C}} d^2\lambda_B\ L_n(|\lambda_B|^2)\exp\big(-a|\lambda_A|^2 \\ -(b+1/2)|\lambda_B|^2 - 2c\text{Re}[\lambda_A\lambda_B] - 2i\text{Im}[\lambda_B\alpha^*]\big)\end{aligned} \tag{3.29}$$

In order to see that this expression depends on $|\alpha|$ only we can implement the change $\alpha \to \alpha' \equiv e^{i\theta}\alpha$ and we have

$$\begin{aligned}\chi[\varrho^{\alpha'}_{A|n}](\lambda_A) = \frac{1}{\pi p_n}\int_{\mathbb{C}} d^2\lambda_B \quad L_n(|\lambda_B|^2)\exp\big(-a|\lambda_A|^2 \\ -(b+1/2)|\lambda_B|^2 - 2c\text{Re}[\lambda_A\lambda_B] - 2i\text{Im}[\lambda_B\alpha^*e^{-i\theta}]\big)\end{aligned}$$

By changing variable $\lambda_B \to e^{-i\theta}\lambda_B$ we see that

$$\chi[\varrho^{\alpha'}_{A|n}](\lambda_A) = \chi[\varrho^\alpha_{A|n}](\lambda_Ae^{-i\theta}) \tag{3.30}$$

Therefore, we have $\chi[\varrho^{\alpha'}_{A|n}] \neq \chi[\varrho^\alpha_{A|n}]$, hence $\varrho^{\alpha'}_{A|n} \neq \varrho^\alpha_{A|n}$. However, $\varrho^{\alpha'}_{A|n}$ and $\varrho^\alpha_{A|n}$ have the same spectrum. Indeed $\chi[\varrho^\alpha_{A|n}](\lambda_A)$ and $\chi[\varrho^\alpha_{A|n}](\lambda_Ae^{i\theta})$ are related by a simple quadrature rotation

$$a_A \to a_Ae^{i\theta} \quad a_A^\dagger \to a_A^\dagger e^{-i\theta} \tag{3.31}$$

which means that

$$\varrho^{\alpha'}_{A|n} = U\varrho^\alpha_{A|n}U^\dagger \tag{3.32}$$

where $U$ is the free evolution of mode $A$, $U = e^{i\theta a_A^\dagger a_A}$. Since $\varrho^{\alpha'}_{A|n}$ and $\varrho^\alpha_{A|n}$ are related by a unitary, they have the same spectrum. Therefore, the spectrum (hence, the entropy) of the reduced post-measurement state $\varrho^\alpha_{A|n}$ does not depend on the phase of

$\alpha$ but just on $|\alpha|$. If follows that the non-Gaussian quantum discord of $\varrho^{\alpha}$ does not depend on the phase of $\alpha$. *QED*.

We have evaluated the Gaussian and non-Gaussian quantum discord for STS and MTS states with a wide range of two-mode squeezing and thermal parameters. Non-Gaussian measurements are done in the displaced photon number basis,

$$P_n = D(\alpha)|n\rangle\langle n|D(\alpha)^{\dagger}$$

with variable $\alpha \in [0, 2.5]$. In Fig. 3.5 and Fig. 3.6 we plot the Gaussian and non-Gaussian quantum discord. We see that greater displacements lead to lower values of the non-Gaussian quantum discord, but the decrease is insufficient to match the Gaussian quantum discord, which remains optimal. However, the non-Gaussian quantum discord approximates the Gaussian one as $\alpha \to \infty$. Indeed, we find that for both STS and MTS

$$\varrho^{\alpha}_{A|n} \to \varrho^{\alpha}_{A|0} \qquad \text{as} \quad \alpha \to \infty \tag{3.33}$$

**Proof.** In order to show that $\varrho^{\alpha}_{A|n} \to \varrho^{\alpha}_{A|0}$ as $\alpha \to \infty$ we adopt the characteristic function formalism. The post-measurement state of mode $A$ has the characteristic function (3.29). Since the phase of $\alpha$ is irrelevant for the discord, we will assume $\alpha \in \mathbb{R}$ in the following. The post-measurement state characteristic function, Eq. (3.29), is the Gaussian integral of a polynomial. By using a well-known trick of Gaussian integrals, we can rewrite

$$\chi[\varrho^{\alpha}_{A|n}](\lambda_A) = \frac{1}{\pi p_n} e^{-a|\lambda_A|^2} \int_{\mathbb{C}} d^2\lambda_B \quad L_n(d/d\gamma) \times$$
$$\exp\left(-\gamma|\lambda_B|^2 + 2c\mathrm{Re}\lambda_A\mathrm{Re}\lambda_B - (2c\mathrm{Im}[\lambda_A] + 2i\alpha)\mathrm{Im}[\lambda_B]\right)$$

where $\gamma = b + 1/2$ and the formal expression $L_n(d/d\gamma)$ means $\sum_{i=0}^{n} \binom{n}{n-i} \frac{1}{i!} \frac{d^n}{d\gamma^n}$. This expression can now be moved outside the integral, so that we are now left with a purely Gaussian integral of the form

$$\int_{\mathbb{R}} d^2\mathbf{\Lambda}_B \; e^{-\frac{1}{2}\mathbf{\Lambda}_B^T \mathcal{M} \mathbf{\Lambda}_B + \mathbf{\Lambda}_B^T \mathcal{B}}$$

where $\mathcal{M} = \mathrm{diag}\{4\gamma, 4\gamma\}$, $\mathcal{B} = (2c\mathrm{Re}\lambda_A, -2c\mathrm{Im}\lambda_A + 2i\alpha)$, $\mathbf{\Lambda_B} = (\mathrm{Re}\lambda_B, \mathrm{Im}\lambda_B)$. The integral gives $\frac{2\pi}{\sqrt{\det\mathcal{M}}} e^{\frac{1}{2}\mathcal{B}^T\mathcal{M}^{-1}\mathcal{B}}$ so that we finally get

$$\chi[\varrho^{\alpha}_{A|n}](\lambda_A) = \frac{1}{p_n} e^{-\frac{1}{2}a|\lambda_A|^2} L_n(-d/d\gamma) \times \tag{3.34}$$
$$\frac{1}{\gamma} \exp\left(\frac{c^2|\lambda_A|^2 - \alpha^2 - 2i\alpha c\mathrm{Im}\lambda_A}{2\gamma}\right)$$

Let us define $x = c^2|\lambda_A|^2 - \alpha^2 - 2i\alpha c\mathrm{Im}\lambda_A$. Then we have

$$L_n(-d/d\gamma)\frac{1}{\gamma}\exp\left(\frac{c^2|\lambda_A|^2 - \alpha^2 - 2i\alpha c\mathrm{Im}\lambda_A}{2\gamma}\right) \quad =$$
$$= L_n(-d/d\gamma)\frac{1}{\gamma}e^{x/2\gamma} = F_n(\gamma, x)e^{x/2\gamma}$$

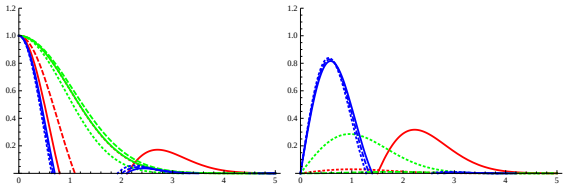

(a) Re (b) Im

Figure 3.7: $\chi[\varrho^{\alpha}_{A|n}](\lambda)$ for $\alpha = 0.1$ (red), $\alpha = 1$ (green), $\alpha = 5$ (blue) and $n = 0$ (solid), $n = 1$ (dashed), $n = 2$ (dotted). Here, we have $A = (N + 1/2)\cosh\lambda$, $C = (N + 1/2)\sinh\lambda$ with $\lambda = 0.5$, $N = 0.5$.

where $F_n(\gamma, x) = \sum_k f_k(\gamma)x^k$ is necessarily a polynomial of degree $n$ in with $\gamma$-dependent coefficients $f_k(\gamma)$. Therefore,

$$\chi[\varrho^{\alpha}_{A|n}](\lambda_A) = \frac{1}{p_n} e^{-(a-c^2(b+1/2)^{-1})|\lambda_A|^2} \times e^{-ic(b+1/2)^{-1}\alpha Im\lambda_A} e^{-\alpha^2/2\gamma} F_n(\gamma, x) \tag{3.35}$$

The norm is

$$p_n = e^{-(a-c^2(b+1/2)^{-1})|\lambda_A|^2} e^{-ic(b+1/2)^{-1}\alpha Im\lambda_A} \times e^{-\alpha^2/2\gamma} F_n(\gamma, x)\Big|_{\lambda_A=0} = e^{-\alpha^2/2\gamma} F_n(-\alpha^2)$$

so that

$$\chi[\varrho^{\alpha}_{A|n}](\lambda_A) = e^{-(a-c^2(b+1/2)^{-1})|\lambda_A|^2} \times e^{-ic(b+1/2)^{-1}\alpha Im\lambda_A} \frac{F_n(\gamma, x)}{F_n(\gamma, -\alpha^2)} \tag{3.36}$$

This function is exponentially decaying as $e^{-s|\lambda_A|^2}$ where $s = a - c^2/(b + 1/2)$, hence it is vanishing for $|\lambda_A|^2 \gg 1/s$. Therefore, we can consider values of $|\lambda_A|^2$ in the region $\lambda_A^2 \lesssim 1/s$. In this region, we we have $\lim_{\alpha\to\infty} x = -\alpha^2$ because $\alpha \gg \lambda_A$ and thus

$$\lim_{\alpha\to\infty} \frac{F_n(\gamma, x)}{F_n(\gamma, -\alpha^2)} = \frac{f_n(\gamma)\alpha^2 n}{f_n(\gamma)\alpha^2 n} = 1$$

In conclusion, as $\alpha \to \infty$ we have

$$\chi[\varrho^{\alpha}_{A|n}](\lambda_A) \to \chi[\varrho^{\alpha}_{A|0}] \tag{3.37}$$

which implies the desired result (3.33), *QED*.

This result means that the conditional state of $A$ is independent of $n$ and equal to the $n = 0$ result. In Fig. 3.7 we show $\chi[\varrho^{\alpha}_{A|0}], \chi[\varrho^{\alpha}_{A|1}], \chi[\varrho^{\alpha}_{A|2}]$ for growing values of

$\alpha$. The three curves converge already for $\alpha \sim 5$. As a consequence of $n$-independence, we have

$$S^{\mathcal{NG}}(A|\Pi^B) = \sum_n p_n S(\varrho^{\alpha}_{A|n}) \to S(\varrho^{\alpha}_{A|0}) \tag{3.38}$$

But $\varrho^{\alpha}_{A|0}$ is just the post-measurement state corresponding to POVM element

$$D(\alpha)|0\rangle\langle 0|D^{\dagger}(\alpha) = |\alpha\rangle\langle\alpha|$$

i.e, a Gaussian state with covariance matrix $\sigma_P = A - C(B + \mathbb{I}/2)^{-1}C^T$ (Schur complement), and mean $\mu_P = X(B + \mathbb{I}/2)^{-1}C^T$, where $X = (\alpha, 0)$. On the other hand, from the discussion in § 3.2 we know that the optimal Gaussian POVM is a heterodyne measurement $\{\Pi_\beta = D(\beta)|0\rangle\langle 0|D^{\dagger}(\beta) = |\beta\rangle\langle\beta|\}$. In this case, as already explained in § 3.2, the entropy of the post measurement state $\varrho_{A|\beta}$ is independent of the measurement result $\beta$, hence the conditional entropy coincides with the entropy of of the $\beta = \alpha$ result. Therefore, we also have $S^{\mathcal{G}}(A|B) = S(\varrho^{\alpha}_{A|0})$. Therefore, we conclude that the non Gaussian discord $D^{\mathcal{NG}}(A|\Pi^B)$ in the displaced number basis tends to the Gaussian discord $D^{\mathcal{G}}(A|B)$ as $\alpha \to \infty$, *QED*.
To be rigorous, we did not prove that the $D^{\mathcal{NG}}(A|\Pi^B)$ is lower bounded by $D^{\mathcal{G}}(A|B)$, and we cannot rule out the possibility that $D^{\mathcal{NG}}(A|B) < D^{\mathcal{G}}(A|B)$ for intermediate values of $\alpha$. However, our numerical data do not support this possibility since we never observe $D^{\mathcal{NG}}(A|\Pi^B) < D^{\mathcal{G}}(A|B)$ and we expect that $D^{\mathcal{NG}}(A|\Pi^B) \to D^{\mathcal{G}}(A|B)$ from above as $\alpha \to \infty$.
In conclusion, we have analytical and numerical evidence that the heterodyne measurement remains optimal also with respect to measurement in the displaced number basis.

## 3.7 Geometric discord

In this section, we briefly consider geometric discord (1.47), defined as

$$D_G(A|B) \equiv \inf_{\varrho_{qc} \in QC} ||\varrho_{AB} - \varrho_{qc}||_2^2$$

We recall that this quantity can also be evaluated as a minimum over local measurements

$$D_G(A|B) = \inf_{\Pi^B} ||\varrho_{AB} - \Pi^B(\varrho_{AB})||_2^2$$

Notice that $D_G$ and $D$ are not monotonic functions of one another and the relation between them is still an open question. However, in many cases $D_G$ is much simpler to evaluate than $D$.

Analogous to the case of Gaussian discord, a Gaussian version of the geometric discord can be defined by restricting to Gaussian measurements [63]. Again, it can be analytically computed for two-mode Gaussian states. With the same reasoning of § 3.2 one easily obtains

$$D^{\mathcal{G}}_G(A|B) = \min_{\sigma_M} \mathrm{Tr}[(\varrho_{AB} - \varrho_P \otimes \varrho_M)^2] \tag{3.39}$$

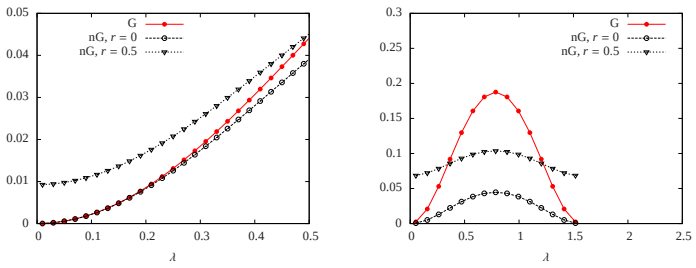


Figure 3.8: (Top) Gaussian and non-Gaussian geometric discord for STS with $N_1 = 1$ as a function of $\lambda$ and for different values of local squeezing $r$; (Bottom) Gaussian and non-Gaussian geometric discord for MTS states for $N_1 = 1$, $N_2 = 0$ as a function of $\phi$ and for different values of local squeezing $r$

Exploiting the property that $\mathrm{Tr}[\varrho_1\varrho_2] = 1/\det[(\sigma_1+\sigma_2)/2]$, for any two Gaussian states $\varrho_1$ and $\varrho_2$,

$$D_G^{\mathcal{G}}(A|B) = \min_{\sigma_M}\{1/\sqrt{\det\sigma_{AB}} + \\ +1/\sqrt{\det(\sigma_P\oplus\sigma_M)} - 2/\sqrt{\det[(\sigma_{AB}+\sigma_P\oplus\sigma_M)/2]}\} \tag{3.40}$$

For for the relevant case of STS and MTS, the minimum is obtained with the $\sigma_M$ elements given by $\alpha = \beta = \frac{\sqrt{ab}(\sqrt{4ab-3c^2}+\sqrt{ab})}{3a}$, $\gamma = 0$. The least disturbing Gaussian POVM for STS, according to the Hilbert-Schmidt distance, is thus a (noisy) heterodyne detection, a result which is analogous to what found in the case of quantum discord. If one constrains the mean energy per mode, the Gaussian quantum discord gives upper and lower bounds to the Gaussian geometric discord. In absence of such a provision, the geometric discord can vanish for arbitrarily strongly nonclassical (entangled) Gaussian states, as a consequence of the geometry of CV state spaces.

Also in this case, we may consider non-Gaussian measurements and evaluate a non-Gaussian geometric discord:

$$D_G^{\mathcal{NG}}(A|\Pi^B) = \mathrm{Tr}[(\varrho_{AB} - \Pi^B(\varrho_{AB}))^2] \tag{3.41}$$

For measurement in the number basis, we can easily obtain

$$D_G^{\mathcal{NG}} = \mu(\varrho) + \sum_{npq} |\langle pn|\varrho|qn\rangle|^2 \tag{3.42}$$

where $\mu(\varrho) = \frac{1}{4\sqrt{\det(\sigma)}}$ is the (Gaussian) state purity [145]. In the case of measurements in the squeezed or displaced number basis, we have to use $\varrho^r$ and $\varrho^\alpha$ instead of $\varrho$ in Eq. (3.42). In general, in order to compute the geometric discord we need to compute matrix elements, and we use the same numerical methods described above. Note that by the same arguments leading to Eq. (3.32) we can easily find that the geometric discord noes not depend on the phase of $\alpha$ like the normal discord.

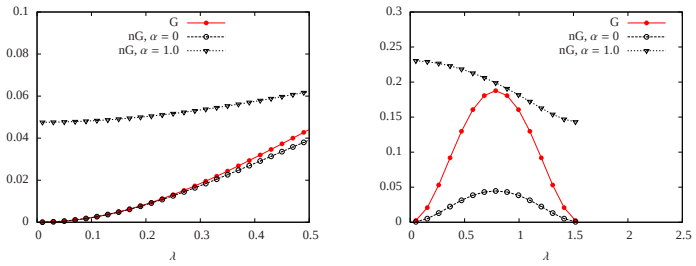


Figure 3.9: (Top) Gaussian and non-Gaussian geometric discord for STS with $N_1 = 1$ as a function of $\lambda$ and for different values of local displacement $\alpha$ (Bottom) Gaussian and non-Gaussian geometric discord for MTS states for $N_1 = 1$, $N_2 = 0$ as a function of $\phi$ and for different values of local displacement $\alpha$

### 3.7.1 Results

We have compared the Gaussian and non-Gaussian geometric discord for STS and MTS in a wide range of parameters. We have considered measurements in the number, squeezed number and displaced number basis for the same values of the parameters given in the preceding sections. Results are plotted in Figs. 3.8 and 3.9. In general, at variance with the results for quantum discord, we find that non-Gaussian measurements can provide lower values of geometric discord than Gaussian ones. Among the class of non-Gaussian measurements we have considered, the optimal one is provided by the number basis, which gives values of geometric discord that are always lower than those given by the optimal Gaussian measurement. The non-Gaussian geometric discord increases for increasing $r$ and $\alpha$, and it can become greater than its Gaussian counterpart. These results are very different from the quantum discord case: on one hand, the (non-Gaussian) geometric discord is substantially affected by the local squeezing; on the other hand, it does not approach the Gaussian one when the displacement $\alpha \to \infty$, but it grows monotonically. Indeed if we increase the squeezing or displacement in the measurement basis, the post-measurement state is more distant (in Hilbert-Schmidt norm) from the original one. As already noticed, performing the measurement is the squeezed (displaced) number basis in equivalent to first squeezing (displacing) the state and then measuring it in the number basis. The local squeezing and displacement have the effect of increasing the energy of the state, shifting the photon number distribution $P(B = n)$ towards greater values of $n$. This causes the overlap between the post measurement state and the original state to decrease, and therefore their distance to increase.

Let us further comment on the difference between the quantum discord and the geometric discord cases. Quantum discord and geometric discord both vanish for classical states, but are not monotonic functions of one another, and thus they are truly different quantities. The geometric discord, based on the Hilbert-Schmidt distance, is a geometric measure of how much a state is perturbed by a local measurement, while quantum discord assesses to which extent correlations are affected by a local measurement. While for the quantum discord well-defined operational and informational

interpretations can be found [71, 82], for the geometric discord the situation is more problematic. Indeed, one can design protocols in which the geometric discord can in some cases be related to the protocols' performances [70, 81]; however, recent discussions [31], show that, as consequence of the non-invariance of the Hilbert-Schmidt norm under quantum evolutions, it is difficult to find a conclusive argument about the relevance of geometric discord as a measure of quantumness of correlations. Our data show that non-Gaussian measurements can yield optimal values of the geometric discord, contrary to the case of quantum discord. Hence, the behavior of quantum discord and geometric discord with respect to different types of measurements is different. This is a further indication that the geometric discord cannot be used as a good benchmark for the quantum discord and that the degree of quantumness measured, if any, by such a quantity has a fundamentally different nature.

## 3.8 Discussion and conclusions

The definition of discord involves an optimization over all possible local measurements (POVMs) on one of the subsystems of a bipartite composite quantum system. In the realm of continuous variables (CV), initial research efforts on quantum discord restricted the minimization to the set of (one-mode) Gaussian measurements.

In this work we have investigated CV quantum discord beyond this restriction. We have focused on Gaussian states, asking whether Gaussian measurements are optimal in this case, i.e., whether the Gaussian discord is the true discord for Gaussian states. While a positive answer to this question had already been given for the special case of two-mode Gaussian states having one vacuum normal mode (by means of an analytical argument based on the Koashi-Winter formula), no general result was available so far. We have addressed our central question upon considering two large classes of two-mode Gaussian states, the squeezed thermal states (STS) and the mixed thermal states (MTS), and allowing for a wide range of experimentally feasible non-Gaussian measurements based on orthogonal bases: the photon number basis, the squeezed number basis, the displaced number basis. For both STS and MTS states, in the range of parameters considered, the Gaussian measurements always provide optimal values of discord compared to the non-Gaussian measurements under analysis. Local squeezing of the measurement basis has no appreciable effect on correlations, while local displacement leads to lower values of the non-Gaussian discord, which approaches the Gaussian one in the limit of infinite displacement.

Overall, for the explored range of states and measurements, we have evidence that the Gaussian discord is the ultimate quantum discord for Gaussian states. We note that the optimality of Gaussian measurements suggested by our analysis is a property which holds only for Gaussian states. In the case of non-Gaussian states, e.g., CV Werner states, non-Gaussian measurements such as photon counting can lead to a better minimization, as was recently proven in Ref. [62].

We also have investigated the CV geometric discord [63], comparing the Gaussian and non-Gaussian cases. We have shown that the behavior of geometric discord is completely different from that of quantum discord. On one hand, non-Gaussian measurements can lead to lower values of the geometric discord, the number basis measure-

ment being the optimal one; on the other hand, the effects of both local squeezing and displacement are strong and consist in a noteworthy increase in the non-Gaussian geometric discord. The remarkable differences between quantum and geometric discord imply that the latter cannot be used as a benchmark of the former.

Both in the case of the discord and geometric discord a definite answer on the optimal measurement minimizing the respective formulas would require the extension of the set of non-Gaussian measurements to possibly more exotic ones and the application of those realizable in actual experiments to a broader class of Gaussian and non-Gaussian states. While we leave this task for future research, our results on discord support the conjecture that Gaussian measurements are optimal for Gaussian states and allow to set, for the class of states analyzed, a tighter upper bound on the entanglement of formation for $1 \times 2$ modes Gaussian states, via the Koashi-Winter relation.

# Chapter 4

# An introduction to decoherent histories

## 4.1 Introduction

Few topics in physics have ever been a source of wider disagreement, and have ignited a fiercer debate than the interpretation of quantum mechanics. Most of the times, purported solutions to the problem have encountered more difficulties that they wished to get rid of, and aroused more skepticism than they wished to overcome. Among the most contentious solutions, I may just remind Everett's many-worlds interpretation – whose awkwardness can elicit an almost rabid rejection on the part of many people, or Bohm's pilot wave theory – that many consider nothing more than a convoluted and unnecessary effort to save realism in quantum physics. For many a physicist, the whole topic of *decoherent* or *consistent histories* [163, 164, 165] may be just another chapter in the endless book on interpretations of quantum mechanics. True, purely interpretational and foundational issues have played a key role in the developement of this topic. But there is much more to it.

This thesis is not concerned with the foundations of quantum mechanics and the related quarrels. Rather, I wish to show how foundational discussions, apparently detached from the urges of the "working physicist", have often led to the development of new concepts and tools that have later proved useful (if not indispensable) to solve and discuss more mundane physical problems. According to this spirit, I view decoherent histories not as an interpretation, but rather as a *language* that, under diverse conditions, may prove effective in formulating and analyzing physical problems of interest. In this sense, I believe that the study of decoherent histories has something in common with the whole field of decoherence [167]: It contributes to clarifying how information is produced by, and how it can be extracted from quantum systems. This fact is epitomized by a tight relation between decoherent histories and the notion of quantum dynamical entropy, which will be the subject of Chapter 5.

This chapter is intended to be a concise review of decoherent histories. My way of presentation will be tailored to my main goals, i.e., provide the reader with the mini-

mal range of notions needed to understand to the work exposed in subsequent chapters. Nevertheless, for the sake of completeness I will briefly mention some interpretational issues and difficulties that have inspired the creation of the formalism, and still make it a disputed topic.
This chapter is organized as follows: In § 4.2 I will review the basics concepts of the decoherent histories formalism. In § 4.3 I will briefly discuss the connection between decoherent histories and the wider notion of decoherence. I claim no originality as for any of the concepts exposed in this chapter, except for the way of presenting them.

## 4.2 quantum histories

The formalism of decoherent (or consistent) histories has been developed by several authors under slightly different perspectives. The approach has been pioneered by Griffiths [163], who named it *consistent histories* and whose main goal was to provide quantum mechanics with an interpretational framework devoid of the concept of measurement. Griffiths' approach was was later embraced by Omnès [164]. Griffiths and Omnès' basic achievement was to find a consistency condition under which quantum mechanics can be applied to closed systems, giving predictions for specific sequences of events in time (histories). Later, Hartle and Gell-Mann essentially rediscovered the formalism of consistent histories while trying to apply quantum mechanics to cosmology [165]. They called their approach *decoherent histories*, the terminology that we will use throughout this work. Gell-Mann and Hartle's formalism is nearly equivalent to Griffiths', apart from a slight reformulation of the consistency condition and a higher emphasis on physical mechanisms of decoherence that secure its fulfillment.
What unites all authors is the yearning to consistently apply quantum mechanics to closed systems - what is precluded in the standard interpretation of quantum mechanics. According to the latter, quantum mechanics can only predict the probabilities of experiment outcomes. Experiments must be performed by some agent (a device or an observer) that is external to the system, which then by definition ought to be open. Furthermore, it is postulated that the measuring agent obey classical mechanics - a requirement macroscopic devices or observers are generically assumed to satisfy. This framework is totally satisfactory for the original aim of quantum mechanics, that was developed as a theory to describe macroscopic observations of microscopic (atomic and subatomic) systems. In this setting, the quantum object-classical observer dualism is neither a problem nor a limit. However, after quantum mechanics was successfully applied to explain the behavior of matter from elementary particles to large molecules, people started to think of it as a universal theory that should adequately describe any physical system, regardless of its size. In principle, it should be even possible to consistently describe the whole universe in quantum mechanical terms, a mission that defines the field of quantum cosmology.
Decoherent histories were born to address these challenges and set up an interpretational framework for quantum mechanics that does not require measurements and observers (even if it can consistently include those, too). In this framework, the physics is essentially the same as in the standard formalism, but experiments are replaced by the consistency condition and probabilities of measurement outcomes are replaced by a

prescription to compute the probabilities of *histories*. The key role assigned to histories has several motivations [169]. First, histories are so general to cover virtually all situations one may be interested in describing. Second, their classical limit are classical trajectories, which makes the decoherent histories formalism particularly convenient to study the quantum-classical transition. Third, in cosmology one needs to reconstruct a "narrative" of past events: Histories are the right tool to construct a narrative that is compatible with quantum mechanics.

### 4.2.1 Events and histories

In what follows, I will introduce the notion of histories of a closed quantum system. As I mentioned above, I look at histories primarily as an effective language to talk about quantum physics. In my opinion, such a language is strongly affine to the so-called *quantum logic* developed by von Neumann in the classic paper [168]. Since quantum logic provides us a nice conceptual toolkit and a useful lexicon, I will glean a few words and concepts from it.
Let us consider a finite-dimensional quantum system characterized by a Hilbert space $\mathcal{H}$ with $\dim \mathcal{H} = d$ and a unitary dynamics $U(t) = e^{-iHt}$ generated by a Hamiltonian $H$. We can start by introducing quantum *events*, that are the elementary building blocks of histories. According to von Neumann, "saying something" about a quantum systems, i.e., specifying a property thereof, is equivalent to specifying a linear subspace $\mathcal{P} \subseteq \mathcal{H}$. For instance, the proposition "the system has energy $E$" is encoded the subspace $\mathcal{P}_E$, the energy eigenspace corresponding to $E$:

$$\mathcal{P}_E = \sum_s |E, s\rangle\langle E, s| \qquad \text{where} \qquad H|E, s\rangle = E|E, s\rangle$$

Linear subspaces of $\mathcal{H}$ are in one-to-one correspondence with projectors, i.e., operators $P$ such that $P^2 = P$. To any $\mathcal{P}$ we can indeed associate the projector $P$ such that $\forall|\phi\rangle \in \mathcal{H}, P|\phi\rangle = |\phi'\rangle \in \mathcal{P}$. In what follows, we will then identify $P$ and $\mathcal{P}$.

Hence, *any quantum proposition can be identified with a projector* $P$. This allows to develop a logical calculus based on projectors:

- The logical negation of $P$ is given by $\mathbb{I} - P$, which projects onto the subspace complementary to $\mathcal{P}$.
- Given $P_1$ and $P_2$, their logical product ("and") is given by $P = P_1 P_2$. This is well-defined only when the two projectors commute, $P_1 P_2 = P_2 P_1$, which implies that $P$ is a projector too. The product $P_1 P_2$ specifies joint properties of the system. Two propositions $P_1$, $P_2$ are *exclusive* if the projectors (and the corresponding subspaces) are orthogonal, $P_1 P_2 = 0$.
- Given two exclusive propositions $P_1$ and $P_2$ we can define their logical sum ("or") by summing projectors, $P = P_1 + P_2$. Orthogonality guarantees that $P$ is a projector too.

- A set of $n$ exclusive propositions $P_j, j = 1, \ldots, n$, $P_i P_j = \delta_{ij}$ is *exhaustive* if the projectors sum up to the identity, $\sum_{j=1}^{n} P_j = \mathbb{I}$.

A quantum *event* is defined as a pair $P, t$ of a projector $P$ and a time $t$. It can be interpreted as an objective statement that the proposition $P$ holds at time $t$. A logical calculus with events immediately stems from the above logical calculus for propositions. Accordingly, two events $P_1, t$, $P_2, t$ are *exclusive* if their projectors are orthogonal $P_1 P_2 = 0$. A set of $n$ exclusive events $\{t, P_j\}$, $P_i P_j = 0, \forall i, j \in \{1, \ldots, n\}$ at time $t$ is *exhaustive* if the projectors sum up to the identity, $\sum_{j=1}^{n} P_j = \mathbb{I}$. An exhaustive set of exclusive events corresponds to the possible outcomes of an orthogonal measurement (von Neumann measurement) at time $t$.

Given an ordered sequence of times $t_1 < \cdots < t_N$, a *history* is defined as a sequence of events $\mathfrak{h} = P^1, t_1 \ldots, P^N, t_N$. If we have $N$ exhaustive sets of events $\{t_\ell, P^\ell_{j_\ell}\}, j_\ell = 1, \ldots, n_\ell$ with $P^\ell_{j_\ell} P^\ell_{k_\ell} = \delta_{j_\ell k_\ell}$, $\sum_{j_\ell} P_{j_\ell} = \mathbb{I}$, we can define an exhaustive set of exclusive histories as $\Sigma = \{\mathfrak{h}_\mathbf{j}\}$, where $\mathfrak{h}_\mathbf{j} = t_1, P^1_{j_1}, \ldots, t_N, P^N_{j_N}$ and the multi-index $\mathbf{j} \equiv j_1, \ldots, j_N$ labels different alternative histories. For simplicity, in the following we will always denote a history with the corresponding multi-index, $\mathbf{j}$ instead of the "heavier" notation $\mathfrak{h}_\mathbf{j}$. The projectors $P^\ell_{j_\ell}$ are formally equivalent to a projective measurement for each $t_\ell$.

### 4.2.2 fine-graining and coarse-graining

#### coarse-graining

A set of histories $\Sigma$ corresponds to a description of the system in time. A less detailed description $\Sigma'$ can be obtained from it by a process called *coarse-graining*, whereby the events of the new histories of $\Sigma'$ are defined by taking the logical sum of events of histories in $\Sigma$ for all times. For instance, given two exclusive histories $\mathbf{j}, \mathbf{k}$ the coarse-grained history $\mathbf{j} \vee \mathbf{k}$ is defined by $t_\ell, P^\ell_{j_\ell} + P^\ell_{k_\ell}, \forall \ell$, that is by taking the sum of projectors for each time.
In general, given a set $\Sigma$ of exclusive and exhaustive histories, we can obtain a set $\Sigma'$ of coarse-grained histories by the following coarse-graining procedure. For each $t_\ell$, there are $n_\ell$ projectors $P^\ell_{j_\ell}, j_\ell = 1, \ldots, n_\ell$. We can partition the set $\Sigma^\ell = \{1, \ldots n_\ell\}$ into $m_\ell < n_\ell$ disjoint subsets $\Sigma^\ell_{\bar{j}_\ell}, \bar{j}_\ell = 1, \ldots, m_\ell$. To each $\bar{j}_\ell$, we associate the projector $\bar{P}_{\bar{j}_\ell} = \sum_{j_\ell \in \Sigma_{\bar{j}_\ell}} P_{j_\ell}$. The resulting set of histories labelled by $\bar{\mathbf{j}} = \bar{j}_1, \ldots, \bar{j}_N$ is a set of coarse-grained exclusive and exhaustive histories. Obviously, by applying a similar coarse-graining procedure to $\Sigma'$ we obtain a new set of histories $\Sigma''$ with a higher degree of coarse-graining.
A special type of coarse-graining is the *temporal coarse-graining*. Consider a coarse-graining such that at some time $t_\ell$ we have $m_\ell = 1$ and correspondingly we have only one coarse-grained projector $\bar{P}^\ell_1 = \sum_{j_\ell \in \Sigma^\ell_1} P^\ell_{j_\ell} = \mathbb{I}$. Then histories in $\Sigma'$ contain no event at time $t_\ell$, because $\mathbb{I}$ is a trivial event that can be neglected and hence removed from the string of projectors defining the history.

**fine-graining**

Conversely, given a set $\Sigma$ of exclusive and exhaustive histories, we can obtain a set $\Sigma'$ of less coarse-grained (more fine-grained) histories through the opposite procedure called *fine-graining*. For each $t_\ell$, there are $n_\ell$ projectors $P^\ell_{j_\ell}, j_\ell = 1, \ldots, n_\ell$. If $n_\ell < d$, at least one of the $P^\ell_{j_\ell}$ is not one-dimensional. We can thus define a set of $m_\ell$ fine-grained projectors ($d \geq m_\ell > n_\ell$) $P^\ell_{\tilde{j}_\ell}$ by "splitting" projectors with $\mathrm{Tr}P_{j_\ell} > 1$ into projectors on lower-dimensional subspaces. Let $\mathrm{Tr}P_{j_\ell} = n_{j_\ell}$ and partition the set $1, \ldots, m_\ell$ into $n_\ell$ disjoint subsets $\Sigma_{j_\ell}$ with $|\Sigma_{j_\ell}| \leq n_{j_\ell}$. We can then define fine-grained projectors $\tilde{P}_{\tilde{j}_\ell}$ as $P_{j_\ell} = \sum_{\tilde{j}_\ell \in \Sigma_{j_\ell}} \tilde{P}_{\tilde{j}_\ell}$ The resulting set of histories labeled by $\tilde{\mathbf{j}} = \tilde{j}_1, \ldots, \tilde{j}_N$ is a set of fine-grained exclusive and exhaustive histories. A temporal fine-graining at time $t_\ell$ is obtained by inserting events at $t_\ell$, that is, by splitting the trivial event $\mathbb{I}$ at $t_\ell$ into the sum of more events.

**complete fine-graining**

In the literature histories that have one-dimensional projectors for all times (and hence admit no further fine-graining except for temporal ones) are often simply called *fine-grained*. A history is *completely fine-grained* if it admits no further coarse-graining tout court. Completely fine-grained histories are given by sequences of one-dimensional projectors $P_{j_t}$ for all times $t > 0$. A completely fine-grained set of histories affords to the maximally detailed description of a system. Completely fine-grained histories constitute the basis of Feynman's sum-over-histories formulation of quantum mechanics, which we now briefly review in the decoherent histories language.
The quantum-mechanical amplitude between state $|\psi_0\rangle$ at time $t_0$ and state $|\phi_f\rangle$ at time $t_f$ is given by $\langle\phi_f|U(t_f - t_0)|\psi_0\rangle$. Upon inserting $N$ decompositions of the identity $\sum_{j_\ell} P_{j_\ell} = \mathbb{I}$ at times $t_\ell = t_0 + \ell\Delta t$ with $\Delta t = |t_f - t_0|/(N+1)$, we get

$$\begin{aligned}\langle\phi_f|U(t_f - t_0)|\psi_0\rangle = \sum_{\mathbf{j}=j_1\ldots j_N} &\langle\phi_f|U(t_f - t_N)P_{j_N}U(t_N - t_{N-1})P_{j_{N-1}}\times \\ &U(t_{N-1} - t_{N-2})\ldots P_{j_1}U(t_1 - t_0)|\psi_0\rangle\end{aligned}$$

Using the Heisenberg representation

$$P^\ell_{j_\ell}(t) \equiv U^\dagger(t - t_0)P^\ell_{j_\ell}U(t - t_0), \qquad |\phi^{(h)}_f\rangle = U^\dagger(t_f - t_0)|\phi_f\rangle, \qquad |\psi^{(h)}_0\rangle = |\psi_0\rangle$$

as well as the notation $C_{\mathbf{j}} \equiv P^N_{j_N}(t_N)\ldots P^1_{j_1}(t_1)$, we get

$$\langle\phi_f|\psi_0\rangle = \sum_{\mathbf{j}}\langle\phi^{(h)}_f|C_{\mathbf{j}}|\psi^{(h)}_0\rangle = \sum_{\mathbf{j}}\langle\phi^{(h)}_f|\psi^{(h)}_{\mathbf{j}}\rangle$$

where $|\psi^{(h)}_{\mathbf{j}}\rangle \equiv C_{\mathbf{j}}|\psi^{(h)}_0\rangle$. Thus we can express the transition amplitude as a sum over amplitudes, each amplitude corresponding to a specific fine-grained history $\mathbf{j}$. The histories become maximally fine-grained in the limit $N \to \infty, \Delta t \to 0$. For an infinite-dimensional system we can consider projections corresponding to sharp values of the

continuous coordinates $P_q = |q\rangle\langle q|$. Hence in the limit $N \to \infty, \Delta t \to 0$ histories can be labeled by a continuous index $q(t)$ and the sum becomes a path integral,

$$\langle \psi_f | \psi_0 \rangle = \int Dq \, \langle \psi_f^{(h)} | e^{i\mathcal{S}[q(t)]} | \psi_0^{(h)} \rangle$$

Here, $\mathcal{S}[q(t)]$ is the fundamental action associated with history $q(t)$. The physical meaning of $q$ depends on the system at hand and its configuration space. For a particle living in a one-dimensional space it is a real spatial coordinate. More in general, $q$ is a shorthand for an arbitrarily long string of values that specify coordinates in a configuration space of arbitrary dimension. In the extreme case, we may looking at histories of the whole universe: then $q(t)$ should include the values of all fundamental physical fields.

### 4.2.3 Probabilities of histories

In the standard formulation of quantum mechanics, given a sequence of $N$ projective measurements we can predict the probability of any sequence of outcomes $\mathbf{j} \equiv j_1 \dots j_N$, provided that we know the initial state and the dynamics governing the system, which is unitary for a closed system. If the initial state is pure – hence represented by a vector $|\psi_0\rangle$ – outcomes $\mathbf{j} = j_1 \dots j_N$ are obtained at times $t_1, \dots, t_N$ with probability

$$p_{\mathbf{j}} = ||P^N_{j_N} U(t_N - t_{N-1}) P^{N-1}_{j_{N-1}} U(t_{N-1} - t_{N-2}) \dots P_{j_1} U(t_1 - t_0) |\psi_0\rangle||^2 \equiv |||\psi_{\mathbf{j}}\rangle||^2$$

where $|\psi_{\mathbf{j}}\rangle$ is an un-normalized *path-projected vector*. After outcomes $\mathbf{j} = j_1 \dots j_N$ are obtained at times $t_1, \dots, t_N$, the system is left in the state $\frac{1}{\sqrt{p_{\mathbf{j}}}} |\psi_{\mathbf{j}}\rangle$.
Upon adopting the Heisenberg representation $P_{j_\ell}(t) = U^\dagger(t - t_0) P_{j_\ell} U(t - t_0)$ we can rewrite the formula above as

$$p_{\mathbf{j}} = ||P^N_{j_N}(t_N) P^{N-1}_{j_{N-1}}(t_{N-1}) \dots P_{j_1}(t_1) |\psi_0\rangle||^2 \tag{4.1}$$

If the initial state is mixed – hence represented by a density matrix $\varrho_0$, outcomes $\mathbf{j} = j_1 \dots j_N$ are obtained at times $t_1, \dots, t_N$ with probability $p_{\mathbf{j}} = \mathrm{Tr}[\varrho_{\mathbf{jj}}]$, where

$$\begin{aligned} \varrho_{\mathbf{jj}} \equiv & P^N_{j_N} U(t_N - t_{N-1}) P^{N-1}_{j_{N-1}} U(t_{N-1} - t_{N-2}) \dots P_{j_1} U(t_1 - t_0) \varrho_0 \times \\ & U^\dagger(t_1 - t_0) P_{j_1} \dots U^\dagger(t_{N-1} - t_{N-2}) P^{N-1}_{j_{N-1}} U^\dagger(t_N - t_{N-1}) P^N_{j_N} \end{aligned}$$

is an un-normalized path-projected density matrix. After outcomes $\mathbf{j} = j_1 \dots j_N$ are obtained at times $t_1, \dots, t_N$, the system is left in the state $\frac{1}{p_{\mathbf{j}}} \varrho_{\mathbf{j}}$. In the Heisenberg representation, we can write

$$p_{\mathbf{j}} = \mathrm{Tr}[P^N_{j_N}(t_N) \dots P_{j_1}(t_1) \varrho_0 P_{j_1}(t_1) \dots P^N_{j_N}(t_N)] \tag{4.2}$$

Introducing the *history operators* $C_{\mathbf{j}} \equiv P^N_{j_N}(t_N) \dots P^1_{j_1}(t_1)$, we thus have:

$$p_{\mathbf{j}} = ||C_{\mathbf{j}} |\psi_0\rangle||^2 \quad \text{(pure states)} \qquad p_{\mathbf{j}} = \mathrm{Tr}[C_{\mathbf{j}} \varrho_0 C^\dagger_{\mathbf{j}}] \quad \text{(mixed states)} \tag{4.3}$$

In the decoherent histories formulation, formulas (4.3) are still of use, but the interpretation is different. *Probabilities are not assigned to measurement outcomes, but to histories within an exhaustive set of exclusive histories* $\Sigma$. Alternatives at each time are characterized by projectors, that are generally not associated with measurements, as they would be in the standard view. Probabilities are assigned to sequences of events, independent of whether a system interacts with an external measuring device (or any system whatsoever). However, probabilities cannot be *consistently* assigned to each and any $\Sigma$. Indeed, for an arbitrary $\Sigma$, probabilities (4.3) do not comply with the classical rules of probability logic, as we will shortly demonstrate. Probabilities can assigned only to those $\Sigma$ that satisfy a particular consistency condition, called *decoherence condition*.

### 4.2.4 the decoherence (or consistency) condition

Classically, for a coarse-grained history we would expect $p_{\mathbf{j}\vee\mathbf{k}} = p_{\mathbf{j}} + p_{\mathbf{k}}$. Instead, what we find applying formula (4.3) is

$$p_{\mathbf{j}\vee\mathbf{k}} = \mathrm{Tr}[(C_{\mathbf{j}} + C_{\mathbf{k}})\varrho(C_{\mathbf{j}} + C_{\mathbf{k}})^\dagger] = p_{\mathbf{j}} + p_{\mathbf{k}} + 2\mathrm{Re}(\mathrm{Tr}[(C_{\mathbf{j}}\varrho C_{\mathbf{k}}^\dagger])$$

Thus, the classical rule for the sum of probabilities is violated. The non-classical term $\mathrm{Re}(\mathrm{Tr}[(C_{\mathbf{j}}\varrho C_{\mathbf{k}}^\dagger])$ represents quantum interference, or *coherence* between the two histories. The interference can be constructive or destructive depending on whether $\mathrm{Re}(\mathrm{Tr}[(C_{\mathbf{j}}\varrho C_{\mathbf{k}}^\dagger]) > 0$ or $\mathrm{Re}(\mathrm{Tr}[(C_{\mathbf{j}}\varrho C_{\mathbf{k}}^\dagger]) < 0$.

In the standard approach, coherence manifests itself in the fact that probabilities for a sequence of measurement outcomes depend on whether some of the experiments are performed or not, and with which accuracy. The most common example is the double slit experiment. Let us consider a photon emitted by a source $S$ at $t_0$, passing through either of two slits ($L$ or $R$) at time $t_1$ and hitting the screen at time $t_2$. The probabilities $p_x$ that the photon will hit different points $x$ on the screen depend on whether detectors are placed in front of the slit to determine which slit the photon goes through. If $A_x^L, A_x^R$ represent the amplitudes for the photon to reach $x$ having passed through $L$ or $R$ we have $p_x = |A_x^L + A_x^R|^2$ if no detectors are present, else $p_x = |A_x^L|^2 + |A_x^R|^2$. In the language of decoherent histories, the two histories $t_1, L, t_2, x$ and $t_1, R, t_2, x$ do not decohere, and thus the probability $p_{L\vee R}$ of the coarse grained history $t_2, x$ (which is a temporally coarse-grained history where we ignore the alternatives a time $t_1$) is not given by $p_L + p_R$.

The condition under which the classical probability rule holds is that interference vanish,

$$\mathrm{Re}(\mathrm{Tr}[(C_{\mathbf{j}}\varrho C_{\mathbf{k}}^\dagger]) = 0 \tag{4.4}$$

Given a set $\Sigma$ of exclusive and exhaustive histories, if interference vanishes for all pairs of histories,

$$\mathrm{Re}(\mathrm{Tr}[(C_{\mathbf{j}}\varrho C_{\mathbf{k}}^\dagger]) = 0, \forall \mathbf{j} \neq \mathbf{k} \tag{4.5}$$

we say that histories in $\Sigma$ are *weakly decoherent* or *weakly decohere*, and $\Sigma$ obeys *weak decoherence* (the specification "weakly" is needed to distinguish this criterion

from stronger ones that we will mention below).
Weak decoherence in $\Sigma$ is necessary and sufficient to ensure that the classical probability rules apply to histories in $\Sigma$. Assume indeed that weak decoherence holds for $\Sigma$ and consider a coarse-graining $\Sigma'$ of $\Sigma$. The probabilities the histories of $\Sigma'$ are

$$p_{\bar{\mathbf{j}}} = \sum_{j_1 \in \bar{j}_1} \sum_{k_1 \in \bar{j}_1} \cdots \sum_{j_N \in \bar{j}_N} \sum_{k_N \in \bar{j}_N} \mathrm{Tr}[P_{j_N}(t) \dots P_{j_1}(t) \varrho P_{k_1}(t) \dots P_{k_N}(t)]$$

where we have used the notation $j_\ell \in \bar{j}_\ell$ as a shortcut of $j_\ell \in \Sigma^\ell_{\bar{j}_\ell}$. Due to weak decoherence, this formula simplifies to

$$\begin{aligned} p_{\bar{\mathbf{j}}} &= \sum_{j_1 \in \bar{j}_1} \cdots \sum_{j_N \in \bar{j}_N} \mathrm{Tr}[P_{j_N}(t) \dots P_{j_1}(t) \varrho P_{j_1}(t) \dots P_{j_N}(t)] = \\ &= \sum_{j_1 \in \bar{j}_1} \cdots \sum_{j_N \in \bar{j}_N} p_{j_1 \dots j_N} \end{aligned}$$

Oviously, if $S$ obeys weak decoherence, so does $S'$ as well as any futher coarse-graining $S''$, since probability sum rules continue to be valid.

The basic axiom of the decoherent histories approach is the following: *probabilities can be assigned only to individual members of a set of weakly decoherent histories*. A set of exclusive, exhaustive, and weakly decoherent histories provides a set of alternative descriptions of the system in time that complies with the rules of classical probability theory. Within such a set, we can make predictions and retrodictions. The conditional probability of a subset of events $\{t_\ell, j_\ell\}, \ell \in A \subset \{1, \dots, N\}$ given the remaining events $\{t_\ell, j_\ell\}, \ell \in \bar{A} = \{1, \dots, N\}/A$ can be defined as

$$p_{\{j_\ell\}, \ell \in A | \{j_\ell\}, \ell \in \bar{A}} = \frac{p_{j_1 \dots j_N}}{p_{\{j_\ell\}, \ell \in \bar{A}}} \tag{4.6}$$

For instance, the probability of events $j_{\ell+1}, \dots, j_N$ given that events $j_1, \dots, j_\ell$ have already occurred (prediction) is

$$p_{j_{\ell+1} \dots j_N | j_1 \dots j_\ell} = \frac{p_{j_1 \dots j_N}}{p_{j_1 \dots j_\ell}} \tag{4.7}$$

The probability that events $j_1, \dots, j_{N-1}$ happened in the past, given the present event $j_N$ (retrodiction) is

$$p_{j_1 \dots j_{N-1} | j_N} = \frac{p_{j_1 \dots j_N}}{p_{j_N}} \tag{4.8}$$

Weak decoherence ensures that all the above defined conditional probabilities correctly add up to 1.
A particular usefulness of retrodictions is in cosmology, where an important goal is to reconstruct the past of our universe on the base of current data. Within the standard interpretation, no statement can be made about what happened in the far past, not even in probabilistic terms, because no measurement was performed at that time. On the contrary, the framework of decoherent histories can easily accommodate such statements. Within this framework, one can legitimately speak of what "happens" or "happened" in the universe (the number of possible histories for the observable universe has been evaluated in Ref. [182]).

### 4.2.5 The decoherence matrix

The matrix

$$\mathcal{D}_{\mathbf{jk}} = \mathrm{Tr}[C_{\mathbf{j}} \varrho C_{\mathbf{k}}^\dagger] = \mathrm{Tr}[P_{j_N}^N(t_N) \dots P_{j_1}^1(t_1) \varrho_0 P_{j_1}^{1\dagger}(t_1) \dots P_{j_N}^{N\dagger}(t_N)]. \tag{4.9}$$

is called *decoherence matrix* or *decoherence functional* (I will reserve the latter term to the case of infinite-dimensional systems). The diagonal elements in $\mathcal{D}$ are probabilities of histories and its off-diagonal elements are coherences between pairs of histories. Weak decoherence implies that the real parts of the off-diagonal elements of the decoherence matrix vanish.
We can immediately verify that $\mathcal{D}_{\mathbf{jk}}$ is diagonal in $j_N, k_N$,

$$\begin{aligned}\mathcal{D}_{\mathbf{jk}} =& \mathrm{Tr}[P_{j_N}^N U(t_N - t_{N-1}) \dots P_{j_1} U(t_1 - t_0) \varrho_0 U^\dagger(t_1 - t_0) P_{k_1} \dots U(t_N - t_{N-1}) P_{k_N}^N] = \\ =& \delta_{j_N k_N} \mathrm{Tr}[P_{j_N}^N U(t_N - t_{N-1}) \dots P_1 U(t_1 - t_0) \varrho_0 U^\dagger(t_1 - t_0) P_1 \dots U(t_N - t_{N-1})]\end{aligned}$$

due to the orthogonality $P_{j_N} P_{k_N} = \delta_{j_N k_N}$. Stated otherwise, $\mathcal{D}_{\mathbf{jk}}$ is block diagonal with each block corresponding to a fixed $j_N$. Furthermore, the following properties hold

- $\mathcal{D} = \mathcal{D}^\dagger$ ($\mathcal{D}_{\mathbf{jk}} = \mathcal{D}_{\mathbf{kj}}^*$)
- $\mathrm{Tr}[\mathcal{D}] = 1$, indeed $\mathrm{Tr}[\mathcal{D}] = \sum_{\mathbf{j}} \mathcal{D}_{\mathbf{jj}} = \sum_{\mathbf{j}} p_{\mathbf{j}} = 1$
- the size of the off-diagonal elements is bounded by the size of diagonal elements,

$$|\mathcal{D}_{\mathbf{jk}}|^2 \leq \mathcal{D}_{\mathbf{jj}} \mathcal{D}_{\mathbf{kk}} \tag{4.10}$$

  and hence the matrix is positive (semidefinite), $\mathcal{D} \geq 0$.

For a pure initial state, the last property immediately follows from the Schwartz inequality for the scalar product in $\mathcal{H}$, since $\mathcal{D}_{\mathbf{jk}} = \langle \psi_0 | C_{\mathbf{j}}^\dagger C_{\mathbf{k}} | \psi_0 \rangle = \langle \psi_{\mathbf{j}} | \psi_{\mathbf{k}} \rangle$, $\mathcal{D}_{\mathbf{jj}} = \langle \psi_0 | C_{\mathbf{j}}^\dagger C_{\mathbf{j}} | \psi_0 \rangle = |||\psi_{\mathbf{j}}\rangle||^2$, $\mathcal{D}_{\mathbf{kk}} = \langle \psi_0 | C_{\mathbf{k}}^\dagger C_{\mathbf{k}} | \psi_0 \rangle = |||\psi_{\mathbf{k}}\rangle||^2$. For a general density matrix, consider

$$\mathrm{Tr}[C_{\mathbf{j}} \varrho C_{\mathbf{k}}^\dagger] = \mathrm{Tr}[C_{\mathbf{j}} \varrho^{1/2} \varrho^{1/2} C_{\mathbf{k}}^\dagger] = \mathrm{Tr}[C_{\mathbf{j}} \varrho^{1/2} (C_{\mathbf{k}} \varrho^{1/2})^\dagger] \tag{4.11}$$

Since the Hilbert-Schmidt scalar product between two operators is defined as $(A, B) \equiv \mathrm{Tr}[A^\dagger B]$, the last expression is just the Hilbert-Schmidt product of $C_{\mathbf{j}} \varrho^{1/2}$ and $C_{\mathbf{k}} \varrho^{1/2}$. The Hilbert-Schmidt respects the Schwarz inequality $|\mathrm{Tr}[A^\dagger B]|^2 \leq \mathrm{Tr}[A^\dagger A] \mathrm{Tr}[B^\dagger B]$. By applying the latter, the desired result follows. Finally, the expression $\mathcal{D}_{\mathbf{jk}} = \mathrm{Tr}[(C_{\mathbf{j}} \varrho^{1/2} (C_{\mathbf{k}} \varrho^{1/2})^\dagger]$ implies that $\mathcal{D}_{\mathbf{jk}}$ is the Gram matrix of the set of linearly independent vectors $\{C_{\mathbf{j}} \varrho^{1/2}\}$. Thus, it is a semipositive definite matrix.
The decoherence matrix is a Hermitian, positive, trace-one matrix and thus has the same properties of a density matrix. In the next chapter (§ 5.1) we will show that such an interpretation is indeed warranted, because $\mathcal{D}$ can be seen as the density matrix of a set of registers interacting with the system in such a way as to effectively induce the projective measurements $P_{j_\ell}$ on it.

### 4.2.6 Medium decoherence

While the weak decoherence condition is sufficient to ensure that the probability rules apply, several authors – most notably, Gell-Mann and Hartle – have proposed to replace it with the stronger condition that both the real and imaginary parts of the off-diagonal terms of the decoherence matrix vanish:

$$\mathrm{Tr}[C_{\mathbf{j}}\varrho C_{\mathbf{k}}^{\dagger}] = 0, \forall \mathbf{j}, \mathbf{k} \tag{4.12}$$

This condition is called *medium decoherence* in the literature. It implies that the decoherence matrix is diagonal, $\mathcal{D}_{\mathbf{jk}} = \delta_{\mathbf{jk}} p_{\mathbf{j}}$.
There are several strong arguments in favour of medium decoherence, as opposed to weak decoherence as the right condition to assign probabilities to a set of histories. First, there are several physical mechanisms that can lead to medium decoherence, but it is hard to think of any that may lead to weak decoherence alone, without inducing medium decoherence at the same time. Indeed, in most in most situations weak decoherence between histories arises only as a consequence of coarse-graining (see § 4.3) and environmental noise. In this case, weak decoherence is always accompanied by medium decoherence. Second, there are strong conceptual arguments [179] pointing out the inadequacy of weak decoherence, of which I will mention the most striking. Consider two independent systems $A$ and $B$ with density matrices $\varrho_A$ and $\varrho_B$ and two independent sets of histories $\Sigma_A = \{\mathbf{j}\}$ and $\Sigma_B = \{\mathbf{j}'\}$ for $A$ and $B$ respectively. Independence implies that the compound system $AB$ has density matrix $\varrho_{AB} = \varrho_A \otimes \varrho_B$. From $\Sigma_A$ and $\Sigma_B$ we obtain a natural set of histories $\Sigma = \{\mathbf{jj}'\}$ for the joint system by taking $P^{\ell}_{j_\ell j'_\ell} = P^{A\ell}_{j_\ell} \otimes P^{B\ell}_{j'_\ell}$, with a decoherence matrix

$$\mathcal{D}^{AB}_{\mathbf{jj}'\mathbf{kk}'} = \mathrm{Tr}[C^A_{\mathbf{j}} \otimes C^B_{\mathbf{j}'}\ \varrho_1 \otimes \varrho_2\ C^{A\dagger}_{\mathbf{k}} \otimes C^{B\dagger}_{\mathbf{k}'}] = \mathcal{D}^{A}_{\mathbf{jk}}\mathcal{D}^{B}_{\mathbf{j}'\mathbf{k}'} \tag{4.13}$$

If $\Sigma_A$ and $\Sigma_B$ are weakly decoherent, we would expect $\Sigma$ to be weakly decoherent as well. However, we can immediately verify that

$$\mathrm{Re}(\mathrm{Tr}[C^A_{\mathbf{j}}\varrho_A C^A_{\mathbf{k}}]) = 0, \forall \mathbf{j} \neq \mathbf{k}, \qquad \mathrm{Re}(\mathrm{Tr}[C^B_{\mathbf{j}'}\varrho_B C^B_{\mathbf{k}'}]) = 0, \forall \mathbf{j}' \neq \mathbf{k}'$$

does not ensure

$$\mathrm{Re}[\mathcal{D}^{AB}_{\mathbf{jj}'\mathbf{kk}'}] = 0, \forall \mathbf{jj}' \neq \mathbf{kk}'$$

If weak decoherence holds for two statistically independent systems, it is not guaranteed that it holds for the composite system that joins them. In other words, if we can separately assign well-defined probabilities to given sets of histories for $A$ and $B$, which are independent systems, it might be impossible to assign well-defined probabilities to the corresponding histories for the joint $AB$ system. This can be regarded as a serious drawback, since it collides with any notion of statistical independence. By inspection, on can see that the medium decoherence condition does not suffer from the same flaw: medium decoherence for independent component systems *does* imply medium decoherence for the composite system.

For the case of pure states, medium decoherence is equivalent to the presence of so-called *generalized records* . Indeed the medium decoherence condition can be rewritten

as $\langle\psi_{\mathbf{j}}|\psi_{\mathbf{k}}\rangle = \langle\psi_0|C_{\mathbf{j}}^\dagger C_{\mathbf{k}}|\psi_0\rangle = 0$. The orthogonality of the $|\psi_{\mathbf{j}}\rangle$ is equivalent to the existence of orthogonal projectors

$$P_{\mathbf{j}}P_{\mathbf{k}} = \delta_{\mathbf{jk}}P_{\mathbf{j}}, \qquad \sum_{\mathbf{j}} P_{\mathbf{j}} = \mathbb{I}, \qquad P_{\mathbf{j}}C_{\mathbf{k}}|\psi_0\rangle = \delta_{\mathbf{jk}}C_{\mathbf{j}}|\psi_0\rangle$$

Remind that $C_{\mathbf{j}}$ need not be themselves projectors. The $P_{\mathbf{j}}$ together constitute a projective measurement on different histories of the system, and so they yield *generalized records* of the history. This suggests that medium decoherence may arise as a consequence of physical decoherence, when each branch $|\psi_{\mathbf{j}}\rangle$ becomes correlated with orthogonal states of the degrees of freedom that are traced over by the coarse-graining procedure (see the discussion in § 4.3).

### 4.2.7 Decoherent histories and generalized measurements

In the literature, one finds also a more general definition of event [180, 181]. Instead of a (time,projector) pair $t, P$, we can specify a time $t$ and a positive operator $E$. A positive operator has an eigendecomposition $E = \sum_\lambda q_\lambda P_\lambda$ where $P_\lambda$ are orthogonal projectors and $q_\lambda > 0$. As a weighted sum of orthogonal projectors, a positive operator defines and "unsharp" event where Hilbert subspaces $\mathcal{P}_\lambda$ are assigned weights $q_\lambda$. An exhaustive set of events at time $t$ can be defined as a set $\Sigma$ of $n \leq d^2$ positive operators $E_j$ such that $\sum_{j=1}^n \mathcal{E}_j = \mathbb{I}$. An exhaustive set of events thus defines a generalized measurement, or POVM at time $t$. Events in the set are not required to be exclusive, i.e. we can have $E_j E_k > 0$ for $k \neq j$.

Given an ordered sequence of times $t_1 < \cdots < t_N$, a *history* is defined as a sequence of events $\mathfrak{h} = E^1, t_1 \ldots, E^N, t_N$. If we have $N$ exhaustive sets of events $\{t_\ell, E^\ell_{j_\ell}\}, j_\ell = 1, \ldots, n_\ell$ with, $\sum_{j_\ell} E_{j_\ell} = \mathbb{I}$, we can define an exhaustive set of (non-exclusive) histories as

$$\Sigma = \{\mathfrak{h}_{\mathbf{j}}\} = \{t_1, E^1_{j_1}, \ldots, t_N, E^N_{j_N}\}$$

where the multi-index $\mathbf{j} = j_1, \ldots, j_N$ labels different alternative histories. As already done in the case of projective measurements, we will denote a history with the corresponding multi-index, $\mathbf{j}$ instead of the "heavier" notation $\mathfrak{h}_{\mathbf{j}}$.

When a POVM is performed on a state $\varrho$, the post-measurement state corresponding to $E_i$ is given by $\frac{1}{p_j} A_j \varrho A_j^\dagger$, where $A_i$ is a square-root of $E_i$, i.e., an operator such that $A_i A_i^\dagger = E_i$ and where $p_j = Tr[\varrho E_j] = Tr[A_j \varrho A_j^\dagger]$. In other terms, the effect of a POVM on a state is specified only if we specify a corresponding quantum operation with Kraus operators given by the $A_j$. Given a given a sequence of generalized measurements, we we can predict the probability of each sequence of outcomes $\mathbf{j} = j_1 \ldots j_N$, provided that i) we know the initial state and the unitary dynamics governing the system. ii) for each $E^\ell_{j_e ll}$ we specify a quantum operation with Kraus operators $A^\ell_{j_\ell}$ such that that $E^\ell_j = \mathcal{A}^{\ell\dagger}_j \mathcal{A}^\ell_j$.

If the initial state is pure, outcomes $\mathbf{j} = j_1 \ldots j_N$ are obtained at times $t_1, \ldots, t_N$ with probability $p_{\mathbf{j}} = |||\psi_{\mathbf{j}}\rangle||^2$, where

$$|\psi_{\mathbf{j}}\rangle \equiv \mathcal{A}^N_{j_N} U(t_N - t_{N-1}) \mathcal{A}^{N-1}_{j_{N-1}} U(t_{N-1} - t_{N-2}) \ldots \mathcal{A}_{j_1} U(t_1 - t_0)|\psi_0\rangle$$

is an un-normalized path-projected vector (after outcomes $j_1 \dots j_N$ are obtained, the state of the system is $\frac{1}{\sqrt{p_{\mathbf{j}}}}|\psi\rangle_{\mathbf{j}}$).
If the initial state is mixed, outcomes $\mathbf{j} = j_1 \dots j_N$ are obtained at times $t_1, \dots, t_N$ with probability $p_{\mathbf{j}} = \mathrm{Tr}[\varrho_{\mathbf{j}}]$, where

$$\varrho_{\mathbf{jj}} = \mathcal{A}^N_{j_N} U(t_N - t_{N-1}) \mathcal{A}^{N-1}_{j_{N-1}} U(t_{N-1} - t_{N-2}) \dots \mathcal{A}_{j_1} U(t_1 - t_0) \varrho_0 \times$$
$$U^\dagger(t_1 - t_0) \mathcal{A}_{j_1} \dots U^\dagger(t_{N-1} - t_{N-2}) \mathcal{A}^{N-1}_{j_{N-1}} U(t_N - t_{N-1}) \mathcal{A}^N_{j_N}$$

is an un-normalized path-projected density matrix (after outcomes $\mathbf{j} = j_1 \dots j_N$ are obtained the system is left in the state $\frac{1}{p_{\mathbf{j}}}\varrho_{\mathbf{j}}$).
Upon adopting the Heisenberg representation $\mathcal{A}_{j_\ell}(t) = U^\dagger(t)\mathcal{A}_{j_\ell}U(t)$ and the history operators $C_{\mathbf{j}} \equiv \mathcal{A}^N_{j_N}(t_N) \dots \mathcal{A}^1_{j_1}(t_1)$, we can rewrite formulas above as

$$p_{\mathbf{j}} = ||C_{\mathbf{j}}|\psi_0\rangle||^2 \quad \text{(pure states)} \qquad p_{\mathbf{j}} = \mathrm{Tr}[C_{\mathbf{j}} \varrho_0 C^\dagger_{\mathbf{j}}] \quad \text{(mixed states)} \tag{4.14}$$

In the decoherent histories formulation for generalized measurements, formulas (4.14) represent the probabilities of histories within an exhaustive set. Again, probabilities are to be assigned only to sets of histories that satisfy the weak decoherence (consistency) condition

$$\mathrm{Re}(\mathrm{Tr}[C_{\mathbf{j}} \varrho_0 C^\dagger_{\mathbf{k}}]) = 0, \forall \mathbf{j} \neq \mathbf{k}$$

or the medium decoherence condition

$$\mathrm{Tr}[C_{\mathbf{j}} \varrho_0 C^\dagger_{\mathbf{k}}] = 0, \forall \mathbf{j} \neq \mathbf{k}$$

The decoherence matrix is expressed as

$$\mathcal{D}_{\mathbf{jk}} = \mathrm{Tr}[C_{\mathbf{j}} \varrho_0 C^\dagger_{\mathbf{k}}] = \mathrm{Tr}[\mathcal{A}^N_{j_N}(t_N) \dots \mathcal{A}^1_{j_1}(t_1) \varrho_0 \mathcal{A}^{1\dagger}_{j_1}(t_1) \dots \mathcal{A}^{N\dagger}_{j_N}(t_N)]. \tag{4.15}$$

### 4.2.8 criticisms to the histories interpretation

To close this section, we briefly mention some main criticisms that have been raised against the decoherent histories interpretation (for a critical review, see [174]). The first issue is that several consistency conditions have been proposed in the literature: in addition to weak decoherence and medium decoherence, other authors have proposed different criteria called feasibility [178], linear consistency [177], ordered consistency [175]. There is disagreement over which condition is the most appropriate. Second, and more important, the weak decoherence condition (or for what matters, any other consistency condition among those proposed) is in general insufficient to single out a single set of histories. Thus the pictures of physics given by the many different consistent sets have to be assigned equal fundamental status, even if they are generally incompatible with one another. Third, examples can be found where two contrary propositions – statements corresponding to orthogonal projections – can be retrodicted from the same data, each with probability one, in different sets [176]. Fourth, given a proposition $P$ that should be logically implied by $Q$, $PQ = QP = P$ (or $P \leq Q$), if $Q$ can be assigned a given probability within a decoherent set of histories, it is not guaranteed that also $P$ can. Thus strictly speaking $P$ cannot be inferred from $Q$. For

instance, we cannot generally infer from the observation that a particle was in a given region at a given time that the particle was in a larger region containing the first [175]. While these points are of fundamental importance for interpretational concerns, and affect the status of decoherent histories as a theory, we will not dwell longer in this discussion since it is outside the scope of this thesis. As mentioned above, we take a rather pragmatic view and regard decoherent histories mainly as a useful language to discuss physics, independent of interpretational subtleties.

## 4.3 quantum histories and decoherence

In Hartle and Gell-Mann's view, one of the central goals of the decoherent histories approach is to explain the transition from the quantum world to the classical world of familiar experience. In the latter domain, one can give a consistent description of a system where the values of all classical variables (such as position and momentum) can be simultaneously specified, and, furthermore, show correlation patterns that are well described by classical laws. Such a description can be formulated in terms of classical histories, that are always decoherent no matter what variables they include. On the contrary, in the quantum domain the consistency (decoherence) condition forces the observer to choose between different alternative, incompatible descriptions of a system that can include only some observables but not others.
To explain how the loss of coherence is achieved in the macroscopic domain, one should, not surprisingly, invoke decoherence. But now by decoherence we intend what is normally intended in the quantum physics paradigm, i.e, a loss of quantum features due to the limited information that is available to the observer. In a word, decoherence - in the sense of histories - can be related to decoherence - as a physical process. This is indeed the ultimate justification behind Gell-Mann and Hartle's choice of the name "decoherent histories". In standard decoherence theory, a variety of physical mechanisms cause quantum information (usually encoded in quantum phases) to be scattered in quantum correlations among a huge number of degrees of freedom, most of which out of the observer's control, so that coherent effects become locally inaccessible. Similarly, in the decoherent histories approach coherent features are washed out by a coarse-graining procedure that conceals correlations between the variables that are distinguished by the coarse-graining and those that are ignored.

### 4.3.1 Decoherence and coarse-graining

When sets of histories satisfy the consistency condition (4.5) as a result of physical decoherence and coarse-graining, they typically satisfy, in addition, medium decoherence.
Among the types of coarse-graining that can lead to (medium) decoherence, the most common is the type involving a factorization of the Hilbert space in a subsystem of interest and the rest, $\mathcal{H} = \mathcal{H}_S \otimes \mathcal{H}_\mathcal{E}$. In general, given such a factorization, the events of a history take the form $P^\ell_{j_\ell j'_\ell} = \tilde{P}^\ell_{j_\ell} \otimes \Pi^\ell_{j'_\ell}$ where $\tilde{P}^\ell_{j_\ell}$ and $\Pi^\ell_{j'_\ell}$ are projectors onto Hilbert subspaces of $\mathcal{H}_S$ and $\mathcal{H}_\mathcal{E}$. Histories for $S$ alone can be obtained upon consid-

ering appropriate coarse-grainings over the environment degrees of freedom, such that the events are $\tilde{P}^{\ell}_{j_\ell} \otimes \mathbb{I}_{\mathcal{E}}$ where $\mathbb{I}_{\mathcal{E}}$ is the identity over $\mathcal{H}_{\mathcal{E}}$.
The crucial point is that when histories for the joint system form a coherent set, coarse-grained histories for the system alone can decohere. In several cases, depending on the dynamics, the coarse-graining over the environment yields indeed a decoherent set of histories for the system for an appropriate choice of the $\tilde{P}^{\ell}_{j_\ell}$. In particular, in many physical cases the resulting decoherent histories are composed by projectors in some given, *fixed* basis. In this case the standard rules of probability theory apply for histories in that basis. An important research effort has been devoted to the to show that (at least approximate decoherence) arises for macroscopically coarse-grained histories in the bases corresponding to the classical variables such as position, momentum, energy[172, 171]. The relation between physical decoherence and history decoherence will be explored more in detail in Chapter 7.

### 4.3.2 Example: decoherence for a particle coupled to a bath of oscillators

One can demonstrate how medium decoherence and quasiclassical trajectories follow from physical decoherence and coarse-graining, by looking at decoherent histories in a model where a particle is linearly coupled to a bath of oscillators [166]. Here we will briefly mention some main results (without a proof or discussion) for the purpose of illustration. For an infinite-dimensional system, the maximally fine-grained decoherence functional can be expressed in terms of the fundamental action as follows,

$$\mathcal{D}[q(t), q'(t)] = \delta(q(t_f), q'(t_f)) e^{i(\mathcal{S}[q(t)-\mathcal{S}[q'(t)])} \varrho(q(t_0), q'(t_0)) \tag{4.16}$$

A coarse graining is peformed where the coordinates are divided into those ($x$) of the particles, that are distinguished by the coarse graining, and those ($Q$) of the bath that are ignored. This division corresponds to a factorization of the total Hilbert space $\mathcal{H} = \mathcal{H}_x \otimes \mathcal{H}_Q$. The fine grained decoherence functional for the particles (upon coarse-graining over the bath modes) reads

$$\mathcal{D}[x(t), x'(t)] = \int DQDQ' \delta(q(t_f), q'(t_f)) e^{i(\mathcal{S}[q(t)-\mathcal{S}[q'(t)])} \varrho(q(t_0), q'(t_0)) \tag{4.17}$$

The action for the system can be written as $\mathcal{S}_{free}[x(t)] + \mathcal{S}_0[Q(t) + \mathcal{S}_{int}[x(t), Q(t)]]$. The term $\mathcal{S}_{free}[x(t)]$ depends only on $x(t)$ (it is free of interaction with the $Q$). We can then express $\mathcal{D}[x(t), x'(t)]$ as follows:

$$\mathcal{D}[x(t), x'(t)] = \delta(x(t_f), x'(t_f)) e^{i(\mathcal{S}_{free}[x(t)-\mathcal{S}_{free}[x'(t)]} \int DQDQ' \delta(Q(t_f), Q'(t_f)) \times$$
$$e^{i(\mathcal{S}_0[Q(t)+\mathcal{S}_{int}[x(t),Q(t)]-\mathcal{S}_0[Q'(t)]-\mathcal{S}_{int}[x'(t),Q'(t)])} \varrho(x(t_0), Q(t_0), x'(t_0), Q'(t_0))$$

The integral over the $Q$s defines $\mathcal{W}$, a functional of the paths $x(t)$ and $x(t')$ and their endpoints $x(t_0)$ and $x'(t_0)$ as follows:

$$e^{i\mathcal{W}[x(t),x'(t);x(t_0),x'(t_0)]} \tilde{\varrho}(x(t), x'(t)) = \int DQDQ' \delta(Q(t_f), Q'(t_f)) \times$$
$$e^{-i(\mathcal{S}_0[Q(t)+\mathcal{S}_{int}[x(t),Q(t)]-\mathcal{S}_0[Q'(t)]-\mathcal{S}_{int}[x'(t),Q'(t)])} \varrho(x(t_0), Q(t_0), x'(t_0), Q'(t_0))$$

where $\tilde{\varrho}(x(t), x'(t)) = \mathrm{Tr}_Q[\varrho(q(t), q'(t))]$ is the reduced density matrix associated with the coarse-graining. The functional $\mathcal{W}$ is called *influence phase*. It depends on the endpoints $x(t_0)$ and $x'(t_0)$ implicitly through the paths $x(t)$ and $x(t')$ and explicitly $\varrho(x(t_0), Q(t_0), x'(t_0), Q'(t_0))$. This double dependence is remarked through the notation $\mathcal{W}[x(t), x'(t); x(t_0), x'(t_0)]$. Conventionally, it is assumed that the initial density matrix of the system factorizes,

$$\varrho(q(t_0), q'(t_0)) = \tilde{\varrho}(x(t_0), x'(t_0)) \times \varrho_B(Q(t_0), Q'(t_0))$$

In this case, $\mathcal{W}$ contains no explicit dependence on $x(t_0)$ and $x'(t_0)$: $\mathcal{W} = \mathcal{W}[x(t), x'(t)]$ and thus the fine-grained decoherence functional per the particle reads

$$\mathcal{D}[x(t), x'(t)] = \quad \delta(x(t_f), x'(t_f)) e^{-i(\mathcal{S}_{free}[x(t)-\mathcal{S}_{free}[x'(t)]+\mathcal{W}[x(t),x'(t)])} \tilde{\varrho}(x(t), x'(t))$$

The imaginary part of $\mathcal{W}$ is causes an exponential suppression of the off-diagonal terms $x \neq x'$. If the particle is a linear oscillator, since all terms in the action are quadratic, $\mathcal{W}$ can be computed by performing Gaussian integrals (a strategy first suggested by a classical study of Feynman and Vernon). By looking at a linear oscillator with frequency $\omega_R$ interacting with an thermal bath of oscillators at temperature $T$ characterized by a spectral density with cut-off at a frequency $\Omega$ when the bath of oscillator is at a temperature $kT \gg \hbar\Omega \gg \hbar\omega_R$ one finds

$$\mathrm{Im}\mathcal{W}[x(t), x'(t)] = \frac{i2M\gamma kT}{\hbar} \int dt (x' - x)^2 \tag{4.18}$$

where $\gamma$ summarized the interaction strength with the bath of oscillators, and $M$ is the oscillator mass. Im$\mathcal{W}$ squeezes together the paths $x$ and $x'$, thus creating (approximate) decoherence for paths $q$ and $q'$ differing by $d$ will decohere after a time scale

$$t \geq \frac{1}{\gamma} \left( \frac{\hbar}{\sqrt{2Mkt}} \frac{1}{d} \right)^2 . \tag{4.19}$$

Upon looking at the history probabilities $p(x(t)) = \mathcal{D}[x(t), x'(t)]$, one can verify the the probability is peaked around the classical trajectory, and analyze non-classical deviations modeled as an effective Langevin force [166].

### 4.3.3 Decoherence, subsystems and Markovian dynamics

As was mentioned above, the most common type of coarse-graining involves the factorization of the system into a subsystem of interest $S$ and an environment $\mathcal{E}$. The physical theory of decoherence devotes significant attention to the problem of finding the reduced dynamics of $S$ when the environment is traced over. In the case of decoherent histories, one asks under which conditions the decoherence matrix can be written in terms of reduced quantities alone, i.e., in terms of the reduced density matrix $\varrho_S(t_0) = \mathrm{Tr}_{\mathcal{E}}[\varrho(t_0)]$ and a reduced propagator for $S$. One encounters thus problem whenever one wants to analyze deocoherent histories in open quantum systems, as we will see for instance in Chapter 7.

Given a factorization $\mathcal{H} = \mathcal{H}_S \otimes \mathcal{H}_\mathcal{E}$, and considering a coarse graining over the environment degrees of freedom, such that the events are $\tilde{P}^\ell_{j_\ell} \otimes \mathbb{I}_\mathcal{E}$, the decoherence matrix for $S$ reads:

$$\mathcal{D}_{\mathbf{jk}} = \mathrm{Tr}[\tilde{P}_{j_N} U(t_N - t_{N-1}) \dots \tilde{P}_{j_1} U(t_1 - t_0) \varrho(t_0) U(t_1 - t_0)^\dagger \tilde{P}_{k_1} \dots U(t_N - t_{N-1}) \tilde{P}_{k_N}]$$

where $U$ is the joint evolution of system and environment. For convenience, let us first introduce the propagator $\mathcal{K}_{t\ t_0}$ as

$$\varrho(t) = U(t - t_0)\varrho(t_0)U(t - t_0)^\dagger \equiv \mathcal{K}_{t\ t_0}[\varrho(t_0)] \tag{4.20}$$

We can rewrite the above equation as:

$$\mathcal{D}_{\mathbf{jk}} = \mathrm{Tr}[\tilde{P}^N_{j_N} \mathcal{K}_{t_N\ t_{N-1}}[\tilde{P}_{j_{N-1}} \mathcal{K}_{t_{N-1}\ t_{N-2}}[\dots \mathcal{K}_{t_1\ t_0}[\varrho_0] \dots] \tilde{P}_{k_{N-1}}] \tilde{P}^N_{k_N}] \tag{4.21}$$

If the initial state is factorized $\varrho(t_0) = \tilde{\varrho}_S(t_0) \otimes \varrho_\mathcal{E}(t_0)$, then the reduced density matrix $\varrho_S(t) = Tr_\mathcal{E}[\varrho(t)]$ evolves according to $\varrho_S(t) = \tilde{\mathcal{K}}_{t\ t_0} \varrho_S(t_0)$ where $\tilde{\mathcal{K}}$ is the (non-unitary) reduced propagator defined by

$$\mathrm{Tr}[U(t - t_0)\tilde{\varrho}_S(t_0) \otimes \varrho_E(t_0) U^\dagger(t - t_0)] = \tilde{\mathcal{K}}_{t\ t_0} \tilde{\varrho}_S(t_0) \tag{4.22}$$

We would like to write the decoherence matrix in terms of reduced quantities alone, i.e., in the form:

$$\mathcal{D}_{\mathbf{jk}} = \mathrm{Tr}[\tilde{P}^N_{j_N} \tilde{\mathcal{K}}_{t_N\ t_{N-1}}[\tilde{P}_{j_{N-1}} \tilde{\mathcal{K}}_{t_{N-1}\ t_{N-2}}[\dots \tilde{\mathcal{K}}_{t_1\ t_0}[\varrho_0] \dots] \tilde{P}_{k_{N-1}}] \tilde{P}^N_{k_N}] \tag{4.23}$$

This reformulation is possible only if the trace over the environment $Tr_\mathcal{E}$ can "seep in" inside expression (4.21) up to the initial density matrix, i.e. if we have

$$\begin{aligned}
&Tr_\mathcal{E}[U(t_N - t_{N-1})\tilde{P}_{j_{N-1}} U(t_{N-1} - t_{N-2}) \dots \tilde{P}_{j_1} U[(t_1 - t_0)\varrho_0 \times \\
&U^\dagger[(t_1 - t_0)\tilde{P}_{k_1} \dots U^\dagger(t_{N-1} - t_{N-2})\tilde{P}_{k_{N-1}} U^\dagger(t_N - t_{N-1})] = \\
&= \tilde{\mathcal{K}}_{t_N\ t_{N-1}} Tr_E[\tilde{P}_{j_{N-1}} U(t_{N-1} - t_{N-2}) \dots \tilde{P}_{j_1} U[(t_1 - t_0)\varrho_0 \times \\
&U^\dagger[(t_1 - t_0)\tilde{P}_{k_1} \dots U^\dagger(t_{N-1} - t_{N-2})\tilde{P}_{k_{N-1}}]
\end{aligned}$$

This is true if the evolution of the system and environment is Markovian. In this case, the semigroup property holds $\tilde{K}_{t_2\ t_0} = \tilde{\mathcal{K}}_{t_2\ t_1} \tilde{\mathcal{K}}_{t_1\ t_0}$ and we can write $\tilde{\mathcal{K}}_{t\ t'} = \tilde{\mathcal{K}}_{t-t'}$. The semigroup property implies

$$\mathrm{Tr}[U(t - t')\varrho(t')U^\dagger(t - t')] = \tilde{\mathcal{K}}_{t-t'}[\tilde{\varrho}_S(t')].$$

Obviously, the system evolution can be Markovian only over time intervals $\Delta t \gg \tau_C$ where $\tau_C$ is the system-environment correlation time. Thus, Eq. (4.23) is valid only if the time interval $\Delta t$ between projections (the temporal coarse-graining) is much higher than $t_C$.

# Chapter 5

# Decoherent histories and dynamical entropy

In this chapter, we will prove that quantum dynamical entropy (the quantum counterpart of the classical Kolmogorov-Sinai entropy) can be naturally embedded in the decoherent histories formulation of quantum mechanics, and will elucidate the consequences for its interpretation. The link between histories and dynamical entropy exists because partitions of the identity (which enter the definition of dynamical entropy) are equivalent to POVMs, and the latter can be used to define a set of quantum histories with the same POVM repeated at regular times. As we will show, the most widespread definition of dynamical entropy, the Alicki-Fannes (ALF) entropy, is determined the von Neumann entropy of the decoherence matrix for a set of histories constructed in this way (to be precise, ALF-entropy is obtained by maximizing over all POVMs, taking the limit of the von Neumann entropy per measurement step as of the number of measurements goes to infinity). As we will show, any decoherence matrix can be intepreted as a density matrix over a set of registers, that subsequently interact with the system, effectively performing the "measurements" that define the set of histories under attention. Thus the von Neumann entropy of the decoherence matrix that defines ALF entropy can be seen as the amount of quantum information stored in a set of registers. This will justify an interpretation of ALF entropy as the rate of production of *quantum* information by the dynamics, in the same way as the classical Kolmogorov-Sinai entropy can be interpreted as the rate at which classical information is produced by the dynamics.

As a byproduct of our analysis, we will be able to define a general measure of coherence between histories. Due to coherence, the von Neumann entropy of a decoherence matrix is lower the Shannon entropy of its diagonal enties (history probabilities). Upon taking the difference between the two, which can be also interpreted as the quantum relative entropy between the decoherence matrix and a corresponding diagonal decoherence matrix, we will define a measure of coherence between histories, called *relative entropy of decoherence*.

This chapter is organized as follows. In § 5.1 I will derive the interpretation of the

decoherence matrix as a density matrix. In § 5.2 I will review classical dynamical entropy. In § 5.3 I will discuss the quantum dynamical entropy. In § 5.3.1 I will introduce ALF entropy in a way that immediately show its connection with decoherent histories. Since ALF entropy is defined for infinite-dimensional systems, in § 5.3.2 I will briefly discuss how it can be extended to finite-dimensional ones. Finally, in § 5.3.3 I will introduce the relative entropy of decoherence.
To the best of my knowledge, the content of this chapter represents an original contribution, as neither the connection between decoherent histories and dynamical entropy nor the interpretation of the decoherence matrix as a density matrix over a set of registers have been presented in previous literature.

## 5.1 The decoherence matrix as a density matrix

In this section, we will prove that the decoherence matrix can be interpreted as the density matrix of an ensemble of registers that subsequently interact with the system, effectively performing the measurements that define the set of histories under attention. This feature will be crucial for our interpretation of the dynamical entropy in the following section.
Consider a projective measurement $P_j, j = 1 \ldots, n$ at time $t$ on a system with Hilbert space $\mathcal{H}_S$. Assume that there is a register with Hilbert space $\mathcal{H}_R$, $\dim \mathcal{H}_R = n$. If $P_j = \sum_{a_j} |a_j\rangle_S\langle\alpha_j|$, the measurement can be realized by a unitary operator $W$ acting jointly on the system and register as follows

$$W|a_j\rangle_S\langle a_j| \otimes |0\rangle_R\langle 0| = |a_j\rangle_S\langle a_j| \otimes |j\rangle_R\langle j| \tag{5.1}$$

The operator $W$ leaves the state of $S$ invariant and shifts $R$ according to $j$. We assume that $W$ has a duration $\tau$ and that the register does not change with time (its internal dynamics is given by $U_R = \mathbb{I}$).
If the initial system-register state is $|\psi_0\rangle_S \otimes |0\rangle_R$, and assuming that $W$ acts on a timescale much smaller than the system's evolution timescales, the joint $SR$ evolution up to time $t_f > t$ can be approximated by

$$|\Psi(t_f)\rangle_{SR} \simeq (U(t_f - t + \tau/2) \otimes \mathbb{I})W(U(t - t_0 - \tau/2) \otimes \mathbb{I})|\psi_0\rangle_S \otimes |0\rangle_R \tag{5.2}$$

If $W$ acts quasi-instantaneously, within a time $\tau \to 0$, the approximation becomes exact,

$$|\Psi(t_f)\rangle_{SR} = (U(t_f - t) \otimes \mathbb{I})W(U(t - t_0) \otimes \mathbb{I})|\psi_0\rangle \otimes |0\rangle \tag{5.3}$$

If $U(t - t_0)|\psi_0\rangle = \sum_j \sum_{a_j} c_{a_j}|a_j\rangle$, we find

$$|\Psi(t_f)\rangle_{SR} = \sum_j \sum_{a_j} c_{a_j}(U(t_f - t) \otimes \mathbb{I})|a_j\rangle \otimes |j\rangle = \sum_j U(t_f - t)P_jU(t - t_0)|\psi_0\rangle \otimes |j\rangle$$

By using the Heisenberg representation, $P_j(t) = U^\dagger(t - t_0)P_jU(t - t_0)$

$$|\Psi(t_f)\rangle_{SR} = U(t_f - t_0) \sum_j P_j(t)|\psi_0\rangle_S \otimes |j\rangle_R$$

A sequence of $N$ measurements $P^\ell_{j_\ell}$ at times $t_\ell, \ell = 1,\dots,N$ can be realized by interaction with $N$ registers $R_1,\dots,R_N$ with Hilbert space spaces $\mathcal{H}_{R_\ell}$, $\dim \mathcal{H}_{R_\ell} = n_\ell$, $\ell = 1,\dots,N$. If $P^\ell_{j_\ell} = \sum_{\alpha^\ell_{j_\ell}} |\alpha^\ell_{j_\ell}\rangle\langle\alpha^\ell_{j_\ell}|$, the interaction at time $t_\ell$ is given by unitary operator $W^\ell$ acting jointly on the system and register $\ell$ as follows

$$W^\ell |\alpha^\ell_{j_\ell}\rangle_S\langle\alpha^\ell_{j_\ell}| \otimes |k\rangle_{R_\ell}\langle k| = |\alpha^\ell_{j_\ell}\rangle_S\langle\alpha^\ell_{j_\ell}| \otimes |(j_\ell + k) \mathrm{mod}\, n_\ell\rangle_{R_\ell}\langle (j_\ell + k) \mathrm{mod} n_\ell|$$

For all $R_\ell$, we assume that $W^\ell$ acts on a vanishing timescale $\tau \to 0$ and that the registers are static, i.e., their internal dynamics is $U_{R_\ell} = \mathbb{I}$. If the initial system-registers state is $|\psi_0\rangle_S \otimes |0\rangle_{R_1} \otimes \dots |0\rangle_{R_N}$, the joint evolution up to time $t_f > t_N$ can be easily computed as:

$$\begin{aligned} |\Psi(t_f)\rangle_{SR_1\dots R_N} = \sum_{j_1\dots j_N} U(t_f - t_N) P^N_{j_N} U(t_N - t_{N-1}) P^{N-1}_{j_{N-1}} \dots P^1_{j_1} U(t_1 - t_0) \times \\ \times |\psi_0\rangle \otimes |j_1\rangle_{R_1} \otimes \dots \otimes |j_N\rangle_{R_N} \end{aligned} \tag{5.4}$$

By using the Heisenberg representation, the history operators $C_{\mathbf{j}} = P_{j_N}(t_N)\dots P_{j_1}(t_1)$ and the path-projected vectors $|\psi_{\mathbf{j}}\rangle = U(t_f - t_0) C_{\mathbf{j}} |\psi_0\rangle$ (see § 4.2.3), we can write

$$\begin{aligned} |\Psi(t_f)\rangle_{SR_1\dots R_N} &= U(t_f - t_0) \sum_{\mathbf{j}} C_{\mathbf{j}} |\psi_0\rangle_S \otimes |\mathbf{j}\rangle_{R_1\dots R_N} = \\ &= \sum_{\mathbf{j}} |\psi_{\mathbf{j}}\rangle_S \otimes |\mathbf{j}\rangle_{R_1\dots R_N} \end{aligned}$$

Taking the trace over the registers, we obtain

$$\varrho_S = \sum_{\mathbf{j}} |\psi_{\mathbf{j}}\rangle_S\langle\psi_{\mathbf{j}}| = \sum_{\mathbf{j}} p_{\mathbf{j}} \Big( \frac{1}{\sqrt{p_{\mathbf{j}}}} |\psi_{\mathbf{j}}\rangle_S\langle\psi_{\mathbf{j}}| \frac{1}{\sqrt{p_{\mathbf{j}}}} \Big) \tag{5.5}$$

which is a weighted sum of all post-measurement states corresponding to successive outcomes $\mathbf{j}$. If instead we take the trace over the system, the registers are left in the state

$$\varrho_{R_1\dots R_N} = \sum_{\mathbf{jk}} \mathrm{Tr}_S [C_{\mathbf{j}} |\psi_0\rangle\langle\psi_0| C^\dagger_{\mathbf{j}}]\ |\mathbf{j}\rangle\langle\mathbf{k}|_{R_1\dots R_N} = \sum_{\mathbf{jk}} \mathcal{D}_{\mathbf{jk}} |\mathbf{j}\rangle\langle\mathbf{k}|_{R_1\dots R_N} \tag{5.6}$$

where $\mathcal{D}_{\mathbf{jk}}$ is the decoherence matrix defined in Eq. (4.9). If the initial system state is mixed ($\varrho_0$), by repeating essentially the same calculations we immediately arrive at a formula analogous to (5.4),

$$\varrho_{SR_1\dots R_N} = \sum_{\mathbf{jk}} U(t_f - t_0) C_{\mathbf{j}} \varrho_0 C^\dagger_{\mathbf{k}} U^\dagger (t_f - t_0) \otimes |\mathbf{j}\rangle\langle\mathbf{k}|_{R_1\dots R_N}$$

Taking the trace over the registers, we obtain

$$\varrho_S = \sum_{\mathbf{j}} \varrho_{\mathbf{j}} = \sum_{\mathbf{j}} p_{\mathbf{j}} \Big( \frac{1}{p_{\mathbf{j}}} \varrho_{\mathbf{j}} \Big) \tag{5.7}$$

which is a weighted sum of all post-measurement states corresponding to successive outcomes **j**. If we take the trace over the system, the registers are left in the state

$$\varrho_{R_1\dots R_N} = \sum_{\mathbf{jk}} \mathrm{Tr}_S[C_{\mathbf{j}}\varrho_0 C_{\mathbf{j}}^\dagger]\ |\mathbf{j}\rangle\langle\mathbf{k}|_{R_1\dots R_N} = \sum_{\mathbf{jk}} \mathcal{D}_{\mathbf{jk}}|\mathbf{j}\rangle\langle\mathbf{k}|_{R_1\dots R_N} \tag{5.8}$$

Therefore, *we can identify the decoherence matrix with the density matrix of $N$ register that, interacting subsequently with the system at times $t_1 \dots t_N$ effectively produce on the latter the projective measurements $P^1_{j_1} \dots P^N_{j_N}$.*

The same picture emerges also in the case of generalized histories with unsharp events. Indeed, an unsharp measurement (POVM) given by operators $E_j = \mathcal{A}_j^\dagger \mathcal{A}_j$ can be realized by a unitary dilation $W$ over an extended space comprising the system and a register $R$ with $\dim R = n \leq d^2$, initialized in some reference state $|0\rangle_R$ [227]:

$$\sum_j \mathcal{A}_j^\dagger \varrho \mathcal{A}_j = \mathrm{Tr}_R[W\varrho \otimes |0\rangle_R\langle 0|W^\dagger]$$

where $\mathcal{A}_j = {}_R\langle j|W|0\rangle_R$. We have indeed:

$$W\varrho \otimes |0\rangle_R\langle 0|W^\dagger = \sum_{jk} |j\rangle_R\langle j|W\varrho|0\rangle_R\langle 0|W^\dagger|k\rangle_R\langle k| = \tag{5.9}$$

$$= \sum_{jk} \big({}_R\langle j|W|0\rangle_R\big)\varrho\big({}_R\langle 0|W^\dagger|k\rangle_R\big) \otimes |j\rangle_R\langle k| = \sum_{jk} \mathcal{A}_j\varrho\mathcal{A}_k^\dagger \otimes |j\rangle_R\langle k|$$

and upon tracing $R$ we obtain $\sum_j \mathcal{A}_j\varrho\mathcal{A}_j^\dagger$.
Let us consider an unsharp measurement at time $t$. We assume, in the same way as above, that $W$ has a quasi-instantaneous duration $\tau \to 0$ and that the register is static (its internal dynamics is given by $U_R = \mathbb{I}$). If the initial system-register state is $|\psi_0\rangle \otimes |0\rangle$, the joint evolution up to time $t_f > t$ is

$$\begin{aligned}|\Psi(t_f)\rangle_{SR} =& (U(t_f - t) \otimes \mathbb{I})W(U(t - t_0) \otimes \mathbb{I})|\psi_0\rangle_S \otimes |0\rangle_R = \\ =& \sum_j U(t_f - t)\mathcal{A}_j U(t - t_0)|\psi_0\rangle \otimes |j\rangle\end{aligned}$$

A sequence of $N$ unsharp measurements $E^\ell_{j_\ell}$ at times $t_\ell, \ell = 1, \dots, N$ can be realized by interaction with $N$ registers $R_1, \dots, R_N$ with Hilbert spaces $\mathcal{H}_{R_\ell}$, $\dim \mathcal{H}_{R_\ell} = n_\ell$, $\ell = 1, \dots, N$. The interaction at time $t_\ell$ is given by unitary operator $W^\ell$ acting jointly on the system and register $\ell$ as

$$\sum_{j_\ell} \mathcal{A}_{j_\ell}^\dagger \varrho \mathcal{A}_{j_\ell} = \mathrm{Tr}_{R_\ell}[W^\ell \varrho \otimes |0\rangle_R\langle 0|W^{\ell\dagger}]$$

where $\mathcal{A}_{j_\ell} = {}_{R_\ell}\langle j_\ell|W^\ell|0\rangle_{R_\ell}$. For all $R_\ell$, we assume that $W^\ell$ has a vanishing duration $\tau$ and that the register does not change with time. If the initial system-registers state is

$|\psi_0\rangle \otimes |0\rangle_{R_1} \otimes \ldots |0\rangle_{R_N}$, the joint evolution up to time $t_f > t_N$ can be computed in the same ways as Eq. (5.4), getting:

$$|\Psi(t_f)\rangle_{SR_1\ldots R_N} = \sum_{j_1\ldots j_N} U(t_f - t_N)\mathcal{A}^N_{j_N} U(t_N - t_{N-1})\mathcal{A}^{N-1}_{j_{N-1}} \ldots \mathcal{A}^1_{j_1} U(t_1 - t_0)\times \\ \times|\psi_0\rangle \otimes |j_1\rangle_{R_1} \otimes \cdots \otimes |j_N\rangle_{R_N} \tag{5.10}$$

By using the Heisenberg representation, the history operators $C_{\mathbf{j}} = \mathcal{A}_{j_N}(t_N)\ldots\mathcal{A}_{j_1}(t_1)$ and the path-projected vectors $|\psi_{\mathbf{j}}\rangle = U(t_f - t_0)C_{\mathbf{j}}|\psi_0\rangle$ we can write

$$|\Psi(t_f)\rangle_{SR_1\ldots R_N} = U(t_f - t_0)\sum_{\mathbf{j}} C_{\mathbf{j}}|\psi_0\rangle_S \otimes |\mathbf{j}\rangle_{R_1\ldots R_N} = \sum_{\mathbf{j}} |\psi_{\mathbf{j}}\rangle_S \otimes |\mathbf{j}\rangle_{R_1\ldots R_N}$$

Taking the trace over the system, the registers are left in the state

$$\varrho_{R_1\ldots R_N} = \sum_{\mathbf{jk}} \mathrm{Tr}_S[C_{\mathbf{j}}|\psi_0\rangle\langle\psi_0|C^\dagger_{\mathbf{j}}]\ |\mathbf{j}\rangle\langle\mathbf{k}|_{R_1\ldots R_N} = \sum_{\mathbf{jk}} \mathcal{D}_{\mathbf{jk}}|\mathbf{j}\rangle\langle\mathbf{k}|_{R_1\ldots R_N} \tag{5.11}$$

where $\mathcal{D}_{\mathbf{jk}}$ is the decoherence matrix for generalized measurements defined in Eq. (4.15). If the initial system state is mixed ($\varrho_0$) we obtain

$$\varrho_{R_1\ldots R_N} = \sum_{\mathbf{jk}} \mathrm{Tr}_S[C_{\mathbf{j}}\varrho_0 C^\dagger_{\mathbf{j}}]\ |\mathbf{j}\rangle\langle\mathbf{k}|_{R_1\ldots R_N} = \sum_{\mathbf{jk}} \mathcal{D}_{\mathbf{jk}}|\mathbf{j}\rangle\langle\mathbf{k}|_{R_1\ldots R_N} \tag{5.12}$$

Therefore, we can identify the decoherence matrix with the density matrix of $N$ registers that, interacting subsequently with the system at times $t_1 \ldots t_N$ effectively produce on the latter the unsharp measurements $E^1_{j_1} \ldots E^N_{j_N}$.

## 5.2 Classical dynamical entropy

The concept of dynamical entropy made its appearance in attempts to discriminate between regular and chaotic classical dynamics. Classical chaos is often defined in terms of sensitive dependence to initial conditions. Consider two initially neighboring points in phase space, $x(0)$ and $x'(0)$ such that $\Delta x(0) = |x - x'| = \epsilon \ll 1$. After time $t$, their distance usually diverges exponentially as $\Delta x(t) = e^{\lambda t}\Delta x(0)$. This happens because the chaotic evolution "stretches" phase space along some directions as $e^{\lambda_+ t}, \lambda_+ > 0$ and "squeezes" it along other directions as $e^{\lambda_- t}, \lambda_- < 0$ so that distances in the "stretched" directions are exponentially amplified. The $\lambda$'s are called Lyapunov exponents. This behavior is possible only if the classical equations of motion are nonlinear, since a linear evolution corresponds to vanishing Lyapunov exponents. The essential consequence of sensitivity to initial conditions is a significant loss in predictability, i.e., the possibility of using current information about a system to predict its future evolution. Measurements of a chaotic system, however precise they may be, can never dispel uncertainty about its future state. This intuition can be classically formalized by means of a concept introduced by Kolmogorov and his school: dynamical

entropy.

Dynamical entropy measures how much information we gain when we repeatedly measure the system in time. Given a partition $\Omega$ of phase space $\Phi_S$ into cells, $\Phi_S = \sum_j \Omega_j$, we can assess the information gained in a single measurement of $j$ via the Shannon entropy

$$h(\Omega) = -\sum_j p(\Omega_j) \log p(\Omega_j)$$

The weights $p_j$ are obtained as $p_j = \int_{\Omega_j} d\mu$ where $\mu$ is a suitable integration measure on the phase space (if we take the uniform measure then $p_j$ is simply the phase-space volume of cell $\Omega_j$).
A time evolution map $\mathcal{T}^t$ maps each cell $\Omega_j$ into $\mathcal{T}^t(\Omega_j)$ at time $t$, and conversely $\mathcal{T}^{-t}\Omega_j$ into $\Omega_j$. Consequently, if we measure the system in cell $j$ at time $t$ and in cell $k$ at time $2t$ we can infer that the system was in

$$\Omega^{(2)}_{jk} \equiv \Omega_j \cap \mathcal{T}^{-t}\Omega_k$$

at time $t$. Thus the pair of measurements defines a refined phase space partition $\Omega^{(2)}$. Extending to $N$ measurements at times $1, \ldots, N$ we define the increasingly fine grained partition

$$\Omega^{(N)}_{j_1 \ldots j_N} \equiv \Omega_{j_1} \cap \mathcal{T}^{-t}\Omega_{j_2} \ldots \mathcal{T}^{-Nt}\Omega_{j_N}$$

In general, to measure the information of a sequence of measurements we can consider the Shannon entropy of the fine-grained partition,

$$h_N(\Omega) \equiv h(\Omega^{(N)}) = -\sum_{j_1 \ldots j_N} p(\Omega^{(N)}_{j_1 \ldots j_N}) \log \left(p(\Omega^{(N)}_{j_1 \ldots j_N})\right) \tag{5.13}$$

This represents the amount of information gained in the $N$ measurements. In general, of course, $h_N(\Omega) < N\ h(\Omega)$. Because of correlations, usually new measurements bring about less information then the preceding ones. This can be well understood in terms of conditional entropy:

$$h(\Omega^{(N)}) = h(\Omega^{(N-1)}) + h(\Omega_{j_N}|\Omega^{(N-1)})$$

where the conditional entropy can be expressed as

$$h(\Omega_{j_N}|\Omega^{(N-1)}) = \sum_{j_1 \ldots j_{N-1}} p(\Omega_{j_1 \ldots j_{N-1}}) \sum_{j_N} h(\Omega_{j_N}|\Omega^{(N-1)}_{j_1 \ldots j_{N-1}}) =$$
$$= -\sum_{j_1 \ldots j_{N-1}} p(\Omega_{j_1 \ldots j_{N-1}}) \sum_{j_N} p(\Omega_{j_N}|\Omega^{(N-1)}_{j_1 \ldots j_{N-1}}) \log \left(p(\Omega_{j_N}|\Omega^{(N-1)}_{j_1 \ldots j_{N-1}})\right)$$

In the (extreme) case where the first $N-1$ measurements $j_1, \ldots j_{N-1}$ are sufficient to predict with certainty $j_N$, then

$$h(\Omega_{j_N}|\Omega^{(N-1)}_{j_1 \ldots j_{N-1}}) = 0$$

and hence

$$h(\Omega_{j_N}|\Omega^{(N-1)}) = 0 \Rightarrow h(\Omega^{(N)}) = h(\Omega^{(N-1)})$$

This means that then no further information is gained in the measurement $j_N$. The Kolmogorov-Sinai entropy is defined as the max (over partitions) of the (asymptotic) information gain rate:

$$h_{KS} = \lim_{N\to\infty} \max_{\Omega} \frac{1}{N} h_N(\Omega) \tag{5.14}$$

This is equivalent to the maximum of the asymptotic information gain per step

$$h_{KS} = \lim_{N\to\infty} \max_{\Omega}(h_N(\Omega) - h_{N-1}(\Omega)) = \lim_{N\to\infty} \max_{\Omega}(h(\Omega_{j_N}|\Omega^{(N-1)}) \tag{5.15}$$

For integrable systems, the more measurements we make (the more $j$'s we collect) the more effectively we can predict the future, i.e., later $j$'s. Therefore $h(\Omega_{j_N}|\Omega^{(N-1)})$ rapidly decreases with $N$ and eventually $h_{KS}$ vanishes when the limit $N \to \infty$ is taken. Instead, a chaotic system has a positive $h_{KS}$, implying that we can never collect enough information to definitively constrain the future evolution of the system. According to the theorems of Ruelle and Pesin we have

$$h_{KS} = \sum_k \lambda_{+,k} \tag{5.16}$$

where the sum is over all positive Lyapunov exponents of the system. Thus KS entropy is intimately connected with classical chaos.

## 5.3 Quantum dynamical entropy

A quest for quantum generalizations of the KS entropy has led to several nonequivalent proposals [188, 191, 189], among wich the most important are the Connes-Thirring (CNT) [188] and Alicki-Fannes (ALF) [191] dynamical entropies. Both were developed as non-commutative extensions of the KS-entropy. The latter is based on the idea that repeated measurements at different times can provide information about the system. Its noncommutative extensions differ in that ALF explicitly takes into account measurements (and the corresponding disturbances), while CNT does not. By virtue of semiclassical approximations with generalized coherent states, it has been rigorously shown that both ALF and CNT entropies tend to the KS entropy in the classical limit [192, 187].

### 5.3.1 ALF entropy and decoherent histories

In the following I will focus on ALF entropy, since it is the proper conceptual device needed to discuss issues related to predictability and chaos. I will derive the ALF entropy following a route that slightly differs from the one taken in original papers. I will stress physical aspects like measurements and information rather than strictly mathematical concerns that were a central motivation for the ALF entropy proposal (for the

same reason, we prefer not to frame our discussion into the original $C^*$-algebraic language, but in Hilbert space language).
The construction of ALF entropy can be regarded as a paraphrase of the KS entropy construction into the quantum language, where measurements and phase space partitions are to be replaced by POVMs and identity decompositions. A generic measurement process can be described by a POVM defined by operators $E_j = A_j^\dagger A_j$. Since $\sum_{j=1}^n E_j = \mathbb{I}$, *any POVM defines a partition of unity*, which is the quantum analogue of a phase space partition. Similar to the commutative case, given an initial partition $E$, the dynamics (that is assumed to be a unitary $U(t)$) naturally leads to a sequence of refined partitions. Upon adopting the Heisenberg representation, we can define $\mathcal{A}_j(t) = U^\dagger(t-t_0)\mathcal{A}_j U(t-t_0)$. If we consider the evolution of the partition at times $t, \ldots, Nt$, a sequence of refined partitions $E_{\mathbf{j}}^{(N)}$ is thus obtained:

$$E_{\mathbf{j}}^{(N)} = C_{\mathbf{j}}^{(N)\dagger} C_{\mathbf{j}}^{(N)}, \qquad C_{\mathbf{j}}^{(N)} = \mathcal{A}_{j_N}(Nt)\ldots\mathcal{A}_{j_1}(t) \tag{5.17}$$

Given a density matrix $\varrho$ and a partition $E_{\mathbf{j}}^{(N)}$, the probability of each partition element is given as:

$$p_{\mathbf{j}} = \mathrm{Tr}[\varrho E_{\mathbf{j}}] = \mathrm{Tr}[C_{\mathbf{j}}^{(N)} \varrho C_{\mathbf{j}}^{(N)^\dagger}] \tag{5.18}$$

As we immediately notice, the definition of $C_{\mathbf{j}}$ in Eq. (5.17) and the partition probability $p_{\mathbf{j}}$ in Eq. (5.18) are the same as in Eq. (4.14) defining histories and their probabilities for unsharp measurements. This is not surprising since refined partitions are in fact defined through a set of histories $\Sigma$ where we take the same projections at each times and equal time intervals between projections.
As we know, the $p_{\mathbf{j}}$'s are not true probabilities (they do not obey the sum rule) unless $\Sigma$ obeys the consistency condition. Correspondingly, a definition of dynamical entropy as

$$h_N^{(c)}(E) = -\sum_{\mathbf{j}} p_{\mathbf{j}} \log p_{\mathbf{j}} \tag{5.19}$$

is meaningful only if histories decohere. In this case, as we stress with the apex $(c)$, $h^{(c)}$ represents the amount of *classical* information generated by the decoherent dynamics of the system. If histories do not decohere, then coherent correlations between different histories have to be taken into account. Correspondingly, we can define a dynamical entropy as the von Neumann entropy of the decoherence matrix,

$$h_N(E) = -\mathrm{Tr}[\mathcal{D}^{(N)} \log \mathcal{D}^{(N)}] \tag{5.20}$$

where $\mathcal{D}_{\mathbf{jk}} = \mathrm{Tr}[C_{\mathbf{j}}^{(N)} \varrho C_{\mathbf{k}}^{(N)^\dagger}]$. In § 5.1 we proved that the decoherence matrix can be interpreted as the density matrix of an ensemble of registers that subsequently interact with the system. This allows to give a different interpretation to $h_N(E)$. Since $h_N(E)$ is the von Neumann entropy of the state of the registers, *it represents the amount of quantum information stored therein*. Therefore, we can look at $h_N$ as the the amount of *quantum information* produced by the dynamics.

Mirroring the KS construction, a dynamical entropy is defined as the max (over POVMs) of the (asymptotic) information production rate:

$$h_{ALF} = \lim_{N\to\infty} \max_{E} \frac{1}{N} h_N(E) \tag{5.21}$$

This is exactly the ALF-entropy defined in [192], even if the original derivation was never referring to the decoherent histories formalism. *By casting ALF entropy in the decoherent histories language, we can endow it with a physical interpretation as the (maximal) amount of quantum information produced by the dynamics per time step.*

### 5.3.2 Finite systems

From definition (5.21), ALF entropy can be nonzero only for infinite-dimensional systems. This follows from the general bound [191, 192]

$$h_N \leq \log d + \log(rank(\varrho)) \tag{5.22}$$

that can be simply derived from the discussion in § 5.1. If the initial state is not pure, let us purify the initial $\varrho$ by adding an external $rank(\varrho)$-dimensional ancilla $A$, $\varrho = \mathrm{Tr}_A[|\psi_0\rangle_{SA}\langle\psi_0|]$. Then after the interaction with the $N$ registers, the pure system + ancilla + registers state is

$$\sum_{\mathbf{jk}} |\psi_{\mathbf{j}}\rangle_{SA}\langle\psi_{\mathbf{k}}| \otimes |\mathbf{j}\rangle_{R_1\ldots R_N}\langle\mathbf{k}|$$

where $U^\dagger(t_f - t_0)|\psi_{\mathbf{j}}\rangle_{SA} = C_{\mathbf{j}}|\psi\rangle_{SA}$ and $C_{\mathbf{j}}\varrho C^\dagger_{\mathbf{k}} = \mathrm{Tr}_A[|\psi_{\mathbf{j}}\rangle_{SA}\langle\psi_{\mathbf{k}}|_{SA}]$. The von Neumann entropy of the registers must be equal to the entropy of the system + ancilla state. Since the system - ancilla state has dimension $d + rank(\varrho)$, the entropy of the registers latter is bounded by $\log d + \log(rank(\varrho))$. But the entropy of the registers is exactly $h_N$. QED. If the initial state is pure, then $h_N \leq \log d$.

From the bound 5.22 we conclude that

$$\lim_{N\to\infty} \max_{E} \frac{1}{N} h_N(E) \leq \lim_{N\to\infty} \frac{2\log d}{N} = 0 \tag{5.23}$$

When considering finite-dimensional systems, one can observe a growth of $h_N$ up to a finite $N_{sat}$, after which a saturation effect must happen. In this case, a non-vanishing dynamical entropy reflects into a *linear growth* of $h_N$ up to the $N_{sat}$. A dynamical entropy for a finite-dimensional system of dimension $d$ can be defined as

$$h^d_{ALF} = \frac{h_{N_{sat}(d)}}{N_{sat}(d)} \tag{5.24}$$

which correspond to the slope of the initial growth of $h_N$. The saturation time $N_{sat}(d)$ is $d$-dependent with $N_{sat}(d) \to \infty$ as $d \to \infty$. In particular, if the entropy is evaluated for coarse-grained partitions with $\Delta$-dimensional projectors, then the maximum possible entropy $h_N$ is given by $N \log f$ where $f = d/\Delta$. Thus, we can expect maximal

entropy production up to time $N_{sat} < \frac{\log d}{\log f}$, after which a saturation effect must happen.
Often, one consider quantum systems that are quantizations of classical systems defined on a compact phase space. In this case, the quantized system has a finite dimension $d$ that plays the role of a Planck constant, $\hbar = 1/d$. The classical limit corresponds to taking $d \to \infty$. To address the classical limit of the dynamical entropy, one needs to evaluate $h^d_{ALF}$ for each $d$ and then take $d \to \infty$. This is equivalent to first $d \to \infty$, and then $N \to \infty$ (the limits do not commute).
The saturation effect of dynamical entropy is known as *logarithmic breaking time* in the literature on quantum chaotic systems. Such systems can follow semiclassical trajectories up to the timescale $\frac{\log d}{\lambda_+ \log d/\Delta}$. This can be intuitively explained as follows. After $N$ steps on the dynamics an initial uncertainty $\Delta x = \Delta/d$ in the direction that is exponentially according to $\lambda_- = -\lambda_+$ is reduced as $(\Delta/d)^{-N\lambda_+}$. At the logarithmic breaking time, this quantity reaches the value $1/d$, that minimal phase-space coarse-graining due to the finite dimension. After this time-quantum effects become dominant.

### 5.3.3 The relative entropy of decoherence

The two quantities $h_N(E)$ and $h^{(c)}_N(E)$ defined in § 5.3.1 differ the wider, the more the set of histories is coherent. In fact, we have:

$$\mathcal{C}_N \equiv h^{(c)}_N - h_N = S(\mathcal{D}^{(N)}||\tilde{\mathcal{D}}^{(N)}) \geq 0 \tag{5.25}$$

where $S(A||B)$ is the quantum relative entropy, and we have defined a matrix $\tilde{\mathcal{D}}^{(N)}_{\mathbf{jk}} = \delta_{\mathbf{jk}}\mathcal{D}^{(N)}_{\mathbf{jk}}$ where the off-diagonal entries are set to zero. To prove (5.25), notice that $\mathrm{Tr}[\mathcal{D}^{(N)} \log \tilde{\mathcal{D}}^{(N)}] = \sum_{\mathbf{j}} D^{(N)}_{\mathbf{j},\mathbf{j}} \log D^{(N)}_{\mathbf{j},\mathbf{j}} = \mathrm{Tr}[\tilde{\mathcal{D}}^{(N)} \log \tilde{\mathcal{D}}^{(N)}]$, hence:

$$\begin{aligned} h^{(c)}_N - h_N &= -\mathrm{Tr}[\tilde{\mathcal{D}}^{(N)} \log \tilde{\mathcal{D}}^{(N)}] + \mathcal{D}^{(N)} \log \mathcal{D}^{(N)} = \\ &= -\mathrm{Tr}[\tilde{\mathcal{D}}^{(N)}(\log \tilde{\mathcal{D}}^{(N)} - \log \mathcal{D}^{(N)})] = S(\mathcal{D}^{(N)}||\tilde{\mathcal{D}}^{(N)}) \end{aligned}$$

Since $h^{(c)}_N$ neglects coherences between different histories, it gives a higher estimate of information production than $h_N$. The two quantities coincide in the case of medium decoherence. In this case, the state of the registers is classical (there are no quantum correlations between the registers) and they effectively store classical information.
The quantity $\mathcal{C}_N$ define is suited to be used as a general measure of coherence within a set of histories. We will call it *relative entropy of decoherence*. Recently, Baumgratz *et al.* [132] have introduced a similar quantity to assess the amount of coherence of a density matrix in a given basis and emphasized that it has the properties of a *bona fide* measure of coherence.

# Chapter 6

# Randomness, decoherence, and dynamical entropy

## 6.1 Introduction

In classical physics, the major source of unpredictability is chaos. If the dynamics is chaotic, data collected on the system in time are never sufficient to predict its future behavior because any finite uncertainty is exponentially amplified. A good measure of the ensuing unpredictability is given by the Kolmogorov-Sinai entropy, that measures the amount of information "produced" by the dynamics per unit of time, i.e., the amount of information that cannot be predicted on the basis of previous data on the system. Chaotic systems keep producing information indefinitely as the dynamics unfolds, whereas integrable ones do so only for a short transient.
In the quantum domain, it is less trivial to identify sources of unpredictability. Due to the intrinsic linearity of the theory, sensitive dependence to initial conditions in Hilbert space is strictly forbidden, and Lyapunov exponents cannot be defined. What are commonly referred to as "quantum chaotic systems" in the literature are just quantum systems whose classical limit is chaotic. Such systems are characterized by some relevant properties, as their Hamiltonians exhibit some universal features of the random matrix ensembles (level spacing distribution, spectral rigidity, two-point correlations [186]), but it is not immediately clear how these properties reflect into unpredictability and dynamical entropy production. Conversely, quantum mechanics allows for sources of unpredictability that have no classical analogue, as they essentially stem from noncommutativity. Since almost all observables do not commute with the dynamics, measurement outcomes are generally probabilistic and create an effective source of randomness that impairs predictability reflecting into a positive value of dynamical entropy. This feature is apparent in Ref. [192], where Alicki *et al.* show that ALF entropy (5.21) can achieve a maximum for random POVMs (random partitions) independent of the unitary evolution between measurements and the degree of "chaoticity" the evolution has in the classical limit. The distinction between systems that are chaotic or integrable in the classical limit can be retrieved only by bringing to the surface the classical phase-

space structure underlying the quantum model. Upon restricting to measurements and initial states with a well defined phase-space limit, ALF entropy necessarily tends to the classical KS entropy [187] and hence gleaming differences between the "chaotic" and the "integrable" case appear, as shown, for instance, in Ref. [190].
In this chapter we consider dynamical entropy production for closed quantum systems within the framework of decoherent histories (where ALF entropy can be naturally formulated as we discussed in § 5.3), and address its behavior in presence of two sources of randomness:

- (R1) randomness in the dynamics
- (R2) randomness in the measurements

Our choice of formalism allows us to address for the first time an aspect that was so far neglected, or given only marginal attention in relation to quantum dynamical entropy: *history decoherence and the role of coarse-graining*. Some previous numerical works [190] have considered coarse-grained partitions, but they did not explicitly examine the role of coarse-graining. In Ref. [193], a set of coarse-grained histories for a quantum chaotic system (the quantum baker's map) was studied, and it was shown that it decoheres. However, the generality of this result was not discussed.
The relevance of history decoherence in relation to entropy production is that it allows to see quantum dynamical entropy as a measure of predictability. From the point of view of an observer who wishes to make classical predictions, the relevant sets of histories are only the decoherent ones, that yield alternative descriptions of the system in time with well-defined probabilities. For such sets of histories we have, in the notation introduced in § 5.3.1, $h_N(E) \simeq h_N^{(c)}(E)$, i.e., the system effectively produces classical information at a rate given by $h_N(E)/N$. In order to achieve decoherence, a (large) degree of coarse-graining is in general necessary, as the literature on decoherent histories has extensively shown.
The general picture that we aim to draw is that for $d \to \infty$ both (R1) and (R2) can lead to the same results: Sufficiently coarse-grained histories decohere and yield maximal dynamical entropy production compatible with the coarse-graining size. This picture is supported by a general argument. Unfortunately, the latter is not conclusive, as it is based on an unproven statistical hypothesis, and hence it mandates a search for a more rigorous proof. By using random matrix techniques, we will be able to fully justify the results in the case of dynamical randomness (R1). We still lack a proof for case (R2).
Our general picture will be illustrated upon studying decoherent histories and quantum dynamical entropy in the quantum standard map (QSM) [195, 196, 197, 198, 199, 200], a paradigmatic toy model to study quantum chaos, that has an integrable/chaotic transition. Our numerical data strongly support our general theoretical understanding.
This chapter is organized as follows. First, in § 6.2 we address decoherent histories in presence of randomness of type (R1) and (R2). We provide a heuristic argument showing that sufficiently coarse-grained histories decohere and lead to non-vanishing entropy production. The consequences of this result in chaotic vs. integrable systems are briefly discussed. Then, in § 6.3 we will present a rigorous argument, based on random matrix techniques, that confirms the results of § 6.2 for the case of (R1). For the sake of conciseness, we only report the main results, postponing their derivation to

§ 6.6. In § 6.4 we analyze DH and dynamical entropy in the quantum standard map (QSM) that undergoes an integrable/chaotic transition. We study histories in the integrable and chaotic regime, considering different kinds of partitions, and show how results conform to the analysis in § 6.2,6.3. Finally, § 6.5 summarizes the main conclusions of this chapter.
To the best of my knowledge, the entire content of this chapter is original and has never appeared in any previous publication.

## 6.2 Randomness and decoherence

In this section we show how randomness of type (R1) and type (R2) can cause decoherence between sufficiently coarse-grained histories and lead to a non-vanishing production of dynamical entropy. Our heuristic argument will be corroborated by the rigorous random-matrix argument provided in § 6.3 (which, however, only holds for randomness of type (R1)), and justified by our numerical findings for the QSM.

The general setting we consider is the following. We consider

1. a *closed* quantum system with dimension $d \gg 1$.
2. *pure initial states*, $\varrho_0 = |\psi_0\rangle\langle\psi_0|$.
3. a dynamics given by a *discrete-time unitary map* $U$.
4. a set of histories defined by *fixed orthogonal projectors* $P_j$ for all times, and a *single iteration of the map* $U$ between projections.

The decoherence matrix for such a set of histories can be written as

$$\mathcal{D}^{(N)}_{\mathbf{jk}} = \mathrm{Tr}[P_{j_N} U \dots P_{j_1} U \varrho U^\dagger P_{k_1} \dots U^\dagger P_{k_N}] \tag{6.1}$$

Let us now precisely define the sources of randomness (R1) and (R2) mentioned in the introduction.
In case (R1), randomness is provided by the dynamics (R1). We extract $U$ from the circular random matrix ensemble CUE, which corresponds to the unitary group equipped with Haar measure. Such a $U$ has well-defined spectral properties, represented by a Wigner distribution of the level spacing $P(s) \propto s e^{-s^2}$. Its eigenvectors also have well-defined statistical properties [205]: they form a basis of Haar-distributed orthogonal vectors.
A second source of randomness (R2) may come from measurements, i.e., from the projectors defining the history. We take random projections, meaning that $P_{i_n} = W \tilde{P}_{i_n} W^\dagger$ where the $\tilde{P}_{i_n}$ are fixed projectors $W$ is a unitary selected from CUE, i.e., from the unitary group with Haar measure. For the purpose of evaluating decoherence matrix elements, the randomness in the measurement can be reinterpreted as a randomness on the dynamics. Indeed, introduce

$$\tilde{U} = W^\dagger U W \tag{6.2}$$

If we write histories in terms of $\tilde{P}_j$ and $\tilde{U}$, then $\mathcal{D}^{(N)}_{\mathbf{jk}}$ reads:

$$\mathcal{D}^{(N)}_{\mathbf{jk}} = \mathrm{Tr}[\tilde{P}_{j_N}\tilde{U}\ldots\tilde{P}_{j_1}\tilde{U}\tilde{\varrho}\tilde{U}^\dagger\tilde{P}_{k_1}\ldots\tilde{U}^\dagger\tilde{P}_{k_N}] \tag{6.3}$$

where $\tilde{\varrho} = W^\dagger\varrho W$. In (6.3), all the randomness has been transferred from the projectors to the evolution operator. Thus the case (R2) looks very similar to the previous case (R1), except for one relevant particular: $\tilde{U}$ has the same spectrum as $U$, that in general does not conform to the predictions of random matrix theory since $U$ is assumed to be completely generic. Thus, the statistical properties of $\tilde{U}$ are not the same as those of a matrix extracted from CUE. Nevertheless, due to the "randomization" afforded by $W$, the eigenvectors of $\tilde{U}$ will have the same statistical properties of the eigenvectors of an $U$ taken from CUE, i.e., they will also form a basis of Haar-distributed, randomly selected orthogonal vectors.

We aim to show that *in presence of randomness of type (R1) and (R2), coarse-grained histories approximately decohere and lead to non-vanishing entropy production*.
This is what emerges from our numerical results in § 6.4, and it is also suggested by results in Ref. [190]. At present, we cannot rigorously prove this fact, and we will only present an admittedly heuristic argument that is based on a plausible, yet unproven statistical hypothesis.

Let us consider a pure initial state $\varrho = |\psi_0\rangle\langle\psi_0|$ and a pair of non-coincident histories $\mathbf{j} \equiv j_1,\ldots,j_N$ and $\mathbf{k} \equiv k_1,\ldots,k_N$. If we select an intermediate time $t_\ell$, $1 < \ell < N$, the decoherence matrix element $\mathcal{D}^{(N)}_{\mathbf{jk}}$ reads

$$\mathcal{D}^{(N)}_{\mathbf{jk}} = \mathrm{Tr}[\bar{P}_{j_N}\bar{U}\ldots\bar{P}_{j_\ell}\bar{U}\bar{P}_{j_{\ell-1}}\bar{U}\ldots\bar{P}_{j_1}\bar{U}|\bar{\psi}_0\rangle\langle\bar{\psi}_0|\times \tag{6.4}$$

$$\bar{U}^\dagger\bar{P}_{k_1}\ldots\bar{U}^\dagger\bar{P}_{k_{\ell-1}}\bar{U}^\dagger\bar{P}_{k_\ell}\ldots\bar{P}^\dagger\bar{P}_{k_N}] \tag{6.5}$$

where $\bar{P} = \{P, \tilde{P}\}$, $\bar{U} = \{U, \tilde{U}\}$, $|\bar{\psi}_0\rangle = \{|\psi_0\rangle, W^\dagger|\psi_0\rangle\}$ for (R1) and (R2) respectively. By introducing the notation

$$C_{mn} = \bar{P}_{j_m}\bar{U}\ldots\bar{P}_{j_n}\bar{U} \qquad C'_{mn} = \bar{P}_{k_m}\bar{U}\ldots\bar{P}_{k_n}\bar{U} \tag{6.6}$$

for any $m, n \in 1,\ldots,N$, and the path-projected states $|\chi\rangle$,$|\chi'\rangle$

$$|\chi\rangle = C_{1\ell-1}|\bar{\psi}_0\rangle, \qquad |\chi'\rangle = C'_{1\ell-1}|\bar{\psi}_0\rangle \tag{6.7}$$

we can express (6.4) as

$$\mathcal{D}^{(N)}_{\mathbf{jk}} = \mathrm{Tr}[C_{\ell N}|\chi\rangle\langle\chi'|{C'}^\dagger_{\ell N}] \tag{6.8}$$

We choose $\ell$ such that $j_{\ell-1} \neq k_{\ell-1}$, so $|\chi\rangle$ and $|\chi'\rangle$ are orthogonal vectors. There must be at least one such $\ell$ since we are assuming $\mathbf{j} \neq \mathbf{k}$. Actually, for most pairs of histories $\{\mathbf{j}, \mathbf{k}\}$ we will have $j_\ell \neq k_\ell$, for all $\ell = 1,\ldots,N$ (see Lemma 2 in § 6.6.3).
The degree of coherence between histories $\mathbf{j}$ and $\mathbf{k}$ can be assessed by the *coherence ratio*, i.e., the ratio between the off-diagonal and the diagonal elements of the decoherence matrix

$$\delta^2 = \frac{\mathcal{D}_{\mathbf{jk}}\mathcal{D}^*_{\mathbf{jk}}}{\mathcal{D}_{\mathbf{jj}}\mathcal{D}_{\mathbf{kk}}} = \frac{\langle\chi'|{C'}^\dagger_{\ell n}C_{\ell n}|\chi\rangle\langle\chi|C^\dagger_{\ell n}C'_{\ell n}|\chi'\rangle}{\langle\chi|C^\dagger_{\ell n}C_{\ell n}|\chi\rangle\langle\chi'|{C'}^\dagger_{\ell n}C'_{\ell n}|\chi'\rangle} \tag{6.9}$$

Recall that from (4.10) we have $|\mathcal{D}_{\mathbf{jk}}|^2 \leq \mathcal{D}_{\mathbf{jj}}\mathcal{D}_{\mathbf{kk}}$, hence $\delta^2 \leq 1$. History decoherence is equivalent to $\delta^2 \ll 1$.
For (R1) and (R2), the operator $\bar{U}$ in Eq. (6.4) is selected at random from a matrix ensemble. In the case of (R1), $\bar{U} = U$ is selected at random from the circular ensemble CUE. In the case of (R2), $\bar{U}$ is selected from a matrix ensemble obtained by the adjoint action of matrices $W$ from the CUE ensemble on a fixed unitary, $\bar{U} = W^\dagger U W$.
The key assumption that will enable us to estimate $\delta^2$ for (R1) and (R2) is that the statistical distribution of $|\chi\rangle$ and $|\chi'\rangle$ induced by the statistical distribution of $\bar{U}$ can be approximated by the uniform distribution over the Hilbert space. Our statistical hypothesis thus reads:

- (H0) For randomness of type (R1) or (R2), i.e, of the evolution operator between projections is given by an $U$ taken from CUE or a $\tilde{U} = W^\dagger U W$ where $W$ is taken from CUE, the path-projected vectors $|\chi\rangle$ and $|\chi'\rangle$ can be assumed to be orthogonal vectors randomly selected according to the uniform measure in Hilbert space.

The statistical hypothesis (H0) essentially amounts at assuming that for a "random dynamics" the path-projected vectors $|\chi\rangle, |\chi'\rangle$ are sufficiently randomized that they can be approximated by random vectors selected according to the uniform measure in the Hilbert space $\mathcal{H}$ (note that at between time-step $\ell - 1$ and $\ell$, $U$ takes the path-projected vector $P_{j_\ell - 1} U \dots U P_{j_1} |\psi_0\rangle$ into an effectively random vector).

Assuming the validity of H0, we can find an estimate of $\delta^2$ by averaging the numerator and the denominator in (6.9) separately over $|\chi\rangle, |\chi'\rangle$, finding:

$$\delta^2 \lesssim \frac{1}{\mathrm{Tr}(C^\dagger_{\ell N} C_{\ell N})} = \frac{1}{d \langle p_{j_\ell \dots j_N | \chi} \rangle_{\mathcal{H}}} \tag{6.10}$$

where $\langle p_{j_\ell \dots j_N | \chi} \rangle_{\mathcal{H}}$ is the conditional probability of $j_\ell \dots j_N$, given that the path-projected state at step $\ell$ is $|\chi\rangle$, averaged over $|\chi\rangle \in \mathcal{H}$.

*Proof of (6.10).* If (H0) holds, $|\chi\rangle$ and $|\chi'\rangle$ are random orthogonal vectors selected with uniform measure in Hilbert space. Therefore we can write $|\chi\rangle = V|0\rangle$, $|\chi'\rangle = V|1\rangle$, where $V$ is a unitary matrix selected from $\mathcal{U}(d)$ according to the Haar measure (one should add a normalization factor for $|\chi\rangle, |\chi'\rangle$, but we neglect those terms because they drop from Eq. (6.9) ). The average over $|\chi\rangle, |\chi'\rangle \in \mathcal{H}$ can be replaced by an average over $V \in \mathcal{U}(d)$. For $d \gg 1$, averages over the Haar measure can be computed by means of formulas

$$\langle V_{l_1 m_1} V^*_{l_2 m_2} \rangle_{\mathcal{U}(d)} = \frac{1}{d^2} \delta_{l_1 l_2} \delta_{m_1 m_2} \tag{6.11}$$

$$\langle V_{l_1 m_1} V^*_{l_2 m_2} V_{l_3 m_3} V^*_{l_4 m_4} \rangle_{\mathcal{U}(d)} = \frac{1}{d^2} (\delta_{l_1 l_2} \delta_{m_1 m_2} \delta_{l_3 l_4} \delta_{m_3 m_4} + \delta_{l_1 l_4} \delta_{m_1 m_4} \delta_{l_2 l_3} \delta_{m_2 m_3})$$

where $\langle l | V | m \rangle \equiv V_{mn}$. These formulas stem from a "Wick calculus" for the unitary group that be explained in detail in § 6.3 (for details see Eq. (6.29) below). From

(6.11), we get for any two operators $O_1, O_2$:

$$\Big\langle \langle 1|V^\dagger O_1 V|0\rangle\langle 0|V^\dagger O_2 V|1\rangle \Big\rangle_{\mathcal{U}(d)} = \langle \sum_{ijkl} V^*_{i1}(O_1)_{ij}V_{j0}V^*_{k0}(O_2)_{kl}V_{l1}\rangle_{\mathcal{U}(d)} \quad (6.12)$$

$$= \sum_{ijkl}(O_1)_{ij}(O_2)_{kl}\langle V^*_{i1}V_{l1}V_{j0}V^*_{k0}\rangle_{\mathcal{U}(d)} = \frac{1}{d^2}\sum_{ijkl}(O_1)_{ij}(O_2)_{kl}\delta_{il}\delta_{jk} =$$

$$= \frac{1}{d^2}\sum_{ij}(O_1)_{ij}(O_2)_{ji} = \frac{1}{d^2}\mathrm{Tr}[O_1O_2]$$

By repeating the same method, we find

$$\Big\langle \langle 0|V^\dagger O_1 V|0\rangle\langle 1|V^\dagger O_2 V|1\rangle \Big\rangle_{\mathcal{U}(d)} = \frac{1}{d^2}\mathrm{Tr}[O_1]\mathrm{Tr}[O_2] \quad (6.13)$$

An estimate of $\delta^2$ can be obtained by averaging the numerator and the denominator separately over $V$:

$$\delta^2 \sim \frac{\Big\langle \langle \chi'|C'^\dagger_{\ell n}C_{\ell n}|\chi\rangle\langle\chi|C^\dagger_{\ell n}C'_{\ell n}|\chi'\rangle \Big\rangle_{\mathcal{H}}}{\Big\langle \langle \chi|C^\dagger_{\ell n}C_{\ell n}|\chi\rangle\langle\chi'|C'^\dagger_{\ell n}C'_{\ell n}|\chi'\rangle \Big\rangle_{\mathcal{H}}} = \quad (6.14)$$

$$= \frac{\Big\langle \langle 1|V^\dagger C'^\dagger_{\ell n}C_{\ell n}V|0\rangle\langle 0|V^\dagger C^\dagger_{\ell n}C'_{\ell n}V|1\rangle \Big\rangle_{\mathcal{U}(d)}}{\Big\langle \langle 0|V^\dagger C^\dagger_{\ell n}C_{\ell n}V|0\rangle\langle 1|V^\dagger C'^\dagger_{\ell n}C'_{\ell n}V|1\rangle \Big\rangle_{\mathcal{U}(d)}}$$

Upon performing the average of (6.14) over $V$ with (6.12) and (6.13) we obtain:

$$\delta^2 \approx \frac{\mathrm{Tr}[C'^\dagger_{\ell N}C_{\ell N}C^\dagger_{\ell N}C'_{\ell N}]}{(\mathrm{Tr}[C^\dagger_{\ell N}C_{\ell N}]\mathrm{Tr}[C'^\dagger_{\ell N}C'_{\ell N}])}$$

Since $||C^\dagger_{\ell N}||_\infty \leq 1$, for any vector $|\phi\rangle$, we have $||C^\dagger_{\ell N}C'_{\ell N}|\phi\rangle||^2 \leq ||C'_{\ell N}|\phi\rangle||^2$, therefore $\mathrm{Tr}[C'^\dagger_{\ell N}C_{\ell N}C^\dagger_{\ell N}C'_{\ell N}] \leq \mathrm{Tr}[C'^\dagger_{\ell N}C'_{\ell N}]$. Hence,

$$\delta^2 \lesssim 1/\mathrm{Tr}(C^\dagger_{\ell N}C_{\ell N})$$

Now, the quantity in the denominator in the r.h.s. is

$$\mathrm{Tr}(C^\dagger_{\ell N}C_{\ell N}) = d\Big\langle \langle\chi|C^\dagger_{\ell N}C_{\ell N}|\chi\rangle\Big\rangle_{\mathcal{H}} = d\Big\langle \mathrm{Tr}[C_{\ell N}|\chi\rangle\langle\chi|C^\dagger_{\ell N}]\Big\rangle_{\mathcal{H}}$$

where averages are over $|\chi\rangle$ in $\mathcal{H}$. The expression $\mathrm{Tr}[C_{\ell N}|\chi\rangle\langle\chi|C^\dagger_{\ell N}]$ can be seen as the diagonal element $j_\ell \ldots j_N$ of a decoherence matrix where the "initial state" at step $\ell$ is $|\chi\rangle$, and thus it represents the conditional probability of $j_\ell \ldots j_N$, given that the path-projected state at step $\ell$ is $|\chi\rangle$: $p_{j_\ell \ldots j_N|\chi}$. Therefore, we can finally write

$$\mathrm{Tr}(C^\dagger_{\ell N}C_{\ell N}) = \frac{1}{d\langle p_{j_\ell \ldots j_N|\chi}\rangle_{\mathcal{H}}}$$

*QED.*

The condition under which histories decohere is

$$d \gg 1/\langle p_{j_\ell \ldots j_N|\chi}\rangle_{\mathcal{H}} \quad (6.15)$$

A high degree of coarse-graining is sufficient to ensure that this condition holds. Indeed let $\Delta = d/f$ be the rank of the $P_{j_\ell}$, i.e, the coarse-graining dimension. Assuming that the probabilities $\langle p_{j_\ell \dots j_N|\chi}\rangle$ are all of the same order of magnitude for all choices of $j_\ell, \dots, j_N$, then $\langle p_{j_\ell \dots j_N|\chi}\rangle$ should be of the order of $f^{-|N-\ell|}$. Approximate decoherence occurs for $d \gg f^{|N-\ell|}$ which can be achieved for sufficiently small $f$, i.e., sufficiently gross coarse-graining.
If all $\langle p_{j_\ell \dots j_N}\rangle$ are approximately equal (which is likely for very high coarse-graining), then classical information is produced at a rate given by the (un-maximized) dynamical entropy

$$\frac{h_N(P)}{N} = \frac{h_N^{(c)}(P)}{N} = \log f \tag{6.16}$$

For $d < \infty$, finite-size effects become eventually dominant, as discussed at length in § 5.3.2. Indeed the bound $h_N \leq \log d$ holds [191, 192]. For coarse-grained histories, the maximum entropy $h_N$ is $N \log f$ and thus entropy production must saturate after $N_{sat} \sim \frac{\log d}{\log f}$.
Thus, under the assumption that (H0) is valid, we have shown that both (R1) and (R2) can lead to history decoherence and non-vanishing entropy production.

*Comment: chaotic and integrable systems.* Let us now briefly discuss what the picture obtained in the previous paragraph entails for the behavior of decoherent histories and dynamical entropy for quantum chaotic and integrable systems respectively.
Let us first address chaotic systems. Discrete-time quantum chaotic maps are represented by unitary *Floquet operators* that exhibit some universal features of the unitary random matrix ensembles [186]). Therefore a chaotic Floquet operator $U$ can be usually approximated by a typical element of the circular ensembles (CUE, COE or CSE). Depending on the type of ensemble, $U$ will have different spectral properties, represented by different Wigner distributions of the level spacing $P(s) \propto s^\alpha e^{-s^2}$ where $\alpha = 1, 2, 4$ for CUE, COE and CSE respectively. Also the eigenvectors will present different statistics [205]. Our argument was derived under the hypothesis that $U$ can be taken from CUE, but its generality suggests that if it holds for CUE it may also hold for COE and CSE (essentially, we only require that the dynamics sufficiently randomizes path-projected vectors). If this is true, we conclude that chaotic maps lead to decoherence between coarse-grained histories, and production of classical entropy at a non-vanishing rate.
As for integrable systems, classically their entropy production vanishes because the high degree of symmetry severely constrains the evolution of the system – the latter can only describe a linear motion onto the phase space surface identified by the constants of motion. Quantum mechanically, the constants of the motion imply that the evolution operator $U$ is block diagonal, each block being identified with a set of conserved quantum numbers (if the constants of the motion form a complete set of observables, then they suffice to fully diagonalize $U$). The dynamics creates no coherence between Hilbert space sectors corresponding to different quantum numbers. Consequently, if we take measurements with projections $\tilde{\mathcal{P}}_j$ that commute with the constants of the motion, we expect no entropy production in the quantum case as well. However, let us consider a random measurement, that can be written as $\mathcal{P}_{i_n} = W\tilde{\mathcal{P}}_{i_n}W^\dagger$ where $W$ is a random

unitary. The entropy production associated to $\mathcal{P}$ and $U$ is equivalent to that associated to $\tilde{\mathcal{P}}$ and $\tilde{U} = W^\dagger U W$. The latter is a "randomized" dynamics that coherently couples all Hilbert space sectors corresponding to different values of the quantum numbers. In other words, a generic measurement clamorously breaks the symmetry of the system. Consequently, even an integrable system can keep producing (classical) information at a rate given by the (nonzero) dynamical entropy.

## 6.3 Decoherence and dynamical entropy for a random chaotic dynamics

For a discrete time dynamics given by a random Floquet operator $U$ we can do much more than simply providing an estimate of the coherence ratio $\delta^2$. We are able to derive estimates of the decoherence matrix elements, and achieve much more precise and detailed results. By using Weingarten calculus [201], we can take averages of arbitrary products of matrix elements of the evolution operator $U$ over the suitable circular ensemble (CUE, COE or CSE). Therefore, we can take averages in the decoherence matrix elements and obtain estimates of the diagonal and off-diagonal entries in the limit $d \gg 1$.
In the following, we shall restrict for simplicity to a $U$ belonging to the CUE ensemble, wich coincides with the Haar measure over the unitary group. This is of relevance for the model studied in § 6.4. Indeed, the evolution operator of the QSM in the strongly chaotic regime can be assumed to be a typical element of the CUE ensemble [186].
The calculations of this section only hold for randomness of type (R1), because we assume that $U$ is taken from the CUE ensemble and it has both the spectrum and the eigenvectors of a random matrix from CUE. As we already discussed, this is not true of $\tilde{U}$ in Eq. (6.2) that defines (R2), as $\tilde{U}$ only has a random eigenbasis. Therefore, generalizing the results presented in this section to the case of random measurements would require different techniques than those used here.

In order not to divert the reader's attention from the main line of discussion, here we will only report results. Their derivation is postponed to § 6.6.
We first consider fine-grained histories, i.e., the projectors are one-dimensional. Assuming for simplicity that that the initial state is a pure state $|j_0\rangle$ belonging to the "measurement basis" defined by the projectors, the fine-grained decoherence matrix element can be expressed as:

$$\mathcal{D}_{\mathbf{jk}} = \delta_{j_N k_N} U_{j_N j_{N-1}} \dots U_{j_2 j_1} U_{j_1 j_0} U^*_{k_1 j_0} U^*_{k_2 k_1} \dots U^*_{k_N k_{N-1}} \tag{6.17}$$

where matrix elements $\langle l|U|m\rangle$ are taken in the same basis of the projectors. $\mathcal{D}_{\mathbf{jk}}$ can be averaged over $U$ by using Weingarten's formula [202] (for more details, see § 6.6),

that allows to compute the average of products of arbitrary matrix elements of $U$:

$$\langle U_{l_1 m_1} \dots U_{l_N m_N} U^*_{l'_1 m'_1} U^*_{l'_N m'_N} \rangle_{\mathcal{U}(d)} = \\ \sum_{\sigma,\tau} \delta_{l_1 l'_{\sigma(1)}} \dots \delta_{l_N l'_{\sigma(N)}} \delta_{m_1 m'_{\tau(1)}} \dots \delta_{m_N m'_{\tau(N)}} Wg(d, \sigma\tau^{-1}) \tag{6.18}$$

where $Wg$ is the so-called Weingarten function [202]. Note that the matrix elements in (6.18) are completely general, i.e. the indices $l_1 \dots l_N$ and $m_1 \dots m_N$ are totally arbitrary. Instead, matrix elements in (6.17) have many indices in common, and a few passages are required to apply the general formula (6.18) to (6.17) (for details, see § 6.6).

*Fine-grained decoherence matrix elements.* For the fine-grained elements of the decoherence matrix, we obtain:

$$\begin{aligned} &\langle \mathcal{D}_{\mathbf{jj}} \rangle_{\mathcal{U}(d)} = \frac{\mathcal{N}_{\mathcal{P}}(\mathbf{j})}{d^N} + \mathcal{O}\Big(\frac{1}{d^{N+1}}\Big), \\ &\langle \mathcal{D}_{\mathbf{jj}} \mathcal{D}^*_{\mathbf{jj}} \rangle_{\mathcal{U}(d)} - \langle \mathcal{D}_{\mathbf{jj}} \rangle^2_{\mathcal{U}(d)} = \frac{\mathcal{N}'_{\mathcal{P}}(\mathbf{j})}{d^N} + \mathcal{O}\Big(\frac{1}{d^{2N+1}}\Big), \\ &\langle \mathcal{D}_{\mathbf{jk}} \rangle_{\mathcal{U}(d)} = \delta_{j_N k_N} \Big( \frac{\mathcal{F}_{\mathcal{P}}(\mathbf{j},\mathbf{k})}{d^N} + \Gamma_{\mathcal{P}}(\mathbf{j},\mathbf{k}) \mathcal{O}\big(\frac{1}{d^{N+1}}\big) \Big) \\ &\langle \mathcal{D}_{\mathbf{jk}} \mathcal{D}^*_{\mathbf{jk}} \rangle_{\mathcal{U}(d)} = \delta_{j_N k_N} \frac{\mathcal{F}'_{\mathcal{P}}(\mathbf{j},\mathbf{k})}{d^{2N}} (1 + \mathcal{O}(\frac{1}{d})) \end{aligned} \tag{6.19}$$

where $\mathcal{N}_{\mathcal{P}}, \mathcal{N}'_{\mathcal{P}}, \mathcal{F}_{\mathcal{P}}, \mathcal{F}'_{\mathcal{P}}, \Gamma_{\mathcal{P}}$ are *symmetry factors*. The derivation of Eq. (6.20) is presented in § 6.6.1. While the evaluation of symmetry factors is in principle hard, in § 6.6.3 we prove two statistical lemmas showing that for the overwhelming majority of pairs $\{\mathbf{j}, \mathbf{k}\}$ we simply have

$$\mathcal{N}_{\mathcal{P}} = 1, \quad \mathcal{N}'_{\mathcal{P}} = 2^N - 1, \quad \mathcal{F}_{\mathcal{P}} = 0, \quad \mathcal{F}'_{\mathcal{P}} = 1, \quad \Gamma_{\mathcal{P}} = 0$$

By "overwhelming majority" we mean all pairs $\mathbf{j}, \mathbf{k}$ except a fraction that vanishes in the limit $N/d \to 0$. The proofs in § 6.6.3 are based on statistical arguments inspired by statistical mechanics and graph theory.
Therefore, for almost all cases Eqs. (6.19) simply reduce to:

$$\begin{aligned} &\langle \mathcal{D}_{\mathbf{jj}} \rangle_{\mathcal{U}(d)} = \frac{1}{d^N} (1 + \mathcal{O}(\frac{1}{d})), \\ &\langle \mathcal{D}_{\mathbf{jj}} \mathcal{D}^*_{\mathbf{jj}} \rangle_{\mathcal{U}(d)} - \langle \mathcal{D}_{\mathbf{jj}} \rangle^2_{\mathcal{U}(d)} = \frac{2^N - 1}{d^{2N}} + \mathcal{O}(\frac{1}{d^{2N+1}}), \\ &\langle \mathcal{D}_{\mathbf{jk}} \rangle_{\mathcal{U}(d)} = 0 \\ &\langle \mathcal{D}_{\mathbf{jk}} \mathcal{D}^*_{\mathbf{jk}} \rangle_{\mathcal{U}(d)} = \delta_{j_N k_N} \frac{1}{d^{2N}} (1 + \mathcal{O}(\frac{1}{d})) \end{aligned} \tag{6.20}$$

*Coarse-grained decoherence matrix elements.* Upon evaluating the fine-grained decoherence matrix elements, we can look at a general coarse-graining where we sum over

$\Delta$ fine-grained projectors for each time. Then any coarse-grained decoherence matrix element $\mathcal{D}_{\mathbf{JK}}$ is obtained by summing over $\Delta^{2N}$ histories,

$$\mathcal{D}_{\mathbf{JK}} = \sum_{\mathbf{j}\in\mathbf{J}} \sum_{\mathbf{k}\in\mathbf{K}} \mathcal{D}_{\mathbf{jk}}. \tag{6.21}$$

Indices $\mathbf{J} = J_1 \dots J_N, \mathbf{K} = K_1 \dots K_N$ indentify a $\Delta^N \times \Delta^N$ submatrix of the fine-grained decoherence matrix. In § 6.6.2 we evaluate the mean and the variance of both diagonal elements $\mathcal{D}_{\mathbf{JJ}}$ and off-diagonal ones $\mathcal{D}_{\mathbf{JK}}$. For almost all $\mathbf{J}, \mathbf{K}$, up to corrections of order $\mathcal{O}(\frac{1}{d})$ we get:

$$\begin{aligned} \langle \mathcal{D}_{\mathbf{JJ}} \rangle_{\mathcal{U}(d)} = f^{-N} \quad , \quad \langle \mathcal{D}_{\mathbf{JJ}} \mathcal{D}^*_{\mathbf{JJ}} \rangle_{\mathcal{U}(d)} - \langle \mathcal{D}_{\mathbf{JJ}} \rangle^2_{\mathcal{U}(d)} = \frac{1}{\Delta} f^{-2N} \\ \langle \mathcal{D}_{\mathbf{JK}} \rangle_{\mathcal{U}(d)} = 0 \quad , \quad \langle \mathcal{D}_{\mathbf{JK}} \mathcal{D}^*_{\mathbf{JK}} \rangle_{\mathcal{U}(d)} = \delta_{J_N K_N} \frac{1}{\Delta} f^{-2N} \end{aligned} \tag{6.22}$$

where $f = d/\Delta$.

*Decoherence and entropy production.* The results (6.22) can be used to estimate the coherence ratio between histories. We obtain

$$\delta^2 = \frac{\langle \mathcal{D}_{\mathbf{JK}} \mathcal{D}^*_{\mathbf{JK}} \rangle_{\mathcal{U}(d)}}{\langle \mathcal{D}_{\mathbf{JJ}} \rangle_{\mathcal{U}(d)} \langle \mathcal{D}_{\mathbf{KK}} \rangle_{\mathcal{U}(d)}} \simeq \frac{1}{\Delta} \tag{6.23}$$

This means tha fine-grained histories ($\Delta = 1$) have a significant degree of coherence. On the contrary, for a high coarse-graining $\Delta \gg 1$ the off-diagonal elements are suppressed with respect to diagonal ones as $\delta \sim 1/\sqrt{\Delta}$. Furthermore, the fluctuations of the diagonal elements $\mathcal{D}_{\mathbf{JJ}}$ are suppressed with respect to their mean, and thus coarse-grained histories tend to acquire equal probabilities $1/f^N$.
The degree of coherence between histories can be evaluated by the relative entropy of decoherence ( 5.25) introduced in § 5.3.3:

$$\mathcal{C}_N = S(\tilde{\mathcal{D}}^{(N)}) - S(\mathcal{D}^{(N)}) = S(\mathcal{D}^{(N)} || \tilde{\mathcal{D}}^{(N)}) \geq 0$$

where $S(A||B)$ is the quantum relative entropy and $\tilde{\mathcal{D}}^{(N)}_{\mathbf{jk}} = \delta_{\mathbf{jk}} \mathcal{D}^{(N)}_{\mathbf{jk}}$. An upper bound to the latter can be found by Fannes inequality

$$|S(\varrho) - S(\sigma)| \leq T_1 \log d/T_1$$

where $T_1 = \frac{1}{2}||\varrho - \sigma||_1$. By applying Fannes inequality to $\mathcal{D}^{(N)}$ and $\tilde{\mathcal{D}}^{(N)}$, we can compute $\mathcal{C}_N$. To obtain an etimate of $T_1$, consider that $\mathcal{D}^{(N)} - \tilde{\mathcal{D}}^{(N)}$ has $f$ blocks of size $f^{N-1} \times f^{N-1}$. In each block, diagonal elements vanish, while off-diagonal ones are bounded above by $f^{-N}/\sqrt{\Delta}$. Assuming that for each block all-off diagonal elements are equal to $f^{-N}/\sqrt{\Delta}$, we get a bound for $||\mathcal{D}^{(N)} - \tilde{\mathcal{D}}^{(N)}||_1$:

$$T_1 \leq f(f^{-N}/\sqrt{\Delta}) \cdot (f^{N-1} - 1) < 1/\sqrt{\Delta}$$

since if a matrix $A$ of size $l$ has constant off-diagonal entries equal to $a$, it has $||A||_1 = 2(l-1)a$. Thus $\mathcal{C}_N$ is upper-bounded by

$$\mathcal{C}_N < \frac{1}{\sqrt{\Delta}} \log(d\sqrt{\Delta})) \tag{6.24}$$

that tends to 0 for $\Delta \gg 1$. Thus we obtain $h_N \simeq h_N^{(c)} \simeq N \log f$. *The chaotic system produces classical information at a rate given by the (un-maximized) dynamical entropy* $h_N/N \sim \log f$.

## 6.4 Decoherent histories in the quantum standard map

In this section, we will numerically address decoherent histories in the quantum standard map [195, 196, 197, 198, 199, 200] and test the predictions of preceding sections. From § 6.2 and § 6.3 we expect to see approximate decoherence among coarse-grained histories, as well as maximal entropy production for the following cases: (R1) random chaotic dynamics (R2) random projections.

*The quantum standard map.* Starting from the quantum kicked rotor

$$H = \frac{p^2}{2} + k/T \cos q \, \delta(t/T) \tag{6.25}$$

where $p$ and $q$ are the rotor's position and momentum variable respectively, and $\delta(t/T) = \sum_{j=-\infty}^{\infty} \delta(t - jT)$, the quantum standard map is defined by integrating the dynamics over a period $T$. One obtains the Floquet operator:

$$U = e^{-ip^2 T} e^{-k \cos q} \tag{6.26}$$

For $k = 0$ the system is integrable and it becomes chaotic for $k > k_c \sim 1$. For $k \gg 1$ the system is strongly chaotic. In our model, following Ref. [215], the phase space is discretized on a torus, i.e., both position and momentum variables are subject to periodic boundary conditions. Thus the Hilbert space has a finite dimension $d$ and $T = \frac{2\pi}{d}$ where $\frac{1}{d}$ plays the role of an effective Planck constant for the system (the classical limit is $d \to \infty$). In our numerics, we take $d = 1024 = 2^{10}$.
Since the phase space is compact, the "angle" observable $q$ has eigenstates

$$|n\rangle, \quad n = 0, 1, \ldots, d-1, \qquad q|n\rangle = \frac{\pi}{N}(2n+1)|n\rangle$$

The momentum eigenstates are obtained via discrete Fourier transform:

$$|k\rangle = \frac{1}{\sqrt{N}} \sum_{n=0}^{N-1} e^{ik\frac{2\pi}{N}n}|n\rangle \qquad p|k\rangle = \frac{\pi}{N}(2k+1)|k\rangle$$

*Decoherent histories in the QSM.* We consider coarse-grained histories with projectors of dimension $\Delta = d/f$. Without loss of generality, we take $f$ to be a power of 2, $f = 2^n$. Thus $n$ is the effective "number of qubits" that are "measured". The coarse-grained history projectors are obtained as $P_J = \sum_{j=(J-1)\cdot\Delta}^{J\cdot\Delta} |e_j\rangle\langle e_j|$ where $|\{e_j\rangle\}$ is an orthogonal basis in the Hilbert space.
From the discussion in § 5.3.2, we know that since the system is finite-dimensional, we can observe a growth of $h_N$ (5.20) up to a finite $N_{sat}$, after which a saturation

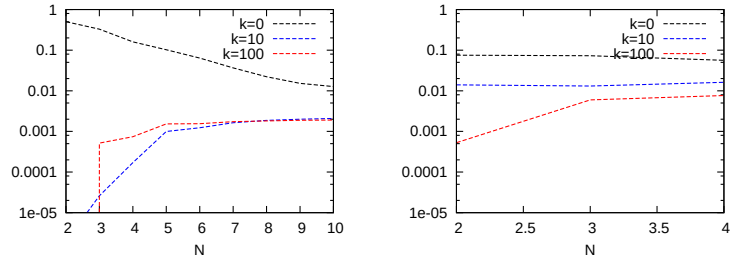


(a) $n = 1$, $|\psi_0\rangle = |0\rangle$ (b) $n = 3$, $|\psi_0\rangle = |0\rangle$

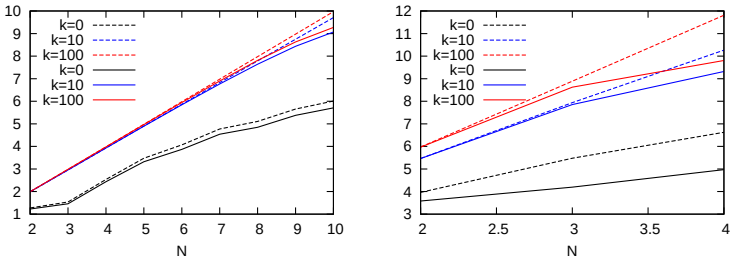


(c) $n = 1$, $|\psi_0\rangle = |0\rangle$ (d) $n = 3$, $|\psi_0\rangle = |0\rangle$

Figure 6.1: (top) average coherence $\langle\delta\rangle$ for histories with projections in the $X$ eigenbasis. (bottom) $h_N^{(c)}$ (dashed curves) and $h_N$ (full curves) for histories with projections in the $X$ eigenbasis. History projectors are of dimension $d/2^n$. Entropies are evaluated in bits.

effect must happen. In this case, a non-vanishing dynamical entropy reflects into a *linear growth* of $h_N$ up to $N_{sat}$ and the entropy production rate is defined as the slope of the initial growth of $h_N$. If the entropy is evaluated for coarse-grained partitions with $\Delta$-dimensional projectors, then the maximum possible entropy $h_N$ is given by $N \log f$ where $f = d/\Delta$ and we can expect maximal entropy production up to time $N_{sat} < \frac{\log d}{\log f}$. After this time, histories can no longer decohere and the relative entropy of decoherence $\mathcal{C}_N > 0$ due to coherent effects. That histories must show coherent effects after a give time is also confirmed by refs. [184, 185], that prove that the maximum number of exactly decoherent histories is $n_d \leq d$. Following other numeric studies, e.g. Ref. [192], we will focus on the initial transient $N \lesssim \log d$, which represents an upper bound to $N_{sat}$ achieved for maximal coarse-graining. We have performed numerical computations for different bases, different pure initial states, different degrees of coarse-graining and different values of the chaos parameter $k$ in the range $[0, 100]$. In Figs. 6.1 and 6.2 we present a selection of results that best illustrate the conclusions reached in § 6.2 and § 6.3. We show the average over all histories of the coherence ratio $\delta^2 = \frac{\mathcal{D}_{\mathbf{j},\mathbf{k}}\mathcal{D}^*_{\mathbf{j},\mathbf{k}}}{\mathcal{D}_{\mathbf{j},\mathbf{j}}\mathcal{D}_{\mathbf{k},\mathbf{k}}}$, as well as the dynamical entropies $h_N^{(c)}$ and $h_N$ (Eqs. (5.19) and (5.20)) in different regimes: $k = 0$ (integrable regime), $k = 10$ (weakly chaotic regime), $k = 100$ (strongly chaotic regime).

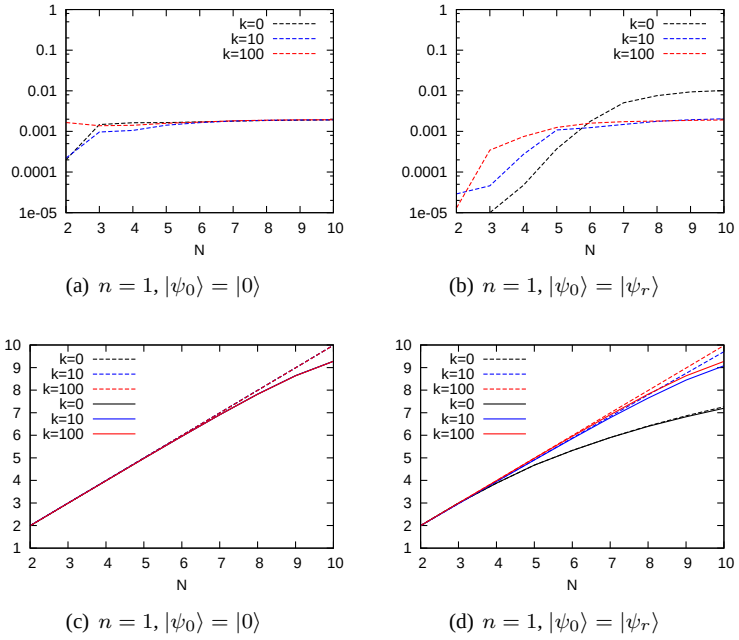


(a) $n = 1$, $|\psi_0\rangle = |0\rangle$ (b) $n = 1$, $|\psi_0\rangle = |\psi_r\rangle$

(c) $n = 1$, $|\psi_0\rangle = |0\rangle$ (d) $n = 1$, $|\psi_0\rangle = |\psi_r\rangle$

Figure 6.2: (top) average coherence $\langle\delta\rangle$ for histories with projections in a random eigenbasis. (bottom) $h_N^{(c)}$ (dashed curves) and $h_N$ (full curves) for histories with projections in a random eigenbasis. History projectors are of dimension $d/2^n$. Entropies are evaluated in bits

In Fig. 6.1 (a) and (c) we consider histories in the $X$ basis for $f = 2$, i.e., the partition is composed by two projections for each time (maximal coarse-graining). The initial state $|0\rangle$ is an eigenstate of $X$. With this choice of partition and initial state (that both have a well-defined phase space limit) we expect significant differences between the chaotic and integrable regime according to the analysis above and the results of Ref. [190, 187]. We can see that histories approximately decohere in the chaotic regime, where randomness of type (R1) is present. We find $\delta^2 < 10^{-3}$, consistent with the value $1/\Delta \simeq 2\cdot 10^{-3}$ expected from Eq. (6.23). Instead, histories have a significant amount of coherence in the integrable regime, where no (R1) randomness is present. In the chaotic regime we have a vanishing relative entropy of decoherence,

$$\mathcal{C}_N = h_N^{(c)} - h_N \simeq 0$$

The system is producing classical entropy at a rate $\sim 1 = \log 2$ (recall that we are taking logs in base 2), which is the maximum allowed by the partition size. In the integrable regime the entropy production is significantly lower. In Fig. 6.1 (b) and (d) we give the same figures for a different coarse-graining $n = 3$ (i.e., 8 projections for each time). We observe the same qualitative features of the previous $n = 1$ case. However, while the system in the chaotic regime starts producing classical entropy at a rate given

by $h_N \sim h_N^{(c)} = 3$, for $N \gtrsim 3$ we can observe finite size effects in the deviation of $h_N$ from $h_N^{(c)}$ for $N \gtrsim 3$ due to the finite-size bound $h_N \leq 10$.

In Fig. 6.2, we show that in presence randomness of type (R2) decoherence and entropy production are the same in the chaotic and in the integrable regime. In Fig. 6.2 (a) and (c), we consider histories in a random basis for $n = 1$ and initial state $|0\rangle$ that is an eigenstate of $X$. In both regimes, histories decohere and there is production of classical entropy at a rate $\sim 1$, i.e, the same behavior of the strongly chaotic regime. In Fig. 6.2 (b) and (d), we consider histories in the $X$ basis for $n = 1$ and initial state $|\psi_r\rangle$ that is a randomly generated state. In both regimes, histories decohere and there is production of classical information, even if the rate of entropy production is higher in the chaotic regime. This data suggest that also randomization of the initial state can lead to history: at present we don't have a proof of this feature, and further investigations are needed to establish whether it may hold in general.

## 6.5 Conclusions

In this chapter, we have addressed the problem of dynamical entropy production by quantum systems in presence of two sources of randomness: (R1) randomness in the dynamics, i.e. in the evolution operator (R2) randomness in the choice of of measurements. Our analysis of entropy production has been carried over in the decoherent histories formalism, with a focus on decoherence and coarse-graining. We have shown that (R1) and (R2) can lead to i) decoherence between coarse-grained histories ii) maximal entropy production compatible with coarse-graining size. As a consequence, both chaotic and integrable quantum systems can produce classical information at a rate given by the (un-maximized) dynamical entropy $h_N^{(c)}/N \simeq h_N/N$.
To conclude this chapter, we mention a link between our analysis and a well-known paper [165] where Gell-Mann addressed the general problem of unpredictability in physics. Gell-Mann identified four *fundamental sources of unpredictability*: (a) the coarse-graining required to make predictions (b) the probabilistic nature of future events (c) limited information about past and present events coupled with unpredictability amplification mechanisms such as chaos (d) limits to computational power. Computational power (d) depends on the nature of the observer - in the terminology of Gell-Mann, the information gathering and utilizing system [229]. Casting aside (d), one can focus on (a)-(c) that are are intrinsic to the system under observation. In this chapter we have analyzed the behavior of dynamical entropy by taking into account (a),(b) and (c) together. In fact, (c) includes dynamical randomness related to chaos (R1), while (b) includes unpredictability caused from measurements (R2). The analysis of (a), i.e., coarse-graining and decoherence, is essential for a physical interpretation of the ALF entropy in terms of predictability, and it is what distinguishes the present work by previous ones in the literature. We have demonstrated that (a),(b) and (c) together lead to the production of classical information at a non-vanishing rate given by the dynamical entropy.

## 6.6 Proofs of random-matrix results

### 6.6.1 Estimation of fine-grained decoherence matrix elements

The decoherence matrix element for a pair of histories reads:

$$\begin{aligned}\mathcal{D}_{\mathbf{jk}} = \mathrm{Tr}\Big[&|j_N\rangle\langle j_N|U|j_{N-1}\rangle\langle j_{N-1}|U\ldots U|j_1\rangle\langle j_1|U|j_0\rangle\times\\ &\langle j_0|U^\dagger|k_1\rangle\langle k_1|U^\dagger\ldots U^\dagger|k_{N-1}\rangle\langle k_N|U^\dagger|k_N\rangle\langle k_N|\Big] =\\ =&\delta_{j_N k_N} U_{j_N j_{N-1}}\ldots U_{j_2 j_1} U_{j_1 j_0} U^*_{k_1 j_0} U^*_{k_2 k_1}\ldots U^*_{k_{N-1}k_N}\end{aligned}$$

where we use the notation $\langle l|U|m\rangle \equiv U_{lm}$ and we assume that the initial state is a pure state $|j_0\rangle$ belonging to the measurement basis. We assume that the unitary $U$ is selected at random with the Haar measure on $\mathcal{U}(d)$ where $d \gg 1$. For almost all $U$ the value of

$$U_{j_N j_{N-1}}\ldots U_{j_2 j_1} U_{j_1 j_0} U^*_{k_1 j_0} U^*_{k_2 k_1}\ldots U^*_{k_{N-1}k_N}$$

will be close to its Haar-average. The latter can be evaluated by Weingarten's calculus [201], which is a generalization of Wick's calculus to unitary group. Weingarten's formula reads [202]:

$$\begin{aligned}&\langle U_{l_1 m_1}\ldots U_{l_N m_N} U^*_{l'_1 m'_1} U^*_{l'_N m'_N}\rangle_{\mathcal{U}(d)} = \\ &\sum_{\sigma,\tau}\delta_{l_1 l'_{\sigma(1)}}\ldots\delta_{l_N l'_{\sigma(N)}}\delta_{m_1 m'_{\tau(1)}}\ldots\delta_{m_N m'_{\tau(N)}} Wg(d,\sigma\tau^{-1})\end{aligned} \tag{6.27}$$

where $\sigma$ and $\tau$ are permutations of $\{1,\ldots,N\}$ and $Wg(d,\sigma\tau^{-1})$ is the so-called Weingarten function, that depends on the dimension $d$ and on the permutation $\sigma\tau^{-1}$. The $\delta$ functions imply that the multi-index $\mathbf{l}'$ must be a permutation of the multi-index $\mathbf{l}$, and at the same time the multi-index $\mathbf{m}'$ must be a permutation of the multi-index $\mathbf{m}$. The Weingarten function can be further evaluated as:

$$Wg(d,\sigma) = d^{-(N+|\sigma|)}(Mob(\sigma) + \mathcal{O}(d^{-2})) \tag{6.28}$$

where $|\sigma|$ is the length of $\sigma$, i.e., the minimum number of permutations that multiply to $\sigma$ and $Mob(\sigma)$ is the so called Möbius function. Therefore $Wg(d,\sigma\tau^{-1})$ is suppressed by a factor $d^{|\sigma\tau^{-1}|}$ that grows larger the more $\sigma$ and $\tau$ differ. If $\sigma = \tau$, then $Wg(d,\sigma\tau^{-1}) = Wg(d,\mathfrak{e}) = \frac{1}{d^N}(1+\mathcal{O}(d^{-2}))$ where $\mathfrak{e}$ is the identical permutation. To first order, we thus find:

$$\begin{aligned}&\langle U_{l_1 m_1}\ldots U_{l_N m_N} U^*_{l'_1 m'_1} U^*_{l'_N m'_N}\rangle_{\mathcal{U}(d)} = \\ &\frac{1}{d^N}\sum_{\sigma}\delta_{l_1 l'_{\sigma(1)}}\ldots\delta_{l_N l'_{\sigma(N)}}\delta_{m_1 m'_{\sigma(1)}}\ldots\delta_{m_N m'_{\sigma(N)}} + \mathcal{O}\Big(\frac{1}{d^{N+1}}\Big)\end{aligned} \tag{6.29}$$

that is essentially a Wick's theorem for the unitary group, asymptotically as $d\to\infty$. The $U_{lm}$ must be coupled with the corresponding complex conjugates $U^*_{lm}$. The essential reason behind the effectiveness of Weingarten calculus is that for $d\to\infty$, given a

random (Haar-distributed) unitary, the matrix elements of any finite $k \times k$ matrix converge (in distribution) to independent complex Gaussians with mean 0 and variance 1, renormalized by $\sqrt{d}$[203]:

$$P[U_{lm}] = P[|U_{lm}|e^{-i\phi_{lm}}] \to \frac{1}{2\pi\sqrt{d}} e^{-1/2|U_{lm}|^2}$$

As a consequence, unitary matrix elements become Gaussian variables and we can apply the original Wick's theorem: the average vanishes unless each $U_{lm}$ is matched by the corresponding $U^*_{lm}$.

In order to apply formula (6.27) to the decoherence matrix

$$\begin{aligned}&\langle \mathcal{D}_{\mathbf{jk}} \rangle_{\mathcal{U}(d)} \equiv \langle \mathcal{D}_{j_1 \dots j_N k_1 \dots k_N} \rangle_{\mathcal{U}(d)} = \\ &= \delta_{j_N k_N} \delta_{j_0 k_0} \langle U_{j_N j_{N-1}} \dots U_{j_2 j_1} U_{j_1 j_0} U^*_{k_1 k_0} U^*_{k_2 k_1} \dots U^*_{k_N k_{N-1}} \rangle_{\mathcal{U}(d)}\end{aligned}$$

we must implement the following substitutions:

$$l_\ell \to j_\ell, \quad l'_\ell \to k_\ell, \quad m_\ell \to j_{\ell-1}, \quad m'_\ell \to k_{\ell-1}$$

for all $1 \leq \ell \leq N$. We have to satisfy the following constraints

- $k_1 \dots k_N$ is a permutation of $j_1 \dots j_N$, $k_{\sigma(\ell)} = j_\ell$
- $k_0 \dots k_{N-1}$ is a permutation of $j_0 \dots j_{N-1}$, $k_{\tau(\ell)-1} = j_{\ell-1}$
- $k_N = j_N$ and $k_0 = j_0$.

By plugging the third condition into the first two, ge get:

- $k_1 \dots k_N$ is a permutation of $j_1 \dots j_N$, $k_{\sigma(\ell)} = j_\ell$ satisfying $k_{\sigma(N)} = k_N$
- $k_0 \dots k_{N-1}$ is a permutation of $j_0 \dots j_{N-1}$, $k_{\tau(\ell)-1} = j_{\ell-1}$ satisfying $k_{\tau(1)-1} = k_0$

So, we obtain *a fortiori* the following **proposition 1**: *unless* **j** *is a permutation of* **k** *we have* $\langle \mathcal{D}_{\mathbf{jk}} \rangle_{\mathcal{U}(d)} = 0$.

By virtue of (6.28), to first order only the permutations $\tau = \sigma$ contribute. We must then have up to corrections of $\mathcal{O}(1/d)$:

$$k_{\sigma(\ell)} = j_\ell, \;\; k_{\sigma(\ell)-1} = j_{\ell-1}$$

the transition pairs $\{k_0 k_1\}, \; \dots, \{k_{N-1} k_N\}$ must be a permutation of the transition pairs $\{j_0 j_1\}, \; \dots, \{j_{N-1} j_N\}$ into transition pairs $\{k_{\sigma(\ell)-1} k_{\sigma(\ell)}\}$. Notice that this is a much stronger condition than saying that **k** is a permutation of **j**.

Thus we obtain the following **proposition 2**: *Up to corrections of* $\mathcal{O}(1/d)$, $\langle \mathcal{D}_{\mathbf{jk}} \rangle_{\mathcal{U}(d)} = 0$ *unless the list of pairs* $\{j_0 j_1\}, \dots, \{j_{N-1} j_N\}$ *is a permutation of the list pairs* $\{k_0 k_1\}, \dots, \{k_{N-1} k_N\}$.

We denote by $\mathcal{P}(\mathbf{j},\mathbf{k})$ the set of permutations on $j_1,\ldots,j_N$ such that the pairs $\{j_0j_1\},\ldots,\{j_{N-1}j_N\}$ are a permutation of the pairs $\{k_0k_1\},\ldots,\{k_{N-1}k_N\}$. Under this notation, for the matrix element $\mathcal{D}_{\mathbf{jk}}$ we obtain:

$$\langle \mathcal{D}_{j_1\ldots j_N k_1\ldots k_N}\rangle_{\mathcal{U}(d)} = \frac{\delta_{k_N j_N}}{d^N}\sum_{\sigma\in\mathcal{P}(\mathbf{j},\mathbf{k})}\delta_{j_1 k_{\sigma(1)}}\ldots\delta_{j_N k_{\sigma(N)}} + \mathcal{O}\Big(\frac{1}{d^{N+1}}\Big) \quad (6.30)$$

Note that this formula could have been obtained directly from (6.29) - we choose not to follow this route as we wanted to derive proposition 1 first.

*Diagonal elements.* Let us use Eq. (6.30) to evaluate

$$\langle \mathcal{D}_{\mathbf{jj}}\rangle_{\mathcal{U}(d)} \equiv \langle \mathcal{D}_{j_1\ldots j_N j_1\ldots j_N}\rangle_{\mathcal{U}(d)}$$

If all transition pairs $\{j_0j_1\},\ldots,\{j_{N-1}j_N\}$ are different from one another we must have $\sigma=\mathfrak{e}$ and we get:

$$\langle \mathcal{D}_{\mathbf{jj}}\rangle_{\mathcal{U}(d)} = \frac{1}{d^N} + \mathcal{O}\Big(\frac{1}{d^{N+1}}\Big) \quad (6.31)$$

If some of the transition pairs $\{j_0j_1\},\ldots,\{j_{N-1}j_N\}$ coincide, let us partition them into $r<N$ equivalence classes, each class comprising $m_i$ elements with $\sum_{i=1}^r m_i = N$. Then we have to add a symmetry factor

$$\mathcal{N}_{\mathcal{P}}(\mathbf{j}) = m_1!\ldots m_r!$$

that properly accounts for the number of possible permutations among equal transition pairs. As a result,

$$\langle \mathcal{D}_{\mathbf{jj}}\rangle_{\mathcal{U}(d)} = \frac{\mathcal{N}_{\mathcal{P}}(\mathbf{j})}{d^N} + \mathcal{O}\Big(\frac{1}{d^{N+1}}\Big) \quad (6.32)$$

In the in § 6.6.3, we shall prove that $\mathcal{N}_{\mathcal{P}}(\mathbf{j}) = 1$ for the overwhelming majority of histories (Lemma 2).
In order to evaluate fluctuations, we compute the variance:

$$\langle \mathcal{D}_{\mathbf{jj}}\mathcal{D}^*_{\mathbf{jj}}\rangle_{\mathcal{U}(d)} - \langle \mathcal{D}_{\mathbf{jj}}\rangle^2_{\mathcal{U}(d)}$$

Assuming that all pairs $\{j_1j_2\},\ldots,\{j_{N-1}j_N\}$ differ, since now each pair $\{j_{\ell-1}j_\ell\}$ appears twice we get a symmetry factor 2 for each pair, hence a global factor $2^N$. Thus, we obtain:

$$\langle \mathcal{D}_{\mathbf{jj}}\mathcal{D}^*_{\mathbf{jj}}\rangle_{\mathcal{U}(d)} - \langle \mathcal{D}_{\mathbf{jj}}\rangle^2_{\mathcal{U}(d)} = \frac{2^N-1}{d^{2N}} + \mathcal{O}\Big(\frac{1}{d^{2N+1}}\Big) \quad (6.33)$$

If some of the pairs $\{j_1j_2\},\ldots,\{j_{N-1}j_N\}$ coincide, we have a symmetry factor

$$\mathcal{N}'_{\mathcal{P}}(\mathbf{j}) = (2m_1)!\ldots(2m_r)!$$

Again, because of Lemma 2, $\mathcal{N}'_{\mathcal{P}}(\mathbf{j}) = 1$ for the overwhelming majority of histories.
Equation (6.33) implies that fluctuations of the diagonal elements (as measured by the

standard deviation) will remain of order $\mathcal{O}(d^{-N})$.

*Off-diagonal elements.* Let us use Eq. (6.30) to evaluate

$$\langle \mathcal{D}_{\mathbf{jk}} \rangle_{\mathcal{U}(d)} \equiv \langle \mathcal{D}_{j_1 \dots j_N k_1 \dots k_N} \rangle_{\mathcal{U}(d)}$$

with $\mathbf{j} \neq \mathbf{k}$. If $j_N \neq k_N$ , we have $\mathcal{D}_{\mathbf{jk}} = 0$ (exactly). From (6.30) we get

$$\langle \mathcal{D}_{\mathbf{jk}} \rangle_{\mathcal{U}(d)} = \delta_{j_N k_N} \Big( \frac{\mathcal{F}_{\mathcal{P}}(\mathbf{j},\mathbf{k})}{d^N} + \Gamma_{\mathcal{P}}(\mathbf{j},\mathbf{k}) \mathcal{O}\big(\frac{1}{d^{N+1}}\big) \Big) \tag{6.34}$$

In (6.34), $\mathcal{F}_{\mathcal{P}}(\mathbf{j},\mathbf{k})$ represents the number of permutations such that bring the list of pairs $\{j_0 j_1\}, \dots, \{j_{N-1} j_N\}$ into the list pairs $\{k_0 k_1\}, \dots, \{k_{N-1} k_N\}$ (from proposition 2, unless such a permutation exists, the lowest order term in $1/d$ vanishes). It is an immediate consequence of Lemma 2 that for the overwhelming majority of pairs $\mathbf{j}, \mathbf{k}$ transition pairs cannot be matched (Corollary 1). Thus, for almost all histories $\mathcal{F}_{\mathcal{P}} = 0$. As for $\Gamma_{\mathcal{P}}(\mathbf{j},\mathbf{k})$, it includes permutations that bring $\mathbf{j}$ into $\mathbf{k}$. From proposition 1 we have that $\Gamma_{\mathcal{P}} = 0$ unless $\mathbf{k}$ is a permutation of $\mathbf{j}$. We shall prove below that $\mathbf{k}$ is not a permutation of $\mathbf{j}$ for the overwhelming majority of histories (Lemma 1), so for most pairs $\mathbf{j}, \mathbf{k}$, both the factors $\mathcal{F}_{\mathcal{P}}$,$\Gamma_{\mathcal{P}}$ vanish and $\langle \mathcal{D}_{\mathbf{jk}} \rangle_{\mathcal{U}(d)} = 0$.
In order to estimate the deviation from the mean, we can evaluate the variance. For pairs of histories with $k_N \neq j_N$ the variance of course vanishes, since $\mathcal{D}_{\mathbf{jk}} = 0$ exactly. For all other pairs,

$$\begin{aligned} \langle \mathcal{D}_{\mathbf{jk}} \mathcal{D}^*_{\mathbf{jk}} \rangle_{\mathcal{U}(d)} \equiv \langle \mathcal{D}_{j_1 \dots j_N k_1 \dots k_N} \mathcal{D}^*_{j_1 \dots j_N k_1 \dots k_N} \rangle_{\mathcal{U}(d)} = \\ \langle U_{j_N j_{N-1}} \dots U_{j_2 j_1} U_{j_1 j_0} U^*_{k_1 j_0} U^*_{k_2 k_1} \dots U^*_{k_{N-1} k_N} \times \\ U^*_{j_N j_{N-1}} U^*_{j_2 j_1} U^*_{j_1 j_0} U_{k_1 j_0} U_{k_2 k_1} \dots U_{k_{N-1} k_N} \rangle_{\mathcal{U}(d)} \end{aligned} \tag{6.35}$$

Since now all pairs of indices can be matched, we get

$$\langle \mathcal{D}_{\mathbf{jk}} \mathcal{D}^*_{\mathbf{jk}} \rangle_{\mathcal{U}(d)} = \frac{\mathcal{F}'_{\mathcal{P}}}{d^{2N}} + \mathcal{O}(\frac{1}{d^{2N+1}}) \tag{6.36}$$

where the symmetry factor $\mathcal{F}_{\mathcal{P}}$ accounts for permutations that bring the list $\{j_1 j_2\}, \dots, \{j_{N-1} j_N\}$ into the list $\{k_1 k_2\}, \dots, \{k_{N-1} k_N\}$. From Corollary 1 we can assume that transition pairs $\{j_1 j_2\}, \dots, \{j_{N-1} j_N\}$ and $\{k_1 k_2\}, \dots, \{k_{N-1} k_N\}$ in the two sets differ, obtaining

$$\langle \mathcal{D}_{\mathbf{jk}} \mathcal{D}^*_{\mathbf{jk}} \rangle_{\mathcal{U}(d)} = \frac{1}{d^{2N}} + \mathcal{O}(\frac{1}{d^{2N+1}}) \tag{6.37}$$

Thus, we can predict a standard deviation scaling as $\frac{1}{d^N}$. This means that off-diagonal elements have a size of $\mathcal{O}(\frac{1}{d^N})$. The estimation of diagonal and off-diagonal elements of the decoherence matrix is summarized in Table 6.6.1.
Putting together Eqs. (6.31) and (6.37), we obtain an estimate of coherences, that are of $\mathcal{O}(1)$:

$$\frac{\langle \mathcal{D}_{\mathbf{jk}} \mathcal{D}^*_{\mathbf{jk}} \rangle_{\mathcal{U}(d)}}{\langle \mathcal{D}_{\mathbf{jj}} \rangle_{\mathcal{U}(d)} \langle \mathcal{D}_{\mathbf{kk}} \rangle_{\mathcal{U}(d)}} \sim \mathcal{O}(1)$$

Thus, fine-grained histories have a significant degree of coherence. The situation will change when we consider coarse-grained histories.

| Case | Element | Average | Stardard deviation |
|---|---|---|---|
| 1 | $\mathcal{D}_{\mathbf{jj}}$ | $\frac{1}{d^N}$ | $\frac{2^N}{d^N}$ |
| 2 | $\mathcal{D}_{\mathbf{jk}}, \quad j_N = k_N$ | 0 | $\frac{1}{d^N}$ |
| 3 | $\mathcal{D}_{\mathbf{jk}}, \quad j_N \neq k_N$ | 0 | 0 |

Table 6.1: Estimation of fine grained elements of the decoherence matrix. Summary.

### 6.6.2 Coarse-graining

In the following paragraph, we start from the above Eqs. (6.31),(6.34), (6.37),(6.33) and consider coarse-grained histories for a random basis (or equivalently for a random evolution). We will show that coarse-graining leads to stronger decoherence between histories and also enforces approximately equal weights for histories.
We consider a coarse-graining where we sum over $\Delta$ projectors for each time. Then any coarse-grained decoherence matrix element $\mathcal{D}_{\mathbf{JK}}$ is obtained by summing over over $\Delta^{2N}$ histories:

$$\mathcal{D}_{\mathbf{JK}} = \sum_{\mathbf{j}\in\mathbf{J}} \sum_{\mathbf{k}\in\mathbf{K}} \mathcal{D}_{\mathbf{jk}} \tag{6.38}$$

The values of $\mathbf{J} = J_1 \dots J_N, \mathbf{K} = K_1 \dots K_N$ identify a $\Delta^N \times \Delta^N$ submatrix of the fine-grained decoherence matrix. We take $1 \ll \Delta < d$.

*Off-diagonal elements.* Consider first $\mathbf{J} \neq \mathbf{K}$. Then $\mathcal{D}_{\mathbf{JK}}$ is obtained by summing $\Delta^{2N}$ off-diagonal elements of the fine-grained decoherence matrix $\mathcal{D}_{\mathbf{jk}}$ and we get

$$\langle \mathcal{D}_{\mathbf{JK}} \rangle = \sum_{\mathbf{j}\in\mathbf{J}} \sum_{\mathbf{k}\in\mathbf{K}} \langle \mathcal{D}_{\mathbf{jk}} \rangle$$

If $J_N \neq K_N$, then for all terms in the sum (6.6.2) $j_N \neq k_N$, thus from Table 6.6.1, case 2, we have $\mathcal{D}_{\mathbf{jk}} = 0$. Therefore also $\langle \mathcal{D}_{\mathbf{JK}} \rangle$ vanishes exactly.
Let us assume $J_N = K_N$. Only pairs of histories with $j_N = k_N$ contribute to the sum (6.6.2), that is then over $\Delta^{2N-1}$ terms:

$$\langle \mathcal{D}_{\mathbf{JK}} \rangle = \sum_{\mathbf{j}\in\mathbf{J}} \sum_{\mathbf{k}\in\mathbf{K}} \delta_{j_N k_N} \langle \mathcal{D}_{\mathbf{jk}} \rangle$$

From Lemma 2, we can assume that for nearly all terms in the sum, $\langle \mathcal{D}_{\mathbf{jk}} \rangle = 0$. We thus get $\langle \mathcal{D}_{\mathbf{JK}} \rangle = 0$. The fluctuations around this value can be evaluated as:

$$\langle \mathcal{D}_{\mathbf{JK}} \mathcal{D}^*_{\mathbf{JK}} \rangle = \sum_{\mathbf{j}\in\mathbf{J}} \sum_{\mathbf{k}\in\mathbf{K}} \sum_{\mathbf{j}'\in\mathbf{J}} \sum_{\mathbf{k}'\in\mathbf{K}} \delta_{j_N k_N} \delta_{j'_N k'_N} \langle \mathcal{D}_{\mathbf{jk}} \mathcal{D}^*_{\mathbf{j'k'}} \rangle$$

To this sum only terms $\mathbf{j} = \mathbf{j}'$, $\mathbf{k} = \mathbf{k}'$, contribute:

$$\langle \mathcal{D}_{\mathbf{JK}} \mathcal{D}^*_{\mathbf{JK}} \rangle = \sum_{\mathbf{j}\in\mathbf{J}} \sum_{\mathbf{k}\in\mathbf{K}} \delta_{j_N k_N} \langle \mathcal{D}_{\mathbf{jk}} \mathcal{D}^*_{\mathbf{jk}} \rangle$$

and from the previous analysis we finally obtain

$$\langle \mathcal{D}_{\mathbf{JK}} \mathcal{D}^*_{\mathbf{JK}} \rangle = \frac{1}{\Delta} \frac{\Delta^{2N}}{d^{2N}} = \frac{1}{\Delta} f^{-2N} \tag{6.39}$$

where $f = d/\Delta$.

*Diagonal elements.* Now $\mathbf{J} = \mathbf{K}$. Then $\mathcal{D}_{\mathbf{JK}}$ is obtained by summing $\Delta^N(\Delta^N - 1)$ off-diagonal and $\Delta^N$ diagonal elements of the fine-grained decoherence matrix $\mathcal{D}_{\mathbf{jk}}$,

$$\langle \mathcal{D}_{\mathbf{JJ}} \rangle = \sum_{\mathbf{j} \in \mathbf{J}} \sum_{\mathbf{k} \in \mathbf{J}} \delta_{j_N k_N} \langle \mathcal{D}_{\mathbf{jk}} \rangle$$

where again only pairs of histories with $j_N = k_N$ contribute to the sum, that effectively includes only $\Delta^N(\Delta^{N-1} - 1)$ off-diagonal terms. From Lemma 2, we can assume that for nearly all off-diagonal terms in the sum, $\langle \mathcal{D}_{\mathbf{jk}} \rangle = 0$. We thus get the estimate:

$$\langle \mathcal{D}_{\mathbf{JJ}} \rangle = \frac{\Delta^N}{d^N} = f^{-N} \tag{6.40}$$

The fluctuations around this value can be evaluated as $\langle \mathcal{D}_{\mathbf{JJ}} \mathcal{D}^*_{\mathbf{JJ}} \rangle - \langle \mathcal{D}_{\mathbf{JJ}} \rangle^2$. We have:

$$\langle \mathcal{D}_{\mathbf{JJ}} \mathcal{D}^*_{\mathbf{JJ}} \rangle = \sum_{\mathbf{j} \in \mathbf{J}} \sum_{\mathbf{k} \in \mathbf{J}} \sum_{\mathbf{j}' \in \mathbf{J}} \sum_{\mathbf{k}' \in \mathbf{J}} \delta_{j_N k_N} \delta_{j'_N k'_N} \langle \mathcal{D}_{\mathbf{jk}} \mathcal{D}^*_{\mathbf{j'k'}} \rangle$$

To this sum contribute i) $\Delta^N$ terms such $\mathbf{j} = \mathbf{k} = \mathbf{j}' = \mathbf{k}'$ ii) $\Delta^N(\Delta^N - 1)$ terms such $\mathbf{j} = \mathbf{k} \neq \mathbf{j}' = \mathbf{k}'$ iii) $\Delta^N(\Delta^{N-1} - 1)$ terms such $\mathbf{j} = \mathbf{j}' \neq \mathbf{k}' = \mathbf{k}'$

$$\begin{aligned} \langle \mathcal{D}_{\mathbf{JJ}} \mathcal{D}^*_{\mathbf{JJ}} \rangle = & \sum_{\mathbf{j} \in \mathbf{J}} \langle \mathcal{D}_{\mathbf{jj}} \mathcal{D}^*_{\mathbf{jj}} \rangle + \sum_{\mathbf{j} \in \mathbf{J}} \sum_{\mathbf{j}' \in \mathbf{J}} \langle \mathcal{D}_{\mathbf{jj}} \mathcal{D}^*_{\mathbf{j'j'}} \rangle \\ & + \sum_{\mathbf{j} \in \mathbf{J}} \sum_{\mathbf{k} \in \mathbf{J}} \delta_{j_N k_N} \langle \mathcal{D}_{\mathbf{jk}} \mathcal{D}^*_{\mathbf{jk}} \rangle \end{aligned}$$

From the previous analysis we know the magnitudes of each contributions. Summing up all contributions, we obtain

$$\begin{aligned} & \langle \mathcal{D}_{\mathbf{JK}} \mathcal{D}^*_{\mathbf{JK}} \rangle = \Delta^N \frac{2^N - 1}{d^{2N}} + \Delta^N(\Delta^N - 1) \frac{1}{d^{2N}} + \\ & \Delta^N(\Delta^{N-1} - 1) \frac{1}{d^{2N}} = \frac{1}{d^{2N}} (\Delta^N(2^N - 3) + \Delta^{2N} + \Delta^{2N-1}) \end{aligned}$$

Upon subtracting $\langle \mathcal{D}_{\mathbf{JJ}} \rangle^2$, the variance is:

$$\begin{aligned} & \langle \mathcal{D}_{\mathbf{JJ}} \mathcal{D}^*_{\mathbf{JJ}} \rangle - \langle \mathcal{D}_{\mathbf{JJ}} \rangle^2 = \frac{1}{d^{2N}} (\Delta^N(2^N - 3) + \Delta^{2N-1}) = \\ & = \frac{1}{\Delta} \frac{\Delta^{2N}}{d^{2N}} (1 + \Delta \cdot \mathcal{O}(\frac{\Delta^N}{d^N})) = \frac{1}{\Delta} f^{-2N} (1 + \Delta \cdot \mathcal{O}(f^{-N}) \end{aligned} \tag{6.41}$$

### 6.6.3 Proofs of statistical lemmas

In this section we prove some lemmas anticipated above. The proofs require simple heuristic arguments based on statistical-mechanical analogies and graph theory.

**Lemma 1**

Consider the set of pairs $\{\mathbf{j}, \mathbf{k}\}$. if $d \gg N$, the overwhelming majority of them, except a fraction that vanishes in the limit $N/d \to 0$, are such that **j** is not related to **k** by a permutation.

*Proof.* The total number of histories is $d^N$. The problem of choosing the multi-index **j** is equivalent to the problem in statistical mechanics of placing $N$ particles into $d$ phase-space cells. By adopting a statistical-mechanical language, we can say consider each choice of **j** as a microstate. Then if the microstates **j** and **k** are related by a permutation they belong to the same macrostate $M(\mathbf{n})$, defined by the occupation numbers $\mathbf{n} = n_1 \dots n_d$ of each cell. Its volume is given by the multinomial factor:

$$V(\mathbf{n}) = \frac{N!}{n_1! \dots n_d!}$$

and the corresponding probability is then:

$$p(\mathbf{n}) = \frac{1}{d^N} \frac{N!}{n_1! \dots n_d!}$$

The total number of macrostates equivalent to the number of ways one can distribute $N$ objects to $d$ parties, which is known in combinatorics as number of combinations of $N$ objects of class $d$ and is given by:

$$\binom{d-1+N}{N} = \frac{(d+N-1)!}{N!(d-1)!}$$

The probability that **j** and **k** are related by a permutation is thus equivalent to the probability that two microstates belong to the same macrostate. This is simply given by

$$\mathcal{P} = \sum_{\mathbf{n}} p(\mathbf{n})^2 = \sum_{\mathbf{n}} \frac{V(\mathbf{n})^2}{d^{2N}}$$

In the "thermodynamic limit" $N \gg d$, most microstates will be absorbed in the Maxwell-Boltzmann macrostate where the $n_k$ are equal and we will have $\mathcal{P} \to 1$: very long histories "equilibrate" in the sense that most of them have the same number of projections on each partition member. However, in the opposite limit $N \ll d, N \leq \log d$ that is relevant for our calculations we can easily find a bound to this quantity. Since $V(\mathbf{n}) \leq N!$ we get

$$\mathcal{P} \leq \frac{(d+N-1)!}{N!(d-1)!} \frac{N!^2}{d^{2N}} \tag{6.42}$$

Upon explanding in series of $1/d$, we get:

$$\mathcal{P} \leq \frac{1}{d^{N+3}} N!(1+\mathcal{O}(1/d)) \leq \frac{1}{d^{N+3}} (\log d)^{\log d}(1+\mathcal{O}(1/d))$$

whence we conclude that $\mathcal{P} \ll 1$ when $d \gg 1$.

**Lemma 2**

Consider the set of histories **j**. The overwhelming majority of them, except a fraction that vanishes in the limit $N/d \to 0$, is such that all transition pairs $\{j_1 j_2\}, \ldots, \{j_{N-1} j_N\}$ differ, hence the the combinatorial factor $\mathcal{N}_{\mathcal{P}}$ in (6.32) is 1.

*Proof.* Our argument will be based on graph theory. There are $d^N$ possible choices of the indices $j_1 \ldots j_N$. We ask how many choices are such that the transition pairs $\{j_1 j_2\}, \ldots, \{j_{N-1} j_N\}$ all differ. We look at $j_1 \ldots j_N$ as describing possible paths on a directed graph $\mathcal{G}$ whose vertices are $1, \ldots, N$. The graph is totally connected, i.e., there is an edge between all ordered pairs of nodes (including loops $j \to j$). Therefore the graph's adjacency matrix is $A_{jk} = 1, \forall j, k$. The total number of edges is $N^2$. Each edge corresponds to a transition pair $\{j, k\}$ with $j, k \in \{1, \ldots, N\}$. The transition pairs can be seen as the vertices of another graph, which is the dual graph $\tilde{\mathcal{G}}$ of $\mathcal{G}$. We can label the $N^2$ vertices of $\tilde{\mathcal{G}}$ as follows: transition $\{i, j\}$ is labeled with the number $N \cdot (j-1) + k$. Under this labeling, we can easily compute the adjacency matrix of $\tilde{\mathcal{G}}$. The upper $N \times N^2$ block comprising the first $N$ rows looks as follows:

$$A = \begin{pmatrix} 1\ldots1 & 0\ldots0 & \ldots & 0\ldots0 \\ 0\ldots0 & 1\ldots1 & \ldots & 0\ldots0 \\ \vdots & & & \vdots \\ 0\ldots0 & 0\ldots0 & \ldots & 1\ldots1 \end{pmatrix}$$

and all $N \times N^2$ blocks comprising rows $m \cdot N \ldots (m+1) \cdot N$, $m = 1 \ldots N-1$ have the same form. This structure simply reflects the fact that each pair $\{j_1, j_2\}$ is linked only to pairs of the form $\{j_2, j_3\}$ (the second element in the first pair is the same as the first element in the second pair). The powers of $\tilde{A}$ are easily calculated as $(\tilde{A}^l)_{jk} = d^{k-2}, \forall j, k$.

Now, each of the $d^N$ admissible paths $j_1 \ldots j_N$ of length $N$ on $\mathcal{G}$ induces an admissible "dual" path $j_1 j_2, \ldots, j_{N-1} j_N$ of length $N-2$ on $\tilde{\mathcal{G}}$. It is known that the number of paths of length $l$ between $j$ and $k$ is given by $(\tilde{A}^l)_{jk}$. From above we can easily calculate the total number of dual paths of length $N-2$ as $\sum_{jk} (\tilde{A}^{N-2})_{jk} = d^N$ which corresponds (correctly) to the number of paths on $\mathcal{G}$.

Now, let us turn back to our original problem. If there are recurring transition pairs $\{j, k\}$ in the path on $\mathcal{G}$ (i.e. if some pairs of consecutive indices coincide) then the dual path on $\tilde{\mathcal{G}}$ must contain some loops. Thus, the total number of paths of length $N$ on $\mathcal{G}$ without recurrent transition pairs is equal to the number of loop-free paths of length $N-2$ on $\tilde{\mathcal{G}}$. This number can be estimated as follows. On $\mathcal{G}$, each of the $d^2$ vertices just has outgoing edges to a subset of $d$ vertices. Hence there there is a probability

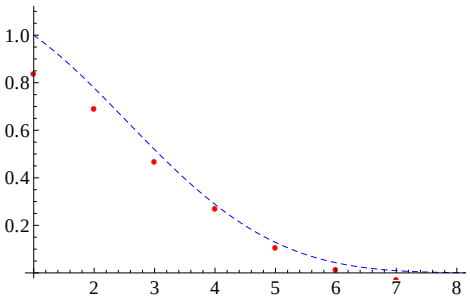


Figure 6.3: Fraction of histories for which all transition pairs $\{j_1, j_2\}, \ldots, \{j_{N-1}, j_N\}$ differ. Exact calculation (dots) and approximate formula $f(N) = \frac{(d^2-2)!}{(d^2+1-N)!} d^{-2N+6}$ (dashed line). The space dimension is $d = 3$.

$p = 1/d$ for the existence of a direct link between a specific pair of vertices. As all links of a path have to exist if the path should exist, the probability for the existence of a specific path of length $l$ is $p_{path} = p^l$ . Taking this into account, an estimate for the number of loop-free paths between two vertices can be expressed as:

$$\#(l) = \frac{(d^2-2)!}{(d^2-1-l)!} p^l = \frac{(d^2-2)!}{(d^2-1-l)!} d^{-l}$$

Thus, the total fraction of loop-free paths of length $N-2$ is give as

$$d^4 \cdot \frac{(d^2-2)!}{(d^2+1-N)!} d^{-N+2} = \frac{(d^2-2)!}{(d^2+1-N)!} d^{-N+6}$$

and the total fraction of loop-free paths of length $N-2$ is finally:

$$f(N) = \frac{(d^2-2)!}{(d^2+1-N)!} d^{-2N+6}$$

In Fig. 6.3 we plot the exact fraction of loop-free paths, numerically evaluated, and our approximation for $d = 3$. It can be seen that there is a very good agreement (note that the approximation is expected to be increasingly accurate as $d$ grows). Upon taking the limit $d \to \infty$, and expanding in powers of $1/d$, we get

$$f(N) = 1 - (1 - \frac{N}{2} - \frac{N^2}{2})(1/d^2) + \mathcal{O}(1/d^3) \tag{6.43}$$

which proves that in the limit $d \to \infty$, the decoherence matrix is dominated by elements of the form (6.31) that have $\mathcal{N}_P = 1$.

**Corollary 1**. Consider the set of pairs $\{\mathbf{j}, \mathbf{k}\}$ such that $\mathbf{k}$ is a permutation of $\mathbf{j}$. if $d \gg N$, the overwhelming majority of them, except a fraction that vanishes in the limit $N/d \to 0$, are such that transition pairs $\{j_1 j_2\}, \ldots, \{j_{N-1} j_N\}$ $\{k_1 k_2\}, \ldots, \{k_{N-1} k_N\}$ differ, hence the factor $\mathcal{F}_\mathcal{P}$ in (6.34) can be assumed to be is 0 and the factor $\mathcal{F}'_\mathcal{P}$ in (6.36) can be assumed to be is 1.

# Chapter 7

# Einselection and decoherent histories

## 7.1 Introduction

Since its modern incipit, physics has been in conflict with intuition. According to Newton's mechanics, an object in motion tends to stay in motion with the same speed and in the same direction unless acted upon by an external force. In the light of our ordinary experiences this assertion looks paradoxical, namely, at odds with common sense. In fact, what we usually observe is rather the opposite: bodies do not stay in motion unless acted upon by a constant force. Accordingly, before Newton people used to split the whole into two domains, the celestial one, where bodies would naturally retain perpetual motions, and the terrestrial one, where bodies would rest in their natural positions and move only when "violently" acted upon by some force. Newton overcame this dichotomy, postulating that the same laws hold everywhere in the universe. What impairs direct observation of the first law in the terrestrial domain we live in is the fact that bodies *are never really isolated*, which results in friction leading to momentum and energy dissipation.

With quantum mechanics, bigger paradoxes came out. One of the main conundrums of quantum theory is that everyday experience seems to contradict one of its cornerstones [206, 207]: the superposition principle. The linearity of the Schrödinger equation entails that the manifold of allowed kinematic states is a linear space. Consequently, for any two orthogonal states corresponding to different values of some observable (say, position), there should exist states where those different values are coherently superposed. Furthermore, most initial conditions are likely to evolve into such a superposition. Yet, we never happen to observe such coexistence of alternatives. In particular, familiar macroscopic systems tend to be well localized with respect to the usual phase-space observables such as position and momentum. The traditional interpretation elaborated by Bohr[225] coped with this issue by splitting the universe into two domains, the quantum one and the classical one. The interaction of a quantum object with the ultimate macroscopic "classical apparatus" would automatically reduce

the plurality of alternatives to a single one. Thus, the paradox was solved at the price of denying the universal validity of quantum mechanics.

The dissatisfaction with this interpretation has motivated a huge effort aimed at restoring the universality of quantum mechanics, while giving at the same time a satisfactory account of the disappearance of coherent effects in macroscopic reality. Contrary to proposals that require a significant modification of quantum theory (such as nonlinear stochastic models[226]), the two most successful approaches to the problem do not involve a change in the fundamental equations. These approaches are environment-induced superselection (EIS) and decoherent histories (DH). Both strive to consistently apply quantum mechanics to *closed* systems, including the universe as a whole. Yet, both recognize that a consistent description must acknowledge that the objects we observe, especially in the macroscopic realm, *are never isolated, hence never closed*. They do not interact with an elusive "classical domain", but with their (quantum) surroundings, and must be consequently treated as *open quantum systems*.

Openness is identified as the root of the problem: like friction prevents observation of the uniform rectilinear motion predicted by Newton's law, so interaction with the environment prevents observation of superposition and interference phenomena predicted by Schrödinger's equation. Indeed the theory of open quantum systems shows that open systems evolution generally results in a dynamical suppression of superpositions. In the EIS approach, this suppression reflects into the emergence of preferred *pointer bases* in Hilbert space such that coherent superpositions in those bases are dynamically ruled out. The off-diagonal entries of the *density matrix* of the in the preferred bases tend to vanish. In the DH approach, we observe history decoherence within preferred sets of coarse-grained histories. The off-diagonal entries of the *decoherence matrix* for these sets tend to vanish.

Thus the aim to understand the quantum/classical transition from a fundamental standpoint fueled interest in the problem of the suppression of coherence, or, simply, *decoherence*. Driven by this goal, research in decoherence initially focused on simple, solvable models devised to realize a well-defined classical macroscopic limit, like a particle interacting linearly with a set of oscillators. In these "semiclassical" models coherence is simultaneously suppressed in several bases, corresponding to phase-space observables (position, momentum, etc.), which is in agreement with the emergence of classicality. From the EIS viewpoint, semiclassical models not not exhibit a single pointer basis, but several ones: Superpositions of eigenstates of phase-space observables with macroscopically different eigenvalues are simultaneously suppressed [211]. Analogously, from the DH viewpoint, coarse-grained histories with projections over macroscopically different values of several phase-space observables decohere [165, 171]. A comparison between EIS and DH for a bosonic mode subject to a Markovian noise including dissipation and thermal hopping from the environment has been done by Twamley [221]. He showed that off-diagonal elements of the density matrix in the position, momentum and coherent-state bases are suppressed, while histories defined by Gaussian quasiprojections in the same bases approximately decohere.

As Zurek stressed, these results cannot be regarded as a complete phenomenological characterization of decoherence in any possible regime [212]. In particular, the behavior of decoherence for microscopic systems with a low number of degrees of freedom and undergoing different interactions with the environment can be richer, more various

and more complicated than the initial results on semiclassical systems might suggest. Thus decoherence becomes an interesting phenomenon in its own right, and not just as a mechanism for achieving classical behavior. Studies of decoherence in microscopic systems have been carried in the EIS picture, and have shown that the emergence of pointer bases crucially depends on the magnitude of the coupling between the system of interest and the environmental degrees of freedom. It has been established that pointer bases emerge in the opposite limits of strong and weak coupling: for weak coupling, a pointer basis is given by the system's energy eigenbasis, while for strong coupling the pointer basis is the eigenbasis of the interaction Hamiltonian. In a recent paper [217], some evidence has been presented that for intermediate values of the coupling there exist pointer bases that interpolate between those two extremes in a continuous fashion. In Refs. [219, 220] a comparison of the EIS and DH pictures for the decoherence of a microscopic system was presented. It was concluded that the relation between pointer bases and sets of decoherent histories is not one-to-one: the existence of a pointer basis is sufficient, but not necessary to construct a set of decoherent histories.

In the present chapter, I analyze decoherence in a microscopic system comparing the EIS and the DH approach in a wide range of system-environment coupling regimes. My aim is twofold. One one side, I will better clarify the relation between the two approaches (EIS and DH) in characterizing a decoherence process. On the other side, I will shed more light onto the intermediate coupling regime. I will cast doubt on previous results in [217], arguing that no *stable* pointer bases arise in this regime, a result that will be confirmed by the the analysis of DH. A crucial tool to compare DH and EIS will be the relative entropy of decoherence (5.25) defined in § 5.3.3, that will hold as a quantifier of coherence within a set of histories. The system under attention is a two-level system interacting with a non-Markovian environment composed by another two level system (near environment) interacting in a Markovian way with a bath (far environment). The choice of this model is motivated by several considerations. First, this is the simplest non-trivial model of small system subject to decoherence. While the the choice of a Markovian bath may be unduly restrictive for such a system, studying a non-Markovian bath is non-trivial from the DH viewpoint, as the decoherence matrix cannot be simply expressed in terms of reduced quantities alone (see § 4.3.3). Second, this is essentially the same model studied in Ref. [217], except that the far environment is a Markovian bath instead of a chaotic system (this replacement is convenient if not mandatory for numerically analyzing DH, and should not affect results, at least qualitatively, as discussed below). Therefore, this will allow for immediate comparison with results in [217].

This chapter is organized as follows. In § 7.2 I will review EIS and discuss previous results comparing EIS and DH. § 7.3 contains the core of the chapter, presenting numeric results for the model under study. § 7.4 will close the chapter summarizing the main conclusions.

To the best of my knowledge, the entire content of this chapter is original and has never appeared in any previous publication.

## 7.2 Environment-induced superselection

### 7.2.1 EIS in a nutshell

Environment-induced superselection [209, 210, 207, 206, 208] or *einselection* is grounded on the idea that most kinematically admissible superpositions are dynamically ruled out from observation due to the effect of the unavoidable interaction with external degrees of freedom collectively denoted as environment. Interaction of the system $S$ with the environment $\mathcal{E}$ leads to an entangled $S\mathcal{E}$ state. As a result, under general conditions $\mathcal{E}$ "monitors" an observable $\mathcal{A} = \sum_i \alpha_i |a_i\rangle_S\langle a_i|$ of the system, in the sense that the $|a_i\rangle_S$ become correlated, and remain stably correlated, with quasi-orthogonal states of the environment $|\phi_i\rangle_\mathcal{E}$:

$$\sum_i \alpha_i |a_i\rangle_S \otimes |\phi\rangle_\mathcal{E} \quad \rightarrow \quad \sum_i \alpha_i |a_i\rangle_S \otimes |\phi_i\rangle_\mathcal{E}$$

where $\langle\phi_i|\phi_j\rangle_\mathcal{E} \ll 1$ for $i \neq j$. In other words, $|a_i\rangle_S|\phi_i\rangle_\mathcal{E}$ is an approximate Schmidt basis of the entangled $S\mathcal{E}$ state, irrespective of the initial state of $S$.
If the environment is sufficiently big, irreversibility appears. We have $\langle\phi_i|\phi_j\rangle_\mathcal{E} \simeq \delta_{ij}$ and the reduced density matrix of the system becomes approximately diagonal in the *preferred basis* or *pointer basis* $|a_i\rangle$. The time required for entanglement to be created between $S$ and $\mathcal{E}$ is usually much shorter that the time required for $S$ and $\mathcal{E}$ to thermally equilibrate. Therefore decoherence of $S$ in the pointer basis usually occurs within a *decoherence time* time $\tau_D$ that is much shorter than the relaxation time $\tau_R$.
The original goal of EIS theory was to depict a measurement process, whence the name "pointer basis" stems. Consider a measurement situation where that the system $S$ interacts with a measuring apparatus $A$ so as to produce the entangled state

$$|\psi\rangle_{SA} = \sum_i \alpha_i |s_i\rangle_S |a_i\rangle_A$$

where $|s_i\rangle$ and $|a_i\rangle$ are orthogonal bases of $S$ and $A$ respectively. A mentioned above in § 1.2, correlations in $|\psi_{SA}\rangle$ show a basis ambiguity problem: they can be expressed in several different bases. Nevertheless, if the apparatus $A$ is subject to interaction with the environment, that "monitors" $\mathcal{A}$, one ends up with the entangled $SA\mathcal{E}$ state

$$\sum_i \alpha_i |s_i\rangle_S \otimes |a_i\rangle_A \otimes |\phi_i\rangle_\mathcal{E} \tag{7.1}$$

where states $|a_i\rangle_A$ of the apparatus become correlated with quasi-orthogonal states of the environment $|\phi_i\rangle_\mathcal{E}$. The reduced $SA$ state is now

$$\sum_i |\alpha_i|^2 |s_i\rangle\langle s_i| \otimes |a_i\rangle\langle a_i| \tag{7.2}$$

displaying only classical correlations between $S$ and $A$. In particular, correlations are between states $|s_i\rangle_S$ of $S$ and states $|a_i\rangle_A$ of $A$. The latter are called *pointer states* because they can be seen as states of the measuring apparatus allowing to discriminate unambiguously the states $|s_i\rangle_S$ of $S$. Whenever such a pointer basis exists, superpositions

in that basis cannot be registered by observers: the environment imposes effective *superselection rules* in the Hilbert space. The only system-observer correlations that are stable under environmental noise are classical correlations in the preferred basis[207]. The environment thus creates well-defined, classical outcomes for any (macroscopic) observation. Correlations that are spoiled by noise are useless: the observer cannot use his records to make inferences on the future behavior of the system.

### 7.2.2 Pointer bases

Pointer bases depend on a subtle balance between the system's self-Hamiltonian and the interaction Hamiltonian. Let

$$H = H_S + H_{\mathcal{E}} + \lambda H_{int} \tag{7.3}$$

be the Hamiltonian that generates the joint system-environment evolution, where $\lambda$ is the system-environment coupling strength and

$$H_S = \sum_i E_{S,i}|E_i\rangle_S\langle E_i|, \qquad H_{\mathcal{E}} = \sum_j E_{\mathcal{E},j}|E_j\rangle_{\mathcal{E}}\langle E_j|$$

#### Strong coupling

If the system-environment coupling is large, the pointer basis is dictated by $H_{int}$ [209]. In this limit, we can neglect $H_S$ and $H_{\mathcal{E}}$ and just focus on $H_{int}$. Exact pointer states emerge if there is a *pointer observable*, i.e., a local observable $\mathcal{A} = \sum_i a_i|a_i\rangle\langle a_i|$ of the system that commutes with the interaction Hamiltonian,

$$[\mathcal{A}, H_{int}] = 0 \tag{7.4}$$

This implies that the interaction Hamiltonian has a form of the type

$$H_{int} = \sum_{ijk} \lambda_{ijk}|a_i\rangle_S\langle a_i| \otimes |b_j\rangle_{\mathcal{E}}\langle b_k| + H.c.$$

In this case eigenstates of $\mathcal{A}$ are perfectly stable under interaction with the environment. Furthermore, they become correlated with states of the environment in such a way as to suppress off-diagonal terms in the density matrix. We can illustrate this process for the simplified case where $H_{int}$ is approximately diagonal in a product basis:

$$H_{int} = \sum_{ij} \gamma_{ij}|a_i\rangle_S\langle a_i| \otimes |b_j\rangle_{\mathcal{E}}\langle b_j|$$

Starting from the initial state:

$$|\psi\rangle_S \otimes |\phi\rangle_{\mathcal{E}} = \sum_i \alpha_i|a_i\rangle_S \otimes \sum_j \beta_j|b_j\rangle_{\mathcal{E}}$$

the time evolution yields:

$$\sum_{ij} \alpha_i\beta_j e^{-i\gamma_{ij}t}|a_i\rangle_S \otimes |b_j\rangle_{\mathcal{E}} = \sum_i \alpha_i|a_i\rangle_S \otimes |\phi_i(t)\rangle_{\mathcal{E}}$$

where $|\phi_i(t)\rangle_{\mathcal{E}} = \sum_j \beta_j e^{-i\gamma_{ij}t}|b_j\rangle_{\mathcal{E}}$ The reduced density matrix for $S$ is given by:

$$\varrho_S(t) = \sum_{ij} \alpha_i\alpha_j^*|a_i\rangle_S\langle a_j|\ \langle\phi_j(t)|\phi_i(t)\rangle_{\mathcal{E}} =$$
$$= \sum_i |\alpha_i|^2|a_i\rangle_S\langle a_i| + \sum_{i\neq j} \alpha_i\alpha_j^*|a_i\rangle_S\langle a_j|\ \langle\phi_j(t)|\phi_i(t)\rangle_{\mathcal{E}}$$

If the environment states $|\phi_i(t)\rangle_{\mathcal{E}}$ become orthogonal, the state becomes diagonal in the $|a_i\rangle_S$ basis. This can occur, for instance, if the environment is large. Consider

$$z_{ij}(t) \equiv \langle\phi_j(t)|\phi_i(t)\rangle_{\mathcal{E}} = \sum_k |\beta_k|^2 e^{-i(\gamma_{ik}-\gamma_{jk})t} = \sum_k p_k e^{-i\omega_{ij}^k t}$$

That $z_{ij}(t)$ give a decay can be easily seen. Indeed compute the long-time average ($t \to \infty$)

$$\langle|z_{ij}|^2\rangle_T = \frac{1}{T}\int_0^T |z_{ij}(t)|^2 dt = \sum_k p_k p_{k'}\Big(\delta(\omega_{ij}^k - \omega_{ij}^{k'}) + \frac{1-e^{-i(\omega_{ij}^k-\omega_{ij}^{k'})T}}{iT(\omega_{ij}^k-\omega_{ij}^{k'})})\Big)$$
$$\longrightarrow_{t\to\infty} \sum_k p_k\delta(\omega_{ij}^k - \omega_{ij}^{k'})$$

If all $\omega_{ij}^k$ are distinct, we get

$$\Delta_z^2 = \langle|z_{ij}|^2\rangle_T - \langle z_{ij}\rangle_T^2 = \sum_{k=1}^N p_k^2$$

If the dimension $N$ of the environment is large, assuming that all $p_k \sim 1/N$ then $\Delta_z \sim 1/\sqrt{N}$.

**Weak coupling**

In the opposite limit of small system-environment coupling $\lambda$, several nontrivial and diverse arguments based on adiabaticity [214], echo dynamics [215] and ergodicity [216] lead to the conclusion that the pointer basis is the energy eigenbasis of the system, i.e., the eigenbasis of $H_S$. We briefly sketch the "adiabatic" argument. Assume that the frequencies (i.e., the energies) of the environment are much lower than those of the system. Consider an initial state $|\Psi(0)\rangle_{S\mathcal{E}} = \sum_k c_k|E_k\rangle_S \otimes |\phi_k(0)\rangle_{\mathcal{E}}$. Since the environment is "slow", from the adiabatic theorem, we have

$$|\Psi(0)\rangle_{S\mathcal{E}} = \sum_k c_k e^{-iE_{S,k}t}|E_k\rangle_S \otimes |\phi_k(t)\rangle_{\mathcal{E}}$$

where $|\phi_k(t)\rangle_{\mathcal{E}} = e^{-itH_{int,k}}|\phi(0)\rangle_{\mathcal{E}}$ with $H_{int,k} = \langle E_k|H_{int}|E_k\rangle_S$. As discussed in [214], often $H_{int,k}$ acts as a "displacement operator" for the environment, then the states $|\phi_k(t)\rangle_{\mathcal{E}}$ of the environment tend to become orthogonal as

$$\langle\phi_k(t)\rangle|\phi_l(t)\rangle_{\mathcal{E}} \sim e^{-\gamma_{kl}t^2}$$

Therefore, for the off-diagonal elements of the reduced density matrix in the energy eigenbasis of the system we get

$$\langle E_k|\varrho^S|E_l\rangle \sim c_k c_l^* e^{-i(E_k-E_l)t} e^{-\gamma_{kl}t^2}$$

**More general cases**

For intermediate coupling, it has been argued that approximate pointer bases exist and interpolate between the pointer basis and the energy eigenbasis[217]. This case will be discussed in detail below (§ 7.3).
In general, it is nontrivial to identify the set of pointer states for a given system/environment dynamics. In the simplest models, such pointer states are eigenstates of the pointer observable which commutes with the system-environment interaction. In more general cases, one may resort to several criteria aimed at identifying the set of states that is least affected by the interaction. One such criterion is the so-called *predictability sieve* [207]. The evolution of a pure state $|\psi\rangle_S$ is considered predictable if it is deterministic, i.e., if the state maintains its purity. The loss of predictability, in this sense, is measured by the von Neumann entropy of the evolved state $S(\varrho(t))$ where $\varrho(0) = |\psi\rangle_S\langle\psi|$. If states are ranked according to their predictability, the environment is seen as a sieve that selects the states that "survive" best to the interaction with the environment. The set of states that minimize $S(\varrho(t))$ is a good candidate to represent the set of pointer states. In fact, when a true pointer observable exists its eigenstates can be retrieved with this predictability sieve criterion.

### 7.2.3 EIS and consistent histories

EIS and DH yield two possible descriptions of a decoherence process. The goal of understanding the relation between the two pictures has prompted several studies [218, 219, 220]. These works have shown that there is an asymmetric relation between pointer bases and decoherent sets of histories, that may be summarized as follows. One one side, the mere existence of a set of decoherent histories may not be related to a physical process of einselection. The vanishing of *interference* between histories may or may not be caused by *decoherence*. In fact, it can occur even in closed systems, as we saw in Chap. 6. On the other side, the existence of a pointer basis implies that a decoherent set of histories can be obtained by fixing projectors in the pointer basis for all times, since histories in the pointer basis will have vanishing interference.

**history decoherence $\not\Rightarrow$ EIS**

Systematic procedures to find a decoherent set of histories exist irrespective of whether einselection is acting or not. Let us consider generic histories defined by projectors $P^\ell_{j_\ell}$, where $\ell = 1, \ldots, N$. The superscript $\ell$ indicates that projectors for each $t_\ell$ may be different, while the subscript $j_\ell$ labels the alternative at time $t_\ell$ (notations are the same introduced in § 4.2.1).
For a closed system we can simply take $P^\ell_{j_\ell} = |e_{j_\ell}(t_\ell)\rangle\langle e_{j_\ell}(t_\ell)|$ where the $|e_k(t)\rangle$ form

the instantaneous eigenbasis of the density matrix,

$$\varrho(t_\ell)|e_k(t_\ell)\rangle = e_k(t_\ell)|e_k(t_\ell)\rangle \quad \text{where} \quad \varrho(t_\ell) = U(t_\ell)\varrho(t_0)U^\dagger(t_\ell)$$

Indeed the decoherence matrix reads

$$\begin{aligned}\mathcal{D}_{\mathbf{jk}} &= \mathrm{Tr}[\dots P^2_{j_2} U(t_2-t_1) P^1_{j_1} U(t_1-t_0)\varrho(t_0)U^\dagger(t_1-t_0)P^1_{k_1}U^\dagger(t_2-t_1)P^2_{k_2}\dots] = \\ &= \mathrm{Tr}[\dots P^2_{j_2} U(t_2-t_1) P^1_{j_1} \varrho(t_1) P^1_{k_1} U^\dagger(t_2-t_1)U^\dagger P^2_{k_2}\dots]\end{aligned}$$

In order to get decoherence in the first index, one simply chooses $P^1_{j_1} = |e_{j_1}(t_1)\rangle\langle e_{j_1}(t_1)|$, getting

$$\begin{aligned}\mathcal{D}_{\mathbf{jk}} &= \delta_{j_1k_1}\mathrm{Tr}[\dots P^2_{j_2}U(t_2-t_1)|e_{j_1}(t_1)\rangle\langle e_{j_1}(t_1)|U^\dagger(t_2-t_1)P^2_{k_2}\dots] = \\ &= \delta_{j_1k_1}\mathrm{Tr}[\dots P^2_{j_2}|e_{j_1}(t_2)\rangle\langle e_{j_1}(t_2)|P^2_{k_2}\dots] =\end{aligned}$$

Taking $P^2_{j_2} = |e_{j_2}(t_2)\rangle\langle e_{j_2}(t_2)|$ one gets decoherence in the second index, etc. This choice requires to adjust the measurement at $t_\ell$ align the projectors to the instantaneous eigenbasis of $\varrho$. However, there is another way to get a decoherent set. It suffices to take histories in the energy eigenbasis of for all times, $P^\ell_{j_\ell} = |E_{j_\ell}\rangle\langle E_{j_\ell}|$. Now the Projectors commute with the dynamics, hence we have

$$\begin{aligned}\mathcal{D}_{\mathbf{jk}} &= \mathrm{Tr}[U(t_N-t_0)P^N_{j_N}\dots P^1_{j_1}\varrho(t_0)P^1_{k_1}\dots P^N_{k_N}U^\dagger(t_N-t_0)] = \\ &= \delta_{\mathbf{jk}}\delta_{i_1i_2}\delta_{i_2i_3}\dots\delta_{i_{N-1}i_N}\mathrm{Tr}[P^1_{j_1}\varrho(t_0)P^1_{j_1})]\end{aligned}$$

Again, we can have no interference and we achieve a decoherent set of histories.
For an open system a set of exactly decoherent histories can be automatically constructed in the Markovian limit (i.e., for time intervals $\Delta t > \tau_M$) where the evolution of $S$ is described by a reduced propagator $\tilde{\mathcal{K}}_{t'\,t}$. From Eq. (4.23) we see that the decoherence matrix $\mathcal{D}_{\mathbf{ij}}$ will be diagonal in the first index $j_1$ if the projectors $P^1_{j_1}$ are taken in the eigenbasis of $\varrho(t_1) = \tilde{\mathcal{K}}_{t_1\,t_0}[\varrho(t_0)]$, referred to as *Schmidt basis* in the literature (obviously, $\tilde{\mathcal{K}}$ does not coherently couple the eigenbases of $\varrho(t_0)$ and $\varrho(t_1)$). Next, $\mathcal{D}_{\mathbf{ij}}$ will be diagonal in the second index $j_2$ if projectors $P^2_{j_2}$ are taken in the eigenbasis of the path-projected reduced density matrix

$$\varrho_{j_1}(t_2) = \tilde{\mathcal{K}}_{t_2\,t_1}[P^1_{j_1}\varrho_0 P^1_{j_1}]$$

for each $j_1$. As thoroughly discussed by Zurek [218], in general the eigenbasis of $\varrho_{j_1}(t_2)$ conditionally depend on $j_1$. In fact, non-unitary evolution does not preserve commutators (*environment-induced noncommutativity*). So, the states $\varrho_{j_1}(t_2)$ obtained for different $j_1$ may not commute, even if $P_{j_1}\varrho_0 P_{j_1}$ did. In order to achieve full decoherence, projectors at each $t_\ell$ must be taken in the eigenbasis of the path-projected density matrix

$$\varrho_{j_{\ell-1}\dots j_1}(t_\ell) = \tilde{\mathcal{K}}_{t_\ell\,t_{\ell-1}}[P^{\ell-1}_{j_{\ell-1}}\varrho_{j_{\ell-2}\dots j_1}(t_{\ell-1})P^{\ell-1}_{j_{\ell-1}}] \tag{7.5}$$

Due to environment-induced noncommutativity, in general the eigenbasis of $\varrho_{j_{\ell-1}\dots j_1}(t_\ell)$ conditionally depends on previous projectors at times $t_1\dots t_{\ell-1}$:

$$P^\ell_{j_\ell} = P^j_{j_\ell|j_{\ell-1}\dots_1}$$

This entails that the resulting histories are "unstable". The choice of projectors $P^{\ell}_{j_\ell}$ depends on the choice of previous times $t_1, \dots t_{\ell-1}$. Moreover, if one effects a temporal coarse-graining over time $t_\ell$, projectors at later times are substantially modified. Thus in general we cannot obtain a decoherent set by taking projector in a fixed basis, as was the case for closed systems (where one could take projectors in the energy eigenbasis). This can be done only if the system-environment interaction creates a true pointer basis.

**EIS $\Rightarrow$ history decoherence**

An einselection process, leading to well-defined pointer basis $|a_j\rangle$, guarantees the existence of a preferred set of decoherent histories. If the environment is ignored and we take for all times coarse-grained projections in the pointer basis, $P^{\ell}_{j_\ell} = |a_{j_\ell}\rangle\langle a_{j_\ell}|$, we observe history decoherence as soon as the time interval $\Delta t$ between projections is $\Delta t \geq \tau_D$. In this case, the Schmidt basis becomes stable (i.e. it does not depend on previous results) and coincides with the pointer basis for all $\ell$ for all $\Delta t > \tau_D$.
In particular, if a true pointer observable exists, and we are in the strong coupling regime (so that $H_S$ and $H_{\mathcal{E}}$ can be neglected), it is immediate that histories in the pointer basis decohere however the times $t_\ell$ are chosen.

$$P^{\ell}_{j_\ell}\tilde{\mathcal{K}}_{t_\ell\ t_{\ell-1}}[P^{\ell-1}_{j_{\ell-1}}]P^{\ell}_{j_\ell} = |a_{j_\ell}\rangle\langle a_{j_\ell}|\left(\tilde{\mathcal{K}}_{t_\ell\ t_{\ell-1}}[|a_{j_{\ell-1}}\rangle\langle a_{j_{\ell-1}}|]\right)|a_{j_\ell}\rangle\langle a_{j_\ell}| =$$
$$= |a_{j_\ell}\rangle\langle a_{j_\ell}|\left(|a_{j_{\ell-1}}\rangle\langle a_{j_{\ell-1}}|\right)|a_{j_\ell}\rangle\langle a_{j_\ell}| = 0 \quad \forall j_\ell \neq j_{\ell-1}$$

This case is analogous to the case of the energy eigenbasis for closed systems. In fact, the states $|a_j\rangle$ are stationary states, as the $|E_j\rangle$ in the closed system case.

To sum up, the DH approach yields a necessary, but not sufficient condition for the existence of a stable pointer basis. If $|a_i\rangle$ is a stable pointer basis, then histories with fixed projections in this basis must decohere, at least for sufficiently large $\Delta t$. Conversely, if histories in a given, fixed basis $|a_i\rangle$ decohere, this does not imply that einselection in a stable pointer basis is acting. It only implies that transitions between the basis elements have vanishing interference. This condition that can be realized both by a coherent (unitary) dynamics that does not couple different basis elements, and by a decoherent (non-unitary) dynamics under which the basis elements are stable. For instance, the DH approach cannot distinguish the situation where the system is weakly coupled to the environment - and hence einselection in the system's eigenbasis occurs - from the situation where the system is closed - and hence, no einselection occurs. In both cases, histories in the system energy eigenbasis will decohere.

## 7.3 EIS and DH in a simple model

### The model

In the following, we shall investigate the relation EIS and DH in a simple model: a qubit coupled to a non-Markovian environment. The system $S$ is a qubit coupled to a

second qubit $\mathcal{E}$ that plays the role of the near environment. The two-qubit Hamiltonian is:

$$H = H_S + H_{\mathcal{E}} + H_{int} = (\sin\alpha\sigma_x + \cos\alpha\sigma_z) \otimes \mathbb{I} + \mathbb{I} \otimes \sigma_z + \lambda\sigma_x \otimes \sigma_x \quad (7.6)$$

with $\alpha = \frac{\pi}{6}$ (we have chosen to rotate $H_S$ away from $\sigma_z$ in the x-z plane for reasons that will become apparent later). The near environment $\mathcal{E}$ is further coupled to an external reservoir (far environment) whose effect is to cause decoherence on $\mathcal{E}$. We will analyze two kinds of Markovian decoherence.

- dephasing in the $\sigma_x$ basis of $\mathcal{E}$. The joint $S\mathcal{E}$ evolves under the Lindblad equation :
$$\dot{\varrho}_{S\mathcal{E}} = -i[H, \varrho_{S\mathcal{E}}] + \gamma L[\mathbb{I} \otimes \sigma_x](\varrho_{S\mathcal{E}}) \quad (7.7)$$
where $L[a](\varrho) = 2a\varrho a^\dagger - a^\dagger a\varrho - \varrho a^\dagger a$ and $\gamma$ is the dephasing constant.

- thermal relaxation in the energy eigenbasis of $\mathcal{E}$. The joint $S\mathcal{E}$ system evolves under the Lindblad equation:
$$\dot{\varrho}_{S\mathcal{E}} = -i[H, \varrho_{S\mathcal{E}}] + \frac{\Gamma}{2}(n_T + 1)L[\mathbb{I} \otimes \sigma_-](\varrho_{S\mathcal{E}}) + \frac{\Gamma}{2}n_T L[\mathbb{I} \otimes \sigma_+](\varrho_{S\mathcal{E}}) \quad (7.8)$$
where $\sigma_+ = \frac{1}{2}(\sigma_x + i\sigma_y)$, $\Gamma$ is the thermal relaxation constant, and $n_T$ is the thermal number.

In both cases, the reduced dynamics of $S$ is non-Markovian. A similar model was studied in [217], with the major difference that the role of the far environment was played there by a quantum kicked rotor $R$ with Hamiltonian

$$H_R = \frac{p^2}{2} + v\cos q\ \delta(t/T) \quad (7.9)$$

where $\delta(t/T) = \sum_{j=-\infty}^{\infty} \delta(t - jT)$, coupled to $\mathcal{E}$ through an interaction Hamiltonian

$$H_{R\mathcal{E}} = \kappa\sigma_x \cos q\ \delta(t/T) \quad (7.10)$$

Although this model appears to be much more complicated than ours due to chaotic dynamics induced by the kicked rotor, in the limit $T \to 0$ the sole effect of the coupling with the rotor is to induce a Markovian dephasing on $\mathcal{E}$ [204]. In [217], a relatively short kick period $T = \frac{2\pi}{4096} \sim 1.5 \cdot 10^{-3}$ was used. Therefore, we do not expect strong qualitative differences between our model and that model as for the general features of decoherence on $S$.

**Methods to predict and find pointer bases**

In [217] it was argued that the system $S$ admits approximate pointer bases for intermediate values of the system-near environment coupling $\lambda$, a feature that was explained by the following heuristic argument. Given an orthogonal basis $\mathcal{B} = \{|b_0\rangle, |b_1\rangle\}$ of $S$, the $S\mathcal{E}$ state can be expanded as

$$|\psi(t)\rangle = |b_0\rangle|\phi_0(t)\rangle + |b_1\rangle|\phi_1(t)\rangle \quad (7.11)$$

so that the off-diagonal elements of $\varrho_S(t)$ are $\langle\phi_0(t)|\phi_1(t)\rangle$. Approximate decoherence in the $\mathcal{B}$ basis corresponds to approximate orthogonality of the "expansion states" $|\phi_0(t)\rangle$ and $|\phi_1(t)\rangle$. If we neglect the effect of the far environment, the expansion states $|\phi_\alpha\rangle$ ($\alpha = 0, 1$) evolve according to

$$i\frac{d}{dt}|\phi_\alpha\rangle = H_{\alpha\alpha}|\phi_\alpha\rangle + i|\xi_\alpha\rangle \tag{7.12}$$

where $H_{\alpha\alpha} = \langle b_\alpha|H|b_\alpha\rangle$ and $|\xi_\alpha\rangle = -iH_{\alpha\beta}|\phi\rangle_\beta$ with $\alpha \neq \beta$. The $|\xi_\alpha\rangle$ evolve according to

$$i\frac{d}{dt}|\xi_\alpha\rangle = Z_\alpha|\xi\rangle_\alpha - iJ_\alpha|\phi_\alpha\rangle \tag{7.13}$$

where $Z_\alpha = H_{\alpha\beta}H_{\beta\beta}H^{-1}_{\beta\alpha}$, $J_\alpha = H_{\alpha\beta}H_{\beta\alpha}$. Thus, the expansion states $|\phi_0(t)\rangle$ and $|\phi_1(t)\rangle$ undergo two distinct evolutions. The discrepancy is due to the difference between $H_{00}, |\xi_0\rangle$, and $H_{11}, |\xi_1\rangle$. It can be estimated by considering the operator differences $\Delta H = H_{00} - H_{11}$, $\Delta Z = Z_0 - Z_1$, $\Delta J = J_0 - J_1$. Actually, one can easily verify that $\Delta J = 0$ in the model and it can be further shown that $\Delta Z \simeq -\Delta H$, so that the discrepancy can be assessed by the single quantifier $||\Delta H||$. The crucial hypothesis in [217] is that the basis $\mathcal{B}$ maximizing $||\Delta H||$ should correspond to an approximate pointer basis for the system. In my point of view, this argument must be taken with a grain of salt for at least reasons: i) the argument totally neglects the effect of the far environment ii) a high $\Delta H$ entails that the two expansion states undergo divergent evolutions, but this does not necessarily and immediately imply their quasiorthogonality, $\langle\phi_0(t)|\phi_1(t)\rangle \simeq 0$.

Whether an approximate pointer basis actually exists can be verified with the following procedure, that was also described in [217] (including both the method to find a pointer basis candidate, Eq. (7.16) and the method to verify its stability, Eq. (7.19)). Ideally, if a stable pointer basis exists all initial states should approximately decohere into the same basis after a decoherence time $\tau_D$. The existence of an approximate pointer basis should mirror in the temporal stability of the Schmidt basis, (i.e., the eigenbasis of $\varrho_S(t)$) for all times $t > \tau_D$ as well as in the stability with respect to the choice of initial states. Notice that it is possible that each initial state decoheres into some basis (i.e., shows a *stable Schmidt basis* for all times $t > \tau_D$ ) but this basis differs depending on the initial state. We will talk about the existence of a *pointer basis* only if the stable Schmidt basis is the same for all initial states.

A stable Schmidt basis can be identified through the following procedure. Consider the Schmidt states $|e_k(t)\rangle, k = 0, 1$ with

$$\varrho_S(t)|e_k(t)\rangle = e_k(t)|e_k(t)\rangle \tag{7.14}$$

with $0 \leq e_k(t) \leq 1,\ e_0(t) + e_1(t) = 1$. If a stable Schmidt basis exists, the $|e_k(t)\rangle$ should be approximately time independent after an initial transient $\tau_D$, so that

$$\varrho_S(t) = \sum e_k(t)|e_k(t)\rangle\langle e_k(t)| \simeq \sum_k e_k(t)|e_k\rangle\langle e_k| \qquad t \gg \tau_D \tag{7.15}$$

Upon integrating $\varrho_S(t)$ in time, $\bar{\varrho}_S = \frac{1}{t_a - t_a}\int_{t_a}^{t_b} \varrho_S(t)dt$ (for sufficiently large $t_a, t_b, t_a - t_b \gtrsim \tau_D$) we thus get

$$\bar{\varrho}_S = \frac{1}{t_b - t_a}\sum_k \int_{t_a}^{t_b} e_k(t)|e_k\rangle\langle e_k|dt = \tag{7.16}$$

$$= \frac{1}{t_b - t_a}\sum_k |e_k\rangle\langle e_k| \int_{t_a}^{t_b} e_k(t)dt = \sum_k \bar{e}_k|e_k\rangle\langle e_k|$$

So the stable Schmidt basis can be identified with the eigenbasis of $\bar{\varrho}_S$: $\bar{\varrho}_S|\bar{e}_k\rangle = \bar{e}_k|\bar{e}_k\rangle$. This basis is well-defined only if the eigenvalue difference $\Delta = \bar{e}_1 - \bar{e}_0$ is non-vanishing. If $\Delta \ll 1$ no unique eigenbasis can be well defined. For the Schmidt basis to be stable, the instantaneous eigenbasis of $\varrho_S(t)$ must be close to the basis identified by the $|\bar{e}_k\rangle$, and we must have

$$|e_k(t)\rangle \simeq |\bar{e}_k\rangle, \forall t \gg \tau_D \tag{7.17}$$

The "distance" between the two bases can be evaluated as

$$D(t) = 1 - |\langle e_k(t)|\bar{e}_k\rangle|^2 \tag{7.18}$$

(we can choose both $k = 0$ or $k = 1$). Hence, the average quantity

$$\delta_s = \frac{1}{t_a - t_a}\int_{t_a}^{t_b} D(t)dt \tag{7.19}$$

is a measure of the stability of the Schmidt basis. If all initial states decohere into the same (approximately) stable Schmidt basis, then the latter is an (approximate) pointer basis. In [217], a specific initial state was considered ant it was shown that a stable Schimidt basis exists for $\lambda \ll 1$ and $\lambda \gg 1$ and it coincides respectively with the $H_S$ eigenbasis and with the eigenbasis of $H_{int}$ (henceforth we will follow a commonplace abuse of notation and call "eigenbasis of $H_{int}$" the eigenbasis of $\mathrm{Tr}_{\mathcal{E}}[H_{int}]$), as expected from previous studies. In case of intermediate coupling, a stable Schmidt basis was found to lay in between these two extremes, interpolating in a continous fashion between the two. The interpolation was shown upon evaluating the angles $\theta_1(\lambda), \theta_2(\lambda)$ needed to rotate the stable Schmidt basis for a given value of $\lambda$ into the eigenbasis of $H_S$ and that of $H_{int}$.

**Environment-induced superselection**

We now follow the procedures described in [217] and sketched in the previous paragraph. We first give a prediction about the pointer bases, following the heuristic argument based on $||\Delta H||$. Next, we check whether pointer bases actually emerge in a wide range of values of $\lambda$.
Any basis can be parametrized by an angle $-\frac{\pi}{2} \leq \theta \leq \frac{\pi}{2}$ and a phase $-\frac{\pi}{2} \leq \chi \leq \frac{\pi}{2}$,

$$|b_0\rangle = \cos\theta|0\rangle + e^{i\chi}\sin\theta|1\rangle, \qquad |b_1\rangle = -\sin\theta|0\rangle + e^{i\chi}\cos\theta|1\rangle \tag{7.20}$$

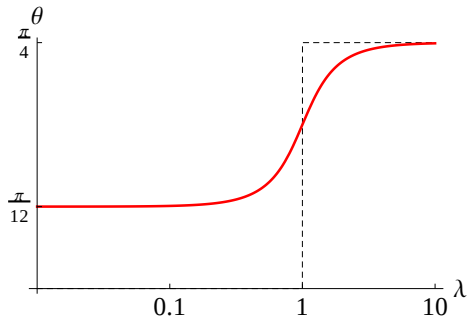


Figure 7.1: Expected pointer basis as a function of $\lambda$ for $\alpha = \frac{\pi}{6}$ (red) and $\alpha = 0$ (black, dashed)

where $|0\rangle$ and $|1\rangle$ represent the $\sigma_z$ eigenstates. We can evaluate $||\Delta H||$ as a function of $\theta, \chi$:

$$\frac{||\Delta H||^2}{8} = (\cos\alpha\cos\theta + \sin\alpha\sin\theta\cos\chi)^2 + \lambda^2\sin^2\theta\cos^2\chi \tag{7.21}$$

$||\Delta H||$ is maximised by $\chi = 0$ and:

$$\theta = \theta_{min} = \frac{1}{4}\arctan\left(\frac{\sin 2\alpha}{\cos 2\alpha - \lambda^2}\right) \quad \text{for} \quad \lambda < \sqrt{\cos 2\alpha} \tag{7.22}$$
$$\theta = \theta_{min} = \frac{\pi}{4} - \frac{1}{4}\arctan\left(\frac{\sin 2\alpha}{\lambda^2 - \cos 2\alpha}\right) \quad \text{for} \quad \lambda > \sqrt{\cos 2\alpha}$$

Thus the basis maximizing $||\Delta H||$ lies in the x-z plane. For $\lambda \to 0$ we get $\theta = \alpha/2$, that corresponds to the eigenbasis of $H_S$. For $\lambda \to \infty$ we get $\theta = \pi/4$, that corresponds to the eigenbasis of $H_{int}$. For intermediate values of $\lambda$, we get a basis interpolating between the two. In Fig. 7.1 we plot $\theta_{min}$ as a function of $\lambda$. It can be seen that if $\alpha = 0$ the change between $\theta = \frac{\alpha}{2}$ and $\theta = \frac{\pi}{4}$ is expected to be abrupt, so that no smooth interpolation is actually expected. This motivates us to choose $\alpha > 0$ in order to look for possible interpolating pointer bases. For $\alpha = \frac{\pi}{6}$ we expect to find $\theta = \frac{\pi}{12} = 0.26$ for $\lambda \ll 1$, corresponding to the eigenbasis of $H_S$, and $\theta = \frac{\pi}{4} = 0.78$ for $\lambda \gg 1$, corresponding to the eigenbasis of $H_{int}$ and smooth interpolation for intermediate values of $\lambda$.

Next, we numerically calculate the eigenbasis of $\bar{\varrho}_S$ for different initial states. We consider an ensemble of $M = 100$ pure $S\mathcal{E}$ states, generated randomly according to the uniform measure on $\mathcal{H}_{S\mathcal{E}} \simeq \mathbb{C}^4$. We first let the ensemble evolve under the dephasing noise. The dephasing constant is $\gamma = 10^{-3}$. We find that all initial states approximately decohere in some basis before $\tau_D \ll \tau_\gamma = 1/\gamma$. In conformity with expectation, we find such stable Schmidt bases to lie in the x-z plane (we always find $\mathrm{Im}(\langle 0|\bar{\varrho}_S|1\rangle) < 10^{-3}$). Therefore, we can characterize any basis with the single parameter $\theta$.

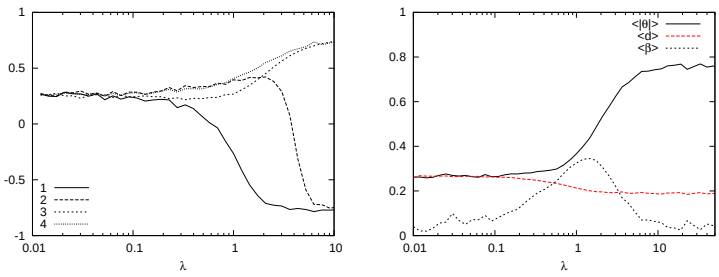


(a) (b)

Figure 7.2: Schmidt bases for state evolving under dephasing noise with $\gamma = 0.001$ (a) Schmidt basis angle $\theta$ as a function of $\lambda$ for some random initial states (b) average distance from the $\sigma_z$ basis $\langle|\theta|\rangle$, average inter-basis angle $\langle\beta\rangle$ and average stability parameter $\langle\delta_s\rangle$ as a function of $\lambda$; the average is over $M = 100$ random initial states.

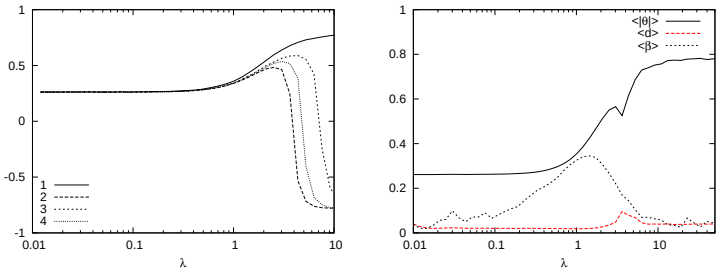


(a) (b)

Figure 7.3: Schmidt bases for state evolving under thermal noise with $\Gamma = 0.001$ and $n_T = 0.5$ (a) Schmidt basis angle $\theta$ as a function of $\lambda$ for some random initial states (b) average distance from the $\sigma_z$ basis $\langle|\theta|\rangle$, average inter-basis angle $\langle\beta\rangle$ and average stability parameter $\langle\delta_s\rangle$ as a function of $\lambda$; the average is over $M = 100$ random initial states.

For $\lambda \ll 1$ all initial states yield $\theta \sim \frac{\pi}{12}$ as expected. For $\lambda \gg 1$, we have $\theta \to \pm\frac{\pi}{4}$ (notice that the values $\pm\frac{\pi}{4}$ correspond to the same basis), again in conformity with expectation. For intermediate values, we would expect to observe a smooth transition with values of $\theta$ in the range $\frac{\pi}{12} \leq \theta \leq \frac{\pi}{4}$. However, contrary to this expectation, we find two kinds of interpolating behavior: i) $\theta$ increases from $\frac{\pi}{12}$ to $\frac{\pi}{4}$ ii) $\theta$ decreases from $\frac{\pi}{12}$ to $-\frac{\pi}{4}$ passing through negative values. This is shown in Fig.7.2(a) where $\theta$ is plotted for four different initial states. In Fig. 7.2(b), we plot $\langle|\theta|\rangle$ (that simply measures the average distance of the dephasing basis from the $\sigma_z$ basis) as a function of $\lambda$, and observe a steady increase from $\langle|\theta|\rangle \sim \frac{\pi}{12}$ to $\langle|\theta|\rangle \sim \frac{\pi}{4}$. The behavior of $\langle|\theta|\rangle$ obscures the fact that the values $\pm\frac{\pi}{4}$ are reached through different pathways. To further highlight this feature, we also consider all pairs of initial states and evaluate the angle $\beta$ between their respective stable Schmidt bases. The average value $\langle\beta\rangle$ is plotted as a function of $\lambda$ for all initial states. We notice that a pointer basis emerges only in the

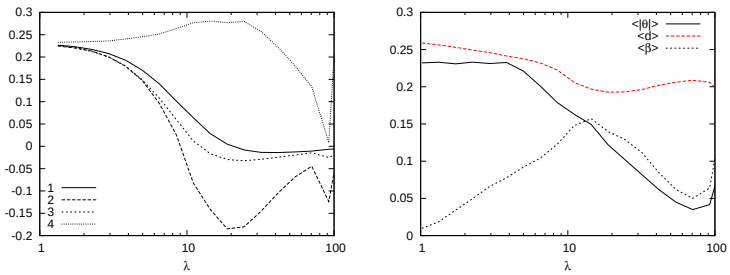


(a) (b)

Figure 7.4: Schmidt bases for state evolving under coupling with a kicked rotor with with $v = 90/T$, $k = 0.1$, $T = \frac{2\pi}{N}$ and $N = 64$. (a) Schmidt basis angle $\theta$ as a function of $\lambda$ for some random initial states (b) average distance from the $\sigma_z$ basis $\langle|\theta|\rangle$, average inter-basis angle $\langle\beta\rangle$ and average stability parameter $\langle\delta_s\rangle$ as a function of $\lambda$; the average is over $M = 100$ random initial states.

opposite limits $\lambda \to 0$ and $\lambda \to \infty$, where $\langle\beta\rangle$ is small. For intermediate values of $\lambda$, $\langle\beta\rangle$ reaches values up to $0.4$ and we cannot really identify a fixed pointer basis. Along with $\langle|\theta|\rangle$ and $\langle\beta\rangle$, in Fig.7.2(b) we also plot the corresponding average values of the stability parameter $\langle\delta_s\rangle$ introduced in Eq. (7.19) to characterize the stability of the Schmidt bases. We observe that the bases found are approximately stable, $\langle\delta_s\rangle \sim 0.2$ in the whole range of $\lambda$. In Fig.7.3, we report the same figures for the thermal noise with $\Gamma = 0.01$ and $n_T = 0.01$. The main qualitative features are unchanged. The main peculiarity of the thermal noise, compared to the dephasing noise, is that it leads to a much stronger stability of the Schmidt bases, i.e., much lower values of $\langle\delta_s\rangle$.

The main message of these plots is that true pointer bases arise only in the limits of small and strong coupling, but not for intermediate coupling. These results seem to be at odds with the main claim made in [217], that a stable pointer basis arises for intermediate values of $\lambda$. We therefore investigate in detail whether there is a significant discrepancy between our model and the kicked-rotor model. We turn to the kicked rotor model studied in [217]. The Hamiltonian is:

$$H = H_S + H_{\mathcal{E}} + H_{int} = (\omega_x\sigma_x + \omega_z\sigma_z) \otimes \mathbb{I} + \mathbb{I} \otimes \omega_A\sigma_x + \lambda\sigma_z \otimes \sigma_z \qquad (7.23)$$

with $\omega_x = 500$, $\omega_z = 1000$, $\omega_A = 500$. The eigenbasis of the system Hamiltonian corresponds to $\theta = 0.23$. The far environment is a kicked rotor represented by a self-Hamiltonian $H_R$ and coupling Hamiltonian $H_{R\mathcal{E}}$:

$$H_R = \frac{p^2}{2} + v\cos q\ \delta(t/T), \quad H_{R\mathcal{E}} = \kappa\sigma_z \cos q\ \delta(t/T) \qquad (7.24)$$

with $v = 90/T$ and $\kappa = 0.1$. The kicking period is $T = \frac{2\pi}{N}$ and $N = 64$. We simulate the model for $M = 100$ random initial states. In Fig. 5a we plot $\theta$ as a function of $\lambda$ for some initial states. We see that for small $\lambda$ there is a pointer basis corresponding to the system's energy eigenbasis, while for large $\lambda$ there is one corresponding to the eigenbasis of $H_{int}$. However, also in this case for intermediate values of $\lambda$ there is no

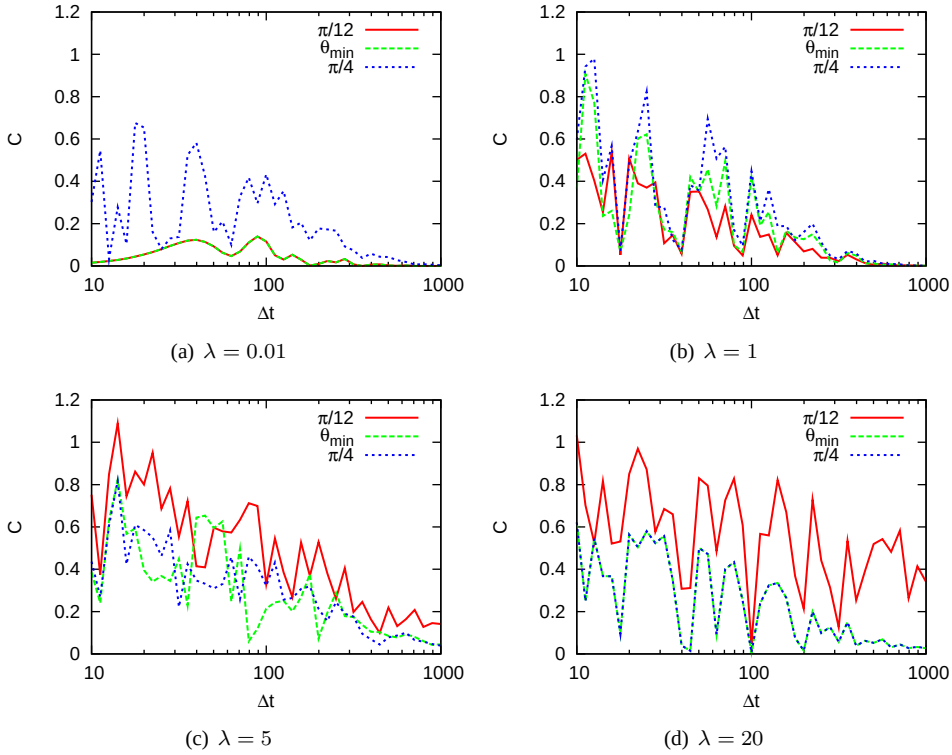


(a) $\lambda = 0.01$ (b) $\lambda = 1$

(c) $\lambda = 5$ (d) $\lambda = 20$

Figure 7.5: Relative entropy of decoherence $\mathcal{C}_4$ for dephasing noise with $\gamma = 0.001$ as a function of the time interval $\Delta t$ between projections for different values of the coupling strength $\lambda$. In all panels, we show $\mathcal{C}_4$ for three different bases in the x-z plane identified by different values of $\theta$: $\theta = \pi/12$ (eigenbasis of $H_S$), $\theta = \pi/4$ (eigenbasis of $H_{int}$), $\theta = \theta_{min}$ (Eq. (7.22))

universal Schmidt basis. This can be seen again by plotting $\beta$ as a function of $\lambda$ (Fig. 5b). Notice that in ref. [217] the behavior of $\theta$ for only one initial state is plotted. This is sufficient to verify the existence of a stable Schmidt basis, but not to infer the existence of a true pointer basis that must coincide for all initial states.

**Decoherent histories**

We now consider decoherent histories of the system. As stated in § 7.2.3, the existence of a pointer basis should reflect into the decoherence of histories with fixed projectors in the pointer basis and $\Delta t \gtrsim \tau_D$. Accordingly, we consider histories with projectors in a fixed basis for all times. We take the time interval $\Delta t_i = t_i - t_{i-1}$ between projections to be the same for all projections, $\Delta t_i = \Delta t$, and consider $N = 4$ projections. We focus on projections in the x-z plane, $P_0 = |\psi_0\rangle\langle\psi_0|,\ P_1 = |\psi_1\rangle\langle\psi_1|$ with

$$|\psi_0\rangle = \cos\theta|0\rangle + \sin\theta(|1\rangle,\ |\psi_1\rangle = -\sin\theta|0\rangle + \cos\theta(|1\rangle \tag{7.25}$$

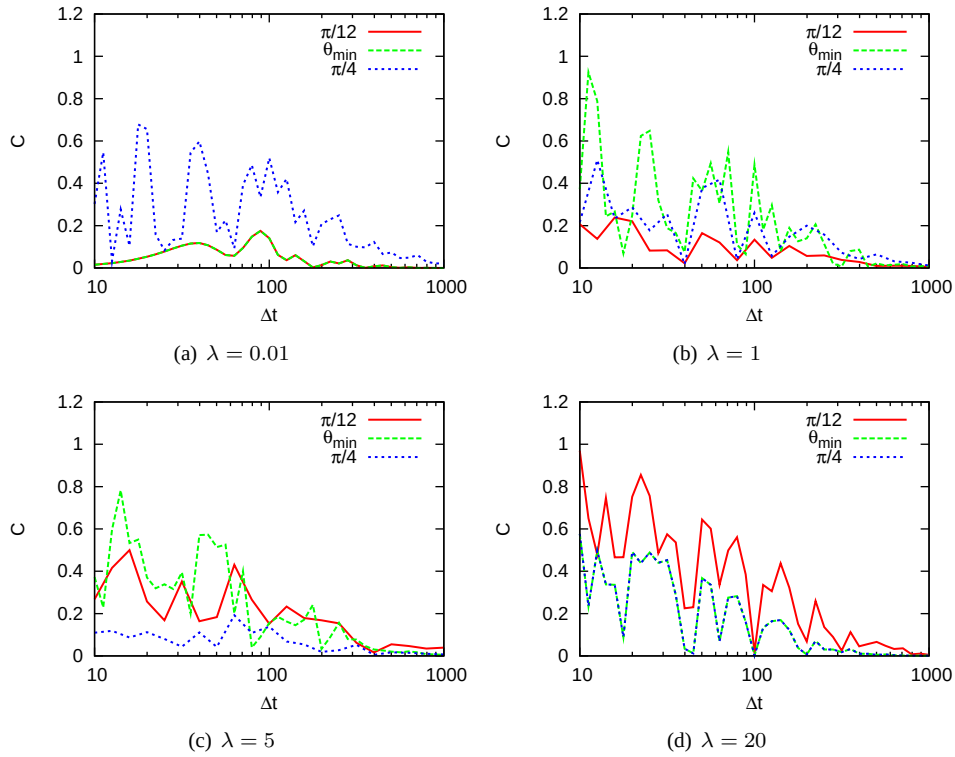


(a) $\lambda = 0.01$ (b) $\lambda = 1$

(c) $\lambda = 5$ (d) $\lambda = 20$

Figure 7.6: Relative entropy of decoherence $\mathcal{C}_4$ for thermal noise with $\Gamma = 0.001$ and $n_T = 0.5$ as a function of the time interval $\Delta t$ between projections for different values of the coupling strength $\lambda$. In all panels, we show $\mathcal{C}_4$ for three different bases in the x-z plane identified by different values of $\theta$: $\theta = \pi/12$ (eigenbasis of $H_S$), $\theta = \pi/4$ (eigenbasis of $H_{int}$), $\theta = \theta_{min}$ (Eq. (7.22))

since we expect to find a pointer basis in the x-z plane. For any choice of basis, we can assess the degree of history coherence by means of the relative entropy of decoherence $\mathcal{C}_N \equiv h_N^{(c)} - h_N = S(\mathcal{D}^{(N)}||\tilde{\mathcal{D}}^{(N)})$ defined in § 5.3.3. $\mathcal{C}_N$ measures how far $\mathcal{D}$ is from its diagonal part, and hence measures the amount of coherence between histories.
We first consider dephasing noise with $\Gamma = 0.001$. In Fig.7.5, we plot $\mathcal{C}_4$ as a function of $\Delta t$ for different values of $\lambda$ and different bases in the x-z plane, corresponding to $\theta = \pi/12$ (eigenbasis of $H_S$), $\theta = \pi/4$ (eigenbasis of $H_{int}$), $\theta = \theta_{min}$ (the basis that should yield a pointer basis according to (Eq. (7.22)). The initial state is $|\psi_0\rangle = |0\rangle$ (we sampled data for several initial states, not shown since the results do not exhibit significant differences). For $\lambda = 0.01$, histories in the eigenbasis of $H_S(\theta = \frac{\pi}{12} \simeq \theta_{min})$ are clearly more decoherent than histories in the eigenbasis of $H_{int}$. In particular, for $\Delta t \gtrsim 200$ they approximately decohere. In the opposite limit of strong coupling, $\lambda = 20$ we observe the converse: histories in the eigenbasis of $H_{int}$ ($\theta = \frac{\pi}{4} \simeq \theta_{min}$) are clearly more decoherent than histories in the eigenbasis of $H_S$. Again, for $\Delta t \gtrsim$

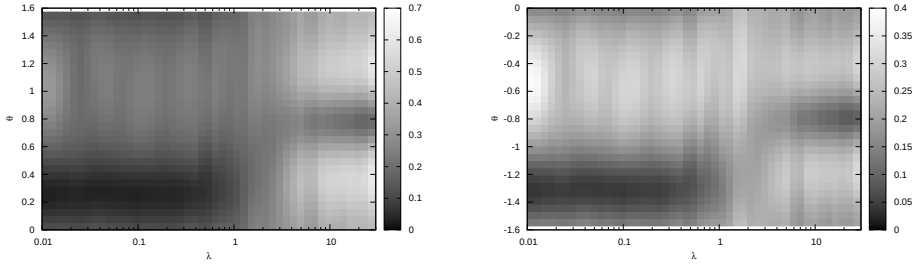


(a) (b)

Figure 7.7: Time-averaged relative entropy of decoherence, $\langle \mathcal{C}_4 \rangle_{\Delta t}$ as a function of the coupling strength $\lambda$ and the basis angle $\theta$ for (a) dephasing noise with $\Gamma = 0.001$ (b) thermal noise with $\Gamma = 0.001$ and $n_T = 0.5$. Darker values indicate that coherence in the basis is lower. Dark "stripes" that appear in the opposite limits of strong and weak coupling clearly identify the emergence of pointer bases

$200$ they approximately decohere. For intermediate values of $\lambda$, though, the degree of coherence between histories, as assessed by $\mathcal{C}_4$, tends to be comparable for all bases. This feature corroborates our view that no true pointer bases exist in the intermediate coupling regime. In Fig.7.6, we plot the equivalent figures for the case of thermal noise. Qualitatively, the behavior matches that of dephasing noise. The main difference can be observed in the strong coupling regime. The disparity between histories in the eigenbasis of $H_S$ and histories in the eigenbasis of $H_{int}$ is less pronounced: for $\Delta t \gtrsim 200$ both sets show low values of coherence. This feature is probably due to the higher decohering effect of the thermal noise with respect to dephasing noise. As we noted above, this effect is responsible for the higher stability of the pointer basis in the case of thermal noise and strong coupling.

The discrepancy in the amount of coherence for histories in different bases can be further synthetically illustrated, as follows. For any value of $\theta$ (i.e., for all bases in the x-z plane) we average $\mathcal{C}_4$ over $\Delta t$ over the period where decoherence is acting, for $\frac{1}{10\Gamma} \leq \Delta t \leq \frac{1}{\Gamma}$ . The result is shown in Fig.7.7. We plot $\langle \mathcal{C}_4 \rangle_{\Delta t}$ as a function of $\lambda$ and $\theta$ for both dephasing and thermal noise with different values of $\Gamma = 0.001$. The two pointer bases are clearly recognizable in the limit of small $\lambda$ and large $\lambda$: they correspond to much lower values of $\langle \mathcal{C}_4 \rangle_{\Delta t}$, compared to the other bases. In the intermediate $\lambda$ regime, it is not possible to single out a clear pointer basis. As we discussed in § 7.2.3, the existence of a pointer basis would imply that histories in the same basis decohere. Indeed, the absence of a clear pointer basis in the regime of intermediate $\lambda$ reflects into all bases having comparable values of $\langle \mathcal{C}_4 \rangle_{\Delta t}$.

## 7.4 Conclusions

While the action of decoherence in the macroscopic limit is well understood, decoherence for microscopic systems with a few degrees of freedom is still a open field of research. A recent work [217] has analyzed decoherence in a simple model, arguing that pointer bases arise for all values of the system-environment coupling.
In this chapter, we have addressed the emergence of pointer bases in a simple model by comparing the standard einselection picture (based on the vanishing of coherence in the density matrix) with the decoherent histories picture based on vanishing interference between histories in a set. On the basis of general considerations, we expect to observe decoherence between histories defined by fixed projections in the pointer basis, if the latter exists and it is stable.
The model we analyze is a qubit coupled to a non-Markovian environment composed by a second qubit (near environment) coupled to a Markovian bath. All together, near and far environment make up a non-Markovian environment. The model is essentially the same as in ref. [217], except that the far environment is a Markovian reservoir instead of a chaotic system (according to Ref. [204]), results should be qualitatively the same.
We have analyzed the emergence of pointer bases for different values of the system-environment coupling, according to the method developed in [217]. In the opposite limits of strong and weak system-environment coupling, we observe stable pointer bases in the system energy eigenbasis and in the interaction Hamiltonian eigenbasis, confirming standard results in the literature [209, 214]. For intermediate values of the coupling, we observe that any initial state decoheres, becoming approximately diagonal in a *stable Schmidt basis*. This basis, however, is state-dependent, while a true pointer basis should coincide for all initial states. Thus, contrary to the opposite claim in [217], our data suggest that no true pointer basis arises for intermediate coupling.
The analysis of decoherent histories in the model corroborates this conclusion. Under general arguments, when a stable pointer basis exists we expect to observe decoherence between histories with projections in the pointer basis. We have analyzed decoherent sets of histories with projections in different bases and for different values of the coupling. For any set, we are able to assess the degree of coherence between histories by means of a single quantifier, the relative entropy of decoherence $\mathcal{C}_N$ introduced in Chap. 5. For strong and weak coupling, $\mathcal{C}_N$ can clearly identify pointer bases, that yield sets of histories that are much less coherent compared to other bases. For intermediate values of the coupling, all sets of histories show a comparable degree of coherence, further indicating the absence of a true pointer basis.

# Chapter 8

# Conclusions and outlook

As we wrote in the introduction, classical records of quantum phenomena can be acquired only at the price of discarding some "coherent" information. Decoherence processes, like those exerted by measurements or interaction with a noisy environment, have two specular consequences: They destroy the excess quantum coherence and stabilize classical information. Throughout this thesis, we have looked at several decoherence processes from an informational viewpoint, using different information-theoretic quantifiers to analyze the effects of decoherence in physically relevant scenarios.
On one side, decoherence processes allow for the definition of suitable measures of "quantumness" in terms of the amount of information that is lost under their action. On the other side, decoherence processes allow to "extract" classical information from quantum systems.
On the first side (measures of quantumness), we have been concerned with a decoherence - related measure of quantumness for correlations between two parties. Local measurements allow to define *quantum discord* (chapter 1), that singles out "coherent" correlations that are unavoidably lost when a subsystem is measured. This measure of quantum correlations is different from the traditional notion of entanglement and may capture quantum effects to which the latter is insensitive, but which can be relevant for the behavior of physical systems. In chapter 2 we have analyzed at length quantum discord in a condensed matter model, the extended Hubbard model, and we have shown a connection between this measure of bipartite correlations and an important physical property of the model (off-diagonal long-range order, ODLRO) that also marks phenomena like superfluidity and superconductivity. Moreover, the splitting of correlations into a quantum and a classical part offered by discord allowed us to discriminate between phase transitions that are physically different. Another measure of quantumness is the *relative entropy of decoherence*, defined in chapter 5. The relative entropy of decoherence can assess coherence in the time evolution of a system, as seen from the interference between different paths or *histories* of the system (chapter 4). Its definition is based on a comparison between the coherent evolution of the system, as represented by the decoherence matrix, and and a fully "decoherent" one represented by a decoherence matrix without interference terms. In chapter 7, we have used the relative entropy of decoherence to characterize einselection, i.e., the emergence of pre-

ferred pointer bases in Hilbert space as a result of interaction with the environment. The consequence of einselection is that coherence in the pointer basis fades and the system becomes "classical" in that basis. By comparing the standard picture based on the density matrix with a decoherent histories picture based on the decoherence matrix, we have analyzed the behavior of an open system subjected to non-Markovian noise and investigated the emergence of pointer bases for different values of the system-environment coupling strength. In the opposite limits of strong and weak coupling clear pointer bases emerge, which is signaled by vanishing off-diagonal elements of a time-averaged density matrix in the pointer basis, and correspondingly by a vanishing relative entropy of decoherence for histories in the same basis. Contrary to previous statements in the literature, we showed that in the intermediate coupling regime no stable pointer basis arises, which is apparent from high values of the relative entropy of decoherence.

On the other side (extraction of classical information), we have seen how decoherence allows to define *classical correlations*, i.e., the part of correlations that are stable under the action of local measurements and are then locally accessible. A key issue is finding the optimal local measurement that allows to maximize the classical correlations. The whole of chapter 3 was essentially devoted to solving this problem in the physically important case of two optical modes in Gaussian states. In particular, we compared Gaussian measurements (such homodyne detection) with non-Gaussian ones (such as photon counting) in order to see whether non-Gaussian measurements can allow for a better extraction of information. We found robust evidence that Gaussian measurements are in fact optimal. Another question related to classical information arising from quantum systems is the *dynamical production of classical information* by quantum dynamics. Decoherent histories provide a natural framework to define a quantum version of dynamical entropy, that measures the maximal rate at which information is produced by the dynamics in time. When histories decohere, the system effectively produces classical information at a maximal rate given by the dynamical entropy. In chapter 6, we have applied quantum dynamical entropy to study how the interplay of coarse-graining, history decoherence and the presence of different sources of unpredictability leads to classical information production by quantum systems. While in classical systems all unpredictability stems from dynamical chaos, in the quantum domain a major source of unpredictability (the probabilistic nature of measurements) appears. Consequently, both chaotic and integrable systems exhibit entropy production. By focusing on decoherence and coarse-graining, we have argued that randomness provided by either the dynamics or measurements can lead to the decoherence of sufficiently coarse-grained histories, as well as maximal entropy production compatible with coarse-graining size. This picture was suggested by a general, heuristic argument and could be rigorously proven in the case of dynamical randomness by means of random matrix techniques. We presented a numerical analysis of decoherent histories in the quantum standard map that agrees with our theoretical predictions.

The results presented in this thesis confirm the importance of decoherence for an understanding of quantum physics at large. Furthermore, they show the power of the information-theoretical approach to the study of physical systems – a power that is now recognized is several fields, from quantum physics to statistical mechanics and complex systems science.

# Bibliography

## Quantum entantlement


[1] R. Horodecki, P. Horodecki, M. Horodecki, and K. Horodecki, *Quantum entanglement*, Rev. Mod. Phys. **81**, 865 (2009).

[2] A. Einstein, B. Podolsky, N. Rosen, *Can quantum-mechanical description of physical reality be considered complete?*, Phys. Rev. **47 (10)**, 777 (1935).

[3] E. Schrödinger, *Die gegenwärtige Situation in der Quantenmechanik*, Naturwissenschaften **23**, 807 (1935); *Discussion of probability relations between separated systems*, Mathematical Proceedings of the Cambridge Philosophical Society **31 (4)** , 555 (1935); *Probability relations between separated systems*, Mathematical Proceedings of the Cambridge Philosophical Society **32 (3)**, 446 (1935).

[4] P. Zanardi, *Virtual quantum subsystems*, Phys. Rev. Lett. **87**, 077901 (2001).

[5] P. Zanardi, D. Lidar and S. Lloyd, *Quantum tensor product structures are observable-induced*, Phys. Rev. Lett. **92**, 060402 (2004).

[6] J. S. Bell, *On the Einstein Podolsky Rosen Paradox*, Physics **1**, 3, 195 (1964); *On the problem of hidden variables in quantum mechanics*, Rev. Mod. Phys. **38**, 447 (1966).

[7] N. Gisin, *Bell's inequality holds for all non-product states*, Phys. Lett. A **154**, 201 (1991).

[8] S. Yu, Q. Chen, C. Zhang, C. H. Lai, and C.H. Oh, *All entangled pure states violate a single Bell's inequality*, Phys. Rev. Lett. **109**, 120402 (2012).

[9] P. Hayden, D. W. Leung, A. Winter, *Aspects of generic entanglement*, Comm. Math. Phys. **265**, 1, 95 (2006).

[10] R. Werner, *Quantum states with Einstein-Podolsky-Rosen correlations admitting a hidden-variable model*, Phys. Rev A **40**, 4277 (1989).

[11] C.H. Bennett, H. Bernstein, S. Popescu, and B. Schumacher, *Concentrating partial entanglement by local operations*, Phys. Rev. A, **53**, 2046 (1996).

[12] E. Chitambar, D. Leung, L. Mancinska, M. Ozols, A. Winter, *Everything you always wanted to know about LOCC (but were afraid to ask)*, arXiv:1210.4583 (2012).

[13] V. Gheorghiu, R.B. Griffiths, *Separable operations on pure states*, Phys. Rev. A **78**, 020304 (2008).

[14] E. Chitambar, W. Cui, and H.-K. Lo, *Increasing entanglement monotones by separable operations*, Phys. Rev. Lett. **108**, 240504 (2012); E. Chitambar, W.Cui, and H.-K. Lo, *Entanglement monotones for W-type states*, Phys. Rev. A **85**, 062316 (2012); E. Chitambar, R. Duan, *Nonlocal entanglement transformations achievable by separable operations*, Phys. Rev. Lett. **103**, 110502 (2009).

[15] L. Gurvits, *Classical deterministic complexity of Edmonds' problem and quantum entanglement*, in Proc. of the 35th ACM symp. on theory of comp., 10-19, New York, ACM Press (2003); S. Gharibian, *Strong NP-hardness of the quantum separability problem*, Quant. Inf. Comp. **10**, 3 & 4, 343 (2010).

[16] G. Vidal, *Entanglement monotones*, J. Mod. Opt. **47**, 355 (2000).

[17] C. H. Bennett, D.P. DiVincenzo, J.A. Smolin, and W. K. Wootters, *Mixed-state entanglement and quantum error correction*, Phys. Rev. A **54**, 3824 (1996).

[18] V. Vedral and M. B. Plenio, *Entanglement measures and purification procedures*, Phys. Rev. A **57**, 1619 (1998); V. Vedral, *The role of relative entropy in quantum information theory*, Rev. Mod. Phys. **74**, 197 (2002).

[19] G. Vidal, R.F. Werner, *A computable measure of entanglement*, Phys. Rev. A **65**, 032314 (2002).

[20] S. Hill, W.K. Wootters, *Entanglement of a Pair of Quantum Bits*, Phys.Rev.Lett. **78**, 5022 (1997); W.K. Wootters, *Entanglement of formation of an arbitrary state of two qubits*, Phys. Rev. Lett. **80**, 2245 (1998).

[21] M. Christandl, A. Winter, *Squashed entanglement - an additive entanglement measure*, J. Math. Phys. **45** (3), 829 (2003); F.G.S.L. Brandão, M. Christandl, J. Yard, *Faithful squashed entanglement*, Commun. Math. Phys. **306**, 805 (2011).

[22] V. Coffman, J. Kundu and W. K. Wootters, *Distributed entanglement*, Phys. Rev. A **61**, 052306 (2000).

[23] T. J. Osborne and F. Verstraete, *General monogamy inequality for bipartite qubit entanglement*, Phys. Rev. Lett. **96**, 220503 (2006).

[24] G. Giedke, M. M. Wolf, O. Krüger, R. F. Werner, and J. I. Cirac, *Entanglement of formation for symmetric Gaussian states*, Phys. Rev. Lett. **91**, 107901 (2003); J. Solomon Ivan, R. Simon, arXiv:0808.1658; P. Marian, T. A. Marian, *Entanglement of formation for an arbitrary two-mode Gaussian state*, Phys. Rev. Lett. **101**, 220403 (2008).

## Quantum discord - general

[25] K. Modi, A. Brodutch, H. Cable, T. Paterek, V. Vedral, *The classical-quantum boundary for correlations: discord and related measures*, Rev. Mod. Phys. **84**(4), 1655 (2012).

[26] H. Ollivier and W. H. Zurek, *Quantum discord: a measure of the quantumness of correlations*, Phys. Rev. Lett **88**, 017901 (2001).

[27] L. Henderson and V. Vedral, *Classical, quantum and total correlations*, J. Phys. A **34**, 6899 (2001).

[28] B. Groisman, S. Popescu, A. Winter, *Quantum, classical, and total amount of correlations in a quantum state*, Phys Rev. A **72**, 032317 (2005).

[29] K. Modi, T. Paterek, W. Son, V. Vedral, M. Williamson, *Unified view of quantum and classical correlations*, Phys. Rev. Lett. **104** (8), 80501 (2010).

[30] S. Luo and S. Fu, *Geometric measure of quantum discord*, Phys. Rev. A **82**, 034302 (2010).

[31] M. Piani, *Problem with geometric discord*, Phys. Rev. A **86**, 034101 (2012).

[32] R. Prabhu, A.K. Pati, A.S. De, U. Sen, *Conditions for monogamy of quantum correlations: Greenberger-Horne-Zeilinger versus W states*, Phys. Rev. A **85** (4), 040102 (2011).

[33] G.L. Giorgi, *Monogamy properties of quantum and classical correlations*, Phys. Rev. A **84**, 054301 (2011).

[34] A. Streltsov, G. Adesso, M. Piani, D. Bruss, *Are general quantum correlations monogamous?*, Phys. Rev. Lett. **109** (5), 050503 (2012).

[35] A. Ferraro, L. Aolita, D. Cavalcanti, F.M. Cucchietti, A. Acín, *Almost all quantum states have nonclassical correlations*, Phys. Rev. A **81** (5), 052318 (2010).

[36] C. C. Rulli, M. S. Sarandy, *Global quantum discord in multipartite systems*, Phys. Rev. A **84**, 042109 (2011).

[37] G.L. Giorgi, B. Bellomo, F. Galve, and R. Zambrini, *Genuine quantum and classical correlations in multipartite systems*, Phys. Rev. Lett. **107**, 190501 (2011).

[38] J. Maziero, L. C. Céleri, R. M. Serra, *Symmetry aspects of quantum discord*, arXiv:1004.2082 (2010).

[39] M. Koashi, A. Winter, *Monogamy of quantum entanglement and other correlations*, Phys. Rev. A **69** (2), 022309 2005.

[40] A. Streltsov, H. Kampermann, and D. Bruß, *Linking quantum discord to entanglement in a measurement*, Phys. Rev. Lett. **106**, 160401 (2011).

[41] M. Piani, S. Gharibian, G. Adesso, J. Calsamiglia, P. Horodecki, A. Winter, *All nonclassical correlations can be activated into distillable entanglement*, Phys. Rev. Lett. **106** (22), 220403 (2011).

[42] M. Piani, and G. Adesso, *Quantumness of correlations revealed in local measurements exceeds entanglement* Phys. Rev. A **85**, 040301(R) (2012); T. Nakano, M. Piani, and G. Adesso, *Negativity of quantumness and its interpretations*, Phys. Rev. A **88**, 012117 (2013).

[43] M. Piani, P. Horodecki, and R. Horodecki, *No-local-broadcasting theorem for multipartite quantum correlations*, Phys. Rev. Lett. **100**, 090502 (2008).

[44] A. Streltsov, W.H. Zurek, *Quantum discord cannot be shared*, Phys. Rev. Lett. **111**, 040401 (2013).

[45] M. Gessner, E.-M. Laine, H.-P. Breuer, J. Piilo, Phys. Rev. A, *Correlations in quantum states and the local creation of quantum discord*, **85**, 052122 (2012).

[46] X. Hu, H. Fan, D.L. Zhou, and W.-M. Liu, *Quantum correlating power of local quantum channels*, Phys. Rev. A **87**, 032340 (2013).

[47] A. Datta, *A condition for the nullity of quantum discord*, arXiv:1003.5256v2 (2010).

[48] D. Cavalcanti, L. Aolita, S. Boixo, K. Modi, M. Piani, A. Winter, *Operational interpretations of quantum discord*, Phys. Rev. A **83** (3), 032324 (2011).

[49] B. Dakić, V. Vedral, Č. Brukner, *Necessary and sufficient condition for nonzero quantum discord*, Phys. Rev. Lett. **105** (19), 190502 (2010).

[50] V. Madhok, A. Datta, *Interpreting quantum discord through quantum state merging*, Phys. Rev. A **83**, 032323 (2011).

[51] A. Al-Qasimi and D. F. V. James, *Comparison of the attempts of quantum discord and quantum entanglement to capture quantum correlations*, Phys. Rev. A **83**, 032101 (2011)

## Quantum discord - evaluation

[52] S. Luo, *Quantum discord for two-qubit systems*, Phys. Rev. A **77**, 042303 (2008).

[53] M. Ali, A. R. P. Rau, and G. Alber, *Quantum discord for two-qubit X states*, Phys. Rev. A **81**, 042105 (2010).

[54] Q. Chen, C. Zhang, S. Yu, X. X. Yi, and C. H. Oh, *Quantum discord of two-qubit X states*, Phys. Rev. A **84**, 042313 (2011).

[55] D. Girolami and G. Adesso, *Quantum discord for general two-qubit states: Analytical progress*, Phys. Rev. A **83**, 052108 (2011).

[56] M. Ali, *Quantum discord for a two-parameter class of states in* $2 \otimes d$ *quantum systems*, J. Phys. A **43**, 495303 (2010).

[57] S. Vinjanampathy and A.R.P. Rau, *Quantum discord for qubit-qudit system*, J. Phys. A **45**, 095303 (2012).

[58] Y. Biao-Liang, L. Yi-Min, L. Xian-Song and Z. Zhan-Jun, *Quantum correlations in a family of bipartite qubit-qutrit separable states*, Chin. Phys. Lett. **30**, 020302 (2013).

[59] P. Giorda and M. G. A. Paris, *Gaussian quantum discord*, Phys. Rev. Lett. **105**, 020503 (2010).

[60] G. Adesso and A. Datta, *Quantum versus classical correlations in Gaussian states*, Phys. Rev. Lett. **105**, 030501 (2010).

[61] F. Galve, G. L. Giorgi and R. Zambrini, *Orthogonal measurements are almost sufficient for quantum discord of two qubits*, Europhys. Lett. **96**, 40005 (2011).

[62] R. Tatham, L. Mišta Jr., G. Adesso, N. Korolkova, *Nonclassical correlations in continuous-variable non-Gaussian Werner states* , Phys. Rev. A **85**, 022326 (2012).

[63] G. Adesso and D. Girolami, *Gaussian geometric discord*, Int. J. Quant. Inf. **9** (2011).

[64] P. Giorda, M. Allegra and M.G.A. Paris, *Quantum discord for Gaussian states with non-Gaussian measurements*, Phys. Rev. A **86**, 052328.

## Quantum discord - applications

[65] A. Datta, *Studies on the role of entanglement in mixed-state quantum computation*, arXiv:0807.4490 (2008).

[66] A. Datta, A. Shaji and C. M. Caves, *Quantum discord and the power of one qubit*, Phys. Rev. Lett. **100**, 050502 (2008).

[67] A. Datta, A. Shaji, *Quantum discord and quantum computing: an appraisal*, Int. J. Quantum Inform. **09**, 1787 (2011).

[68] B. Eastin, *Simulating concordant computations*, arXiv:1006.4402 (2010).

[69] G. Passante, O. Moussa, D. A. Trottier, R. Laflamme, *Experimental detection of nonclassical correlations in mixed-state quantum computation* , Phys. Rev. A. **84**, 044302 (2011).

[70] B. Dakić, Y.O. Lipp, X. Ma, M. Ringbauer, S. Kropatschek, S. Barz, T. Paterek, V. Vedral, A. Zeilinger, Č. Brukner, P. Walther, *Quantum discord as resource for remote state preparation*, Nature Physics **8** (9), 666 (2013); G.L. Giorgi, *Quantum discord and remote state preparation*, Phys. Rev. A **88**, 022315 (2013).

[71] M. Gu, H.M. Chrzanowski, S.M. Assad, T. Symul, K. Modi, T. C. Ralph, V. Vedral, P. K. Lam, *Observing the operational significance of discord consumption*, Nat. Phys. **8** (9), 671 (2013).

[72] S Boixo, L Aolita, D Cavalcanti, K Modi, A Winter, *Quantum locking of classical correlations and quantum discord of classical-quantum states*, Int. J. Quant. Inf. **9**, 1643 (2011).

[73] S. Pirandola, *Quantum discord as a resource for quantum cryptography*, arXiv:1309.2446 (2013).

[74] C. Weedbrook, S. Pirandola, J. Thompson, V. Vedral, M. Gu, *Discord empowered quantum illumination*, arXiv:1312.3332 (2013).

[75] D. Girolami, A. M. Souza, V. Giovannetti, T. Tufarelli, J. G. Filgueiras, R. S. Sarthour, D. O. Soares-Pinto, I. S. Oliveira, G. Adesso, *Quantum discord determines the interferometric power of quantum states*, arXiv:1309.1472 (2013).

[76] L. Roa, J.C. Retamal, M. Alid-Vaccarezza, *Dissonance is required for assisted optimal state discrimination*, Phys. Rev. Lett. **107** (8), 080401 (2011); B. Li, S.M. Fei, Z.X. Wang, H. Fan, *Assisted state discrimination without entanglement*, Phys. Rev. A **85** (2), 022328; F.-L. Zhang, J.-L. Chen, L.C. Kwek and V. Vedral, *Requirement of dissonance in assisted optimal state discrimination*, Sci. Rep. **3**, 2134 (2013).

[77] A. Brodutch, D.R. Terno, *Quantum discord, local operations, and Maxwells demons*, Phys. Rev. A **81** (6), 062103.

[78] W.H. Zurek, *Quantum Discord and Maxwell's Demons*, Phys. Rev. A **67**, 012320 (2003).

[79] J. Oppenheim, M. Horodecki, P. Horodecki, and R. Horodecki, *Thermodynamical approach to quantifying quantum correlations*, Phys. Rev. Lett. **89**, 180402 (2002); M Horodecki, P Horodecki, R Horodecki, J Oppenheim, A.S. De, U. Sen, B. Synak-Radtke, *Local versus nonlocal information in quantum-information theory: formalism and phenomena*, Phys. Rev. A **71** (6), 062307 (2005).

[80] G. L. Giorgi, F. Galve, G. Manzano, P. Colet, R. Zambrini, *Quantum correlations and mutual synchronization* , Phys. Rev. A **85**, 052101 (2012).

[81] T. Tufarelli, D. Girolami, R. Vasile, S. Bose, G. Adesso, *Quantum resources for hybrid communication via qubit-oscillator states*, Physical Review A **86** (5), 052326 (2012).

[82] A. Datta, A. Shaji, *Quantum discord as a resource in quantum communication*, Int. J. Mod. Phys. B **27**, 1345041 (2013).

[83] A. Ferraro, M. G. A. Paris, *Nonclassicality Criteria from Phase-Space Representations and Information-Theoretical Constraints Are Maximally Inequivalent*, Phys. Rev. Lett. **108**, 260403 (2012).

## Entanglement in many-body systems

[84] L. Amico, R. Fazio, A. Osterloh, and V. Vedral, *Entanglement in many-body systems*, Rev. Mod. Phys. **80**, 517 (2008).

[85] A. Osterloh, L. Amico, G. Falci, R. Fazio, *Scaling of entanglement close to a quantum phase transition*, Nature **416** (6881), 608 (2001).

[86] T. J. Osborne and M. A. Nielsen, *Entanglement in a simple quantum phase transition*, Phys. Rev. A **66**, 032110 (2002).

[87] G. Vidal, J.I. Latorre, E. Rico, A. Kitaev, *Entanglement in quantum critical phenomena*, Phys. Rev. Lett. **90** (22), 227902 (2004).

[88] P. Calabrese, J. Cardy, *Entanglement entropy and conformal field theory*, J. Phys. A **42** (50), 504005 (2004).

[89] L. A. Wu, M. S. Sarandy, and D. A. Lidar, *Quantum phase transitions and bipartite entanglement*, Phys. Rev. Lett. **93**, 250404 (2004); L. A. Wu, M. S. Sarandy, D. A. Lidar, and L. J. Sham, *Linking entanglement and quantum phase transitions via density-functional theory*, Phys. Rev. A **74**, 052335 (2006).

[90] T. Roscilde, P. Verrucchi, A. Fubini, S. Haas, and V. Tognetti, *Studying quantum spin systems through entanglement estimators*, Phys. Rev. Lett. **93**, 167203 (2004).

[91] L. Amico, F. Baroni, A. Fubini, D. Patanè, V. Tognetti, and P. Verrucchi, *Divergence of the entanglement range in low-dimensional quantum systems*, Phys. Rev. A **74**, 022322 (2006).

[92] V. Vedral, *High-temperature macroscopic entanglement*, New J. Phys. **6**, 102 (2004).

[93] H. Fan, S. Lloyd, *Entanglement of eta-pairing state with off-diagonal long-range order*, J. Phys. A **38**, 5285 (2005).

[94] S.-J. Gu, S.-S. Deng, Y.-Q. Li, and H.-Q. Lin, *Entanglement and quantum phase transition in the extended Hubbard model*, Phys. Rev. Lett. **93**, 086402 (2004).

[95] A. Anfossi, P. Giorda, A. Montorsi and F. Traversa, *Two-point versus multipartite entanglement in quantum phase transitions*, Phys. Rev. Lett. **95**, 056402 (2005).

[96] A. Anfossi, C. Degli Esposti Boschi, A. Montorsi, and F. Ortolani, *Single-site entanglement at the superconductor-insulator transition in the Hirsch model*, Phys. Rev. B **73**, 085113 (2006).

[97] A. Anfossi, P. Giorda and A. Montorsi, *Entanglement in extended Hubbard models and quantum phase transitions* , Phys. Rev. B **75** 165106 (2007).

[98] A. Anfossi, P. Giorda and A. Montorsi, *Momentum-space analysis of multipartite entanglement at quantum phase transitions* , Phys. Rev. B **78**, 144519 (2008).

[99] P. Giorda and A. Anfossi, *Structure of quantum correlations in momentum space and off-diagonal long-range order in pairing and BCS states*, Phys. Rev. A **78**, 012106 (2008).

## Discord in many-body systems

[100] R. Dillenschneider, *Quantum discord and quantum phase transition in spin chains*, Phys. Rev. B **78**, 224413 (2008)

[101] M. S. Sarandy, *Classical correlation and quantum discord in critical systems*, Phys. Rev. A **80**, 022108 (2009).

[102] T. Werlang and G. Rigolin, *Thermal and magnetic quantum discord in Heisenberg models*, Phys. Rev. A **81**, 044101 (2010).

[103] J. Maziero, H. C. Guzman, L. C. Céleri, M. S. Sarandy, R. M. Serra, *Quantum and classical thermal correlations in the XY spin-*$1/2$ *chain*, Phys. Rev. A **82**, 012106 (2010).

[104] M. A. Yurischev, *Quantum discord in spin-cluster materials*, Phys. Rev. B **84**, 024418 (2011).

[105] J. Maziero, L. C. Céleri, R. M. Serra, M. S. Sarandy, *Long-range quantum discord in critical spin systems* , Physics Letters A **376** (18), 1540 (2012);

[106] Y.-X. Chen and S.-W. Li, *Quantum correlations in topological quantum phase transitions*, Phys. Rev. A **81**, 032120 (2010).

[107] M. Allegra, P. Giorda, A. Montorsi, *Quantum discord and classical correlations in the bond-charge Hubbard model: Quantum phase transitions, off-diagonal long-range order, and violation of the monogamy property for discord*, Phys. Rev. B **84** (24), 245133 (2011).

## Discord in open systems

[108] L. Mazzola, J. Piilo, and S. Maniscalco, *Sudden transition between classical and quantum decoherence*, Phys. Rev. Lett. **104**, 200401 (2010).

[109] R. Vasile, P. Giorda, S. Olivares, M. G. A. Paris and S. Maniscalco, *Nonclassical correlations in non-Markovian continuous-variable systems* , Phys. Rev. A **82**, 012313 (2010);

[110] G. L. Giorgi, F. Galve, R. Zambrini, *Robustness of different indicators of quantumness in the presence of dissipation* , Int. J. Quant. Inf. **9**, 1825 (2011); L. A. Correa, A. A. Valido, D. Alonso. arXiv:1111.0806v2 (2011).

[111] J. Maziero, L. C. Celeri, R. M. Serra, and V. Vedral, *Classical and quantum correlations under decoherence* , Phys. Rev. A **80**, 044102 (2009); J. Maziero, T. Werlang, F. F. Fanchini, L. C. Celeri, and R. M. Serra, *System-reservoir dynamics of quantum and classical correlations* , Phys. Rev. A **81**, 022116 (2010).

[112] F. F. Fanchini, T. Werlang, C. A. Brasil, L. G. E. Arruda, and A. O. Caldeira, *Non-Markovian dynamics of quantum discord*, Phys. Rev. A **81**, 052107 (2010); L. Mazzola, J. Piilo, and S. Maniscalco, *Sudden transition between classical and quantum decoherence*, Phys. Rev. Lett. **104**, 200401 (2010); F. F. Fanchini, L. K. Castelano, and A. O. Caldeira, *Entanglement versus quantum discord in two coupled double quantum dots* , New J. Phys. **12** 073009 (2010); Z.-K. Su and S.-J. Jiang, *Quantum discord dynamics in structured reservoirs*, arXiv:1105.4911 (2011).

[113] J.-S. Xu, X.-Ye Xu, C.-F. Li, C.-J. Zhang, X.-B. Zou, and G.-C. Guo, *Experimental investigation of classical and quantum correlations under decoherence* , Nature Communications **1**, 7 (2010).

## Quantum information theory

[114] V. Vedral, *Introduction to Quantum Information Science*, Oxford University Press, Oxford, (2007); M. A. Nielsen and I. L. Chuang, *Quantum Computation and Quantum Information*, Cambridge University Press, Cambridge, U.K. (2000).

[115] B. Schumacher, *Quantum coding*, Phys. Rev. A **51**, 2738 (1995).

[116] B. Schumacher, *Sending entanglement through noisy quantum channels*, Phys. Rev. A **54**, 2614 (1996); B. Schumacher, M. Nielsen, *Quantum data processing and error correction*, Phys. Rev. A **54**, 2629 (1996).

[117] S. Lloyd, *Capacity of the noisy quantum channel*, Phys. Rev. A **55**, 1613 (1997).

[118] N. J. Cerf and C. Adami, *Negative entropy and information in quantum mechanics*, Phys. Rev. Lett. **79**, 5194 (1997).

[119] J. Oppenheim, M. Horodecki, A. Winter, *Partial quantum information*, Nature **436**, 673 (2005); M. Horodecki, J. Oppenheim, A. Winter, *Quantum state merging and negative information*, Comm. Math. Phys. **269** (1), 107 (2007); A. Abeyesinghe, I. Devetak, P. Hayden, A. Winter, *The mother of all protocols: Restructuring quantum informations family tree*, Proc. of the Royal Soc. A, **465**, 2537 (2009).

[120] E.H. Lieb, M.B. Ruskai, *Proof of the strong subadditivity of quantum-mechanical entropy*, J. Math. Phys., **14** 1938 (1973).

[121] M. B. Ruskai, *Inequalities for quantum entropy: A review with conditions for equality*, J. Math. Phys. **43**, 4358 (2002); P. Hayden, R. Jozsa, D. Petz, and A. Winter, *Structure of states which satisfy strong subadditivity of quantum entropy with equality*, Comm. Math, Phys. **246**, 359 (2004).

[122] M. Christandl, A. Winter, *Uncertainty, monogamy, and locking of quantum correlations*, IEEE Transactions on Information Theory **51** (9), 3159 (2005).

[123] A.S. Holevo, *Bounds for the quantity of information transmitted by a quantum communication channel*, Problems of Information Transmission **9**, 177 (1973).

[124] D.P. DiVincenzo, M.Horodecki, D.W. Leung, J.A. Smolin, B.M. Terhal, *Locking classical correlations in quantum states*, Phys. Rev. Lett. **92** (6), 067902 (2004).

[125] G. Giedke and J. I. Cirac, *Characterization of Gaussian operations and distillation of Gaussian states* , Phys. Rev. A **66**, 032316 (2002); J. Fiuràšek and L. Mišta Jr., *Gaussian localizable entanglement* , Phys. Rev. A (**75**, 060302(R) 2007).

[126] G.M. D'Ariano, P.L. Presti, and P. Perinotti, *Classical randomness in quantum measurements*, J. Phys. A: Math. Gen **38**, 5979 (2005).

[127] V. Giovannetti, S. Lloyd, L. Maccone, *Quantum-enhanced measurements: beating the standard quantum limit*, Science **306** (5700), 1330 (2004); *Quantum metrology*, Phys. Rev. Lett. **96** (1), 010401 (2006).

[128] S. Lloyd, *Enhanced sensitivity of photodetection via quantum illumination*, Science **321** (5895), 1463 (2008).

[129] L. Viola, S. Lloyd, *Engineering quantum dynamics*, Phys. Rev. A **65**, 010101(R) (2001).

[130] S. Hamieh, R. Kobes and H. Zaraket, *Positive-operator-valued measure optimization of classical correlations* , Phys. Rev. A **70**, 052325 (2004).

[131] L. del Rio, J. Åberg, R. Renner, O. Dahlsten and V. Vedral, *The thermodynamic meaning of negative entropy*, Nature **474** 61 (2011).

[132] T. Baumgratz, M. Cramer, M. B. Plenio, *Quantifying Coherence*, arXiv:1311.0275 (2013).

## Quantum communication

[133] B. Schumacher, M. D. Westmoreland, *Quantum mutual information and the one-time pad*, Phys. Rev. A **74**, 042305 (2006).

[134] C. Bennett and S. J. Wiesner, *Communication via one- and two-particle operators on Einstein-Podolsky-Rosen states*, Phys. Rev. Lett. **69**, 2881 (1992).

[135] C.H. Bennett, G. Brassard, C. Crépeau, R. Jozsa, A. Peres, W. K. Wootters, *Teleporting an unknown quantum state via dual classical and Einstein-Podolsky-Rosen channels*, Phys. Rev. Lett. **70**, 1895 (1993).

[136] A. Ekert, *Quantum cryptography based on Bell's theorem*, Phys. Rev. Lett. **67**, 661 (1991).

[137] S. Bose, *Quantum communication through an unmodulated spin chain*, Phys. Rev. Lett. **91**, 207901 (2003). D. Burgarth and S. Bose, *Perfect quantum state transfer with randomly coupled quantum chains*, New J. Phys. **7** 135 (2005); D. Burgarth and S. Bose, *Conclusive and arbitrarily perfect quantum-state transfer using parallel spin-chain channels*, Phys. Rev. A **71**, 052315 (2005).

## Quantum computation

[138] R. Jozsa, N. Linden, *On the role of entanglement in quantum-computational speed-up*, Proc. Roy. Soc. A **459** (2036), 2011 (2003).

[139] G. Vidal, *Efficient classical simulation of slightly entangled quantum computations*, Phys. Rev. Lett. **91** (14), 147902 (2003).

[140] D. Gottesman, *Stabilizer codes and quantum error correction*, PhD thesis, California Institute of Technology (1997).

[141] E. Knill, and R. Laflamme, *Power of one bit of quantum information*, Phys. Rev. Lett. **81**, 5672 (1998).

[142] B.E. Kane, *A silicon-based nuclear spin quantum computer*, Nature **393**, 133 (1998); B. E. Kane, *Silicon-based quantum computation*, Fortschritte der Physik **48**, 1023 (2000).

[143] A. Datta, S.T. Flammia, C.M. Caves, *Entanglement and the power of one qubit*, Phys. Rev. A **72** (4), 042316 (2005).

[144] A. Datta, G. Vidal, *Role of entanglement and correlations in mixed-state quantum computation*, Phys. Rev. A **75** (4), 042310 (2007).

## Quantum optics

[145] A. Ferraro, S. Olivares, M. G. A. Paris, *Gaussian States in Continuous Variable Quantum Information*, Bibliopolis, Napoli (2005), arXiv:quant-ph/0503237.

[146] C. T. Lee, *Two-mode squeezed states with thermal noise*, Phys. Rev. A **42**, 4193 (1990).

[147] A. Furusawa, J. L. Sorensen, S. L. Braunstein, C. A. Fuchs, H. J. Kimble, and E. S. Polzik, *Unconditional quantum teleportation*, Science **282**, 706 (1998); N. Lee, H. Benichi, Y. Takeno, S. Takeda, J. Webb, E. Huntington, A. Furusawa, *Teleportation of nonclassical wave packets of light*, Science, **332**,330 (2011).

[148] V. D'Auria, S. Fornaro, A. Porzio, S. Solimeno, S. Olivares, and M. G. A. Paris, *Full characterization of Gaussian bipartite entangled states by a single homodyne detector*, Phys. Rev. Lett. **102**, 020502 (2009).

[149] A. Agliati, M. Bondani, A. Andreoni, G. De Cillis, M. G. A. Paris, *Quantum and classical correlations of intense beams of light investigated via joint photodetection*, J. Opt. B **7**, 652 (2005).

[150] M. G. A. Paris, *Displacement operator by beam splitter*, Phys. Lett. A **217**, 78 (1996).

[151] F. A. M. de Oliveira, M. S. Kim, P. L. Knight, abd V. Bužek, *Properties of displaced number states*, Phys. Rev. A **41**, 2645 (1990).

[152] H. P. Yuen, *Two-photon coherent states of the radiation field* , Phys. Rev. A **13**, 2226 (1976).

[153] M. S. Kim, F. A. M. De Oliveira and P. L. Knight, *Properties of squeezed number states and squeezed thermal states*, Phys. Rev. A **40**, 2494 (1989).

[154] R. T. Hammond, *Density operator with coherent, number, and squeezed states*, Phys. Rev. A **41**, 1718 (1990).

[155] C. F. Lo , *Generating displaced and squeezed number states by a general driven time-dependent oscillator* , Phys. Rev. A **43**, 404 (1991); M. M. Nieto, *Displaced and squeezed number states*, Phys. Lett. A **229**, 135 (1997).

[156] L. Albano, D.F.Mundarain and J. Stephany, *On the squeezed number states and their phase space representations* , J. Opt. B **4**, 352 (2002).

## Condensed matter and quantum many body theory

[157] P. L. Taylor and O. Heinonen, *A Quantum Approach to Condensed Matter Physics*, Cambridge University Press, Cambridge, UK (2002); P. M. Chaikin and T. C. Lubensky, *Principles of Condensed Matter Physics*, Cambridge University Press, Cambridge, U.K., (2000).

[158] B. Sutherland, *Model for a multicomponent quantum system*, Phys. Rev. B **12**, 3795 (1975).

[159] C. N. Yang, *Concept of off-diagonal long-range order and the quantum phases of liquid He and of superconductors*, Rev. Mod. Phys. **34**, 694 (1962); *$\eta$ pairing and off-diagonal long-range order in a Hubbard model*, Phys. Rev. Lett. **63**, 2144 (1989).

[160] L. Arrachea and A. A. Aligia, *Exact solution of a Hubbard chain with bond-charge interaction*, Phys. Rev. Lett. **73**, 2240 (1994); A. Schadschneider, *Superconductivity in an exactly solvable Hubbard model with bond-charge interaction* , Phys. Rev. B **51**, 10386 (1995).

[161] C. Vitoriano, and M.D. Coutinho-Filho, *Fractional statistics and quantum scaling properties of the hubbard chain with bond-charge interaction* , Phys. Rev. Lett. **102**, 146404 (2009).

[162] M. E. Simón and A. A. Aligia, *Brinkman-Rice transition in layered perovskites*, Phys.Rev. B **48**, 7471 (1993); J. E. Hirsch, *Bond-charge repulsion and hole superconductivity*, Physica C **158**, 326 (1989); F. Marsiglio and J. E. Hirsch, *Hole superconductivity and the high-$T_c$ oxides*, Phys.Rev. B **41**, 6435 (1990).

## Decoherent histories

[163] R. B. Griffiths, *Consistent histories and the interpretation of quantum mechanics*, J. Stat. Phys. **36**, 219 (1984).

[164] R. Omnès, *Logical reformulation of quantum mechanics I, II, III, IV*, J. Stat. Phys. **53**, 893, 933, 957 (1988), **57**, 357 (1989); *Consistent interpretations of quantum mechanics*, Rev. Mod. Phys. **64**, 339 (1992).

[165] M. Gell-Mann and J. B. Hartle, *Quantum mechanics in the light of quantum cosmology*, in *Complexity, Entropy, and the Physics of Information*, W. H. Zurek, ed. (Addison-Wesley, Reading, Massachusetts, 1990); *Alternative decohering histories in quantum mechanics*, in Proceedings of the 25th International Conference on High Energy Physics, Singapore, August 2-8, 1990, K. K. Phua and Y. Yamaguchi, eds. (South East Asia Theoretical Physics

Association and Physical Society of Japan, distributed by World Scientific, Singapore, 1990).

[166] M. Gell-Mann and J. B. Hartle, *Classical equations for quantum systems*, Phys. Rev. D *47*, 3345 (1993).

[167] D. Giulini, E. Joos, C. Kiefer, J. Kupsch, I.-O. Stamatescu, H. D. Zeh, *Decoherence and the appearance of a classical world in quantum theory*, Springer, Berlin (Germany) (1996).

[168] G. Birkhoff and J. Von Neumann, Ann. of Math., **37**, 4, 823 (Oct., 1936).

[169] J. J. Halliweel, *A review of the decoherent histories approach to quantum mechanics*, Annals of the New York Academy of Sciences, **755**, 726 (1995).

[170] F. Dowker, A. Kent, *Properties of consistent histories*, Phys. Rev. Lett. **75**, 3038 (1995); *On the consistent histories approach to quantum mechanics*, J. Stat. Phys. **82**, 1575 (1996).

[171] M. Gell-Mann, J. Hartle, *Classical equations for quantum systems*, Phys. Rev. D **47**, 3345 (1993).

[172] J. J. Halliwell, *Decoherent histories and the emergent classicality of local densities*, Phys. Rev. Lett. **83**, 2481 (1999).

[173] W. H. Zurek, J. P. Paz, *Environment-induced decoherence, classicality, and consistency of quantum histories*, Phys. Rev. D **48**, 2728 (1993).

[174] A. Kent, *Quantum histories*, Phys.Scripta **T76**, 78 (1998).

[175] A. Kent, *Quantum Histories and Their Implications*, Lect. Notes Phys. **559**, 93 (2000).

[176] A. Kent, *Consistent Sets Yield Contrary Inferences in Quantum Theory*, Phys. Rev. Lett. **78**, 2874 (1997)

[177] S. Goldstein, D. N. Page, *Linearly positive histories: probabilities for a robust family of sequences of quantum events*, Phys. Rev. Lett. **74** 3715 (1995).

[178] I. Pitowsky, *Feasible Histories, Maximum Entropy and a MinMax Choice Criterion*, Physics Letters A **247**, 9 (1998).

[179] L. Diósi, *Anomalies for weakened decoherence criteria for quantum histories*, Phys. Rev. Lett. **92**, 170401 (2004).

[180] S. Lloyd, *Decoherent histories and generalized measurement*s, arXiv:quant-ph/0504155 (2005).

[181] O. Rudolph, *Consistent Histories and Operational Quantum Physics*, Int. J. Theor. Phys. **35**, 1581 (1996); *On the Consistent Effect Histories Approach to Quantum Mechanics*, J. Math. Phys. **37**, 5368, (1996).

[182] J. Garriga, A. Vilenkin, *Many worlds in one*, Phys. Rev. D **64**, 043511 (2001)

[183] T. A. Brun, *Quantum Dissipative Chaos*, arXiv:9307018v2 (1993);

[184] L. Diosi, *On the maximum number of decoherent histories*, Phys. Lett. **203A**, 267 (1995).

[185] F. Dowker, A. Kent, *Properties of consistent histories*, Phys. Rev. Lett., **75** 3038 (1995); *On the consistent histories approach to quantum mechanics*, J.Stat. Phys. **82** 1575 (1996).

## Quantum chaos and quantum dynamical entropy

[186] H. S. Stockmann, *Quantum Chaos*, Cambridge University Press (1999).

[187] F. Benatti, V. Cappellini, M. De Cock, M. Fannes, D. Vampeteghem, *Classical limit of quantum dynamical entropies*, Rev. Math. Phys. **15**, 847 (2003); V. Cappellini, *A survey on the classical limit of quantum dynamical entropies*, Acta Phys. Polon. A **112**(4), 589 (2007).

[188] A. Connes, E. Størmer, *Entropy for automorphisms of II 1 von Neumann algebras*, Acta Mathematica **134**, 289 (1975); A. Connes, H. Narnhofer, W. Thirring, *Dynamical entropy of $C^*$ algebras and von Neumann algebras*, Comm. in Math. Phys. **112**, 691 (1987).

[189] R. Alicki, H. Narnhofer, *Comparison of dynamical entropies for the noncommutative shifts*, Lett. in Math. Phys. **33**, 241 (1995).

[190] R. Alicki, D. Makowiec, and W. Miklaszewski, *Quantum chaos in terms of entropy for a periodically kicked top* Phys. Rev. Lett. **77** (1996).

[191] R. Alicki, M. Fannes, *Defining quantum dynamical entropy*, Lett. in Math. Phys. **32**, 75 (1994).

[192] R. Alicki, A. Łoziński, P. Pakoński and K. Życzkowski, *Quantum dynamical entropy and decoherence rate*, J. Phys. A **37,** 5157 (2004).

[193] A. N. Soklakov and R. Schack, *Decoherence and linear entropy increase in the quantum baker's map* , Phys. Rev. E **66**, 036212 (2002).

[194] W. Słomczyński W and K. Życzkowski, *Mean dynamical entropy of quantum maps on the sphere diverges in the semiclassical limit* , Phys. Rev. Lett. **80**, 1880 (1999).

[195] F.M.Izrailev, *Simple models of quantum chaos: spectrum and eigenfunctions*, Phys. Rep. **196**, 299 (1990).

[196] F.M.Izrailev, G.Casati, J.Ford, B.V.Chirikov, *Stochastic behavior of a quantum pendulum under a periodic perturbation*, Preprint 78-46, Institute of Nuclear Physics, Novosibirsk (1978).

[197] G.Casati *et al.*, *Lecture Notes in Physic*, Springer, Berlin, **93**, 334 (1979).

[198] S.Fishman, D.R.Grempel, R.E.Prange, *Chaos, quantum recurrences, and Anderson localization*, Phys. Rev. Lett. **49**, 509 (1982);

[199] B.V.Chirikov, F.M.Izrailev and D.L.Shepelyansky, *Quantum chaos: localization vs. ergodicity*, Physica D **33** 77 (1988);

[200] F.L.Moore *et al.*, *Atom optics realization of the quantum $\delta$-kicked rotor*, Phys. Rev. Lett. **75**, 4598 (1995).

[201] D. Weingarten, *Asymptotic behavior of group integrals in the limit of infinite rank*, J. Math. Phys. **19**, 999 (1978); B. Collins, S. Matsumoto, *On some properties of orthogonal Weingarten functions*, J. Math. Phys. **50** (2009), 113516.

[202] B. Collins and P. Śniady, *Integration with respect to the Haar measure on unitary, orthogonal and symplectic group* , Comm. Math. Phys. **264**, 773 (2006).

[203] D. Petz, J. Réffy, *On asymptotics of large Haar distributed unitary matrices*, Periodica Mathematica Hungarica **49**, 103 (2004); C. Mastrodonato, R. Tumulka, *Elementary proof for asymptotics of large Haar-distributed unitary matrices* , Lett. Math. Phys. **82**, 51 (2007).

[204] D. Rossini, G. Benenti, and G. Casati, *Conservative chaotic map as a model of quantum many-body environment*, Phys. Rev. E **74**, 036209 (2006).

[205] F. Haake and K. Zyczkowski, *Random-matrix theory and eigenmodes of dynamical systems*, Phys. Rev. A **42**, 1013 (1990).

## Einselection

[206] W. H. Zurek, *Decoherence and the transition from quantum to classical*, Phys. Today **44**(10), 36 (1991).

[207] W.H. Zurek, *Preferred states, predictability, classicality and the environment-induced decoherence*, Progr. Theor. Phys. **89**(2), 281 (1993).

[208] W.H. Zurek, *Decoherence, einselection, and the quantum origins of the classical*, Rev. Mod. Phys. **75** (2003).

[209] W. H. Zurek, *Pointer basis of quantum apparatus: into what mixture does the wavepacket collapse?*, Phys. Rev. D **24**(6), 1516 (1981); *Environment-induced superselection rules*, ibidem **26**(8), 1862 (1982).

[210] E. Joos and H. D. Zeh, *The emergence of classical properties through interaction with the environment*, Zeit. Phys. B **59**, 223 (1985).

[211] W.H. Zurek, S. Habib, J.P. Paz, *Coherent states via decoherence*, Phys. Rev. Lett. **70** (9), 1187 (1993).

[212] JR Anglin, JP Paz, WH Zurek, *Deconstructing decoherence*, Phys. Rev. A **55** (6), 4041 (1997).

[213] L. Diósi, C. Kiefer, *Robustness and diffusion of pointer states*, Phys. Rev. Lett. **85**, 3552 (2000).

[214] J. P. Paz and W. H. Zurek, *Quantum limit of decoherence: environment induced superselection of energy eigenstates*, Phys. Rev. Lett. **82**, 5181 (1999).

[215] W.-g. Wang, J. Gong, G. Casati and B. Li, *Entanglement-induced decoherence and energy eigenstates*, Phys. Rev. A **77**, 012108 (2008).

[216] C. Gogolin, *Environment-induced super selection without pointer states*, Phys. Rev. E **81**, 051127 (2010).

[217] W.-g. Wang, L. He and J. Gong, *Preferred states of decoherence under intermediate system-environment coupling*, Phys. Rev. Lett. **108**, 070403 (2012).

[218] W. H. Zurek, J. P. Paz, *Environment-induced decoherence, classicality, and consistency of quantum histories*, Phys. Rev. D **48**, 2728 (1993).

[219] A. Albrecht, *Investigating decoherence in a simple system*, Phys. Rev. D **46**, 5504 (1992).

[220] A. Albrecht, *Following a collapsing wavefunction*, Phys. Rev. D **48**, 3768 (1993).

[221] J. Twamley, *Phase-space decoherence: a comparison between consistent histories and environment-induced superselection*, Phys. Rev. D **48**, 5730 (1993).

## Other Miscellanea

[222] A. J. MacFarlane, A. Sudbery, and P. H. Weisz, *On Gell-Mann's $\lambda$-matrices, $d$-and $f$-tensors, octets, and parametrizations of $SU(3)$* , Comm. Math. Phys. **11**, 77 (1968).

[223] J. B. Bronzan, *Parametrization of SU (3)*, Phys. Rev. D **38**, 1994 (1988).

[224] K. Zyczkowski and M. Kus, *Random unitary matrices*, J. Phys. A **27**, 4235 (1994).

[225] N. Bohr, *The philosophical writings of Niels Bohr*, Ox Bow Press, Woollbridge, CT (1987).

[226] G. C. Ghirardi, A. Rimini and T. Weber, *Unified dynamics for microscopic and macroscopic systems*, Phys. Rev. D **34**, 470 (1986); A. Bassi and G. C. Ghirardi, *Dynamical reduction models*, Phys. Rept. **379**, 257(2003).

[227] H. P. Breuer, F. Petruccione, *The Theory of Open Quantum Systems*, Oxford University Press (2002).

[228] J. Anandan and Y. Aharonov, *Geometry of quantum evolution*, Phys. Rev. Lett. **65**, 1697 (1990).

[229] M. Gell-Mann, *The Quark and the Jaguar*, W. Freeman, San Francisco (1994).

# Index

# Acknowledgements (Ringraziamenti)

First and foremost, I would like to thank my advisor Paolo Giorda, who has provided me with unvaluable help, encouragement and guidance during the whole PhD training. Paolo has been extremely generous with his time and patience in guiding me through several research projects, carefully adjusting a balance of supervision and freedom, and I owe him a debt of gratitude for making me grow as a scientist. In accordance with his rigor and loyalty, Paolo has made any effort to ensure a smooth course of my PhD despite several obstacles, and he helped to create for me an important opportunity to visit MIT. Finally, his careful reading and suggestions were absolutely essential in completing this thesis.

I am very grateful to Seth Lloyd for accepting me as a visiting student at MIT last year, and for his manifold stimuli and suggestions. Half of the work presented in this thesis would not have existed without his aid and ideas.

My PhD would have been completely different without the wonderful company of several friends and colleagues. I thank all the members of the quantum group at ISI for the great time spent together over lunches, drinks and conversations, in particular Mauro Faccin, Leonardo Banchi, Gianluca Costagliola, Zoltan Kadar, and of course Zoltan Zimboras whose presence was sufficient to create a cheerful and pleasant work environment. I also thank all other colleagues at ISI for their support and company, especially Giovanni Petri, Martina Scolamiero and Irene Donato.

I am obviously indebted to all my collaborators for their time, patience, and help. In particular, I thank Matteo Paris and Arianna Montorsi, who collaborated with me and Paolo on two projects appearing in this thesis. I also thank Xiaoting Wang and Clarice Aiello, for being an example of kindness and endurance, as well as for their nice company at MIT. Finally, I thank Paola Cappellaro for collaborating with me, Clarice and Xiaoting on a long project.

This work would have been impossible without the support of the ISI Foundation, and I thank all the staff and president Mario Rasetti for endorsing my career and my research.

I thank Lorenzo Magnea for taking up the responsibility of being my academic advisor, and I thank Marco Genovese and Michele Caselle for my their careful reading of my PhD thesis and their willingness to take part to the defense committee.

Non è questo il luogo per rendere adeguate testimonianze d'affetto. Posso solo dire che l'intero mio lavoro, e in particolare le ricerche presentate in questa tesi, traggono luce e senso dalla costellazione di rapporti umani che mi circonda. In particolare vorrei ringraziare tutti gli splendidi amici di lunga e meno lunga data che mi hanno accompagnato in questi anni, in particolare Alberto Martinetti, Giovanni Camanni, Pietro Fornara, Arianna Lovera, Elisa Roberi, Marco Spelta, Paolo Giacobbe, Laura Zotti, Giovanni Ciaccio, Luca Valenza, Marco Viola, Neri Marsili, Matteo Grasso. In occasione del completamento di questa tesi, un ringraziamento sentito va a Cosmo Lupo, Ornella Iuorio e Ginevra Favole la cui amicizia, simpatia e calore mi sono stati essenziali per affrontare il difficile periodo di visita al MIT.
Infine, ringrazio di cuore la mia famiglia per l'infinito sostegno e affetto che mi ha dato. Alla mia "gemella diversa" Cecilia va un sincero augurio di trovare la sua strada. Affido alle parole di uno scrittore un ringraziamento ai miei genitori: "Il figlio alto e lontano sentiva che non avrebbe mai potuto ripagarlo, nemmeno in parte centesimale [...]. L'unica maniera di ripagarlo, pensava ora, sarebbe stata d'amare suo figlio come il padre aveva amato lui: a lui non ne verrà niente, ma il conto sarà pareggiato nel libro mastro della vita." (Beppe Fenoglio, *Il partigiano Johnny*)